Remote Sensing for Large-Area, Multi-Jurisdictional Habitat Mapping

by

Gregory John McDermid

A thesis

presented to the University of Waterloo

in fulfillment of the

thesis requirement for the degree of

Doctor of Philosophy

in

Geography

Waterloo, Ontario, Canada, 2005

AUTHOR'S DECLARATION FOR ELECTRONIC SUBMISSION OF A THESIS

I hereby declare that I am the sole author of this thesis. This is a true copy of the thesis, including any required final revisions, as accepted by my examiners.

I understand that my thesis may be made electronically available to the public.

Abstract

A framework designed to guide the effective use of remote sensing in large-area, multi-jurisdictional habitat mapping studies has been developed. Based on hierarchy theory and the remote sensing scene model, the approach advocates (i) identifying the key physical attributes operating on the landscape; (ii) selecting a series of suitable remote sensing data whose spatial, spectral, radiometric, and temporal characteristics correspond to the attributes of interest; and (iii) applying an intelligent succession of scale-sensitive data processing techniques that are capable of delivering the desired information. The approach differs substantially from the single-map, classification-based strategies that have largely dominated the wildlife literature, and is designed to deliver a sophisticated, multi-layer information base that is capable of supporting a variety of management objectives. The framework was implemented in the creation of a multi-layer database composed of land cover, crown closure, species composition, and leaf area index (LAI) phenology over more than 100,000 km^2 in west-central Alberta. Generated through a combination of object-oriented classification, conventional regression, and generalized linear models, the products represent a high-quality, flexible information base constructed over an exceptionally challenging multi-jurisdictional environment. A quantitative comparison with two alternative large-area information sources – the Alberta Vegetation Inventory and a conventional classification-based land-cover map – showed that the thesis database had the highest map quality and was best capable of explaining both individual- and population-level resource selection by grizzly bears.

Acknowledgements

I acknowledge the generous financial support of the Foothills Model Forest Grizzly Bear Research Program, and its many partners in industry and government. From 2002 through 2004, I was employed as a research associate in the project, as funded by an NSERC CRD grant to Dr. Steven Franklin at the University of Calgary/University of Saskatchewan and Dr. Mark Boyce at the University of Alberta. I was also supported by an NSERC Post-Graduate Scholarship, Forestry Canada Graduate Supplement, and Ontario Graduate Scholarship during my time at the Waterloo Laboratory for Earth Observation, University of Waterloo.

Gordon Stenhouse, Jerome Cranston, Julie Dugas, Scott Nielsen, Christian Weik, Robin Munroe, and other colleagues in the Foothills Model Forest Grizzly Bear Research Program have provided me with the environmental imperative and intellectual feedback that has largely driven this work, in addition to on-going assistance in data management and field logistics. I thank the Foothills Model Forest partners who have supported this project, and the colleagues in western Alberta who have lent me their encouragement, advice, …and field data! George Mercer, Landon Shepherd, and Jesse Whittington in Jasper National Park; Ron Hall at the Canadian Forest Service; and Arturo Sanchez, Shasta Rudyk, and Mark Hebblewhite at the University of Alberta all went out of their way to assist me.

I am grateful to my supervisor, Ellsworth LeDrew, for affording me the opportunity to resurrect my graduate career after six years in industry. I didn't think it could be done! Thanks also to my mentor, Steven Franklin, whose infectious comments

at the pool table got this whole ball rolling (again). I came back because I recognized the impact these two gentlemen have had in my life, and I wanted to pass it along.

Thanks also for the support and hard work of my colleagues at the University of Calgary, wherein I was housed ("holed up", some might say) during the course of this research. Julia Linke, Falk Huettman, Alysha Pape, Kirk Montgomery, Barb Schwab, David Couroux, Scott Steeby, and David Nuell all contributed to this work as part of their affiliation with the Earth Systems Modelling Lab, wherein we planned and executed two successful and entertaining field campaigns. Thanks also to Medina Hansen, whose initial efforts in 2000 and 2001 – the infamous "IDT" map – this research builds upon.

A big shout out and thanks must also go to my new faculty colleagues in the Department of Geography, University of Calgary, who thought enough of my work to let me to stick around a while longer, while affording me the patience to finish off a few loose ends. ;-)

Finally, I thank my family: Pat, Derek, and Jonathan McDermid, to whom the brunt of long days at the office and short, distracted days at home largely falls. I did it for you, and I couldn't have done it without you.

Table of Contents

List of Tables

List of Figures

Chapter 1: Introduction

Environmental management and conservation agendas commonly include requirements for mapping and monitoring wildlife habitat for the purpose of estimating population sizes, identifying critical habitat, and predicting the impacts of development or environmental change. While occasionally conducted over small geographic areas (e.g. Radeloff *et al.*, 1999; Lauver *et al.*, 2002) these initiatives commonly require regional, or, increasingly, global perspectives that defy traditional field-based strategies (e.g. Skidmore and Gauld, 1996; Corsi *et al.*, 1997; Osborne *et al.*, 2001; Wulder *et al.,* 2003; Zhu and Waller, 2003). In light of these challenges, remote sensing has often been identified as a key data source for supporting habitat mapping and other large-area wildlife applications (Graetz, 1990; Roughgarden *et al.*, 1991; Wickland, 1991). The promise of the technology lies in its potential to deliver information about key environmental parameters over large areas with regular temporal revisit periods. These sentiments are reflected in the growing number of *integrated* remote sensing-ecology studies in the literature (e.g. Hines and J. Franklin, 1997; Carroll *et al.*, 1999; Kobler and Adamic, 1999; Skidmore, 2002). However, the technology remains a "blunt tool" (Plummer, 2000) requiring a significant amount of multidisciplinary research and joint understanding in order to reach its full potential.

Multidisciplinary approaches to science and management are tremendously appealing, because they bring together individuals with different experience and backgrounds whose constructive exchange of ideas have the potential to generate novel solutions. However, such projects are often challenging in that researchers entering new

disciplines do not possess the necessary background knowledge, and lack the ability to communicate effectively with their new peers. Such is clearly the case with the remote sensing-ecology interface, where significant gaps of understanding exist between the *tools* experts – practitioners of remote sensing, geographic information systems (GIS), and other spatial techniques – and ecologists. Plummer (2000) lamented the issue in the context of ecological process models, but a wider survey of the literature reveals this to be a common pattern. In their review of remote sensing protocols used in the national Gap Analysis Program, Eve and Merchant (1998) offered the following advice to new projects just getting underway with their ecological mapping: "Brace yourself and good luck!"

There is a need for users and producers of remotely sensed information to seek common ground with respect to the capabilities of the tools. Hoffer (1994) referred to the "information needs definition circle" (Figure 1-1) in which resource managers and remote sensing/GIS specialists – lacking a common background and thorough understanding of each other's fields – struggle to communicate with one another. The resource manager requires a variety of information products at a wide range of scales but is unsure of the capabilities of remote sensing and GIS, and so asks "What can the tools do to help me?" The remote sensing specialist, unfamiliar with the complex intricacies of ecology and ecosystem processes, asks in turn "What type of information do you need?"

Figure 1-1: The information needs definition circle. Adapted from Hoffer, 1994.

This research attempts to traverse that knowledge gap, looking specifically at the use of remote sensing and other geospatial tools for large-area habitat mapping. The extent to which wildlife studies have come to rely on remote sensing-derived products is illustrated by the increasing frequency with which they occur in the literature (e.g. May *et al.*, 2004; Osko *et al.*, 2004; Jackson *et al.*, 2005; Hoving *et al.*, 2005). In Alberta, the Foothills Model Forest Grizzly Bear Research Program (FMFGBRP) has pioneered the use of remote sensing-based land-cover maps, derived through a combination of supervised classification, decision rules, and pre-existing GIS information (Franklin *et al.*, 2001), to create *resource selection functions*: statistical models that relate grizzly bear telemetry data with environmental information to create spatially explicit map products that summarize the probability of grizzly bear occurrence (Nielsen, 2004). These products, in turn, serve as management tools to help ameliorate the impact of development in sensitive bear range. The ultimate goal of the FMFGBRP is to map and monitor grizzly bear habitat across the entire province (Stenhouse, 2005), and there is a

critical need for *next generation* remote sensing techniques that are both robust scaleable over very large areas.

The basic premise behind this work is that while many of these collaborative studies have shown substantial promise, an effective framework for applying the remote sensing toolset to wildlife habitat applications has yet to be formally articulated (Glenn and Ripple, 2004). Previous efforts have relied too heavily on single-map, classification-based approaches developed for other applications that fail to recognize the particular needs of the wildlife community, and may therefore fall short of expectations. For example, Throgmartin *et al.* (2004) documented a number of discrepancies and spatial inconsistencies in the National Land Cover Dataset – the most current and widely available representation of land cover in the contimerous United States – in a bird habitat model over the upper Midwestern United States.

While it is unreasonable to expect flawless information from remote sensing, multi-disciplinary collaborators do require high levels of quality and consistency. It is also desirable to produce flexible *high-level* data products wherever possible that can be adjusted to meet the diverse and evolving needs of research and management partners. In developing the methodological framework that is the main subject of this research, the following has served as guiding principles:

1. The process must be sensitive to scale, and avoid over-simplifying complex phenomenon with single *catch-all* maps;
2. The methodological procedures must be robust and scalable enough to be applied effectively over very large areas;

3. The products must be consistent, with no discernable seam lines or sharp breaks in quality; and
4. The information base should be flexible enough to address a variety of management objectives.

1.1 Research Objectives

The central goal of this research is to establish an effective framework for deriving high-quality land and vegetation information over large, multi-jurisdictional areas in order to support contemporary wildlife research and conservation agendas. In working to achieve this goal, three main objectives must be met:

1. A methodological approach for creating high-quality, spatially explicit environmental information over large areas must be articulated,
2. Robust strategies for creating attribute-based maps of land cover, crown closure, species composition, and leaf area index (LAI) phenology must be established, and
3. The effectiveness of these new products for supporting operational wildlife management objectives over large, multi-jurisdictional areas must be determined.

Within the context of these main objectives, a number of specific research questions can be posed:

- What are the most effective methods for mapping physical ground processes and attributes such as land cover, crown closure, species composition, and LAI phenology? What roles do object-oriented classification, per-pixel modelling, and other advanced processing procedures play in the overall strategy?

- How do you make the most effective use of spectral, spatial, geomorphometric, and other supplemental GIS information in this style of mapping? What are the best sources for these data?
- What is the proper series of preprocessing and processing procedures for eliminating seam lines and other spatial inconsistencies in map products generated over large, multi-scene mosaics?
- What strategies can be incorporated into the mapping procedure to maximize the flexibility of the end products and enhance their utility to support multiple research and management objectives?
- How do the information products generated through this research compare to other traditional sources of environmental information? Does the information base generated in this work provide an effective foundation for operational wildlife management?

These objectives and research questions provide the foundation upon which this thesis was organized.

1.2 Organization of Thesis

The introductory chapter provides a brief introduction to the role of remote sensing in multi-disciplinary ecological studies, and an overview of the specific research objectives to be addressed in this thesis. Chapter 2 reviews the use of remote sensing in wildlife habitat research, including a definition of critical terms, an overview of common strategies, and a description of an attribute-based framework for linking environmental information needs with remote sensing techniques that is based on hierarchy theory and the remote sensing scene model. Chapter 3 provides an overview of the applied portion

of this thesis, including a description of the 100,000 km^2 study area in west-central Alberta and the partner projects that have contributed to this work. The next two chapters contain the core remote sensing components of the thesis which describe the creation, testing, and assessment of the environmental database produced in this research: Chapter 4 with methods, and Chapter 5 with results and discussion. Chapter 6 outlines the details of a comparison between the attribute-based layers created in this work with two alternative sources of spatially explicit environmental information: the Alberta Vegetation Inventory, and the Alberta Ground Cover Categorization map. Chapter 7 contains a summary of the thesis, conclusions, and recommendations for future work.

Chapter 2: Remote Sensing for Large-Area Habitat Mapping: A Review

2.1 Definitions and Nomenclature

In 1942, Raymond Lindeman penned a landmark paper that defined *ecosystem* as "the system composed of physical-chemical-biological processes active within a space-time unit of any magnitude, i.e. the biotic community plus its abiotic environment". While the definition is not strictly spatial, it is generally understood that the area referred to by an ecosystem is a common and recognizable environmental unit. *Habitat*, in turn, occupies a somewhat adjunct position, referring specifically to the place or physical environment occupied by a population of organisms (Colinvaux, 1986). Unfortunately, the two terms have become so ubiquitous over time that their potential for misuse is high. For example, authors in the remote sensing community are quick to label their classification products "habitat maps" whenever the work falls within an ecological context (e.g. Dechka *et al.*, 2000; Vinluan and DeAlban, 2001) when, in many cases, the term "land-cover maps" (Wyatt *et al.*, 1994) might be more appropriate. However, the issue is complicated, being hampered in practice by multiple definitions and frequent inconsistencies in the literature.

The fact that habitat is rarely defined suggests that its meaning is generally taken for granted, yet even a simple dictionary search reveals two different definitions: one relating to location – the place where a species is commonly found – and the other relating to condition – the type of environment in which an organism normally occurs (Merriam-Webster, 1998). While Morrison *et al.* (1992) noted this initial dichotomy, a survey of the literature reveals an even more complicated situation. Corsi *et al.* (2000)

partitioned the various meanings of habitat into a nine-cell matrix (Table 2-1), showing that the term can refer to a distinct species or community (e.g. grizzly bear habitat), or a land attribute with no relation to biota (e.g. riparian habitat). Specific definitions can also include elements of Cartesian space, environmental space, or both. The situation is further complicated by frequent examples of ambiguity in the literature; sometimes within the same publication. For example, Lehmkuhl and Raphael (1993) used the terms "old-forest habitat" and "owl habitat" simultaneously in a paper about northern spotted owls in the Olympic Peninsula. All of the above contributes to misunderstanding amongst multidisciplinary colleagues, and prompted Hall *et al.* (1997) to issue a plea for standard terminology.

Table 2-1: The various meanings of the term *habitat,* with selected references from the literature. Modified after Corsi et al. (2000).

	Biota		
	Species	**Species and Communities**	**Land**
Cartesian Space	Begon et al., 1990; Krebs, 1985; Odum, 1971	Zonneveld, 1995,	
Environmental	Collin, 1988; Whittaker et al., 1973; Moore, 1967		
Environmental & Cartesian	Morrison et al., 1992; Mayhew and Penny, 1992	Yapp, 1922; Colinvaux, 1986	Stelfox and Ironside, 1982, USFWS, 1980a, b; Herr and Queen, 1993

Corsi *et al.* (2000) speculated that the origin of the word habitat – Latin for *habitare*, or "to dwell" – reflects its initial purpose as a term to describe the environment a species lives in. Its gradual transformation into more of a land-based concept is likely related to the emergence of widespread habitat and biodiversity mapping, in which individual maps for every species are virtually impossible to produce (Kerr, 1986). The term *habitat type*, defined as a mappable unit of land homogeneous with respect to vegetation and environmental factors (Jones, 1986), is a likely product of this trend. In retrospect, this context likely forms the basis of many remote sensing *habitat maps*, and subsequent confusion over the use of the term.

Considered carefully, the value of habitat type maps is based on the assumption that an area exhibiting similar vegetation cover is also likely to contain homogeneous conditions with respect to other environmental gradients. However, it seems unlikely that the variation of factors affecting the distribution of all species is completely interdependent, which would lead one to conclude that habitat types are not truly homogeneous. It also seems reasonable to speculate that the focus on habitat types as an ecological mapping unit may have arisen from an early lack of sophisticated spatial tools capable of portraying the many environmental factors that affect the distribution of species, such as land cover, soil type, temperature variability, food availability, and shelter (among many others) (Corsi *et al.*, 2000). The recent development of geographic information system (GIS) technology, however, has revolutionized the feasibility of these more sophisticated environmental characterizations, and a subsequent revival of the

original species-specific meaning of habitat. Given these observations, I will adopt the following definition after Hall *et al.*, 1997:

> Habitats are the resources and conditions present in an area that produce occupancy, including survival and reproduction, by a given organism, and, as such, implies more than vegetation and vegetation structure. It is the sum of the specific resources that are needed by an organism.

As a result, habitat is considered to be a species-specific concept, and includes elements of both environmental and Cartesian space. Table 2-2 presents a summary of habitat-related terminology, including several not discussed directly in this work, but commonly encountered in the ecological literature.

Table 2-2: Habitat terminology. Modified after Krausman (1999).

Term	Definition
Habitat	The sum and location of the specific resources needed by an organism for survival and reproduction
Habitat Type	A mappable unit of land considered homogeneous with respect to vegetation and environmental factors
Habitat Use	The way an organism uses the physical and biological resources in a habitat
Habitat Selection	A series of innate and learned behavioural decisions made by an animal about what habitat it would use
Habitat Preference	The consequences of habitat selection
Habitat Availability	The accessibility and procurability of the physical and biological components of a habitat
Habitat Suitability	The ability of the habitat to sustain life and support population growth
Habitat Quality	The ability of the environment to provide conditions appropriate for individual and population persistence
Critical Habitat	A legal term describing the physical or biological features essential to the conservation of a species, which may require special management considerations or protection

It is useful to consider the relationship between the *habitat* concept and that of *land cover*: the attribute most commonly mapped with remote sensing methods. Land cover is generally defined as the observed (bio)physical description of the earth's surface (DiGregio and Jansen, 2000). While land cover is often the first data layer produced in a mapping exercise, it is usually desirable to combine this information with additional ancillary data in order to derive other spatial products that are more useful to managers and researchers. A good example of this is the transformation of land *cover* to land *use*, which describes not only the physical and biological cover of an area, but also contains information on how the land is used by humans. The transformation can either be accomplished indirectly through implied relationships, or directly through the integration of other spatially referenced information (Jensen and Cowen, 1999).

From the practical perspective of a remote sensing scientist, the relationship between land cover and habitat is analogous to that which exists between land cover and land use. Habitat (or other ecological properties) can either be inferred from land cover indirectly or modelled explicitly through integration with other environmental factors (Corsi *et al.*, 2000). The ecological literature contains examples of both strategies.

2.2 Previous Studies

A survey of the literature reveals a variety of remote sensing strategies applied to habitat mapping projects spanning a wide range of spatial scales (Table 2-3). Manual interpretation of aerial photographs has often been employed by studies that involve species with limited ranges and/or the analysis of relatively small areas. For example, Palma (1999) used manual interpretation of 1:10,000 aerial photography to extract a

variety of environmental variables including land cover, land-cover diversity, road density, and drainage density in order to characterize the habitat immediately surrounding confirmed sightings of Iberian lynx in the western Algarve region of Portugal. Lauver *et al.* (2002) used 1:12,000 digital orthophotos to map detailed environmental variables such as tree density and hedgerow location in order to assess loggerhead shrike habitat suitability over a 40,000 ha study area in Kansas. In both these cases, remote sensing served primarily as a complement to field surveys, and made use of skilled interpreters to generate detailed, high-quality information. Unfortunately, the labour-intensive nature of such manual procedures tends to limit the range over which this type of analysis can be conducted.

Researchers faced with larger study areas have typically turned to digital processing of medium-spatial-resolution satellite imagery such as Landsat Multispectral Scanner (MSS), Thematic Mapper (TM), or Enhanced Thematic Mapper Plus (ETM+) for more efficient acquisition of environmental information. Land cover, in particular, plays a prominent role in most regional-scale habitat studies. McClain and Porter (2000), for example, used TM-derived land-cover maps to evaluate white-tailed deer habitat in the Adirondacks of New York. A second study by Nielsen *et al.* (2003) used resource selection functions to link grizzly bear location data to a land-cover map covering more than 10,000 km^2 in the foothills of Alberta, Canada. However, while land-cover maps may contain useful predictive power, they are often not capable of revealing the underlying mechanisms and dynamic nature of complex natural landscapes.

Table 2-3: Literature examples showing the range of scales and remote sensing-derived variables used in previous habitat-mapping studies.

	Local	Regional	National/Continental
Land cover	Palma et al., 1999; Radeloff et al., 1999; Lauver et al., 2002	Hines and Franklin, 1997; Roseberry, 1998; Kurki et al., 1998; Carroll et al., 1999; Smith et al., 1998; McLain and Porter, 2000; Borboroglu et al., 2002; Ciarniello et al., 2002; Danks and Klein, 2002; Norris et al., 2002; Rushton et al., 1997; Woolf et al., 2002; Nielsen et al., 2003	Osborne et al., 2001
Topography	Palma et al., 1999	Ciarniello et al., 2002; Danks and Klein, 2002; Woolf et al., 2002; Nielsen et al., 2003	Osborne et al., 2001
Fragmentation	Radeloff et al., 1999; Palma et al., 1999	Hines and Franklin, 1997; Roseberry, 1998; Kurki et al., 1998; Hargis et al., 1999; Woolf et al., 2002	
Vegetation Greenness/Phenology		Verlinden and Masogo, 1997; Ciarniello et al., 2002	Wallin et al., 1992
Vegetation Structure	Radeloff et al., 1999; Lauver et al., 2002	Hines and Franklin, 1997; Carroll et al., 1999	

Several researchers have attempted to supplement basic land cover information with fragmentation metrics, topographic measures, and vegetation indices, among others. For example, Danks and Klein (2002) used the topographic variables elevation, slope, aspect, and ruggedness to develop predictive models of muskoxen habitat in northern Alaska. Other studies have demonstrated the value of fragmentation metrics as indicators of habitat structure. For example, Hargis *et al.* (1999) employed a suite of spatial statistics to investigate the effects of forest fragmentation on American martens in the

Uinta Mountains of Utah. In a later study, Hansen *et al.* (2001) explored the spatial effects of timber harvesting on woodland caribou habitat in south-eastern British Columbia, Canada. While these approaches seem capable of summarizing complex spatial habitat requirements, the challenge involves selecting the correct metrics and identifying the appropriate scale of observation.

The challenge of balancing the need for detailed information with the cost and complexities involved with producing such information increases directly with study area size. Habitat projects operating at the national and continental level are often forced by practical reasons to use more generalized variables from coarse-resolution satellite data. For example, Wallin *et al.* (1992) used the Normalized Difference Vegetation Index (NDVI) of 4km Advanced Very High Resolution Radiometer (AVHRR) imagery in their analysis of breeding habitat for the red-billed quelea in sub-Saharan Africa. The authors hypothesized that NDVI would be capable of providing a reasonable index of more detailed (and unavailable) measures such as vegetation condition and food availability.

The growing demand for large area environmental information is reflected by the numerous large-area data initiatives, including land cover maps of the United States (Loveland *et al.*, 1991), Canada (National Resources Canada, 1995), and the world (Hansen *et al.*, 2000); the Pathfinder (Maiden, 1994; James and Kalluri, 1994) and Moderate Resolution Imaging Spectroradiometer (MODIS) (Justice and Townshend, 2002) datasets; and the National Gap Analysis Program (Scott *et al.*, 1993). However, these data are likely to lack the spatial grain and environmental detail necessary for most habitat-mapping projects.

At the leading edge of the discipline are studies that have attempted to incorporate detailed vegetation attributes such as taxonomy, age, and structure derived from widely available satellite imagery. The work by Carroll *et al*. (1998) stands out with its use of sophisticated TM-derived estimates of canopy closure, tree size, and percent conifer in a study of fisher habitat in the Klamath region of Oregon and California. In similar works, Hines and J. Franklin (1997) and J. Franklin and Stephenson (1995) demonstrated the value of a high-quality, regional-scale (2 million ha) vegetation database in the San Bernardino Mountains of southern California that included spatially detailed information on forest cover (land cover, fragmentation) and canopy structure (canopy coverage, tree crown size) with an analysis of habitat quality for the California spotted owl.

While obviously expensive and difficult to produce, large-area vegetation databases with at least moderate levels of structural and taxonomic detail are likely required for most large-area habitat studies. Deriving such databases is a tremendous challenge that requires the intelligent coupling of ecological theory and remote sensing technique.

2.3 Remote Sensing Information Extraction Strategies

The application of remote sensing techniques to large-area habitat projects is often hindered by the relative immaturity of the remote sensing/GIS discipline. Researchers both inside and outside the field tend to forget that we have only been working with earth-observing satellites for about thirty years, and that truly large-area projects (those combining information from two or more adjacent scenes) have only been widely attempted within the past decade.

Several works (e.g. Meyer and Werth, 1990; Mladenoff and Host, 1994) have criticized the "overselling" of Landsat data, citing the inconsistent delineation of species composition and detailed vegetation structure, among other issues. In response, some specialists have pointed to the vast technical gains over early MSS instruments (Hoffer, 1994), improved algorithms (e.g. Bolstad and Lillesand, 1992; Cohen *et al.*, 1995; Cohen *et al*., 2003), and the introduction of new sensor technologies (e.g. Asner *et al.*, 2000; Lim *et al.*, 2003). Others (e.g. Trotter, 1991) have questioned the necessity for higher accuracy map products destined for use with data of lesser or unspecified quality. Regardless of the debate, ecologist and resource managers require at least a basic understanding of the techniques and capabilities of remote sensing. Together, these constitute the *toolset* for large-area habitat mapping.

2.3.1 Classification

Image classification – the systematic grouping of remote sensing and other geographically referenced data by categorical or, increasingly, fuzzy decision rules – is the best-known and most widely used information extraction technique in remote sensing. Given a choice, many technicians prefer classification, because (i) the methodological procedures are widely known and available, (ii) the output is generally simple to understand, and (iii) the accuracy of the results is relatively easy to assess.

The vegetation attributes typically mapped through classification include a general typing of physiognomy and dominant species composition. These are reviewed in detail by S. Franklin (2001), and are generally broken down hierarchically into broad classes of land cover at Level I (e.g. forest, non-forest, water, etc), forest types at Level II (e.g. conifer, broadleaf, mixed forest, etc), and more detailed species composition/canopy

structure criteria at Level III (e.g. open-canopy spruce, closed-canopy spruce, trembling aspen, etc). While consistent separation at Level III is challenging (J. Franklin *et al.*, 2003), particularly over mixed forest targets (Reese *et al.*, 2002), acceptable accuracies can generally be obtained with the correct image processing procedures (e.g. Brown de Colstoun *et al.*, 2003).

There are literally dozens – if not hundreds – of classification techniques used in the processing of remotely sensed imagery, and they are well described by other works (e.g. Jensen, 1996; Mather, 1999). The purpose of this review is not to duplicate those efforts, but rather to provide a summary of the major choices required for all classification projects, paying particular attention to the use of satellite imagery over large areas.

2.3.1.1 Variable Selection

Satellite remote sensing instruments deliver spectral measures that are highly related to land cover, and represent a powerful dataset for mapping surface patterns across broad regions (e.g. DeFries and Belward, 2000; Lunetta *et al.*, 2002; Cihlar *et al.*, 2002; Walker *et al.*, 2002; Homer *et al*., 2002). However, the successful application of these data depends largely on the selection of appropriate mapping variables. Raw spectral values can undergo wide variety of mathematical transformations including principal components (Fung and LeDrew, 1987; Piwowar and LeDrew, 1996), tasseled cap (Kauth and Thomas, 1976; Crist and Cicone, 1984), and band ratioing (Satterwhite, 1984) techniques designed to reduce data dimensionality, subsume noise, and enhance specific spectral phenomena. These data can often also benefit from a variety of textural (Haralick *et al.*, 1973; Irons and Peterson, 1981; Clausi, 2002), contextual (Binaghi *et al.*,

1997), and other (Read and Lam, 2002) pattern recognition techniques aimed at capturing additional information in the spatial domain. Numerous studies have also demonstrated the utility of spatially referenced ancillary data for classification, including topography, climate, geology, landform, and soils (e.g. S. Franklin and Moulton, 1990; McDermid and S. Franklin, 1995; Treitz and Howarth, 2000; Gould *et al.*, 2002). Multitemporal analysis – the integration of scenes acquired at different seasons – is often applicable, particularly for detailed forest species discrimination at the stand level (e.g. Wolter *et al.*, 1995; Brown de Colstoun, 2003).

2.3.1.2 Supervised Versus Unsupervised Classification

Classification approaches can generally be considered as either supervised, unsupervised, or hybrid (Fleming and Hoffer, 1975). Unsupervised routines are designed to illuminate the natural groupings or clusters present in the mapping variables, and require no prior knowledge of the study area. Supervised classification techniques, in contrast, use intensive hands-on training in an attempt to extract pre-defined information classes from the explanatory variables, and, as such, require specific *a priori* knowledge.

Because of the reduced need for spatially detailed ground information, many large-area mapping projects have relied heavily on unsupervised techniques. A survey of 21 participants in the National Gap Analysis Program (GAP) who used pure classification approaches as their primary mapping protocol revealed that 41% used unsupervised classification, compared to just 5% for supervised classification (Eve and Merchant, 1998). Unfortunately, the benefits of the unsupervised technique are often outweighed by the difficulty of post-classification labelling (which itself requires substantial ground information) and the procedure has often been shown to produce sub-optimal results.

Huang *et al.* (2003) compared the accuracy of two large-area mapping projects in Utah: one nine-scene application that was classified with a supervised technique, and one 14-scene area classified with unsupervised criterion. While other factors almost certainly played a role, the authors attributed at least some of the roughly 8% overall accuracy improvement to the high-quality training data employed in the supervised classification.

The potential conflict between spectral clusters and desired information classes – combined with the difficulty of obtaining abundant training data over broad areas – has encouraged many researchers to employ hybrid supervised/unsupervised elements to their strategy. Reese *et al.* (2002) used "guided clustering" in the production of a 12-scene land-cover map of Wisconsin from Landsat Thematic Mapper (TM) data. The approach involved the application of an unsupervised routine on training pixels for which the information class was already known. Clusters were merged on the basis of transformed divergence values, spectral space plots, and visual assessment. Eventually, all of the subsets for each information class were assembled into unique signature sets, which were then applied in a standard maximum likelihood classification. Using these methods, the authors were able to achieve overall classification accuracies in the range of 70% to 84% for Anderson Level II/III land cover classes. Early successes with these hybrid methods in the GAP program (e.g. Lillesand, 1994) led to their subsequent adoption by 48% of the states surveyed.

2.3.1.3 Decision Rules

All remote sensing classifiers operate as pattern recognition algorithms that rely on decision rules to define boundaries and assign class membership. While these rules can

be organized along a variety of lines, the parametric/non-parametric categorization presents a convenient basis for discussion.

Many of the most familiar classifiers operate in Euclidean space, and rely on statistical measures such as central tendency, variance, and covariance to perform their functions. These routines – clustering algorithms, discriminant functions, and maximum likelihood, for example – are robust and well-behaved when the input variables conform to basic statistical assumptions, but may perform poorly in the presence of non-parametric distributions (Peddle, 1995). The maximum likelihood classifier (MLC) is perhaps the best-known of the parametric classifiers. A supervised technique, MLC uses training to characterize information classes on the basis of the mapping variables' mean values and covariance matrices. In the decision phase, unknown pixels are assigned a probability-of-membership for each class, and placed in the *most likely* category. While the sensitivity of MLC to variables with non-normal – particularly multimodal – distributions is well-known, the technique remains very popular. In practice, many of the normality issues can be resolved by pre-stratifying the imagery with ancillary data (Hutchinson, 1982; Harris and Ventura, 1995) or unsupervised classification (Homer *et al.*, 1997). However, these procedures can become unwieldy, and MLC remains incapable of incorporating low-level (nominal, ordinal) data directly.

Researchers have invested a significant amount of effort in the search for decision rules free of parametric constraints. The nearest neighbour (NN, or kNN) classifier is a supervised technique that assigns unknown observations to the class of the nearest training vector (or majority of k vectors), and has proven effective in several recent studies (e.g. Kuncheva and Jain, 1999; Barandela and Juarez, 2002). However, NN

classifiers are computationally intensive and highly susceptible to errors in training data (Brodley and Friedl, 1999).

Artificial neural networks (ANNs) are a second non-parametric approach to classification that have recently received a lot of attention in the remote sensing literature (e.g. Ripley, 1996; Atkinson and Tatnall, 1997; Murai and Omatu, 1997; Kimes *et al.*, 1999). The technique falls within a group of machine learning classifiers that *learn* decision rules through training observations without statistical constraints. ANNs learn patterns by iteratively considering the multivariate characteristics of each class, multiplying the explanatory variables by a set of weights, applying a transfer function to their weighted sum, and using these to predict the identity of the original training data. Subsequent iterations are designed to improve the fit between actual and predicted class membership, and increase the utility of the classifier. One of the strengths of ANNs lies in their ability to handle information categories that consist of many spectral subclasses without the explicit stratifying that would be necessary with parametric techniques such as MLC (Pax-Lenney *et al.*, 2001). However, many technicians are uncomfortable with the "black box" nature of ANNs, and they remain poorly integrated into most commercial image processing packages (J. Franklin *et al.*, 2003).

Decision trees are another of the *machine-learning* classifiers, but are far more conceptually transparent than ANNs. Decision trees handle classification by recursively partitioning a data set into smaller and smaller subdivisions on the basis of tests performed at branches or nodes in a tree (Hansen *et al.*, 1996). The tree is composed of a root node (composed of all the data), a set of internal nodes (splits), and a set of terminal nodes (leaves). Within this framework, an image is classified by sequentially subdividing

it according to the decision framework defined by the tree (Friedl and Brodley, 1997). Decision trees work well when the boundaries between classes have well-defined thresholds, and are capable of handling large numbers of dependent variables of all data levels (Fayyad and Irani, 1992). S. Franklin *et al.* (2001) modified the decision tree concept somewhat in a large-area classification of land cover in Alberta by selectively combining parametric (ML), non-parametric (kNN), and GIS decision rule criteria where conditions for each method were optimal. This (S. Frankin *et al.*, 2001) and other (e.g. Borak and Strahler, 1999; Rogan *et al.*, 2002) studies have found decision trees to outperform both MLC and other non-parametric classifiers.

2.3.1.4 Hard Versus Soft Classification

The natural world is a heterogeneous place that does not easily lend itself to the nominal information scales imposed by classification. Traditional *hard* classifiers use binary logic to determine class membership, in that each observation can belong to one and only one category. Classification strategies that employ fuzzy logic, by contrast, assign observations membership in each category (Foody, 1996a; 1999). The result is a more conceptually appealing classification model that seems better capable of representing the partial truth that we observe in the real world. For example, white spruce and trembling aspen species often blend together into mixed stands in the forests of western Alberta, and create a problem for traditional classification schemes. A hard classifier might address the issue by establishing a *mixed* forest class through the placement of decision boundaries along the species composition continuum – made up of, say, stands with more than 25% coniferous trees, but less than 75%. Under this scenario, a stand with 25% conifers would be considered pure, while a stand with 26% would be called mixed. A

fuzzy classifier, on the other hand, could soften these decision boundaries by allowing mixed observations to have membership in each class. Even probabilistic classifiers (like MLC) that are not based on fuzzy set theory can have their decision boundaries softened by retaining the class probability values (Foody, 1996b).

While fuzzy and other soft classification techniques are appealing, they also face challenges. For example, visualizing the results of a fuzzy classification for the purpose of decision-making or thematic map production often requires a *de-fuzzification* process in order to assign observations into definitive classes. Developing methods to better incorporate fuzzy information for ecosystem management and landscape planning still requires more research (J. Franklin *et al.*, 2003).

2.3.2 Sub-pixel Models

While nominal compilations of vegetation at the stand level are normally the domain of image classification procedures, the more detailed biophysical attributes of vegetation are usually better handled by per-pixel models. There are two primary reasons for this: first, because the vegetation elements normally considered at this level – LAI, biomass, crown closure, volume, density, etc. – vary continuously across the landscape and are not well represented by categorical measures, and second, because attributes at this level of detail are commonly smaller than the pixel size of optical satellite imagery. While detailed structural/biophysical factors can be summarized at the stand level and mapped discretely through classification, models that estimate biophysical attributes on a continuum provide much more flexibility with regard to their future use. One can also argue that pixel-based outputs present a more realistic spatial characterization of tree/gap-level information. Cohen *et al.* (2001) used TM imagery and empirical models to map percent conifer,

crown diameter, and age across five million hectares of forest in western Oregon. Besides generating a seamless output over the entire study area, their methods resulted in a forest information database with exceptional flexibility. By maintaining high-order information, the system provides managers with divergent needs the opportunity to define categories that suit their individual application. For example, one manager might use the system to define a GIS layer composed of three age classes: <80 years, 80-200 years, and >200 years (Cohen *et al.*, 1995). While this suits the needs of the first application, a second prospective user may only require two categories, or perhaps three classes with different thresholds.

While simple regression analysis is the most popular method for estimating sub-pixel properties from remote sensing data, it is certainly not the only one. Recent work has illustrated the effectiveness of alternative regression procedures such as canonical correspondence analysis (Cohen *et al.*, 2003; Ohmann and Gregory, 2002), generalized linear models (J. Franklin, 1995; Moisen and Edwards, 1999), and generalized additive models (Frescino *et al.*, 2001; Edwards *et al.*, 2002) that are capable of incorporating non-linear, categorical, or other non-parametric data into the analysis. Mixture models are commonly used to map the fraction of scene elements across an image (e.g. Mustard, 1993; Huguenin *et al.*, 1997) and can be linked with physical scene models to estimate specific structural attributes (e.g. Peddle *et al.*, 1999).

One of the dangers of the modelling approach is the illusion of precision afforded by continuous variable estimation. The experience of many researchers (e.g. Peterson *et al.*, 1987; Cohen and Spies, 1992; S. Franklin and McDermid, 1993; S. Franklin *et al.* 2003) has shown that there are definite limitations to the extent to which specific tree/gap

parameters can be characterized by moderate-resolution sensors. This is particularly true in closed stands, where changes in the physical variable may not translate to a measurable difference in the canopy. While these limitations can be ameliorated somewhat through the introduction of other (non-spectral) environmental variables into the modelling process (J. Franklin, 1995), specific care must be taken to guard against over-extending the limits of the data.

2.3.3 Quantifying Landscape Heterogeneity

While the great majority of remote sensing techniques are designed to extract knowledge concerning land composition and physical dimension, an important additional branch of digital processing is concerned with analysis of spatial structure. Scientists have long been aware that ecological processes are influenced by environmental patterns, and the subject of quantifying environmental heterogeneity has been an active research area for decades (e.g. Pielou, 1975). However, recent interest in the subject has increased dramatically, due to the complementary development of GIS and spatial statistics, coupled with the emergence of orbiting satellites as platforms for large-area ecological observations. It is within this context that the discipline of landscape ecology has emerged to examine landscape pattern, the influence of environmental actions on a landscape mosaic, and changes in landscape pattern and process over time (Turner *et al.*, 2001). Prominent among the discipline's core objectives are efforts to produce quantitative measures of landscape heterogeneity, a pursuit that has culminated in the development of an impressive array of indices designed to capture the various nuances of spatial structure (e.g. McGarigal and Marks, 1995; Elkie et al., 1999). A number of studies (e.g. Hargis et al., 1999; Lawler and Edwards, 2002; Woolf et al., 2002) have

demonstrated the potential of these variables as predictors of habitat quality and other environmental concerns.

In spite of recent accomplishments, the effective quantification of environmental heterogeneity remains problematic (Gustafson, 1998). Despite – some would argue because – of the ready availability of software capable of generating large numbers of spatial pattern indices from many forms of digital maps, many researchers remain unclear regarding which metrics to use and what these measures might mean (Kepner *et al.*, 1995). Whereas early studies relied on as little as three core indices (e.g. O'Neill *et al.*, 1988), recent efforts commonly contain a much larger number of metrics (e.g. Luque *et al.*, 1994; Lawler and Edwards, 2002). In describing the functionality of the software package FRAGSTATS, McGarigal *et al.* (2002) describes well over 150 variables, divided into eight separate categories. Overwhelmed researchers often turn to principal components analysis and other data reduction techniques to reduce redundancy and limit the amount of variables to a more reasonable number (Haines-Young and Chopping 1996). For example, Riitters *et al.* (1995) used factor analysis to explore the redundancy of 55 landscape metrics derived from a variety of land-use and land-cover maps, and concluded that close to 90% of the original variance could be explained by six univariate measures corresponding roughly to the first six factors of the analysis. The search for a relatively small number of meaningful variables that can be effectively applied to diverse landscapes remains an active research issue (Cushman *et al.* in review).

Even more elusive than the pursuit of parsimony is an understanding of the relationship between ecologically meaningful heterogeneity and that which can be mapped and measured by remote sensing. Spatial (and ecological) variability is a

function of both scale and time; the observed structure of a natural landscape is dependent on the spatial resolution of the data (grain), the physical size of the study area (extent), and the time period over which observations were acquired (Gustafson, 1998). Complexities surrounding the issue of scale is one of ecology's primary research focuses (e.g. O'Neill *et al.*, 1986; Wiens, 1989; Allen and Hoekstra, 1992; Hay *et al.*, 2002; Wu *et al.*, 2002).

2.3.4 Large Area Challenges

Knowledge concerning the automated extraction of biophysical information from digital satellite imagery has been the mainstay of research in the remote sensing community for more than 30 years. However, while most would agree that these efforts have resulted in an impressive variety of useful techniques, the fact remains that many of our core procedures have never been thoroughly tested on data sets larger than a single image. Research involving information extraction over large areas – those consisting of two or more adjacent scenes – is currently one of the discipline's key frontiers (Cihlar, 2000; Woodcock *et al.,* 2001, S. Franklin and Wulder, 2003). The following is a brief overview of the core challenges presented by large-area studies.

2.3.4.1 Image Acquisition and Temporal Heterogeneity

The multi-day temporal resolution of many earth-observing satellite systems creates a significant challenge for acquiring high-quality, cloud-free imagery over large study areas – particularly when there are specific temporal objectives. The inability to collect target scenes during specified time periods can derail certain information extraction techniques (multitemporal analysis, for example) and introduce unwanted variance to

others. Substituting historical imagery or data from alternate sensors – including synthetic aperture radar – is often required to meet specific mapping objectives, particularly in areas of persistent shadow or cloud cover (Wagner *et al.*, 2003; S. Franklin and Wulder, 2003).

Even under ideal conditions, study areas that traverse satellite path lines will have to deal with variability caused by temporal heterogeneity. Images acquired on different dates are likely to contain differences caused by changing ground conditions – moisture, vegetation phenology, and biomass (Schriever and Congalton, 1995) – in addition to atmospheric and illumination effects. All of these factors serve to complicate the mosaicking process and confound model and signature extension. While some of these issues can be accounted for in the image preprocessing phase, ground-based differences are difficult to overcome. Strategies for dealing with seam lines – abrupt changes between images caused in part by temporal heterogeneity – remains an active research issue.

2.3.4.2 Image Preprocessing

Radiometric processing in the form of atmospheric and/or topographic correction presents a significant challenge to large-area mapping and modelling activities, which require common radiometric scales across not only space and time, but potentially across sensors as well. Unfortunately, we presently lack a widespread standard for performing such adjustments. While much of the atmospheric correction literature is concerned with absolute calibration via radiative transfer models (e.g. Vermonte and Kaufman, 1995), the detailed atmospheric observations demanded by such solutions are rarely available. As an alternative, many users have come to rely on standard atmosphere parameterization

from commercial image processing packages. However, this is often an unsatisfactory approach; commonly producing poor or unexpected results (Cohen *et al.*, 2001; McDermid *et al.*, in prep.). Relative calibration procedures that normalize *slave* images to a high-quality *master* through histogram matching (Homer *et al.*, 1997), dark object subtraction (Chavez, 1988), or linear transformation (Hall *et al.*, 1991; McGovern, *et al.*, 2002) present an attractive set of alternatives.

Even less well defined is the role of topographic corrections over large areas. While topographically induced variance can be safely ignored over flat terrain, the effects can be significant in high-relief environments (Kimes and Kirchner, 1981; Allen, 2000). Numerous techniques have been devised to correct for terrain illumination differences, including simple cosine correction (S. Franklin, 1991) and the Minnaert correction (Tokola, 2001), among others (Civco, 1989; Conese *et al.*, 1993; Meyer *et al.*, 1993; Townshend and Foster, 2002). However, no geometry-based method seems capable of accounting for all topographic variation, since the issue is complicated by vegetation canopy geometry and the anisotropic behaviour of most cover types (Gu and Gillespie, 1998). At present, most large-area studies have chosen to ignore the topographic effect, dealing with it instead through stratification or the use of non-parametric methods that are less sensitive to its effects.

2.3.4.3 Large-area Diversity and Spatial Heterogeneity

In image classification, the concept of *signature extension* represents the distance over which the training data from one location – say, a pine forest – can represent other similar locations across space (Jensen, 1996), and reflects the overall efficiency of the classification procedure. Spatial heterogeneity is the primarily limitation on signature

extension; for example, phenological differences between pine forests at low elevation and those up high can create the need for additional high-cost training data, limit the ability to map consistent information classes, or both. The frequency with which these factors become an issue increases directly in proportion with the size and spatial detail of the mapping effort, and is one of the core challenges of large-area mapping exercises.

In many respects, large-area projects are crucibles of remote sensing efficiency. With limited resources, researchers are constantly challenging the limits of ground data, and pushing the envelope of spectral/temporal generalization. Previous studies have shown that spectral (Reese *et al.*, 2002) and physiographic (Homer *et al.*, 1997) stratification are the best strategies for maximizing efficiency over large, spatially heterogeneous study areas. Lillesand (1996) described the process of stratifying TM scenes into "spectrally consistent classification units" that attempted to maximize both spectral and physiological homogeneity. Manis *et al.* (2001) developed 74 mapping zones across five southwest states (Utah, Nevada, New Mexico, Colorado, and Arizona) in support of the southwest GAP project. The goal of each of these efforts was twofold: (i) to partition massive volumes of data into manageable and logical units, and (ii) to improve the efficiency of vegetation modelling and land-cover classification. Previous work in Minnesota by Bauer *et al.* (1994) showed that physiographic stratification improved overall classification accuracies by 10 to 15 percent.

Image stratification coupled with robust and/or non-parametric information extraction techniques are the key strategies for dealing with large-area diversity and spatial heterogeneity. Digital elevation models, soils maps, census data, ecoregion zones, and previous classification products can all contribute to the stratification process.

Operators must juggle diverse and potentially contradictory data sources, and define processing units that strike the correct balance between detail and cost.

2.3.4.4 Accuracy Assessment

The quality of a spatial data set is a broad issue that can relate to a variety of properties, including vagueness, precision, consistency, and completeness, among others (Worboys, 1998). The property of most frequent interest, however, is accuracy (Foody, 2002). That a map is not truly complete until its accuracy is properly assessed is one of the discipline's key tenets (Stehman and Czaplewiski, 1998; Cihlar, 2000).

Validation is the process of assessing – by independent means – the accuracy of remote sensing information products (Justice *et al.*, 2000), and the literature contains numerous references on the subject (see annotated bibliography by Veregin, 1989). However, very little has been done to assimilate the wide variety of techniques into a standard set of methods suitable for consistent application over large-areas (Edwards *et al.*, 1998). Outstanding issues include the design of statistically valid and logistically feasible sampling strategies, the adoption of stable and widely understood accuracy metrics, the assessment of positional errors, and the determination of reference data accuracy (S. Franklin and Wulder, 2003).

Ideally, researchers validate maps by way of comparison with some independent data set – preferably ground data – collected for that specific purpose. Unfortunately, these data are expensive, and commonly end up being used for more urgent needs, like training classifiers and establishing empirical relationships. Specific strategies like cluster sampling can be used to increase the efficiency of field data collection, but, in general, these data contain less information per unit sampled than those from pure or

stratified random procedures (Edwards *et al.*, 1998). Air photos and other higher-resolution brands of remote sensing are by far the most common source of validation information for large-area projects (S. Franklin and Wulder, 2003). For example, coarse-resolution AVHRR products are routinely validated with higher-resolution TM imagery (e.g. Fazakas and Nilsson, 1996; Scepan, 1999). IKONOS and QuickBird instruments could perform a similar function for Enhanced Thematic Mapper Plus (ETM+). The ultimate solution could resemble the coordinated use of field- and image-based validation methods similar to the procedures described by Tomlinson *et al.* (1999). Clearly, more research is required.

2.4 Linking Information Needs with Remote Sensing Strategy

Ecosystems are a somewhat abstract concept, and there are competing viewpoints as to which elements are important to map for the purpose of science and management over large areas. Graetz (1990) suggested that the characteristics of ecosystems are determined by the primary trophic level – the vegetation – and that vegetation can therefore be taken as the functional equivalent of terrestrial ecosystems. Remote sensing scientists have been quick to adopt this viewpoint, since vegetative units are much simpler to map than the complex interplay of physical (soils, climate, topography) and biological (wildlife, vegetation, micro organisms) agents that define the alternative viewpoint.

Unfortunately, many remote sensing products can be criticized for presenting an overly simplistic representation of vegetation, perhaps contributed to by historical limitations of satellite data and the ubiquitous use of classification as an information extraction technique. However, both of these factors have undergone recent change, with

the growing number and availability of commercial and non-commercial satellites acquiring data with ever-increasing spatial, spectral, and temporal dimensions (Phinn, 1998). While these newfound choices have the potential to greatly enhance our ability to conduct ecological monitoring and management, they also present unique challenges surrounding the selection of appropriate data and techniques. The discussion of information-extraction strategies for use in large-area ecosystem management applications must therefore begin with a review of the remote sensing scene model, and how it relates to vegetation as a hierarchical, multi-scale phenomenon.

2.4.1 Multi-scale Vegetation Structure

Understanding the structure of complex, natural systems is a key challenge for all disciplines dealing with these phenomena (Marceau and Hay, 1999). Contemporary works in landscape ecology (e.g. Gardner *et al*, 2001; Turner *et al.*, 2003) emphasize the interaction between vegetation stands distributed across the Earth's surface. This *mosaic of patches* implies a certain conceptual model concerning the nature of vegetation, which can be articulated formally as complex systems theory. Complex systems theory describes the behaviour of ecological systems characterized by a large number of components interacting in a non-linear way and exhibiting adaptive properties through time (Kay, 1991; Hay *et al.*, 2002). An important characteristic of complex systems is that they intuitively take the form of a nested hierarchy, in that finer categorical divisions (leaf, canopy) are nested within broader ones (tree, stand). This hierarchical structure is employed by many classification systems in their attempt to organize vegetation by process rate, scale, or taxonomy (see summaries by J. Franklin and Woodcock, 1997 and S. Franklin, 2001).

Woodcock and Harward (1992) presented a hierarchical model that describes patterns of matter and energy flux in a forested scene that consists (in ascending order) of trees/gaps, stands, forest types, and scenes. Their model compares closely to Urban *et al.*'s (1987) process-based organization of vegetation into gaps, stands, cover type, provinces, and biomes. The stand (often referred to as a *patch* in the landscape ecology literature) is defined as a contiguous area of similar species composition, plant cover, and plant size distribution (J. Franklin and Woodcock, 1997). Trees and gaps are nested within stands, which in turn are subsumed by larger landscape units or cover types, defined by Cousins (1993) as a complex of systems that form a recognizable entity. While there is some discussion regarding the scale of cover-type units (e.g. Forman and Godron, 1986; Urban *et al.*, 1987; Turner *et al.*, 2001) they are generally considered to be on the order of 1000s of hectares, and correspond quite closely to the Level II classes of Anderson *et al.* (1976).

While differences between the various classification systems in use (spatial, taxonomic, process-based) can create considerable confusion, the understanding of vegetation as a complex system – and subsequent adoption of one or more hierarchies – is important to large-area habitat mapping projects for the following reasons:

1. They represent the foundation of communication between resource managers and remote sensing specialists,
2. They provide a framework for conducting multi-scale mapping and modeling activities, and
3. They provide a conceptual basis for linking ecological information to the remote sensing scene model and subsequent information extraction techniques.

2.4.2 The Scene Model

Strahler *et al*. (1986) described the remote sensing model as having three distinct components: the sensor, the atmosphere, and the scene. The scene model comprises the area of interest, which, in a forest, is composed of a forested portion of the Earth's surface viewed at a specific scale. For many applications, it is appropriate to consider the scene as a spatial arrangement of discrete two- or three-dimensional objects distributed on a background (Jupp *et al.*, 1988; 1989). In real scenes, objects are formed by spectrally homogeneous pixels, and can take many different forms depending on scale. For example, a conifer forest scene could be modeled at a detailed scale as a series of two-dimensional objects composed of sunlit and shaded patches of forest and understorey, or, at a broader scale, as a mosaic of structurally homogenous forest stands.

The relationship between the size of the objects and the spatial resolution of the scene follows one of two types: H-resolution or L-resolution (Strahler *et al.*, 1986). The H-resolution case occurs when the pixel size of the scene is significantly smaller than the objects of investigation, while the L-resolution case occurs when pixels are larger than objects (Figure 2-1). This designation is important, since it describes the fundamental relationship between the objects of interest and the spatial resolution of the image, which in turn governs the choice of subsequent information extraction techniques.

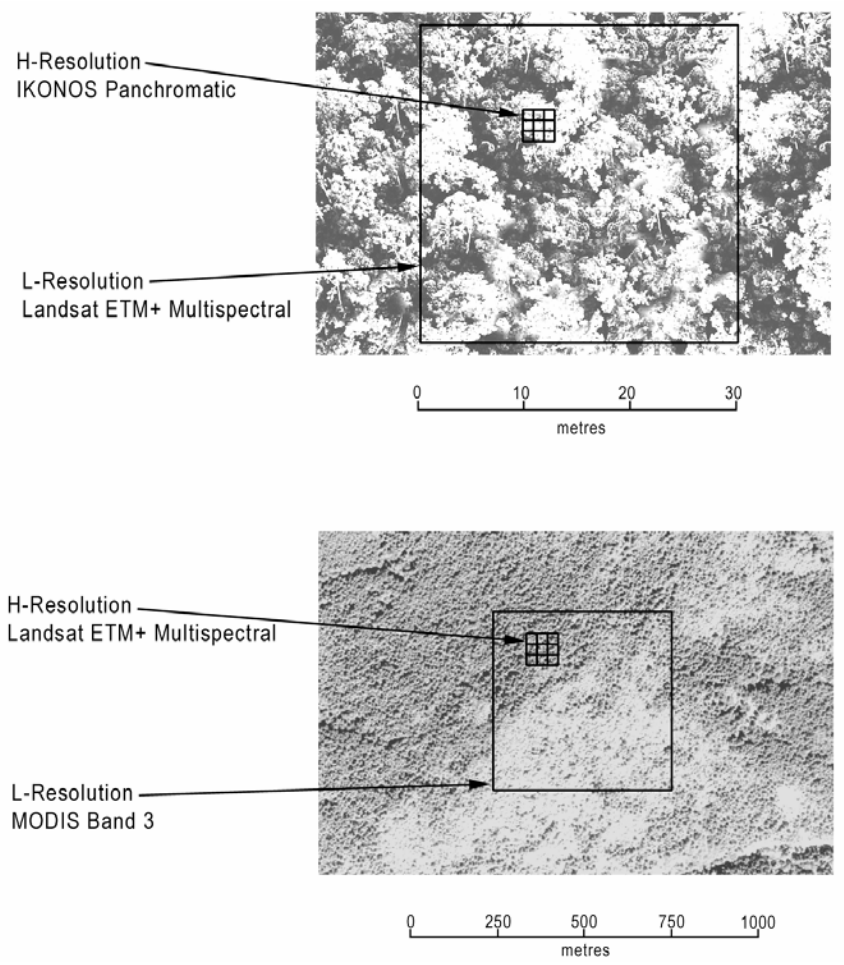

Figure 2-1: H- and L-resolution scene models for a forested scene. At the tree/gap level (top), Landsat ETM+ multispectral pixels are L-resolution, while IKONOS panchromatic pixels are H-resolution. At the stand level (bottom) Landsat ETM+ multispectral pixels are H-resolution, while MODIS band 3 pixels are L-resolution.

Generally speaking, H-resolution images are best suited for classification, since the objects of interest occur over areas larger than individual pixels. Depending on the specific structure of the scene, analysts can employ a wide variety of image processing techniques to extract the variables necessary for consistent discrimination, and may employ re-sampling (S. Franklin and McDermid, 1993) or segmentation (Woodcock and Hayward, 1992) strategies to better define the objects of investigation. L-resolution scenes, on the other hand, are more suited to per-pixel routines such as vegetation indices

(Satterwhite, 1984; Cohen, 1991), empirical (Moisen and Edwards, 1999; Cohen *et al.*, 2002) or physical (Goel, 1988; Scarth and Phinn, 2000) models, and spectral mixture analysis routines (Peddle *et al.*, 1999) that relate sub-pixel biophysical properties to multispectral reflectance measurements.

A critical characteristic of remote sensing scenes is the following: since natural systems are composed of objects in a multi-scale hierarchy, a single image can be both H-resolution with respect to some types of information, and L-resolution with respect to others. Following Woodcock and Harward's (1992) hierarchical forest scene model described earlier, a Landsat ETM+ image would be L-resolution at the tree/gap level, since each 30-metre pixel consumes several tree/gap objects (top part of Figure 2-1). However, the same 30-metre imagery would be considered H-resolution with respect to stands, which may cover 10s or 100s of hectares and consume many individual pixels (bottom part of Figure 2-1). As a result, the *correct* information extraction strategy for ecosystem management can vary greatly, and depends jointly on (i) the scale of information desired, and (ii) the spatial resolution of the image used.

2.4.3 A Framework for Application

Phinn *et al.* (2003) presented a framework for selecting the appropriate remote sensing data for environmental scientists. The process consists of the following six steps: (i) identify the information requirements for the project; (ii) organize the information needs in terms of an ecological hierarchy; (iii) conduct an exploratory analysis using existing digital data; (iv) identify the ideal remote sensing data, considering spatial, spectral, radiometric, and temporal dimensions; (v) select and apply a suitable set of information extraction techniques; and (vi) conduct a cost benefit analysis. This process can be

visualized with the help of Figure 2-2: a hypothetical landscape that is to be the study area of a regional habitat-mapping project. By identifying various vegetation attributes as the required information products, we can adopt a multi-scale hierarchy that organizes the scene in ascending scale as tree/gap, stand, and cover type. Specifications for the ideal remote sensing data can vary, depending on vegetation conditions, study area size, and available image processing techniques. Figure 3 offers H- and L- resolution suggestions at each level of the hierarchy. The choice of data should dictate – at least initially – the subsequent image processing techniques pursued: generally, classification for H-resolution data and physical or empirical modelling for L-resolution cases. Assessing the benefits of the resulting investment should take into account, among other things, the accuracy of the information products generated, the value of the resulting habitat maps, and the utility of the vegetation database for other resource management applications.

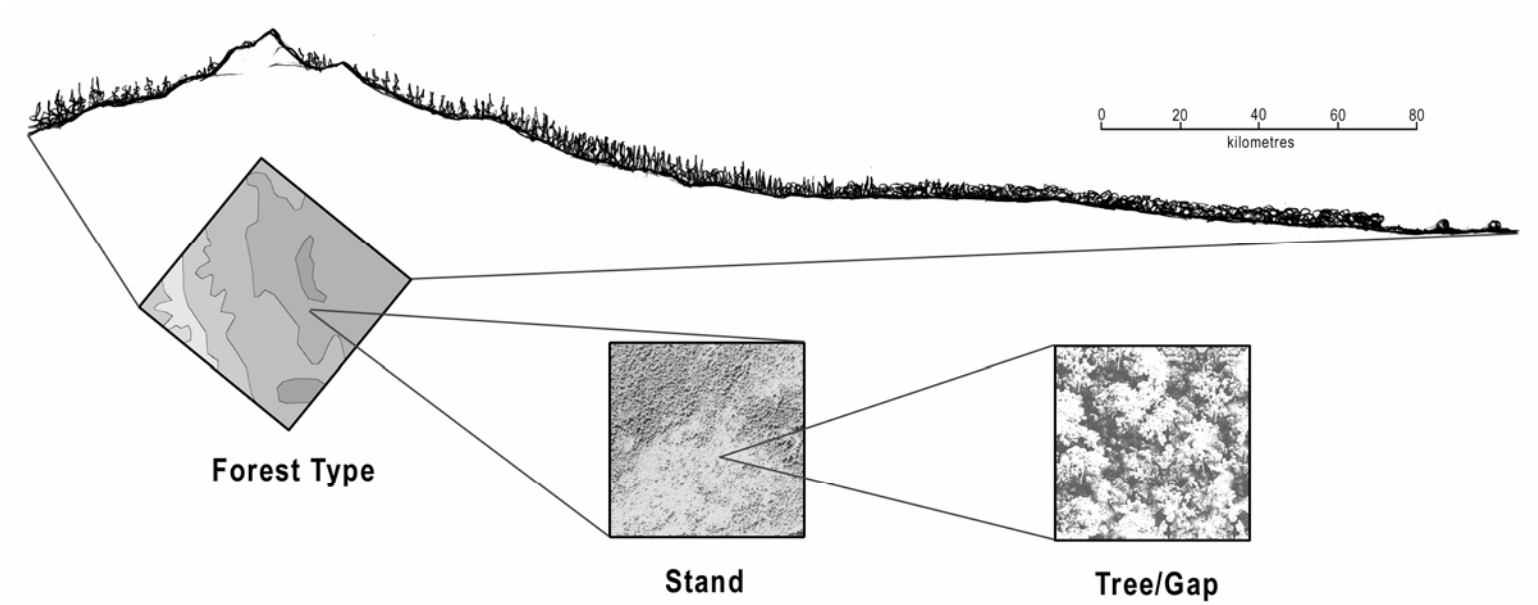

	Attribute		Data Source	Technique
Tree/Gap	LAI, species, crown closure	*H*	IKONOS, Quickbird	Classification
		L	Landsat, SPOT, ASTER	Physical/empirical modelling
Stand	Landcover, composition, fragmentation	*H*	Landsat, SPOT, ASTER	Classification
		L	MODIS, AVHRR	Physical/empirical modelling
Forest Type	Natural subregion	*H*	MODIS, AVHRR	Classification
		L		

Figure 2-2: A vegetation hierarchy is imposed on a theoretical landscape for the purpose of selecting the ideal remote sensing data and information extraction techniques.

2.5 Chapter Summary

A strong alliance is forming between remote sensing and ecology to address the challenge of large-area habitat mapping. However, the harmony of this multidisciplinary approach to science is hindered by miscommunication and a lack of common understanding. Pioneering work has demonstrated the promise of geospatial tools in cross-disciplinary work, but a tremendous amount of research yet remains. Image classification, per-pixel models, and spatial pattern analysis techniques are effective tools for extracting information, but scientists and resource managers require guidance for their effective application. A framework that combines hierarchy theory with elements of the remote sensing scene model presents a mechanism for linking information needs with image processing technique, as well as a foundation for communication between ecologists and specialists in remote sensing. Future research should explore the integrated role of new remote sensing instruments and emerging technologies, develop techniques for constructing multi-scale vegetation databases over large areas, and test the utility of these databases for supporting diverse environmental applications.

Chapter 3: Project Overview and Description of the Study Area

The central purpose of this research is to create a framework for deriving high-quality land and vegetation information for large-area habitat mapping using remote sensing and other geospatial tools. In addition to being applicable over very large areas, it is also desirable that these methods be flexible enough to support multiple objectives. This means avoiding the use of nominal information categories and pre-defined classes, and making use of *continuous* variables to store vegetation information attributes as much as possible.

The land and vegetation information base envisioned in this work is composed of four components – physical landscape attributes – that operate on the landscape and are judged to be important to habitat use patterns observed in grizzly bears and other wildlife species in western Alberta: (i) land cover/physiognomy, (ii) crown closure, (iii) species composition, and (iv) phenology. The approach varies from that used in the generation of most other large-area remote sensing maps in at least two important respects. First is the recognition that land and vegetation information exists at a variety of spatial and temporal scales, and that no single map is capable of capturing the full range of variability observed in reality. While it would be certainly incorrect to claim that a four-level database is capable of simulating reality, I do contend that an attribute-based approach that attempts to identify and account for the major spatial, structural, and temporal patterns observed on the landscape is more appropriate than a single *catch-all* map. The second major difference involves the selective application of remote sensing techniques sensitive to the scale at which these attributes appear on the landscape.

Guided by hierarchy theory and the remote sensing scene model, the framework adopted in this research calls for a variety of information-extraction strategies, including regression analysis and object-oriented classification designed specifically to exploit H- and L-resolution information, as appropriate. Finally, a concerted effort has been made in the construction of the current environmental database to map selected attributes as continuous variables wherever possible, in order to achieve maximum flexibility with the completed product. This decision was the product of hard-won experience gained in previous collaborative experiences, in which decisions concerning class labels and boundaries made early on in the project have a tendency to change over time as new opinions, challenges, and information arise. For example, initial consultation amongst team partners might determine that two categories for crown closure are sufficient: open (6-50%) and closed (51-100%). Upon further review, however, (normally when the products are complete!) it is determined that the classes are too broad, and that a three-category configuration of crown closure would be more appropriate. If the map was a standard ordinal classification, then this request would require thorough revisions, adding weeks or months to the project's timeline. If the underlying product were a continuous-variable model of crown closure, however, then the reconfiguration would be a simple GIS exercise that could be completed within hours. This flexibility is an important advantage, both for preserving harmony within a multi-disciplinary team as well as enabling the finished database to be adapted and applied to other projects with potentially divergent objectives with minimal re-investment.

3.1 Location and Description of the Study Area

The study area for this research is located in the west-central portion of Alberta, Canada (Figure 3-1), along the front range of the Rocky Mountains. This expansive region, covering more than 100,000 km^2, encompasses one of western Canada's most physiographically and biologically diverse landscapes. The area is internationally recognized for the quality of its physical and biological systems, and contains a number of provincially and federally protected reserves (Figure 3-2), including Banff and Jasper National Parks. Outside of these well-known protected areas, however, the region is subject to rapid development and intensive resource extraction. Oil and gas development (Figure 3-3), forestry, mining, and agriculture form the foundation of Alberta's economy and exert a profound influence on the natural and political landscape. This apparent dichotomy places tremendous pressure on the region's management agencies, which must balance the demands of economic activity with the obligations of ecological sustainability.

3.1.1 Natural Regions and Subregions

The Natural Regions and Subregions is a hierarchical land classification system designed for broad-scale description of provincial land resources, and is used by the Alberta government for a variety of planning purposes (Achuff and Wallis, 1977). The system classifies the landscape on the basis of biogeographic features – geology, hydrology, soils, climate, vegetation, etc. – and provides a convenient framework for describing the current study area.

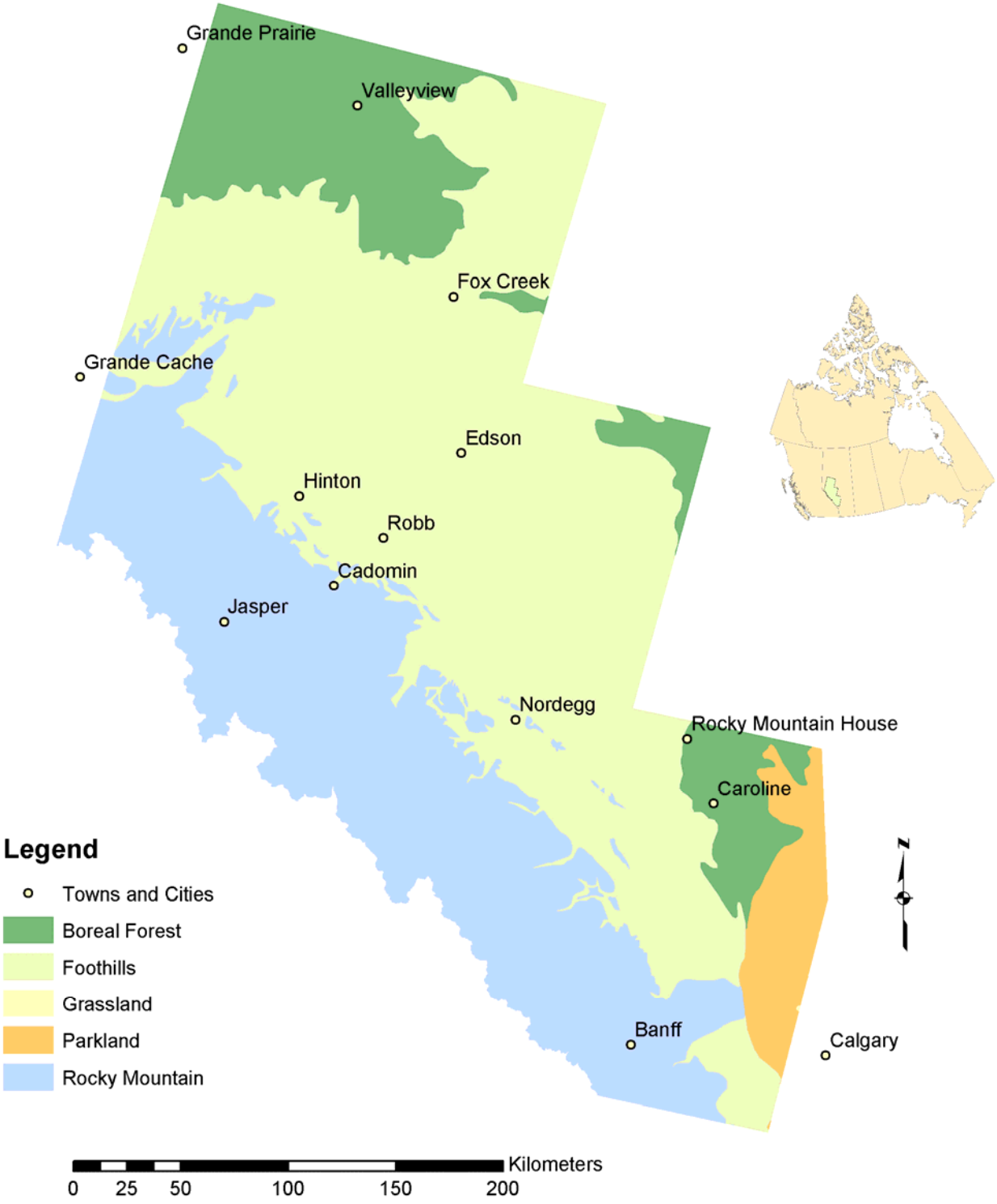

Figure 3-1: Location of the study area in west-central Alberta.

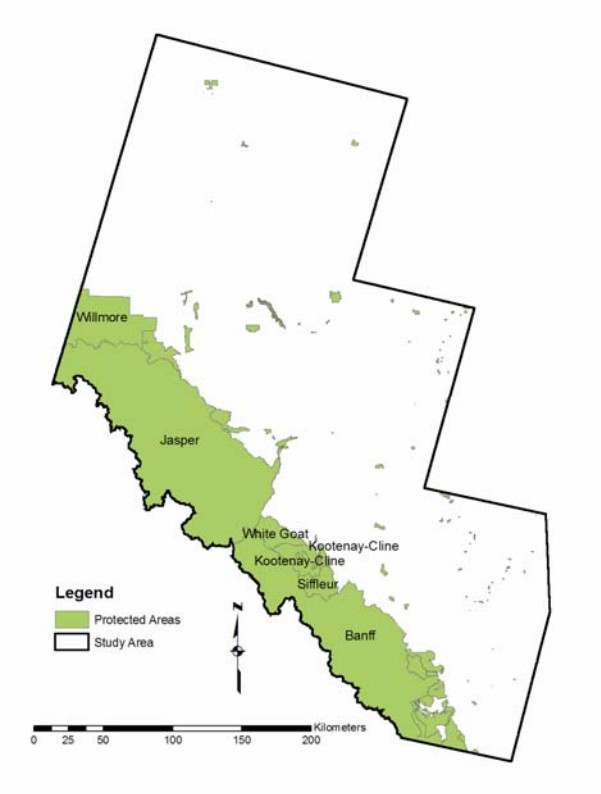

Figure 3-2: Protected regions in the study area. Large reserves (>40,000 Ha) are labelled.

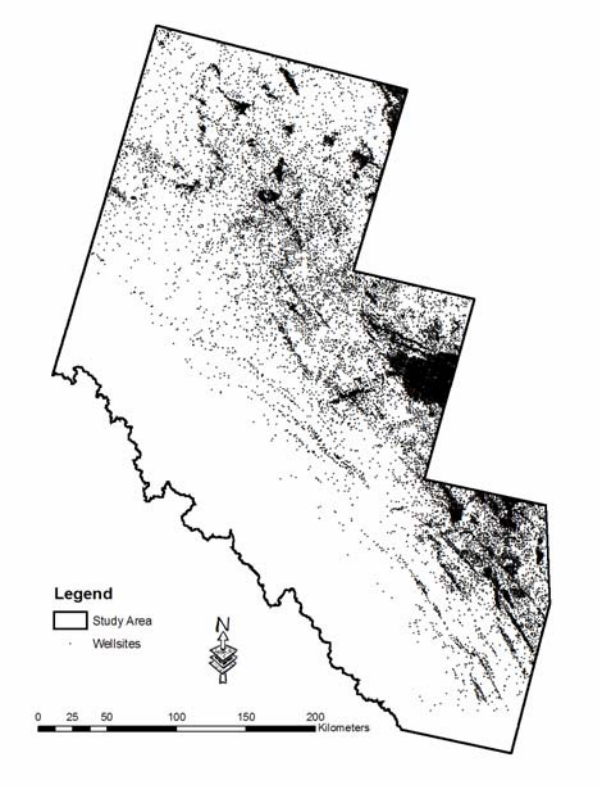

Figure 3-3: Oil and gas well sites in the study area.

The study area contains five of the province's six natural regions: Rocky Mountain, Foothills, Parkland, Boreal Forest, and Grassland (Achuff, 1992). The highest level of the hierarchical system, natural regions reflect broad patterns of vegetation, physiography, soil, and vegetation. Finer-scale landscape patterns are recognized in subregion designations. For example, the Rocky Mountain natural region is divided into three subregions on the basis of vegetation patterns, soil, and climate: alpine, subalpine, and montane. Table 3-1 provides a summary of the common vegetation, geology, and landform patterns observed in the natural regions and subregions occurring in the study area.

3.1.1.1 Rocky Mountain Natural Region

The Rocky Mountain natural region is part of the major geological uplift trending along the western part of the province that forms the continental divide, and makes up 31% of the study area. The region is underlain primarily by upthrust and folded carbonate and quartzitic bedrock, expressed in dramatically rugged topography that ranges from less than 1000 metres in the bottom of the Athabasca valley to the 3747-metre summit of Mount Columbia in the northwest corner of the Columbia Icefields. The region consists of two major mountain ranges: the easterly Front Range, and the westerly Main Range (Gadd, 1986). The major valleys trend south-east/north-west, and represent the origins of some of the largest rivers in Alberta: the Bow, Red Deer, North Saskatchewan, and Athabasca. The climate, soils, vegetation, and wildlife in the Rocky Mountain region

Table 3-1: A summary of the natural regions and subregions found in the study area, including dominant vegetation and characteristic geology and landforms. Information compiled after Achuff, 1992.

Region	Subregion	Vegetation	Geology and Landforms
Rocky Mountain	Alpine	Black alpine sedge, heathers, grouseberry, mountain avens, willow, moss, lichens	Bedrock, snowfields, glaciers, and colluvium in extremely rugged terrain. Rock glaciers and other permafrost features can be found in places
	Subalpine	Lodgepole pine, Englemann Spruce, subalpine fir, whitebark pine, buffaloberry, aster, hairy wild rye, junipers, grouseberry, false azalea, huckleberry, bunchberry, arrowleaf groundsel, willow	Rugged terrain consisting of morainal and colluvial deposits overlying Rocky Mountain strata.
	Montane	Douglas fir, limber pine, white spruce, aspen poplar, pine grass, hairy wild rye, bearberry, juniper, wheatgrass, Idaho fescue	Fluvial and glaciofluvial terraces and deposits in road river valleys.
Foothills	Upper Foothills	White spruce, black spruce, lodgepole pine, buffaloberry, bunchberry, Labrador tea, fireweed, feathermoss, dwarf birch, peat moss	Strongly rolling topography with frequent bedrock outcrops. Ground moraine over bedrock, with some colluvium on steep terrain.
	Lower Foothills	White spruce, black spruce, lodgepole pine, balsam fir, aspen polar, paper birch, balsam poplar, buffaloberry, juniper, Labrador tea, fireweed, dwarf birch, horsetail, willow, peat moss	Rolling topography created by moraine over bedrock. Extensive organic deposits in valleys and wet depressions
Parkland	Foothills Parkland	Aspen poplar, balsam poplar, snowberry, saskatoon, white meadowsweet, glacier lily, Bebb's willow	Hummocky ground moraine, outwash deposits, and extensive river terraces
	Central Parkland	Aspen polar, balsam poplar, snowberry, saskatoon, bunchberry, red osier dogwood, willow, alder, rough fescue	Hummocky ground moraine and fine-textured glaciolacustrine deposits
Boreal Forest	Dry Mixedwood	Aspen poplar, balsam poplar, white spruce, balsam fir, jack pine, black spruce, tamarack, cranberry, red-osier dogwood, feathermoss, bearberry, lichen, Labrador tea, peatmoss, sedge	Low-relief terrain composed of ground moraine and sandy outwash plain
	Central Mixedwood	Aspen poplar, balsam poplar, paper birch, white spruce, balsam fir, jack pine, black spruce, cranberry, red-osier dogwood, dewberry, feathermoss, lichen, bearberry, Labrador tea, peatmoss, sedge	Low relief on a level to undulating surface. Ground moraine, sandy outwash plain, and glaciolacustrine deposits
Grassland	Foothills Fescue	Rough fescue, Idaho fescue, oatgrass, sticky geranium and prairie crocus, balsam-root, narrowleaf cottonwood	Flat to gently rolling terrain made up of moraine and glaciolacustrine deposits

vary substantially with elevation, and combine to produce three distinct natural subregions: Montane, Subalpine, and Alpine (Figure 3-4).

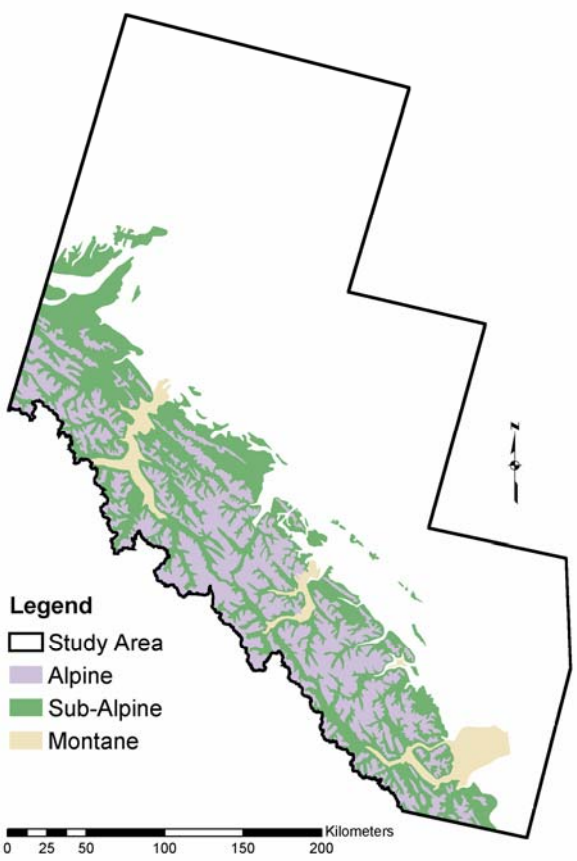

Figure 3-4: Rocky Mountain natural subregions.

Occupying the lower portions of the study area's four major river valleys, the Montane subregion is characterized by the influence of warm, dry chinook events that ameliorate the winter temperatures to create intermittent snow-free zones. Vegetation is typically open forests and grasslands, with Douglas fir (*Pseudotsuga menziesii*), white spruce (*Picea glauca*), trembling aspen (*Populus tremuloides*), and limber pine (*Pinus*

flexilus) occurring in forested areas, and fescues (*Fescuta* spp.), oatgrasses (*Danthonia* spp.), and bluebunch wheatgrass (*Agropyron spicatum*) dominating the grasslands (Achuff, 1992). The abundance of herbs and intermittent winter snow makes the Montane subregion wildlife hotspots for many Rocky Mountain species, including elk, bighorn sheep, wolf, and mule deer.

The Subalpine natural subregion occupies the middle elevations between the Alpine and Montane subregion in the major river valleys and the Upper Foothills and Alpine subregions elsewhere. Lower Subalpine elevations are covered with glacial till and moraine deposits, while the higher elevations are dominated by colluvium and residual bedrock material. Brunisol and Luvisol soils are widespread, but diverse physical conditions produce also produce a variety of regosols, podsols, and cryosols (Achuff, 1992). Closed stands of fire-successional lodgepole pine (*Pinus contorta*) at the lower elevations give way to Englemann spruce (*Picea englemannii*) and subalpine fir (*Abies lasiocarpa*) on the upper slopes. Important understorey species include buffaloberry (*Shepherdia canadensis*), hairy wild rye (*Elymus innovatus*), false azalia *(Menziesia ferruginae*), huckleberry (*Vaccinium membranaceum*), and grouseberry (*Vaccinium scoparium*). Mature mesic forests have a thick carpet of mosses and lichens. Open forests and shrubby areas mark the transition between the subalpine and alpine subregions, with Englemann spruce, subalpine fir, whitebark pine (*Pinus albicaulus*), subalpine larch (*Larix lyallii*), rock willow (*Salix vestita*), heathers (*Phyllodoce* spp.), and arrowleaf groundsel (*Senecio triangularis*) among the common vegetation species.

The Alpine natural subregion represents the highest areas of the Rocky Mountains above treeline - typically about 2100 metres in the study area. Land cover here includes

alpine meadows, non-vegetated rock, snow, and glaciers. Soils are thin or non-existent on deposits of bedrock and colluvium. Vegetation patterns are typically complex, controlled by microclimatic variations of slope, aspect, exposure, and moisture. Communities at the highest elevation are limited to lichens, while lower-elevation meadows may contain alpine sedge (*Carex nigricans*), dwarf shrub heath (*Phyllodoce* and *Cassiope* spp.), grouseberry (*Vaccinium scoparium*), white mountain avens (*Dryas octopetala*) and willow (*Salix* spp.) (Achuff, 1992). Alpine areas form critical seasonal habitat for many Rocky Mountain species, including grizzly bear, bighorn sheep, mountain goat, ptarmigan, and woodland caribou.

3.1.1.2 Foothills Natural Region

The Foothills natural region covers about 50% of the total study area – the largest proportion of the four natural regions occurring therein. Transitional between the Rocky Mountain/Boreal Forest natural regions in the north, and the Rocky Mountain/Parkland regions in the south, the Foothills zone is characterized by rolling to strongly rolling topography underlain by sandstone and shale. The boundaries of the Foothills zone are determined largely by structural geology, with folded bedrock materials contrasting with the thrusts and faults of the Rocky Mountains or the flat-lying terrain of outlying regions (Strong, 1992). However, Achuff (1992) also recognizes distinctive patterns with respect to vegetation, wildlife, and physiography.

The Foothills natural region is divided into two subregions: Upper Foothills and Lower Foothills (Figure 3-5). The Upper Foothills is characterized by strongly rolling topography on the eastern edge of the Rocky Mountain region, with an additional disjunct outlier occurring in the Swan Hills region in the north-eastern part of the study area.

Morainal deposits are widespread throughout the region, with colluvium deposits occurring alongside bedrock outcrops on steeper terrain. Vegetation is strongly dominated by coniferous forests of lodgepole pine, white spruce, black spruce (*Picea mariana*), and (less frequently) subalpine fir. Lodgepole pine forests are widespread on the upland slopes, with understories typically including false azalea, buffaloberry, bunchberry, and fireweed. Spruce communities on mesic sites commonly have a thick carpet of feathermosses (*Hylocomium splendens, Pleurozium shreberi, and Ptilium crista-castrensis*). The limited wet sites host black spruce forests with Labrador tea, dwarf birch (*Betula* spp.) and peat moss (*Sphagnum* spp.). Wildlife species in the Upper Foothills typically includes pine siskin, varied thrush, black bear, grizzly bear, and elk (Achuff, 1992).

The Lower Foothills subregion occurs over rolling topography with morainal deposits laid on top of folded bedrock. The area contains extensive wetlands, with organic deposits and wet depressions common across low-lying terrain. The vegetation in the Lower Foothills is more varied than the coniferous monotone observed in the adjacent Upper Foothills subregion. Mixed forests of white spruce, lodgepole pine, balsam fir, aspen, and paper birch are common throughout the area. Dry upland sites are commonly covered with fire-successional pine forests, where understorey species typically include bearberry (*Actostaphylos uva ursi*), buffaloberry (*Shepherdia canadensis*), and juniper. Mesic sites commonly host mixed stands of white spruce and aspen, with a well-developed understorey of bunchberry, Labrador tea, fireweed, and bog cranberry (*Vaccinium vitis-idaea*). Black spruce forests occupy the moist organic soils in

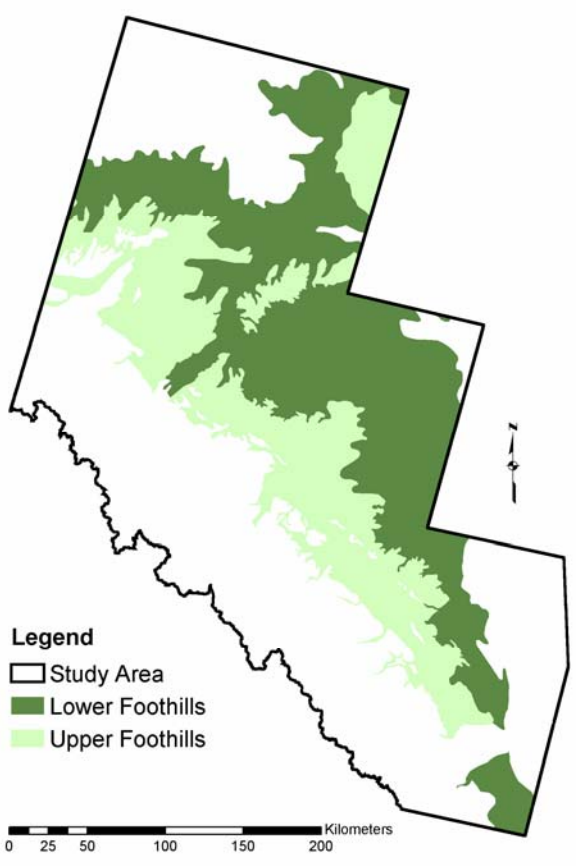

Figure 3-5: Foothills natural subregions.

the central and northern parts of the study area, with Labrador tea, dwarf birch, peat moss, and horsetail (*Equisetum* spp.) occurring commonly in the understorey. Wetland fens are widespread in wet depressions, composed of peat moss, sedge (*Carex* spp.), Labrador tea, dwarf birch, willow, and scattered black spruce and tamarack (*Larix larciana*). The vegetation diversity in the lower foothills contributes to an equally diverse range of wildlife; the area draws wide-ranging species from the adjacent Rocky Mountain and Boreal regions, including moose (*Alces alces*), elk, spruce grouse, and purple finch (Achuff, 1992).

3.1.1.3 Boreal Forest Natural Region

The Boreal Forest natural region occurs in the north and far eastern portions of the study area, and makes up about 15% of the total area. The largest natural region in the province, the Boreal Forest consists of broad lowland plains with deeply buried bedrock, extensive wetlands, and expansive forested areas. Tremendously diverse, the Boreal is composed of six natural subregions, two of which – Dry Mixedwood and Central Mixedwood – are represented in this study (Figure 3-6).

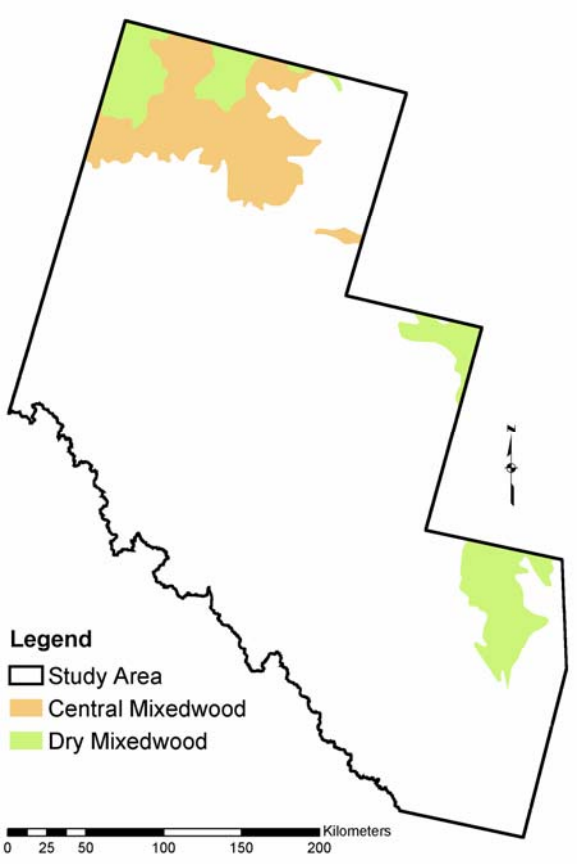

Figure 3-6: Boreal Forest natural subregions.

The Central Mixedwood natural subregion can be found in the far northern part of the study area. The terrain here is relatively flat, with glacial till being the dominant surficial material. Broadleaf species such as aspen, balsam poplar, and paper birch are the widespread, with forests tending successionally towards white spruce and balsam fir in the absence of fire (Achuff, 1992). The understories of upland broadleaf communities are rich and diverse, with low-brush cranberry (*Vibernum edule*), red-osier dogwood, sasparilla (*Rubus pubescens*), and twinflower (*Linnaea borealis*) among the common understorey species. Coniferous-dominated spruce/fir forests are less common, and have a less diverse understorey dominated by mosses and lichens. Black spruce-and peat-dominated fens occur on poorly drained lowland sites, with Labrador tea, dwarf birch, and sedges locally abundant. Wildlife of the Central Mixedwood subregion is the most diverse of the Boreal Forest, including black bear, wolf, lynx, moose, and ermine.

The Dry Mixedwood subregion occurs in four discontinuous patches along the eastern and northern edges of the study area. Vegetation is transitional between Central Parkland and Central Mixedwood subregions, with aspen and balsam poplar occurring in both pure and mixed stands. Forests evolve successionally towards white spruce, but the presence of fire generally prevents this from occurring and upland forests here tend to be largely broadleaf. As with aspen/balsam poplar communities elsewhere in the study area, the understories are typically rich and diverse, with low-brush cranberry, rose (*Rosa* spp.), red-osier dogwood, and twinflower (*Linnaea borealis*) among the common species. Coniferous stands – where they occur – host a more limited understorey, dominated primarily by moss species. Wetlands are common throughout the Dry Mixedwood, but are not as prevalent as in the Central Mixedwood and other Boreal

subregions (Achuff, 1992). Vegetation here is dominated by black spruce, Labrador tea, tamarack, peat mosses, and dwarf birches. Characteristic animals include beaver, moose, wolf, and black bear.

3.1.1.4 Parkland Natural Region

Occupying a transitional zone between Grassland and Foothills, the Parklands natural region makes up about 4% of the study area, split into Central Parklands and Foothills Parklands subregions located along the south-eastern boundary (Figure 3-7).

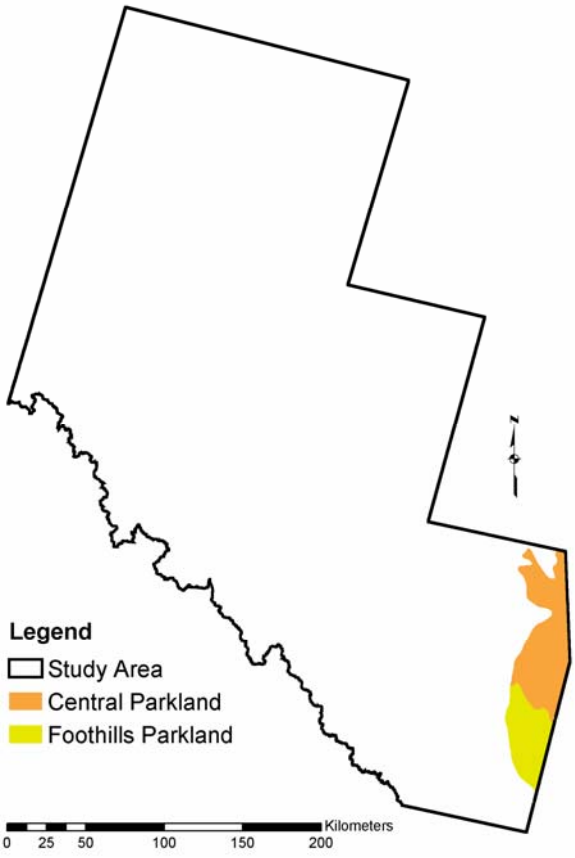

Figure 3-7: Parkland natural subregions.

The Central Parkland subregion is characterized by hummocky moraines, glaciolacustrine deposits, and glacial outwash plains. Black and dark-brown Chernozem soils have historically supported aspen parkland vegetation – dense aspen stands broken by grassy openings – but agricultural developments have displaced virtually all of the native vegetation cover in this subregion (Achuff, 1992). Balsam poplar (*Populus balsamifera*) forests with dense, species-rich understories occur locally on floodplains, and small woodlots of aspen communities with snowberry, saskatoon (*Amelancier alnifolia*), and chokecherry (*Prunus virginiana*) understories remain locally scattered amongst the alfalfa fields. Small wetlands and pothole lakes support a wide variety of birds and amphibians, along side white-tailed deer, porcupine, pocket gophers, and snowshoe hare.

Further south in the study area, the Central Parklands yield to the Foothills Parkland natural subregion. Physiographically similar to the Central Parklands further north, the Foothills Parklands are characterized by distinctive vegetation species, including lupines (*Lupinus* spp.), oatgrass (*Danthonia* spp.), and Idaho fescue (*Fescuta idahoensis*) (Achuff, 1992). However, most of the native species in this subregion have also been cleared for agriculture.

3.1.1.5 Grassland Natural Region

A very small portion of the study area (less than 1%) occupying the Bow valley in the extreme south-eastern portion of the region is categorized as Grassland. Grasslands in Alberta occupy generally flat to gently rolling terrain, with bedrock covered by thick deposits of glacial till (Achuff, 1992). A relatively warm, dry climate coupled with rich

Chernozemic soils results in a natural vegetation cover dominated by grasses and forbs. In this study area, these lands have been converted to agriculture.

3.2 Partner Studies

In order to maximize the effectiveness of this research over its very large study area, a number of partnerships were established with projects operating within the region. Brief descriptions of these studies and their role within the project are provided below.

3.2.1 The Foothills Model Forest Grizzly Bear Research Program

The project to which this work is most closely tied is the Foothills Model Forest Grizzly Bear Research Program (FMFGBRP). The FMFGBRP was created in 1999 to provide knowledge and planning tools to land and resource managers in order to ensure the long-term conservation of grizzly bears in Alberta. It represents a unique partnership amongst more than 50 collaborators and sponsors from various levels of industry, academics, and government. Key to the FMFGBRP's efforts is sound scientific field research, practical results, and a large-area or *landscape level* approach toward grizzly bear conservation. With a focus aimed primarily at grizzly bear management, the program is designed to assess bear populations and evaluate bear responses to both human activities and habitat conditions. Major research activities within the project include:

- Remote sensing tools and procedures allowing the creation of grizzly bear habitat maps over large areas;
- Resource selection function (RSF) models that build on remote sensing maps and other environmental information sources to identify important grizzly bear habitats on the landscape;

- Animal movement models, based on graph theory analysis, that are designed to identify grizzly bear movement corridors across the landscape;
- Techniques to monitor and assess grizzly bear health;
- DNA grizzly bear census techniques to enhance our ability to monitor grizzly bear population status over time; and
- New procedures and techniques for the capture and handling of grizzly bears for research and management purposes.

The FMFGBRP study area has occupied a series of expanding regions since its inception in 1999, as the scope of the program has evolved to encompass larger and larger portions of the province. Starting across an original zone covering approximately 10,000 km^2 south of Hinton in 1999, the study area grew to about 40,000 km^2 in 2003 (Figure 3-8). While the project's area of interest has continued to expand both northwards and southwards since 2003, it is this 40,000-km^2 phase that oversaw the bulk of cooperative research reported here.

The FMFGBRP provides the overriding framework for the activities reported in this thesis. The project was the primary source of funding for this work, and supported nearly every aspect of field research and data collection. In return, the accomplishments reported here represent the primary vehicle for remote sensing research within the FMFGBRP from 2002 through 2004.

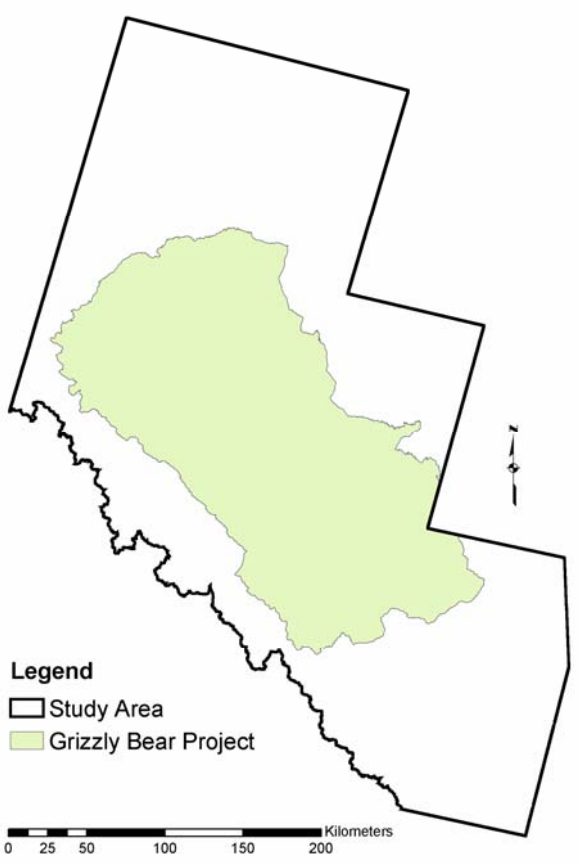

Figure 3-8: The FMFGBRP's core 2003 study area, upon which the bulk of the work in this thesis is based.

3.2.2 The Alberta Ground Cover Characterization Project

The Alberta Ground Cover Characterization (AGCC) project is an on-going initiative between the University of Alberta and its partners in the provincial and federal government to map the land cover across the forested portions of Alberta. Built upon unsupervised classification strategies using medium-spatial-resolution Landsat data, the AGCC has adopted a phased approach to mapping the province, moving more or less systematically from the northeast towards the southwest. In 2003, the AGCC became a partner of this research in an effort to (i) join forces for the purpose of field work for map production and error characterization, and (ii) collaborate on the evaluation of different

large-area satellite mapping strategies for wildlife habitat assessment. These initiatives resulted in the execution of a joint field program in 2003, which contributed towards the development of the remote sensing map products presented in Chapters 4 and 5, and a map comparison study, the results of which can be found in Chapter 6.

3.2.3 The South Jasper Woodland Caribou Project

The South Jasper Woodland Caribou Project (SJWCP) is an initiative of Parks Canada designed to examine the status of the south Jasper woodland caribou herd, a geographically isolated population that has declined by an estimated 39-47% between 1988 and 2003 (Parks Canada unpublished data). The SJWCP began in 2002, and its findings have contributed substantially to the recent Alberta Woodland Caribou Recovery Plan (Herivieux *et al.*, 2005). Based largely around a series of resource selection studies using telemetry data from collared caribou, the project also included substantial land cover and vegetation surveys within Jasper. Through collaboration with SJWCP managers and field personnel, field data collection protocols of Parks field crews were augmented to enhance compatibility with ground measurements acquired by crews contributing to this research. The resulting field data – including valuable points from challenging, high-altitude locations within Jasper National Park – contributed to the development of the remote sensing map products presented in Chapters 4 and 5.

Chapter 4: Remote Sensing Map Production - Methods

4.1 Data Acquisition

In its most common form, information extraction using modern remote sensing involves establishing statistical relationships between ground truth information acquired in the field and digital data acquired from a distance using various airborne or spaceborne instruments. Once established, these relationships are applied spatially in order to create extended information products over larger areas. The following subsections provide an overview of the primary data sources available here to carry out this process, and their respective roles in this research.

4.1.1 Ground Biophysical Data

An extensive database of ground biophysical data was required to create and validate the map products that make up the land/vegetation information base used in this research. Observations and measurements of land cover, crown closure, species composition, and LAI were required to train and test a variety of statistical models and classifications.

Under normal conditions, ground truth data are compiled from a single source – commonly a field campaign carried out by researchers from within the project. However, the size and diversity of this study area necessitated the coordinated use of multiple information sources. The biophysical database used in this study combines field data from the Foothills Model Forest Grizzly Bear project, the South Jasper Woodland Caribou Study, the Alberta Ground Cover Categorization (AGCC) project, and some

manual interpretation of satellite imagery and aerial photographs. Each of these major data sources is described briefly below.

4.1.1.1 Foothills Model Forest Grizzly Bear Project Field Data

A total of four field campaigns have been conducted in support of the remote sensing activities in the Foothills Model Forest Grizzly Bear Research Program from 2000 to 2003, and this research used field data from each campaign. The first two campaigns – carried out in the summers of 2000 and 2001 – were designed primarily to support the initial land cover classification work performed over that project's Phase 1 and Phase 2 study areas, described in the literature as the "integrated decision tree" (IDT) approach to mapping by S. Franklin *et al.* (2001). The field work took place across a stratified random sample generated on the basis of some initial classification work performed by the consulting group GeoAnalytic (GeoAnalytic, 1999). About two-thirds of the 592 sites visited in these early years were ground visits, while inaccessible areas in high-altitude and/or wetland regions received air call visits from field personnel in a helicopter. The ground protocol involved measurements of vegetation composition (species, percent cover) and structure (height, crown closure, and volume) using standard vegetation sampling and timber cruise methods across a 30-metre plot analogous in size to a Landsat Thematic Mapper (TM) pixel. In addition, a field call was used to classify each plot into one of the 16 vegetation/land cover classes that made up the classification legend in use at the time (Table 4-1). The air call protocol was adapted to provide analogous measures of vegetation composition and structure, but relied on ocular estimates and interpretations of photographs recorded from a low-hovering helicopter.

Table 4-1: Vegetated portions of the IDT classification legend from Phases 1 and 2 of the Foothills Model Forest Grizzly Bear Research Program.

Class	Description
Alpine/Subalpine	Mosses, willows, and grasses above 1800m
Recent Burn	Areas burned 2 years prior to image acquisition
Closed Conifer	Conifer vegetation with crown closure between 51 and 100%
Closed Deciduous	Deciduous vegetation with crown closure between 51 and 100%
Cut 0-2	Areas harvested 2 years prior to image acquisition
Cut 3-12	Regenerating vegetation in a cutblock that occurred 3-12 years prior to image acquisition
Cut >12	Regenerating vegetation in a cutblock that occurred greater than 12 years prior to image acquisition
Herbaceous <1800m	Grassy areas below 1800m
Herbaceous Reclamation	Areas planted with non native vegetation associated with mining activities
Mixed Conifer	Forested stands containing >50% conifer stems
Mixed Deciduous	Forested stands containing >50% deciduous stems
Open Conifer	Conifer vegetation with crown closure between 0 and 50%
Open Deciduous	Deciduous vegetation with crown closure between 0 and 50%
Shrub <1800m	Shrub areas below 1800m
Wet Open	Swampy or marshy areas with grassy vegetation
Wet Treed	Swampy or marshy areas with trees or shrubs

In contrast to the first two Grizzly Bear Project field campaigns, which were designed primarily to acquire training and testing data for a categorical land cover classification, the third campaign – conducted in the summer of 2002 – focussed on the characterization of more detailed vegetation attributes such as species composition, crown closure, and leaf area index (LAI). The underlying motivation was a need to provide more depth and

richness to the remote sensing map products than what was provided by the original classification, and laid the foundation for the attribute-based approach to mapping upon which this research is based.

A particular goal of the 2002 field campaign was to assess the seasonal variability of various vegetation attributes by conducting field visits at two different times of the summer growing season. A stratified random sample of 74 sample plots was established across the 15 vegetated IDT classes, limited to areas within 350 metres of a road, seismic cut line, or other access features. The tasseled cap derivative *greenness* (Crist and Cicone, 1984) was used to stratify sample locations within each land cover class in an attempt to better capture the full range of variability observed on the landscape. Instead of a long, drawn-out field season stretched out across an entire summer, the sites were visited during two *focussed* campaigns in order to observe the change in time-sensitive variables such as canopy closure and LAI. The first campaign took place in the early summer between June 20 and July 7, 2002. During this time period, referred to by biologists in the Foothills Model Forest Bear Research Program as the *early hyperphagia*[1] season, the herbaceous understorey plants observed across much of the study area are not fully developed. The second campaign – held during the *late hyperphagia* period from August 15 to September 2, 2002 – took place under conditions when plant canopies and undergrowth were at their maximum.

The field protocol for both 2002 campaigns was the same. A 30- by 30- metre ground plot oriented along a north-bearing transect (Figure 4-1) was established at each sampling location. If trees were present, a prism sweep was conducted from the centre of

[1] The term *hyperphagia* is defined as excessive ingestion of food, and refers to the critical time of year when grizzly bears eat heavily in order to gain the body mass necessary to sustain them through winter.

each plot using a Basal Area Factor 2 or 4 prism. Each tree was labelled, identified for species, and measured for diameter at breast height (DBH). Three representative trees of each species in the sweep were selected for more detailed measurements, including height, height to live crown, and coring with an increment bore. Five 5-metre radius subplots located in the centre and four corners of the master plot provided the basis for a series of cover measurements made at each strata of vegetation: tree, shrub, herb, and ground. At each level, an ocular estimate was made of both the overall cover percentage and the percent exposed to the sky. The same five sub-plots were used as measuring stations for measuring crown closure with a spherical densiometer. Finally, an AccuPAR ceptometer was used to measure photosynthetically active radiation (PAR) in the 400 to 700 nanometer wavelengths at three different heights: 1.3 metres, 0.3 metres, and ground level. The ceptometer measurements were only taken when light conditions were stable – either fully diffuse or fully direct – and only within three hours of solar noon if the light conditions were direct. In order to facilitate later computations of FPAR – the fraction of absorbed PAR – accompanying above-canopy *clearsky* readings were acquired before and after each series of sub-canopy measures in the centre of clearings a minimum of 2x the size of the surrounding vegetation canopy. Additional information regarding global positioning system (GPS) location and error, qualitative plot description, light conditions, disturbance, and photography were recorded on the field sheet found in Appendix A.

The field campaign in 2003 coincided with expansion of the Foothills Model Forest Grizzly Bear Research Program to its Phase 3 study area – the same study area adopted for this research. Field efforts that summer focussed on establishing plot

locations in the new regions north and south of the core. A stratified random sampling procedure was used to select 219 sample locations distributed in an area-weighted

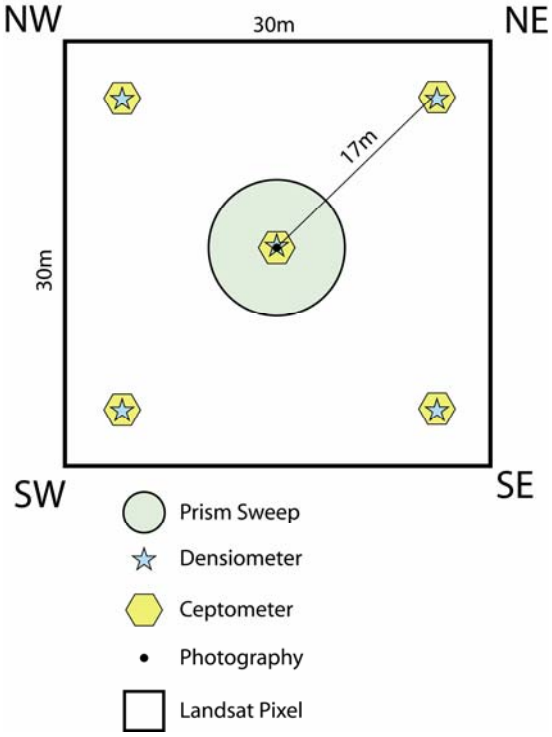

Figure 4-1: Plot layout used to characterize vegetation and ground cover across a 30-metre Landsat pixel.

fashion amongst the six natural subregions occurring in the expanded area. To arrive at the final sample locations, 1000 random points per natural subregion were placed in areas that were within 350 metres of a road. From these, a preliminary land-cover map produced from points in the core area and additional information from the Alberta Vegetation Inventory was used to choose locations stratified across each predicted cover type. The field work was carried out in July and August, 2003, using essentially the same field protocol described previously.

4.1.1.2 EOSD/AGCC Field Data

In order to maximize the amount of ground data, an effort was made to collaborate and share resources amongst other field projects operating in the study area. The Earth Observation for Sustainable Development of Forests (EOSD) is a joint initiative of the Canadian Forest Service and the Canadian Space Agency that aims to map the land cover of all the forested lands in Canada at 30-metre resolution by 2006 (Wulder *et al.*, 2003). The work is designed to permit the ongoing monitoring of Canadian forests for the purpose of carbon accounting (Apps *et al.*, 1999), monitoring of sustainable development (Wood *et al.*, 2002), and contributing to the National Forest Inventory (Gillis, 2001). In Alberta, the mapping is being carried out in concert with a provincial mapping initiative called the Alberta Ground Cover Characterization (AGCC) which aims to produce a 30-metre land-cover map of the entire forested region of the province.

By coordinating the field activities in this research with those in the AGCC project, an additional 86 plots were acquired in the northern portion of the study area. The field protocol for these plots differed somewhat to that adopted by field crews in the Foothills Model Forest Grizzly Bear Research Program, but still contained prism sweep, densiometer, field photographs, and land cover calls useful for product development in this research.

4.1.1.3 South Jasper Woodland Caribou Project Field Data

Field personnel in the South Jasper Caribou Project conducted habitat sampling for 300 field plots in Jasper National Park in the summer of 2003. The plots locations were selected by initially identifying points stratified by caribou telemetry (use, non-use), dominant forest species, (pine, spruce, alpine), forest age (greater than or less than 150

years old), and aspect (northwest or southeast). The physical (non-telemetry) stratification features were based on information from the Parks ecological land classification (Van Tighem and Holroyd, 1983), while the caribou use points were acquired from 11 caribou collared in 2002. Within each stratification, random locations were generated within five and ten kilometres from roads for the subalpine and alpine ecoregions, respectively. Plots were 20 by 20 metres in size. Within these, measurements were made concerning percent tree canopy cover, ground cover, and shrub cover. Tree characteristics including species, DBH, age, and height were measured for all trees falling within two 10 by 10 metre fixed plots located in opposite corners of the plot.

4.1.1.4 Merging Data Sets

The task of merging field data from multiple sources proved to be a more formidable undertaking than was initially envisioned. Some of the data issues – differences in sampling strategies between field programs, for example – were judged to be less important than gaining a more complete coverage of field points. Others, however, were more problematic. For example, while each field dataset contained estimates of crown closure, distinct differences could be detected related to origin of the observations. Some of these differences were expected – ocular estimates of crown closure and species composition made from a helicopter are likely to be inconsistent from instrument readings made on the ground, for example – but others were more subtle. For instance, an examination of the summary statistics of crown closure measurements taken from different field campaigns (Figure 4-2) reveals substantial differences. The spherical densiometer instrument traditionally used to measure crown closure requires counting the

number of squares on a concave mirror covered by the reflected canopy. It is a procedure that takes some skill to master, and one that is prone to errors in judgement.

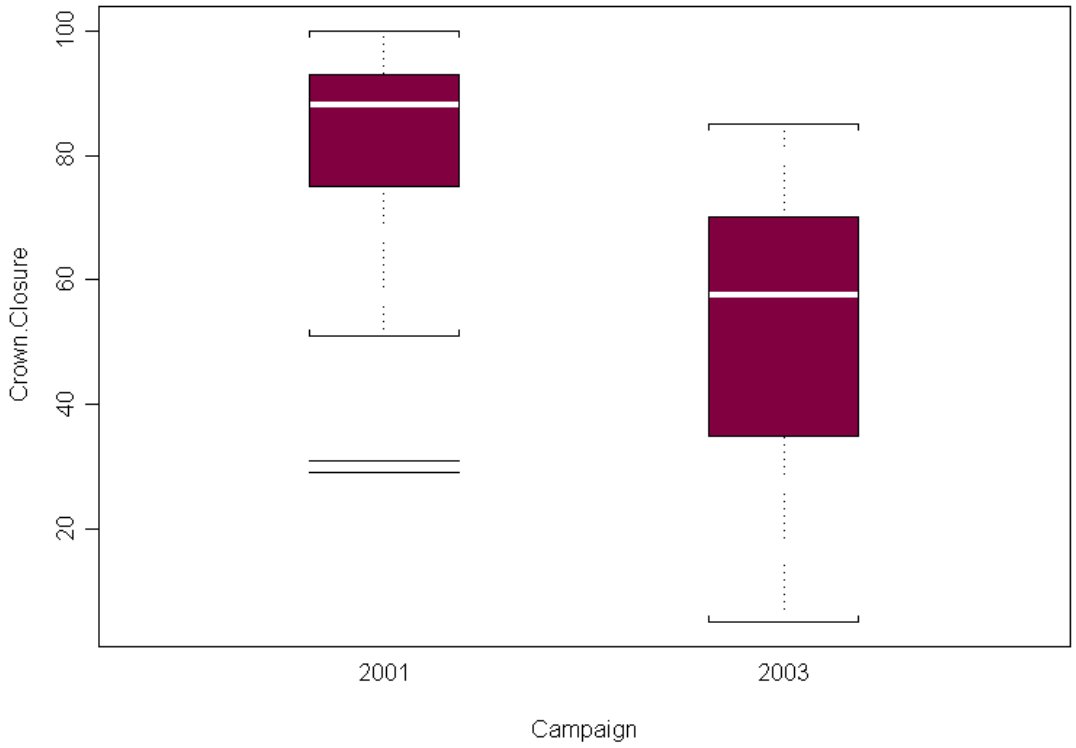

Figure 4-2: Box plots displaying marked differences in crown closure measurements taken in the Foothills natural region during the 2001 and 2003 field campaigns.

In order to ensure quality and consistency amongst field data, each data source was carefully reviewed. Individual field protocols were examined for procedural inconsistencies, plots locations were examined visually in a GIS for location errors and edge effects, and summary statistics were generated. In some cases, procedural differences in data processing were overcome by re-calculating summary variables. For example, some campaigns based species composition measures on basal area proportion

rather than stem counts. By re-processing the original prism sweep data, it was possible to adjust many of these inconsistencies. Translation procedures were created to re-code land cover calls to a common framework to ensure global consistency amongst those observations. However, some differences were too large to overcome. In all cases, decisions were made to err on the side of caution.

Table 4-2 summarizes the source and final sample count of ground biophysical data used in the various mapping phases of this study. In total, 1125 field samples were used for mapping land cover, 321 for crown closure, 241 for species composition, and 76 for leaf area index.

Table 4-2: Sources of ground biophysical data used in the study.

Data Source	Land Cover	Crown Closure	Species Composition	LAI
FMF Grizzly Bear Project 1999-2001	☒	☒	☒	☐
FMF Grizzly Bear Project 2002	☒	☒	☒	☒
FMF Grizzly Bear Project 2003	☒	☒	☒	☐
AGCC Project 2003	☒	☐	☐	☐
South Jasper Caribou Project 2003	☒	☐	☐	☐
Image/Photo Interpretation	☒	☐	☐	☐
SAMPLE SIZE:	1125	321	241	76

4.1.2 Satellite Imagery and Digital Data

Remote sensing imagery from two different satellite sensor systems were acquired in support of this research: Landsat Thematic Mapper (TM) and the Moderate Resolution Imaging Spectrometer (MODIS). Multispectral TM imagery from Landsat 5 were used to map land cover, crown closure, and species composition, while MODIS data were used to map LAI. An additional suite of digital data products, including a digital elevation model (DEM), data from the Alberta Vegetation Inventory, and other miscellaneous GIS layers, helped with various processing tasks and formed ancillary data for subsequent mapping and modelling efforts. A description of these digital data sets and the preprocessing routines used to prepare them follows below.

4.1.2.1 Landsat Imagery

Despite the recent failure of the Enhanced Thematic Mapper Plus (ETM+) instrument on board Landsat 7 and the age of the TM-5 sensor, these data were chosen as the primary data source for mapping land cover, crown closure, and species composition because of their long-term data continuity with other Landsat sensors, well-known radiometric qualities, and compatibility with common image processing procedures. The imagery offers a balanced blend of spatial detail (30-meter pixel size) and expansive ground coverage (more than 3 million hectares per scene) over seven multispectral bands. While the sensor is currently operating well beyond its intended life span, recently revised radiometric calibration procedures (Chander and Markham, 2003) have significantly improved the quality of recent imagery and the sensor continues to perform well.

The study area is covered by five overlapping World Reference System (WRS) scenes, the footprints of which are shown in Figure 4-3. A total of seven images were

acquired for the study from the summers of 2002 and 2003 (Table 4-3). Of these, the 2003 imagery were used to map land cover, crown closure, and species composition, while the 2002 imagery – acquired coincident with the focused field campaigns conducted that year – contributed to the mapping of LAI.

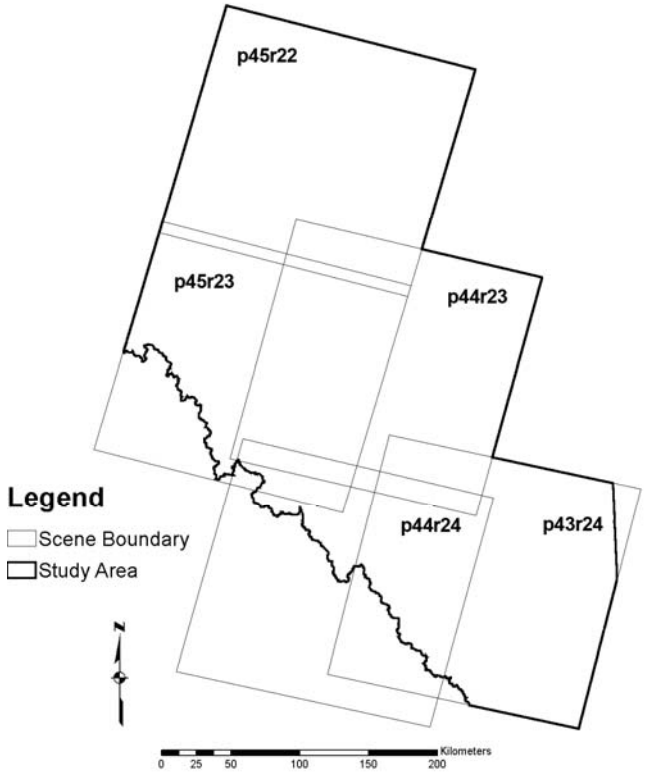

Figure 4-3: Landsat WRS scenes covering the study area.

Table 4-3: Landsat imagery used in the study.

WRS Scene	Acquisition Date(s)
Path 43 Row 24	June 17, 2003*
Path 44 Row 23	June 13, 2002†; July 10, 2003*
Path 44 Row 24	July 10, 2003*
Path 45 Row 22	September 3, 2003*

Path 45 Row 23	August 23, 2002[†]; September 3, 2003*

* Used for land cover, crown closure, species composition
[†] Used for LAI

A series of preprocessing routines were applied to all the Landsat images in order to establish the seamless and consistent geometric and radiometric properties necessary for subsequent mapping work. Radiometric processing in the form of atmospheric and/or topographic correction is a common methodological step in the information extraction process (Jensen, 1996). The electromagnetic radiation signals measured by satellite sensors in the solar spectrum are modified by gases and aerosols in the Earth's atmosphere in complex and often contradictory ways. In cases where the application calls for a common radiometric scale – such as in this research when classification signatures and models need to be extended beyond the border of a single image – the effects of atmospheric attenuation must be accounted for (Song *et al.*, 1999).

Unfortunately, there is no standard, reliable method for performing atmospheric correction. Much of the literature on the subject is concerned with absolute calibration of individual image scenes, whereby sensor characteristics, atmospheric conditions, and illumination angles are modelled explicitly (e.g. Vermonte and Kaufman, 1995). However, the detailed atmospheric observations required to drive these models are rarely available, leading most users to rely on standard atmosphere parameterization from commercial image processing packages. Unfortunately this is often an unsatisfactory approach, commonly producing poor or unexpected results (Cohen *et al*., 2001).

A class of alternative solutions - known collectively as relative calibration - are procedures whereby individual scenes are normalized with respect to each other, using

little or no ancillary data (Hall *et al*., 1991; Narayana *et al*., 1995). The techniques vary widely, and include the use of anniversary dates (Lambin, 1996), histogram matching (Homer *et al*., 1997), dark object subtraction (Chavez, 1988), and linear transformation (McGovern, *et al*., 2002). To date, no single "best" calibration procedure has emerged, due likely to the wide range of ground and atmospheric conditions encountered in practice.

In order to identify a reliable routine, three brands of relative and absolute radiometric correction algorithms were tested on eight Landsat TM and ETM+ images from within the study area. Though not the same scenes used in subsequent mapping work, they did represent a good sample of imagery from a variety of dates and atmospheric conditions over the same region, and were believed to comprise a reliable test on which to base subsequent radiometric processing decisions. Two candidate radiometric correction strategies were performed: (i) an absolute atmospheric correction using the ATCORR radiative transfer model available in PCI Geomatica, and (ii) a relative calibration procedure based on atmospheric normalization through linear transformation. In order to maintain a standard radiometric scale for comparison, the ground reflectance estimates were scaled back to 8-bit digital numbers (DNs) to match the radiometric resolution of the raw and relatively calibrated products.

The quality of the two candidate radiometric preprocessing procedures were judged using pseudo-invariant features (PIFs): locations on the landscape whose surface reflectance properties should not change over time, such as deep clear lakes, large asphalt surfaces, and large flat gravel pads. DNs of a selection of PIFs identified in the overlap portions of adjacent scenes were extracted for each set or transformed imagery, and the

root mean square error (RMSE) was calculated. The RMSE equation takes the following form:

$$RMSE = \sqrt{\frac{1}{n}\sum_{i=1}^{n}(DN_{image1} - DN_{image2})^2}$$

Equation 4-1

where

n	=	the number of pseudo invariant features,
DN_{image1}	=	the DN of a PIF on the first image, and
DN_{image2}	=	the DN of the corresponding PIF on the adjacent image.

A summary of the RMSE values generated for each of the two candidate radiometric processing techniques – as well as those for the original uncorrected imagery – is shown in Figure 4-4. The mean RMS error of the raw imagery (51 DNs) was reduced to 37 through ATCOR's absolute radiometric correction routine. These modest results clearly undermine the perception that absolute correction – at least the parameterized brand performed in the absence of detailed atmospheric observations – as an effective tool for radiometric normalization. In fact, in one of the observed cases (August 17, 2000), conversion to ground reflectance actually increased radiometric variability over that observed in the raw imagery.

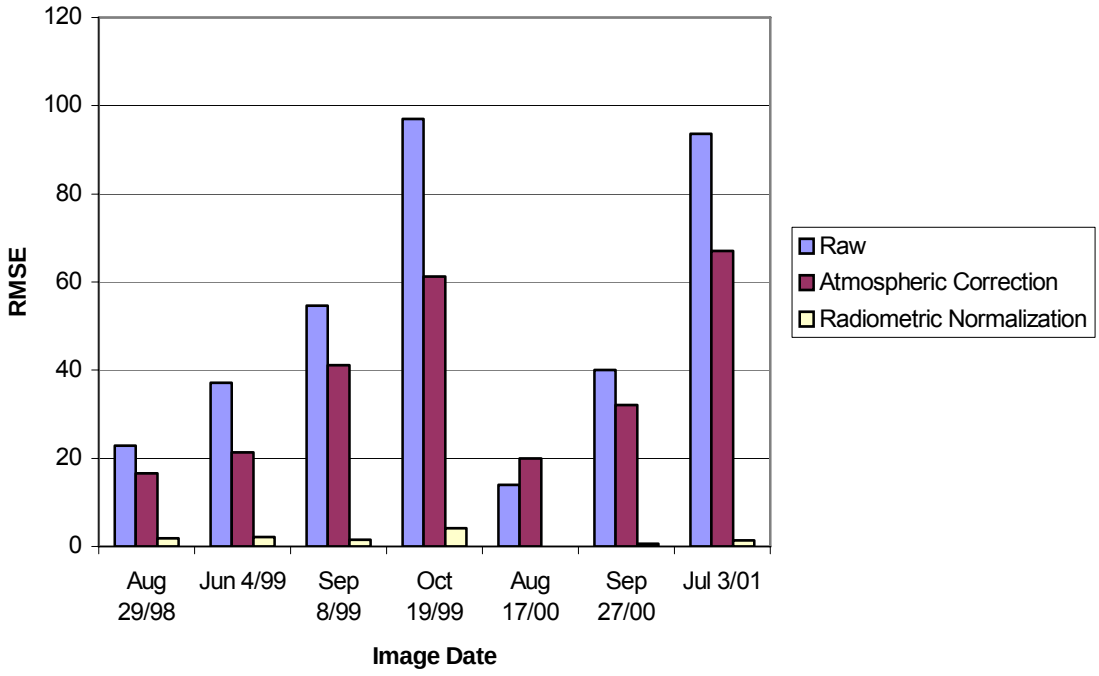

Figure 4-4: RMS errors illustrate the variability of pseudo-invariant features observed across seven Landsat scenes using three strategies of radiometric correction.

The relative radiometric processing routine consistently produced the best results, reducing radiometric variability down to a mean RMS of 2 DNs. In no case was the observed variance higher than 10 DNs. Based on these results, the relative normalization procedure was selected as the most reliable means of reducing radiometric variability, and adopted as the standard for all subsequent preprocessing.

The relative calibration procedure used to perform atmospheric normalization with Landsat images in this research is based on the work of Hall *et al.* (1991) who reported that a "slave" image could be radiometrically normalized to a "master" through a series of empirical transformation models developed for each spectral band. The

models are generated by deriving linear transformations between pixels selected from PIFs in each scene. The models are expressed in the form

$$(DN_{Normalized})_i = a_i + b_i(DN_{Original})_i$$

Equation 4-2

where

$DN_{Normalized}$ = the DN value of a pixel in the normalized image;

$DN_{Original}$ = the DN value of the same pixel in the original image;

b_i = a coefficient that accounts for differences in solar irradiance, downwelling sky radiance, and atmospheric transmission; and

a_i = differences in sensor calibration and path radiance.

While some authors have reported automated means of selecting *no change* pixels (e.g. Elvidge *et al.*, 1995) between two different image datasets, PIFs in these imagery were chosen manually in order to avoid locations in rugged topography or with marked differences in elevation. It should be pointed out that like all relative calibration procedures, the linear transformation technique does not *remove* the effects of the atmosphere, but instead make multiple images look like they were acquired through the *same* atmosphere.

The final radiometric preprocessing routine used on all Landsat data handled in this research involved the following four steps (i) selecting a master image, (ii) converting the DN values of the master image to 8-bit, top-of-atmosphere reflectance, (iii) performing atmospheric normalization through linear transformation on the remaining slave images, and (iv) calculating the tasseled cap components. The master

image chosen for all the mapping work in this study was the WRS path 45, row 23 image acquired on September 3, 2003 – a high-quality image acquired through an exceptionally clear atmosphere. Calculating TOA reflectance values first required converting the digital numbers (DNs) back to the original 32-bit radiance values measures by the sensor with the following equation:

$$L_\lambda = Gain_\lambda * DN_\lambda + Bias_\lambda$$

Equation 4-3

where

λ = TM band number,

L = at-satellite radiance,

Gain = band-specific gain, obtained from header file, and

Bias = band-specific bias, obtained from header file.

Once the physical radiance values were obtained, at-satellite reflectance was calculated as

$$\rho = \frac{\pi * L_\lambda * d^2}{ESUN_\lambda * \sin(\theta)}$$

Equation 4-4

where

λ = TM band number,

L = at-satellite radiance,

ρ = TOA reflectance,

$ESUN$ = mean solar exoatmospheric irradiance, and

θ = sun elevation angle, obtained from the header file.

The exoatmospheric irradiance tables are calculated according to Iqbal (1983), and are available on line from a variety of sources.

Once the *master* image was prepared, the other six *slave* Landsat images were radiometrically matched to it using the linear transformation procedure described previously. The entire five-scene study area was processed sequentially using the overlapping portions of adjacent image scenes (Figure 4-4). No topographic corrections were performed.

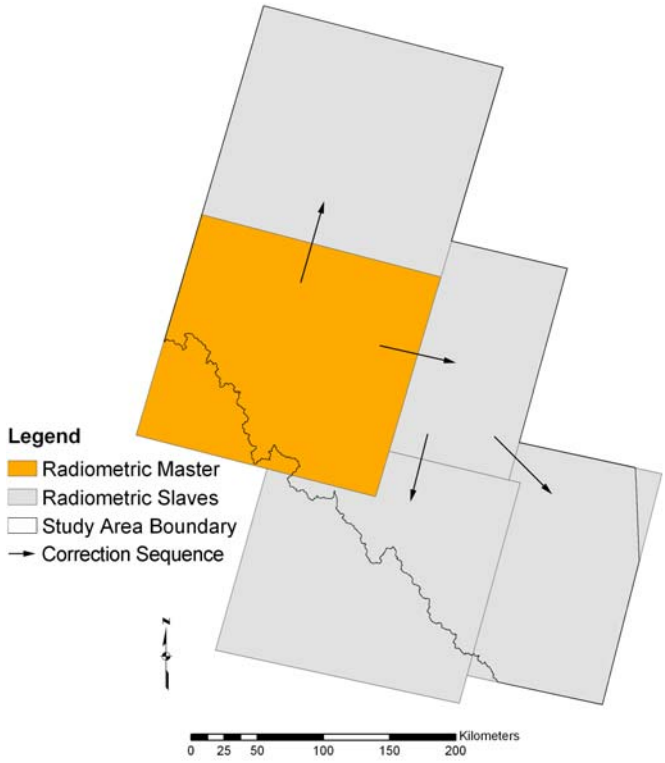

Figure 4-4: Radiometric normalization sequence for Landsat TM imagery.

The final step in the radiometric preprocessing routine involved performing the tasseled cap transformation of Crist and Ciccone (1984) to generate the standard orthogonal components brightness, greenness, and wetness. The components are calculated by performing weighted summations of Landsat's reflective bands using coefficients chosen to match the radiometric state of the imagery. The coefficients for 8-bit, at-satellite reflectance imagery are shown in Table 4-4. The resulting components reduce the dimensionality of the original six-band dataset with minimal loss of variance, and create efficient variables for subsequent classification and modelling.

Table 4-4: Coefficients for calculating the tasseled cap components from 8-bit, at-satellite reflectance imagery.

	Band 1	Band 2	Band 3	Band 4	Band 5	Band 7
Brightness	0.35612057	0.39722876	0.39040367	0.69658643	0.22862755	0.15959082
Greenness	-0.33438846	-0.35444216	-0.45557981	0.69660177	-0.02421353	-0.26298637
Wetness	0.26261884	0.21406704	0.09260517	0.06560172	-0.76286850	-0.53884970

In addition to the radiometric normalization described above, careful geometric preprocessing of the Landsat scenes was necessary in order to permit precise integration of optical satellite imagery with other geographic data in a GIS environment. As with all digital remote sensing imagery, TM data are subject to a variety of systematic and non-systematic distortions including detector delay, slight variations in spacecraft movement, earth rotation, panoramic distortion, and relief displacement (Landsat Project Science Office, 1998). Landsat level 1R data – the type acquired for this study – have been processed at the United States Geological Survey's EROS Data Center to remove many

of these systematic errors, but remain in a path-oriented configuration with imagery aligned in the direction of the satellite orbit. Precision products – orthorectified imagery in which errors caused by relief displacement have been removed and the data re-sampled to a standard map projection – require further refinement with digital elevation models and ground control points. Orthorectification was performed using the satellite orbital math model (Toutin, 1995) found in Geomatica OrthoEngine. Orthorectified Landsat 7 imagery downloaded from the Geogratis collection maintained on the Internet by Natural Resources Canada was used for reference in image-to-image ground point collection, with geometric models generated to within 0.5 pixels using a minimum of 50 ground control points per scene. The project imagery were then re-sampled with bilinear interpolation to 30-metre pixels in UTM zone 11 using the NAD83 datum, based on the GRS80 ellipsoid. The bilinear interpolation method was selected in order to reduce re-sampling artefacts while keeping the dubsequent DN values close to their original values. The geometric quality of the resulting images was inspected visually using roads, cut lines, and other linear features in a GIS environment in order to ensure a high-quality rectification. A complete, radiometrically normalized orthomosaic of the study area using the best cloud-free Landsat imagery available in the archive is shown in Figure 4-5.

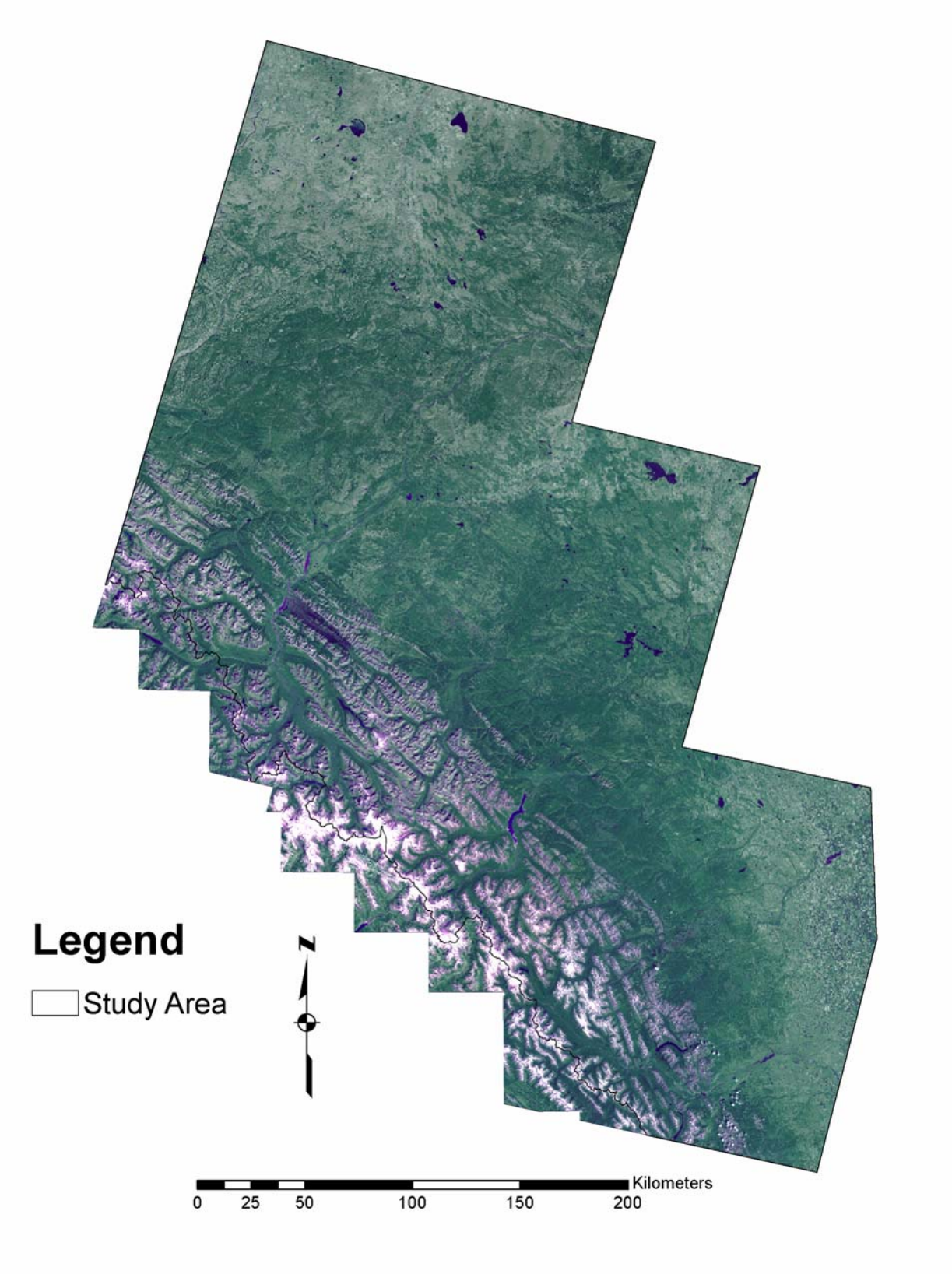

Figure 4-5: False-colour, radiometrically-normalized Landsat orthomosaic of the study area.

4.1.2.2 MODIS Imagery

While Landsat TM data provide exceptional support for long-term land-cover mapping, the 16-day temporal resolution of the sensor seriously limits access to time-sensitive information or multi-temporal analysis. In some locations (e.g. the tropics) and times of the year (e.g. springtime and early summer in Alberta) high-quality Landsat data are extremely difficult to acquire because of persistent cloud cover. MODIS, one of the key instruments on board the Earth Observing System's (EOS's) Terra and Aqua satellites, views the entire surface of the earth every one to two days, acquiring data over 36 spectral bands ranging in spatial resolution from 250 to 1000 metres (Table 4-5). The tremendous frequency with which these data are acquired makes it possible to create high-quality, cloud-free mosaics of areas that are rarely captured by Landsat. In addition to enhanced temporal, spectral, and radiometric resolution, MODIS distinguishes itself from Landsat and most other satellite image platforms in two important respects. First, the development of high-level data products is one of the EOS's core goals, so the MODIS project is supported by an international team of scientists working to develop 44 separate data products in five categories: calibration, atmosphere, land, cryosphere, and ocean (Table 4-6). As a result of this research effort, MODIS data users can choose from dozens of high-end products developed by some of the leading scientists in their discipline.

Table 4-5: MODIS bandset.

Band	Bandwidth	Spatial Resolution	Primary Use
1 2	620-670nm 841-876 nm	250m	Land/Cloud/ Aerosols Boundaries
3 4 5 6 7	459-479 nm 545-565 nm 1230-1250 nm 1628-1652 nm 2105-2155 nm	500m	Land/Cloud/Aerosols Properties
8 9 10 11 12 13 14 15 16	405-420 nm 438-448 nm 483-493 nm 526-536 nm 546-556 nm 662-672 nm 673-683 nm 743-753 nm 862-877 nm	1000m	Ocean Colour/ Phytoplankton/ Biogeochemistry
17 18 19	890-920 nm 931-941 nm 915-965 nm	1000m	Atmospheric Water Vapour
20 21 22 23	3.660 -3.840μm 3.929-3.989μm 3.929-3.989μm 4.020-4.080μm	1000m	Surface Cloud Temperature
24 25	4.433-4.498μm 4.482-4.549μm	1000m	Atmospheric Temperature
26 27 28	1.360-1.390μm 6.535-6.895μm 7.175-7.475μm	1000m	Cirrus Clouds/Water Vapour
29	8.400-8.700μm	1000m	Cloud Properties
30	9.580-9.880μm	1000m	Ozone
31 32	10.780-11.280μm 11.770-12.270μm	1000m	Surface/Cloud Temperature
33 34 35 36	13.185-13.485μm 13.485-13.785μm 13.785-14.085μm 14.085-14.385μm	1000m	Cloud Top Altitude

Table 4-6: MODIS data products.

Calibration MOD 01 - Level 1A Radiance Counts MOD 02 - Level-1B Calibrated Geolocated Radiances MOD 03 - Geolocation Data Set	**Land** MOD 09 - Surface Reflectance MOD 11 - Land Surface Temperature & Emissivity MOD 12 - Land Cover/Land Cover Change MOD 13 - Vegetation Indices MOD 14 - Thermal Anomalies, Fires & Biomass Burning MOD 15 - Leaf Area Index & FPAR MOD 16 - Evapotranspiration MOD 17 - Net Photosynthesis and Primary Productivity MOD 43 - Surface Reflectance MOD 44 - Vegetation Cover Conversion
Atmosphere MOD 04 - Aerosol Product MOD 05 - Total Precipitable Water (Water Vapor) MOD 06 - Cloud Product MOD 07 - Atmospheric Profiles MOD 08 - Gridded Atmospheric Product MOD 35 - Cloud Mask	**Cryosphere** MOD 10 - Snow Cover MOD 29 - Sea Ice Cover
Cryosphere MOD 10 - Snow Cover MOD 29 - Sea Ice Cover	**Ocean** MOD 18 - Normalized Water-leaving Radiance MOD 19 - Pigment Concentration MOD 20 - Chlorophyll Fluorescence MOD 21 - Chlorophyll_a Pigment Concentration MOD 22 - Photosynthetically Available Radiation (PAR) MOD 23 - Suspended-Solids Concentration MOD 24 - Organic Matter Concentration MOD 25 - Coccolith Concentration MOD 26 - Ocean Water Attenuation Coefficient MOD 27 - Ocean Primary Productivity MOD 28 - Sea Surface Temperature MOD 31 - Phycoerythrin Concentration MOD 36 - Total Absorption Coefficient MOD 37 - Ocean Aerosol Properties MOD 39 - Clear Water Epsilon

The second important characteristic that distinguishes MODIS data products from those of Landsat and most other platforms is that the data products from each of the science teams can be acquired from NASA at no charge. The data are housed and distributed through three Distributed Active Archive Centers located in NASA facilities across the United States, and are available for download across the Internet through the EOS Data Gateway. This exceptional availability of high-level data products stands in

stark contrast to the more limited policies of Landsat and most other satellite data platforms, and greatly relieves the burden of data acquisition and preprocessing.

Data from MOD 13 – vegetation indices (VIs) – were used to map and monitor LAI across the study area. Headed up by team leader Alfredo Huete, MOD 13 products are designed to provide consistent spatial and temporal monitoring of global vegetation conditions (Huete *et al*., 1999). MOD 13 uses two different algorithms in its production of global VIs: the normalized difference vegetation index (NDVI) and the enhanced vegetation index (EVI). Both indices exploit the well-known relationship observed between healthy vegetation and reflected energy in the visible and near-infrared portions of the electromagnetic spectrum. Previous studies have shown that most of the near-infrared energy is reflected by the foliage, while much of the visible energy – particularly in the red wavelengths – is absorbed for photosynthesis (Colwell, 1974). Jordon (1969) was the first to exploit this relationship for the derivation of LAI with the simple ratio (SR), calculated as

$$SR = \frac{DN_{nir}}{DN_{red}}$$

Equation 4-5

where

DN_{nir} = Digital number of the near-infrared band, and

DN_{red} = Digital number of the red band.

The NDVI of Deering (1978) normalized the index to values of –1 to +1 with the equation

$$NDVI = \frac{DN_{nir} - DN_{red}}{DN_{nir} + DN_{red}}$$

Equation 4-6

As a vegetation monitoring tool, NDVI has been used to estimate a wide variety of biophysical parameters, including LAI (Curran *et al.*, 1992), green biomass (Reeves *et al.*, 2001), percent green cover (Elvidge and Chen, 1995), and fraction of absorbed photosynthetic radiation (Asrar *et al.*, 1984).

Despite the long history of use, a significant body of research illustrates a series of limitations to NDVI that may impact upon the quality of the index, including atmospheric effects (Goward *et al.*, 1991), anisotropy (Cihlar, *et al.*, 1994), and background contamination (Huete and Warrick, 1990; Qi *et al.*, 1993). The second MOD 13 vegetation index – the EVI – is designed specifically to address some of these issues by reducing canopy background and sub-pixel atmospheric effects not accounted for in the 20km-resolution atmospheric correction algorithms (MOD 09). The equation takes the form

$$EVI = G * \frac{(\rho_{nir} - \rho_{red})}{L + \rho_{nir} + C_1 * \rho_{red} + C_2 * \rho_{blue}}$$

Equation 4-7

where

G = Gain factor

ρ_{nir} = Near-infrared reflectance factor,

ρ_{red} = Red reflectance factor,

ρ_{blue} = Blue reflectance factor,

L = Canopy background brightness correction factor

C_1 = Atmospheric resistance red correction factor, and

C_2 = Atmospheric resistance blue correction factor.

The terms G, L, C_1 and C_2 are each empirically determined constants, the details of which are beyond the scope of this discussion. A complete description of the theoretical foundation of the EVI can be found in Huete *et al.* (1999).

The MOD 13 product list (Table 4-7) consists of 21 variations based on spatial grain (500m, 1km, and 0.05 degree climate modelling grid), composite window (16-day or monthly), platform (Terra, Aqua, Terra/Aqua combined), and version (V003 or V004). The data used for this project were MOD13Q1 16-day composites from the Terra satellite. The V004 designation reflects a "validated" product assessed in a systematic and statistically robust fashion (Huete *et al.*, 1999). The study area is split across MODIS tiles h10v03 and h11v03, and distributed in a sinusoidal projection in the NASA *.hdf* format. The MODIS reprojection tool (downloaded from the Land Processes Distributed Active Archive Center) was used to mosaic the required scenes, reproject to UTM zone 11 (NAD 83), and translate to a more useable file format. Figure 4-6 shows a false-colour composite of the MODIS mosaic containing the study area; the MOD13Q1 NDVI product is shown in Figure 4-7.

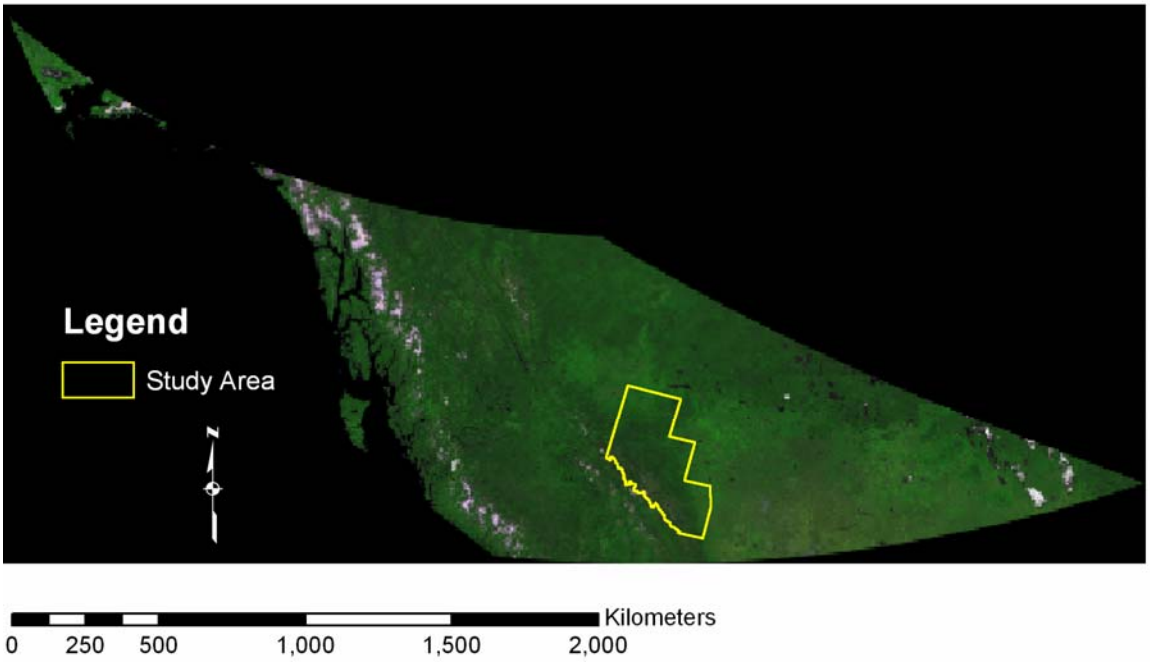

Figure 4-6: False colour MODIS composite (August 18, 2003) containing the study area.

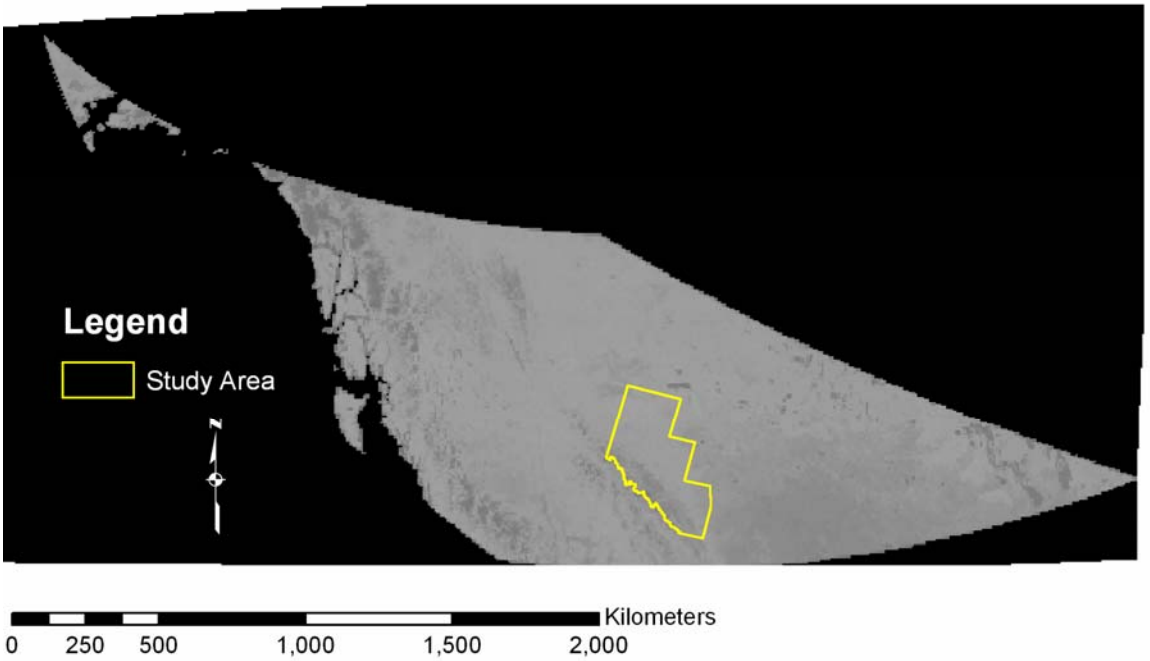

Figure 4-7: MOD13Q1 NDVI mosaic (August 18, 2003) containing the study area.

Table 4-7: MOD 13 data products.

Data Product	Terra V004	Aqua V003	Aqua V004	Terra/Aqua Combined
Vegetation Indices 16-Day L3 Global 500m	MOD13A1	MYD13A1	MYD13A1	MCD13A1
Vegetation Indices 16-Day Global 1km	MOD13A2	MYD13A2	MYD13A2	MCD13A2
Vegetation Indices Monthly L3 Global 1km	MOD13A3	-	MYD13A3	MCD13A3
Vegetation Indices 16-day L3 Global 0.05Deg CMG	MOD13C1	-	MYD13C1	MCD13C1
Vegetation Indices Monthly L3 Global 0.05Deg CMG	MOD13C1	-	MYD13C1	MCD13C1
Vegetation Indices 16-day L3 Global 250m	MOD13Q1	MYD13Q1	MYD13Q1	MCD13Q1

4.1.2.3 Digital Elevation Model

The value of topographic and geomorphometric information from digital elevation models for analyzing vegetation (e.g. Davis and Goetz, 1990; Franklin *et al.*, 1994), land cover (Franklin and Moulton, 1990; Fahsi *et al.*, 2000), hydrology (Moore *et al.*, 1991; Tarboton, 1997), and landforms (McDermid and Franklin, 1993; Macmillan *et al.*, 2003) are well-established. The early IDT map of the Foothills Model Forest Grizzly Bear Research Program's phase 2 study area (Franklin *et al.*, 2001) relied heavily on topographic variables for GIS decision rules and a source of ancillary data for supervised classification. A commercial model from the Canadian company DMTI Spatial was acquired for this study through an academic agreement with the University of Calgary library. The DEM was created through interpolating of the National Topographic Database 1:50,000 digital map contours, contours, spot heights, and water body polygons. A smoothing algorithm (Hutchinson, 1989) was used to eliminate *stepping* and *pit* artefacts commonly associated with similar medium-quality elevation models. The model was created at 30-metre resolution, and distributed by 1:250,000 map sheet.

Samples of the DMTI data were compared with those from the 50-metre provincial DEM, and judged to be of a slightly higher quality.

Wall-to-wall DEM coverage of the study area (Figure 4-6) was achieved by mosaicking 1:250,000 map sheets in ArcView. Further morphometric processing was used to derive topographic variables of slope and angle of incidence for use in subsequent mapping activities. Slope was calculated over a 3x3 neighbourhood surrounding each pixel in the image as the slope of the plane formed by the vector connecting the left and right neighbours and the vector connecting the upper and lower neighbours of the pixel, and ranges between 0 and 90 degrees. The angle of incidence is the angle between a point on the surface and the line connecting this point to a user-selected light source, and ranges from 0 to 90 degrees. A value of 0 indicates that light will not strike the surface, while a value of 90 indicates a direct 90-degree angle. Incidence was calculated using a light source at 152° azimuth and 57° elevation – typical for a late-summer day at the latitude of the study area during which most of the imagery in this study was acquired. Together, the measures of elevation, slope, and incidence provided a basic description of topography for each pixel in the elevation model in linear variables suitable for statistical analysis, classification, and modelling.

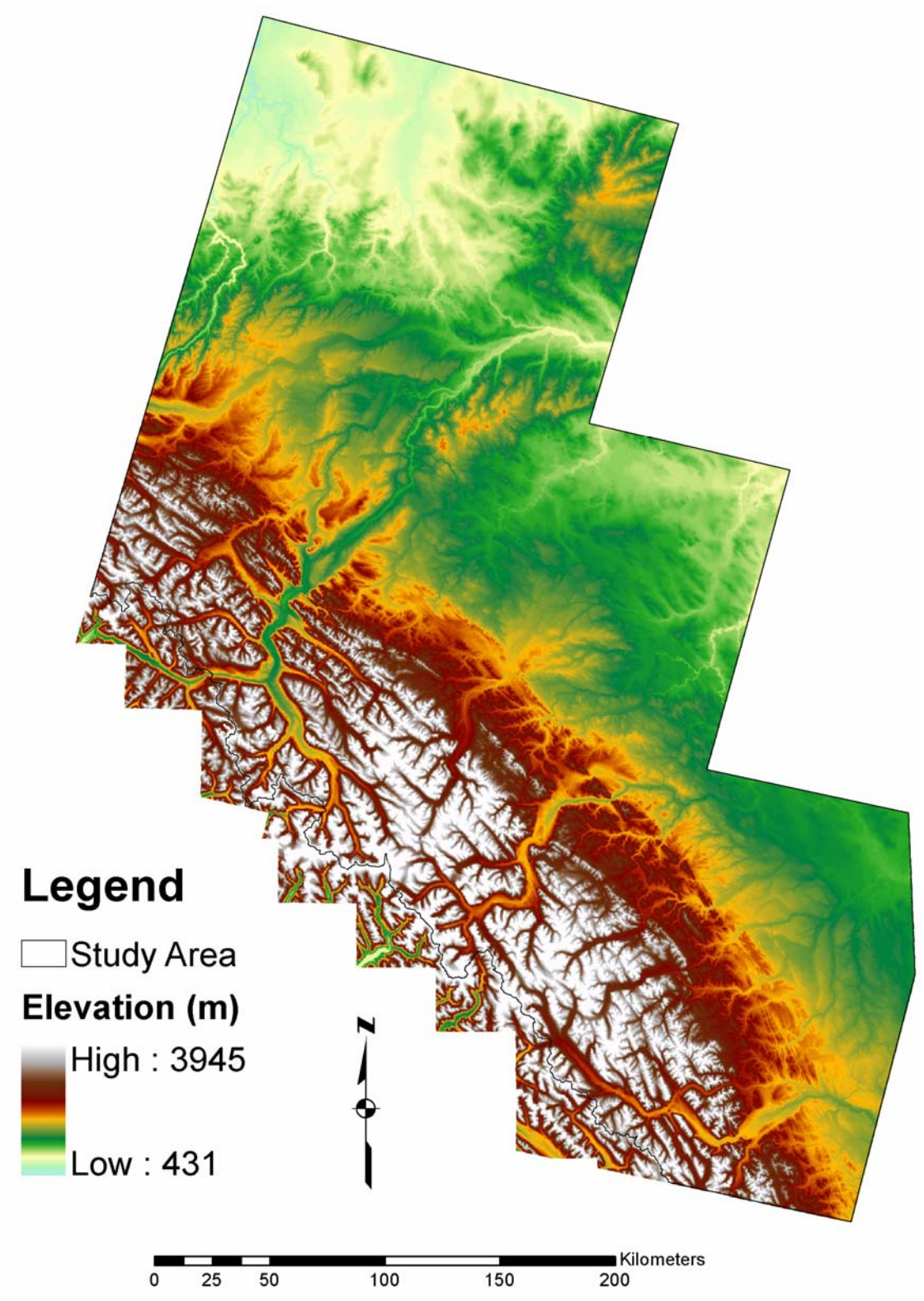

Figure 4-6: Pseudo-coloured digital elevation model containing the study area.

4.1.2.4 Additional Digital Data Sources

4.1.2.4.1 Alberta Vegetation Inventory

The Alberta Vegetation Inventory (AVI) is the provincial standard for forest inventory on Alberta's public lands. Generated through manual interpretation of aerial photographs, the AVI contains a variety of information related to timber productivity, moisture regime, crown closure, height, tree species composition, and age at a scale of about 1:20,000 (Alberta Sustainable Resource Development, 1991). While various issues related to accuracy, consistency, and completeness limit the usefulness of the AVI across the entire study area, it did provide a valuable source of supplemental information in areas where no other ground data were available.

4.1.2.4.2 Cut Block/Forest Regeneration Mask

The land cover/vegetation mapping and modelling work conducted within this research was designed primarily around natural vegetation communities occurring outside of disturbed and regenerating areas formed by cut blocks, burns, and other natural and anthropogenic processes. While the products certainly cover these areas, observations made in the preliminary stages of this project suggested that the patterns and processes operating in cut blocks and other regenerating surfaces are fundamentally different from those in surrounding undisturbed lands, and the quality of products within these areas is expected to be lower. As a result, a cut block/forest regeneration mask covering the study area was created using a combination of object-oriented change detection (McDermid *et al.*, 2003) and manual digitizing. The resulting layer (Figure 4-7) served as the basis for segregating field points acquired in disturbed areas from those in

surrounding undisturbed regions for the purpose of map and model generation, and was included in the package of completed products as a source of additional information. However, it is not considered a core remote sensing derivative, and is therefore not described further within this document.

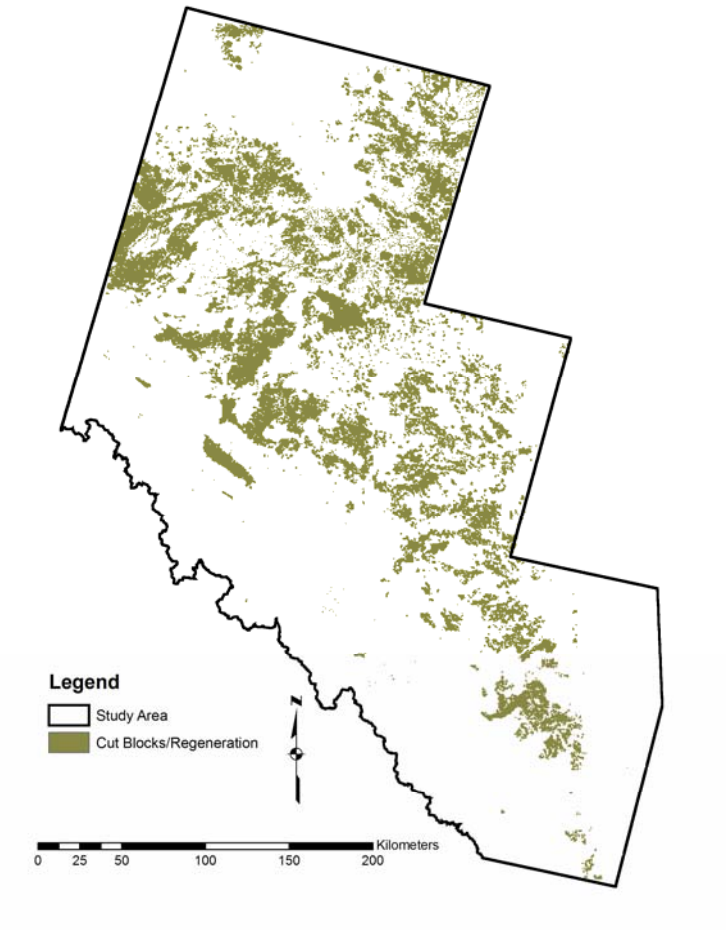

Figure 4-7: Cut blocks and regenerating regions in the study area.

4.1.2.4.3 Additional GIS Layers

A series of additional spatial information products served a variety of miscellaneous functions within this research, including stratification, field work planning, and map/figure production. These layers include roads, cut lines, streams, political

boundaries, protected areas, and populated areas, among others, and were acquired from a variety of local and provincial sources.

4.2 Digital Image Processing and Map Product Development

The flow chart shown in Figure 4-8 provides an overview of the various image processing and map product development procedures used in this study, and serves as a guide for the remainder of this chapter. It outlines a scale-sensitive framework for extracting high-quality information on land cover, forest structure, and vegetation phenology over large areas using remote sensing and other geospatial data sets. Object-oriented classification was used to map land cover with H-resolution TM data, while regression analysis techniques were used to derive continuous-variable models of the L-resolution processes of crown closure and intra-pixel species composition. Multi-temporal derivation of LAI from MODIS imagery was performed to gain insight on seasonal patterns of LAI phenology across the growing season. Combined together with other information layers in a GIS environment, these products provide a powerful database of environmental information suitable for supporting large-area, multi-jurisdictional habitat mapping and other resource-management activities.

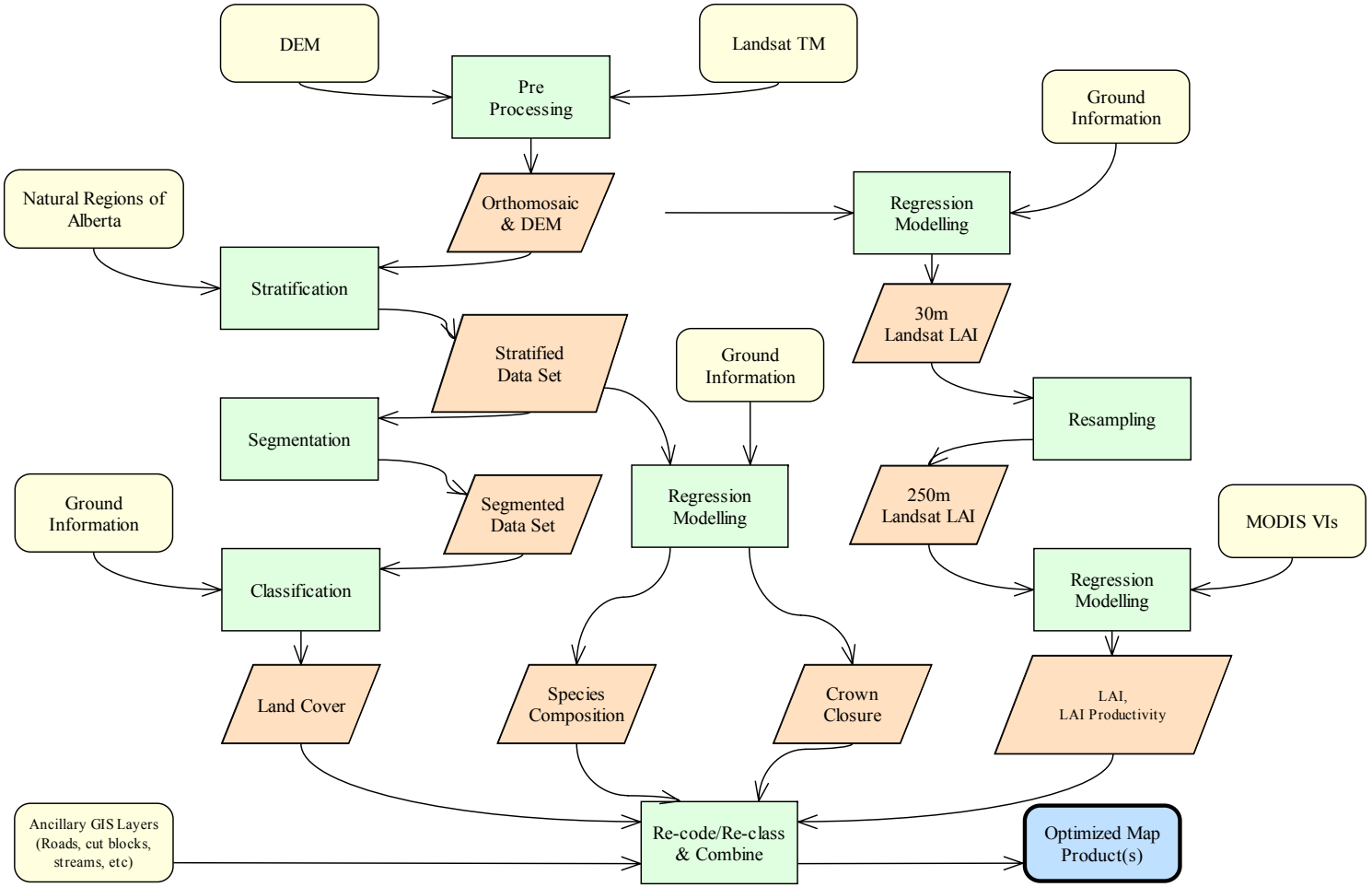

Figure 4-8: Flow chart illustrating the basic methodology for producing the flexible, scale-sensitive land and vegetation information base used in this research.

4.2.1 Land-cover Mapping

Land cover classification was performed using object-oriented image processing techniques implemented within the software package eCognition. The procedure involved performing a multi-resolution segmentation of the five scene comprising the study area to identify a nested hierarchy of image object primitives: homogeneous groups of pixels that formed the basis of all subsequent processing. Classification was performed using fuzzy rule-based and nearest neighbour analysis in a *top-down* approach based on a three-level land classification hierarchy, and evaluated using 249 independent test sites.

4.2.1.1 Segmentation

The segmentation algorithm provided in eCognition uses a region-merging technique that starts with single pixels and creates subsequently larger objects through a clustering process based on weighted heterogeneity (Baatz and Schape, 1999). The size of the resulting objects is controlled by weight, scale, and shape parameters, enabling the user to exercise some control over the size and nature of the resulting objects. To create the objects used in this classification, various combinations of input variables and parameters were experimented with in order to create meaningful object primitives that were judged to be small enough to avoid merging obviously separate objects (e.g. cut block edges, road allowances, stand boundaries, etc), yet large enough to identify meaningful groups of similar pixels. This stage of the analysis relies largely on the skill and judgement of the image analyst, and there is likely no optimal combination of variables and parameters

capable of producing ideal objects over the entire image. Where possible, decisions were made which erred on the side of detail, knowing that post-classification merging could be used to combine contiguous groups of *too small* primitives into larger objects more suitable for the given classification level. The combination ultimately used was based on a blend of the tasseled cap variables brightness, greenness, and wetness (weight 1.0), and the DEM derivatives of slope and incidence (weight 0.3). The scale parameter was 9, and the composition criteria were colour: 0.8, shape: 0.2, smoothness: 0.8, and compactness: 0.2.

4.2.1.2 Classification and Map Product Development

In order to characterize land cover and basic physiognomy of the study area, a hierarchical land cover classification scheme composed of three levels of detail was adopted (Table 4-8). The hierarchy aided in the development of the final land cover product and provided a mechanism for easily tracking accuracy at multiple land-cover scales. The original Landsat orthomosaic was stratified into four pieces, based on the Natural Regions classification of Achuff (1994): mountains, foothills, boreal forest, and parkland/grassland. All subsequent segmentation and classification activities took place within each of these broad units of analysis. Beginning at the most general level in the land cover classification scheme, an iterative process of training, classification, and refinement was adopted until an acceptable level of accuracy (>80%, if possible) had been arrived at. Once achieved, a classification-based segmentation was used to merge the original object primitives into new composite objects appropriate for that level of classification. In this way, an object-based hierarchy that matched the land cover

classification scheme was created, and used to drill down towards the most detailed classification (level III). The technique is similar to the Integrated Decision Tree Approach (IDTA) developed by Franklin *et al.* (2001) that selectively combined supervised, unsupervised, and GIS decision rule criteria in concert with a three-level classification scheme. The hierarchical, multi-step nature of the strategy enabled class-specific decision rules (e.g. water separated from shadow on the basis of slope and elevation) and variable sets to be applied in a selective manner best suited to the particular level of classification.

Table 4-8: Class hierarchy used in object-based land cover classification.

Level I	Level II	Level III
A. Vegetation & Shadow	1. Trees	a. Upland Trees
		b. Wetland Trees
	2. Herbs	c. Upland Herbs
		d. Wetland Herbs
	3. Shrubs	e. Shrubs
	4. Shadow	f. Shadow
B. No Vegetation	5. Water	g. Water
	6. Barren Land	h. Barren Land
	7. Snow/Ice	i. Snow/Ice
	8. Cloud	j. Cloud

The approach to land cover classification adopted in this research differs from the IDTA method used in previous phases of the Foothills Model Forest Grizzly Bear Research Program in several important respects. First, it employs an object-based style of analysis rather than one based on pixels, providing a more appropriate scale for H-

resolution classification, and eliminating the need for majority filters and other post-classification processing procedures. Second, the current methods used eCognition: a software package specifically designed for multi-resolution analysis, decision rules, and supervised classification, thereby reducing the need for complex procedures requiring multiple software packages and making the process more attainable for use in an operational environment. Perhaps the most important difference, however, was the reduced emphasis placed on classification techniques overall in the current methodological framework. The IDTA relied exclusively on classification (augmented substantially with GIS information from the AVI) as an information-extraction technique in the production of 23 information classes. The current approach, by contrast, produces only ten classes at its most detailed level, focussing exclusively on broad, H-resolution information that is well-suited to classification-based techniques using Landsat. Additional information from other more detailed attributes of the landscape – crown closure, intra-pixel species composition, and phenology – are generated separately using other more appropriate strategies.

eCognition uses a fuzzy rule base to classify image objects, with membership boundaries defined by fuzzy membership functions (Definiens, 2003). Membership functions can be created manually through one-dimensional membership classes, or automatically through nearest neighbour analysis of training data. One-dimensional membership functions are defined manually through a graphical user interface, and take the form of decision rules based on one of the many dozens of object features available in the software. For example, a decision rule was used to help define the membership function of *water* at classification level II, in which class membership was limited to

objects with a mean slope less than 2 degrees. This simple rule effectively eliminated confusion between *water* and *shadow* classes – two information categories that are commonly confused in pure multispectral feature space. Function slopes can take on a variety of forms to match such logical conditions as *larger than*, *smaller than*, *boolean*, and *range*, among others, and multiple rules can be combined together with *and/or* operators to define complex heuristics.

While the combined use of one-dimensional functions can be used to cover multi-dimensional feature space, the strategy becomes unwieldy in large, complex classification problems. For that reason, eCognition also offers the ability to generate multi-dimensional membership functions automatically through training sites and nearest neighbour analysis. The analyst identifies a representative set of sample sites and defines the feature space (the spectral, spatial, textural, contextual, and hierarchical attributes associated with each object) to be used for analysis. In the classification phase, the algorithm assigns membership values ranging from 0 (no assignment) to 1 (full assignment) to each unknown object on the basis of its distance to known sample objects. eCognition computes distance as follows:

$$d = \sqrt{\sum_f \left(\frac{v_f^{(s)} - v_f^{(o)}}{\sigma_f} \right)^2}$$

Equation 4-8

where

d = distance sample object s and image object *o*,

$v_f^{(s)}$ = feature value of known sample object for feature *f*,

$v_f^{(o)}$ = feature value of unknown image object for feature *f*, and

σ_f = standard deviation of the feature values for feature *f*.

Dividing the distance in feature space between a known sample object and unknown image object by the standard deviation of all feature values serves to standardize distance measures so that features of varying ranges can be combined. A distance value of d=1 means that the distance equals the standard deviation of all feature values defining the feature space. The *steepness* of the membership function – i.e. the quality that determines the class membership value associated with each value of d – is controlled by the function slope: a variable parameter that can be modified for each class by the user. The default value is 0.2. Values less than that create narrower membership functions in which image objects have to be closer to sample objects in feature space in order to be classified. Larger values relax the membership function and create higher class membership values for unknown objects further away from the sample objects.

In general, the generation of effective multi-dimensional membership functions was found to be training intensive, requiring large numbers of sample sites in order to properly partition the n-dimensional feature space. The final classification products created with eCognition required supplemental training samples beyond the 844 points generated through field work. Additional training points were chosen manually with the help of the AVI combined with image- and air photo-based interpretation. This was particularly true in the Parkland and Boreal Forest portions of the study area, where biophysical ground data were slim.

4.2.1.3 Error Characterization

The number of field data points suitable for land cover assessment was richer and more numerous than for any other ground attribute mapped in this research, with 1125 samples. This data set was divided randomly into 893 points for training, and 232 for testing, using a rough 80/20 rule of thumb that was adopted for most of the analyses conducted in this research. The independent test data were used to construct standard contingency matrices and Kappa coefficient statistics for each level in the land cover hierarchy.

4.2.2 Crown Closure and Species Composition

Vegetation attributes that vary at the tree/gap level are not well-suited to classification procedures using Landsat data, since objects of interest occur over areas that are smaller than individual pixels (L-resolution). In addition, there is an incentive to perform analyses that maintain higher-order data than the nominal and ordinal values produced by most categorical classification procedures, in order to maintain flexibility in the finished product. As a result, a variety of regression analysis techniques were used to produce *continuous variable* models of crown closure and species composition – defined here in the most general sense as percent broadleaf and percent conifer – within each pixel of the geospatial data set.

Box diagrams of the field reference data (Figure 4-9) illustrate the wide range of crown closure and species composition conditions that were sampled across the natural forested regions of the study area. Regenerating forest stands occurring in cut blocks and regenerating forests were not modelled because of the tremendous variability observed here related to re-planting strategy, scarification, and other silvicultural practices. These

disturbed forests likely require separate treatment and additional reference data not available in this study.

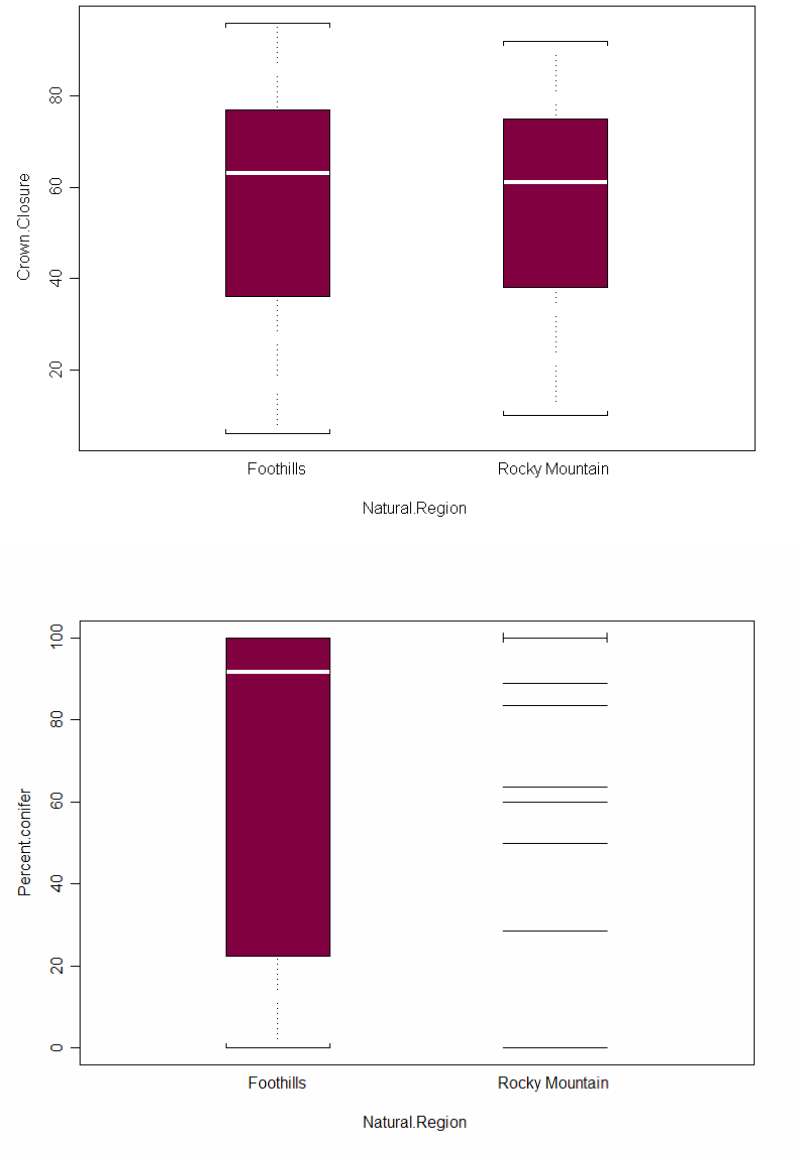

Figure 4-9: Crown closure (top) and species composition (bottom) box plots of the Foothills and Rocky Mountain natural subregions from ground biophysical data.

4.2.2.1 Model Development

Simple linear regression assumes that variance is constant and that the errors are normally distributed. Proportional data such as % conifer and % crown closure often displays ∩-shaped variance patterns that violate these assumptions and require the use of binomial-family generalized linear models (GLM's) with a logit link (Crawley, 2002). The logit transformation takes the form

$$\text{logit} = \ln\left(\frac{p}{q}\right)$$

Equation 4-9

where

p = the number of failures in a proportional data count and

q = the number of successes (i.e. 1 - p).

In addition to producing the linear predictor necessary for analysis, the proportional data are strictly bounded between 0 and 100, eliminating the unreasonable results commonly encountered with untransformed data. The *failure* and *success* counts necessary for constructing the two-vector response variable were obtained from the dot counts and stem counts from densiometer and prism sweep data respectively.

While the binomial-family GLM appeared to work well for the species composition data, preliminary analyses with crown closure models revealed residual deviance more than 10-times the residual degrees of freedom, suggesting a poorly specified model (Crawley, 2002). A survey of the literature revealed that some kinds of proportional data, including percent cover, are best analysed using conventional

regression models following arcsine transformation (e.g. Mazerolle and Hobson, 2002; Austen *et al.*, 2001). The arcsine transformation takes the form

$$y = \sin^{-1}\sqrt{0.01 * p}$$

Equation 4-10

where

y = the response variable in radians, and

p = the proportion (e.g. cover) in percent.

Using the appropriate regression form, six candidate models of crown closure and species composition were constructed from three different groups of predictor variables (Table 4-9). The first two– CCTM and SCTM – were based on TM data alone. CCDEM and SCDEM were based on topographic measures of elevation, slope, and incidence, while CCTMDEM and SCTMDEM drew from both TM and DEM variables together. The variables available for each candidate model were examined for collinearity, and determined to be independent at the $r<0.6$ level. A stepwise procedure based on Akaike's Information Criterion (Burnham and Anderson, 1998) was used to select the best-fitting model with the fewest number of predictor variables, following the principle of parsimony, and verified the results through F-tests and analyses of variance. All statistical analyses were conducted in the software package S-SPLUS.

Table 4-9: A summary of candidate models constructed for crown closure and species composition.

Crown Closure Models	Species Composition Models	Available Predictor Variables
CCTM	SCTM	Brightness, Greenness, Wetness
CCTMDEM	SCTMDEM	Brightness, Greenness, Wetness, Elevation, Slope, Incidence
CCDEM	SCDEM	Elevation, Slope, Incidence

4.2.2.2 Model Application and Map Product Development

Models of crown closure and species composition were initially derived across the entire un-stratified mosaic, but preliminary inspections revealed unwanted seam lines on the boundaries of adjacent scenes (Figure 4-10). In spite of my best efforts at radiometric normalization in image preprocessing, the changing ground conditions observed across the summer growing season (soil moisture, understorey development, shadow component, etc), combined with the sensitivity of continuous-variable parameter estimates, lead to unacceptable variability between Landsat scenes. The same difficulties were not observed in the land cover classification component of this study, suggesting that categorical discrimination of broad land cover types using supervised classification techniques is not as sensitive to subtle changes in ground conditions.

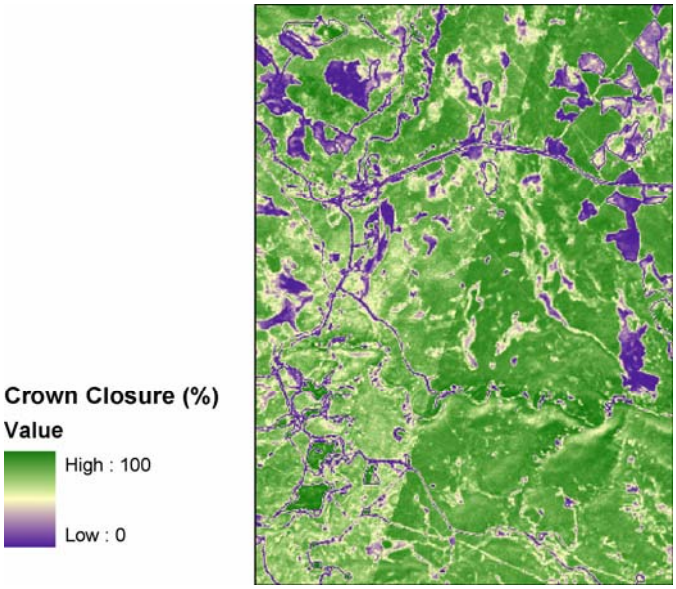

Figure 4-10: Seam lines in a draft version of the crown closure map based on mosaic-level processing across Landsat scenes.

In order to overcome the seam line issues observed in the continuous-variable models, regression processing was conducted on a per-scene basis using the five individual TM scenes that composed the original Landsat mosaic. The complication with the per-scene approach to modelling was that the field points with high-quality prism sweep and densiometer data were concentrated in the middle portion of the region where the bulk of the field work had been conducted (Figure 4-11), rather than distributed evenly across the entire area as would be ideal. In two of the images (path 44, row 23 and path 45, row 23) there was enough field data to enable the models to be both trained and tested, but in the remaining three scenes there was not. In these cases, a procedure described by Cohen *et al.* (2001) was adapted to permit the extension of model predictions from the two source images to the three adjacent destination scenes. The technique involves using model predictions from the source image to train new models with explanatory measures obtained from the overlapping portion of the destination

image. Any field data that existed in the destination imagery were used for model verification and testing. The resulting model parameters for the destination scene were slightly different, accounting for the differences in ground condition and eliminating the unwanted seams. While similar to the linear transformation procedure used in radiometric preprocessing, the model extension method is not limited to pseudo-invariant features in its focus, and is therefore perhaps better-suited to handling the subtle changes in ground condition that can occur temporally.

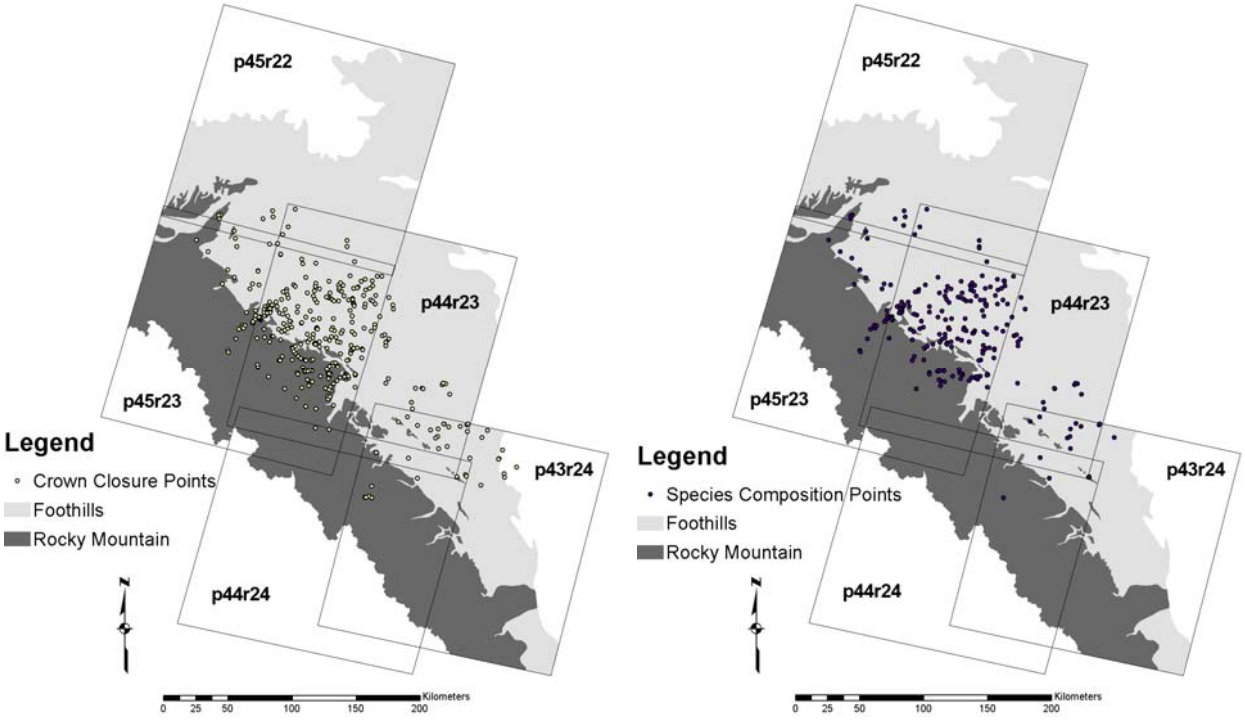

Figure 4-11: Distribution of crown closure (left) and species composition (right) ground points across the study area.

Figure 4-12 illustrates the basic steps necessary to perform model extension from a source image to an adjacent destination scene. The procedure was used to extend the crown closure and species composition from the two source scenes – path 45, row 23 and

path 44, row 23 – to the remaining scenes in the mosaic. The steps are described briefly below:

1. The overlap portion of the source and destination imagery in the target natural region was defined using GIS polygon clipping routines. Necessary layers included source image footprint, destination image footprint, and natural region boundaries. The resulting polygon encompassed the extent of the desired natural region in the area of overlap.
2. The second step involved obtaining the samples necessary for constructing a model that relates predictor variables from the destination scene from the response variable in the source scene (crown closure in the illustrated example). In order to ensure that samples are constrained to forested portions of the overlap area, it is first necessary to mask out all non-forested regions with a forest/non-forest layer. In this case, the results of the Level II land cover classification were used to accomplish this. Five hundred random points were then dropped onto the overlap portion to extract the necessary variables. The large sample size was designed to ensure a broad representation of the spectral and topographic conditions found in the overlap area.
3. The destination model was derived by developing a statistical relationship between the source response variable and the predictor variables from the destination scene. Destination models were developed in a manner consistent with that used to develop the source models – i.e., applying the same transformation, using the same regression strategy, and employing the same predictor variables. Attempts were made to achieve parsimony and the minimum

effective model, but since the purpose of the exercise was the extension of source models across presumably similar terrain, and because the imagery had already been radiometrically normalized to adjust for major differences in illumination angle and atmospheric effects, the number and form of independent variables qualifying for the destination models rarely varied from those observed in the source set.

4. In the final step, the destination model was applied to the appropriate portion of the destination scene. Once again, the forest/non-forest mask was needed to eliminate non-forest pixels from the analysis. Once both models had been applied, the source and destination maps could be merged together to form a seamless extension of the predicted attribute.

The procedure described above differs from Cohen *et al.'s* in two important respects. First, all of the imagery was stratified by natural region in order to refine the creation of source models and limit the inappropriate extension of destination models. The original procedure described by Cohen *et al.* (2001) used un-stratified Landsat scenes as model elements, and the authors observed instances where unique vegetation conditions lead to sub-optimal results. The same might be the case in boreal forest, parkland, and grassland portions this study area, which received models derived from adjacent foothills natural regions, due to a lack of ground points within these natural regions.

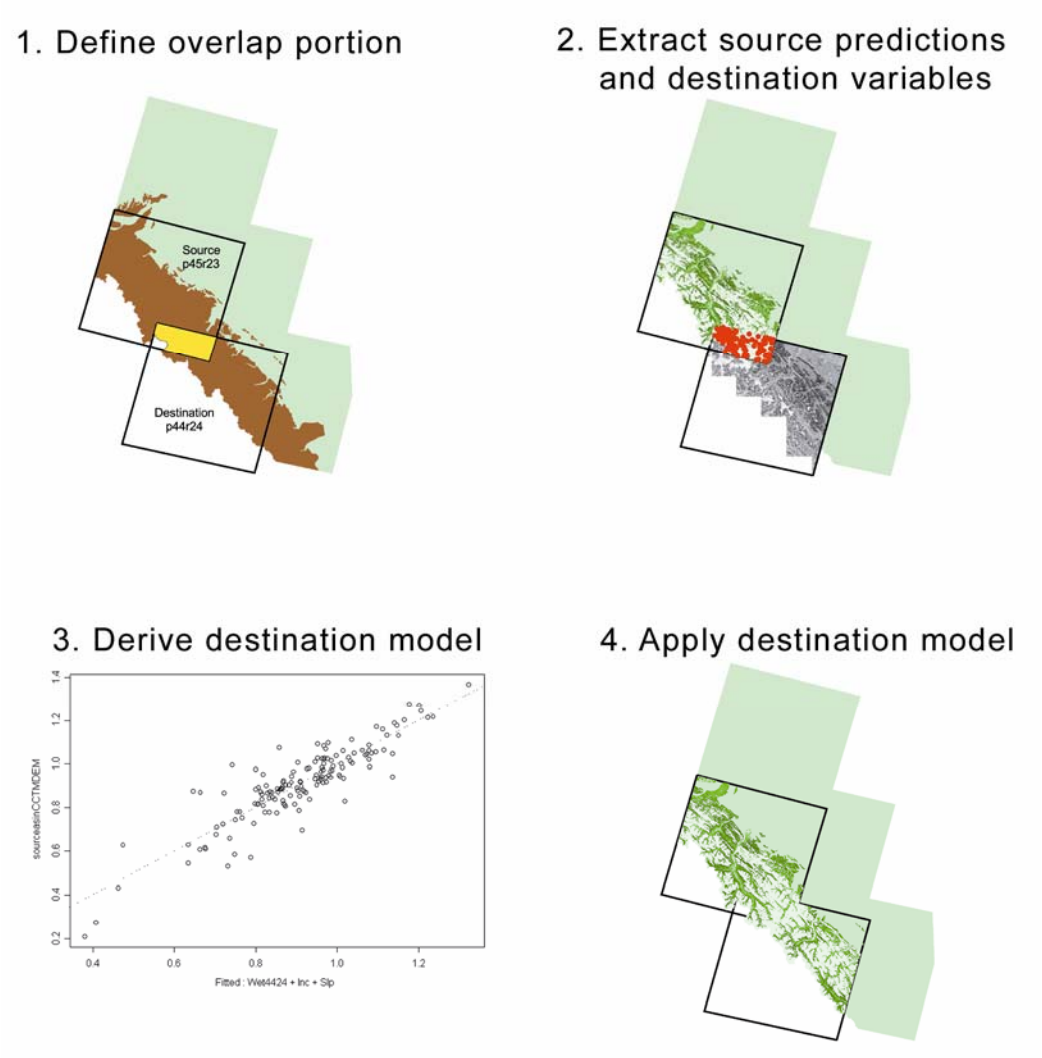

Figure 4-12: Major steps in model extension procedure.

The second procedural difference between the Cohen method and the current technique involves the extraction of sample data for developing the destination models. Cohen *et al.* masked all the pixels for each given integer in the model range (e.g. 6% crown closure, 7% crown closure, 8% crown closure, etc.) and derived mean values for each of the explanatory variables in the overlap portion of the imagery. By doing this, the authors ensured the inclusion of training data across the full range of the source attribute, but assumed that the mean values were good representatives of the explanatory

conditions. By employing random sample techniques, it was thought that a training set that better captured the true variance observed between the two scenes could be developed, which would lead to more consistent transformation functions.

The combination of natural region stratification and per-scene model extension meant that coverage of the entire study area required adopting a piece-wise strategy of deriving and assembling eight sub-models per attribute: four source pieces and four destination pieces (Figure 4-13). The Rocky Mountain region piece labelled 8 in the figure came from path 43, row 24, which did not physically overlap with any other Rocky Mountain source scene, requiring the execution of a *double extension* from p45r23 to p44r24 (piece 1 to piece 6), then p44r24 to p43r23 (piece 6 to piece 8). The small portion of Rocky Mountain region occurring in path 45, row 23 did not contain enough overlap area to create a stable destination model, so the Foothills model was simply applied from piece 5.

4.2.2.3 Error Characterization

The regression analysis techniques used to model crown closure and species composition provide some limited evaluation tools, such as standard errors and coefficients of determination. However, independent test sets provide a much more meaningful means of characterizing error. The reference data set falling within the source portions of the study area was divided randomly into portions for model building (80%) and model testing (20%) (Table 4-10). The source models were tested by applying them to the independent test data, providing new coefficients of determination calculated for the relationship between values observed in the field and predicted by the models.

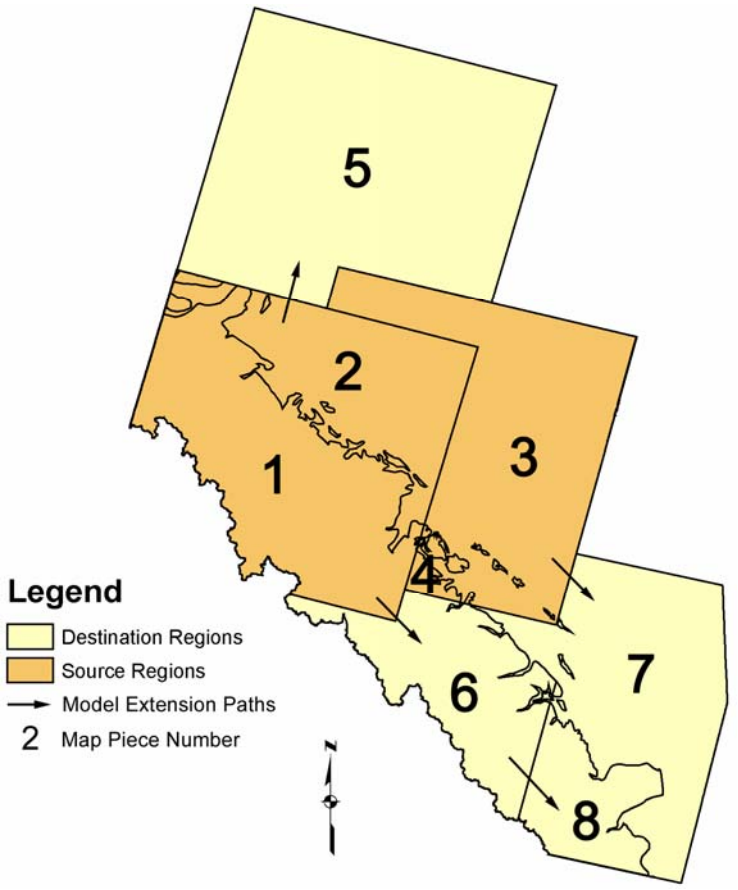

Figure 4-13: Map production strategy for crown closure and species composition.

Additional information regarding error patterns and prediction biases was gained from scatterplots and regression equations of measured versus predicted values.

While model performance in the source areas provides a general indication of quality for the final map product, it does not give a precise estimate of the performance of the aggregated models or incorporate errors from the adjacent destination scenes. One of the benefits of model extension is that any reference points that occur in the destination scenes are not used in the procedure, and are therefore available for map accuracy assessment. These points were added to the original independent test data set and used in a second round of error analysis across the entire study area. Finally, a series of

Table 4-10: Summary statistics for reference data used in model training and testing.

Attribute	Minimum	Maximum	Mean	Standard Dev.	Number
Model Building					
Crown Closure – Mountains	10	92	60.3	21.3	69
Crown Closure – Foothills	8	96	68.5	24.1	150
% Conifer – Mountains	0	100	93.6	22.1	41
% Conifer – Foothills	0	100	65.2	39.9	137
Model Testing					
Crown Closure – Mountains	10	89	58.1	25.2	32
Crown Closure – Foothills	6	96	70.0	23.5	70
% Conifer – Mountains	28	100	87.5	23.5	13
% Conifer – Foothills	0	100	63.4	40.3	50

categorized maps were produced mimicking those that might be generated by end users, both to demonstrate the flexibility of the continuous-variable products and track their categorical accuracy at different levels of detail. Contingency tables and standard accuracy statistics (% correct, Kappa, Weighted Kappa) were to judge the quality of the various map configurations produced under two-, three-, and four-class scenarios (Table 4-11).

Table 4-11: Two-, three-, and four-class configurations of crown closure and species composition used for error characterization.

	Crown Closure (% Closed)	Species Composition (% Conifer)
2-Class	0-50; 51-100	0-50; 51-100
3-Class	0-50; 51-70; 71-100	0-20; 21-79; 80-100
4-Class	0-30; 31-50; 51-70; 71-100	0-20; 21-50; 51-79; 80-100

4.2.3 Leaf Area Index

Leaf area index (LAI) represents the amount of leaf surface per unit ground area, and is a key parameter related to a broad range of biological and physiological processes, including photosynthesis, respiration, transpiration, hydrology, carbon and nutrient cycling (Law and Waring, 1994). Since LAI is a required input to many climate and ecological models (e.g. Sellers *et al.*, 1986; Running and Coughlan, 1988; Bonan, 1993; Dickinson *et al.*, 1993) its derivation stands out as one of the most common contemporary remote sensing tasks (e.g. Curran *et al*, 1992; Chen and Cihlar, 1996; White *et al.*, 1997; Turner *et* al., 1999; Pu and Gong, 2004). Unfortunately, as is the case with many quasi-ubiquitous science terms, the exact definition is more complicated than it may first appear. LAI was initially defined by Watson (1947) as the total one-sided leaf area per unit ground area. For broad-leafed vegetation, this definition is generally appropriate, since both sides of the leaf have roughly the same area. However, if leaves are round, bent, rolled, or wrinkled, the one-sided area is difficult to define. In order to address this problem, several authors have proposed the concept of projected leaf area (e.g. Bolstad and Gower, 1990; Smith, 1991), but the projection coefficient is highly dependant on the shape and orientation of the leaves. Chen and Black (1992) summarized the issues surrounding LAI of non-flat leaves and suggested that half the total leaf area was a more appropriate foundation for the index, since it has a strict physical foundation with important biological implications (e.g. biomass, gas exchange). While examples of all three LAI definitions are still commonly encountered in the literature, the Chen and Black definition – one half the total leaf area per unit ground area – is the most widely accepted (Fassnacht, *et al.*, 1994; Stenberg *et al.*, 1994).

There are several techniques for measuring LAI directly, including manual harvest and litter traps (Chason, *et al.*, 1991; Rhoades *et al.* 2004), but these methods are far too time-consuming and labour-intensive to be used in operational field campaigns concerned with characterizing detailed spatial and temporal dynamics over large areas. Indirect measurement based on allometric relationships between LAI and sapwood area – the *pipe model* theory (Shinozaki *et al.*, 1964a,b) – have been used successfully in several studies (e.g. Waring *et al.*, 1982; Wulder *et al.*, 1998; Meadows and Hodges, 2002). However, the technique relies on site-specific allometrics (Mencuccini and Grace, 1995), and is limited by several potential inaccuracies, including sapwood measurement errors, allometric non-linearity in large trees (Law *et al.*, 2001), and seasonal variability in the sapwood-LAI relationship (Le Dantec *et al.*, 2000).

Optical devices that measure the transmission of photosynthetically active radiation (PAR) through a plant canopy compose an alternative set of strategies for the indirect measurement of LAI (Jonckheere *et al.*, 2004). These techniques operate on the observation that the absorption of PAR by leaves in a plant canopy can be modelled by the Beer-Lambert law: an empirical equation that describes the exponential decay of light through a solution. LAI is related to PAR below the canopy (Q_i), PAR above the canopy (Q_o), and an extinction coefficient (k) by the equation

$$LAI = -\ln(Q_i / Q_o) / k$$

Equation 4-11

The simplicity of the underlying theory makes estimates of LAI relatively easy to obtain in the field. The gap fraction – Q_i/Q_o – can be measured or estimated with a

variety of instruments, including the Accupar Ceptometer and the LI-COR LAI-2000. The extinction coefficient for the canopy must be known or estimated. Jarvis and Leverenz (1983) reported extinction coefficients for 13 needle- and broad-leafed tree species between 0.28 to 0.65; canopies with spherical (random) distributions of leaf inclination angles are well-approximated with an extinction coefficient of 0.5 (Degagon Devices, Inc., 2001).

The assumption of randomly distributed foliage – typical of all techniques based on gap fraction analysis – is commonly violated. The spatial and angular distribution of leaves is often clumped, and optical instruments are unable to distinguish photosynthetically active leaf tissues from stems, branches, boles, flowers, and other non-leaf plant elements that might be present in the canopy (Jonkheere *et al.*, 2004). Chen and Cihlar (1995) used the term "effective LAI" (LAI_e) to describe such estimates, replacing earlier terminology such as "plant area index" (Neumann *et al.*, 1989) and "foliage area index" (Welles and Norman, 1991). While estimates of true LAI can be obtained from LAI_e measurements through *clumping index* corrections obtained with instruments, such as the TRAC, designed to quantify the effects of non-random canopy distribution (e.g. Hall *et al.*, 2003), the extra costs in terms of instrumentation and observation time place this additional step beyond the reach of many large-area studies. Chen and Cihlar (1995) argued that LAI_e is an intrinsic attribute of plant canopies in its own right, and since it is easier to measure and more highly correlated with remote sensing VIs, should be the preferred value for many applications.

4.2.3.1 Ground Measurement and Model Development

Ground observation of LAI and subsequent model development activities were designed to (i) characterize the structure and variability of LAI_e across two important time periods related to grizzly bear habitat use, and (ii) investigate the extent to which these patterns could be characterized with geospatial techniques. LAI is a dynamic parameter that exhibits substantial seasonal fluctuations (Welles, 1990; Curran *et al.*, 1992), due in large part to pronounced changes in herbaceous understorey abundance (Badhwar *et al*., 1986). For many applications, these understorey or *background* effects are considered unwanted noise that interferes with the desired quantity: the LAI of the overstorey canopy. Chen and Cihlar (1996), for example, stated a preference for using Landsat images acquired in the late spring in order to minimize the effects of understorey growth on remote sensing observations. Several studies have experimented with mid-infrared correction factors designed to reduce the effects of background "contamination" (e.g. Huete, 1988; Spanner *et al.*, 1990; Qi *et al.*, 1994). Nemani *et al.* (1993) described a mid-infrared correction factor, *c*, designed to compensate for variations in understorey reflectance:

$$c = 1 - \frac{(MIR - MIR_{\min})}{(MIR_{\max} - MIR_{\min}}$$

Equation 4-12

where MIR_{min} and MIR_{max} are middle infrared radiances from completely closed and completely open canopies from the working image. The correction factor can be applied to a standard VI such as NDVI in the fashion

$$NDVI_c = \frac{NIR - RED}{NIR + RED} * \left[1 - \frac{(MIR - MIR_{\min})}{(MIR_{\max} - MIR_{\min})} \right]$$

Equation 4-13

The theory is that mid-infrared reflectance changes in response to canopy closure (Butera, 1986; Baret *et al.*, 1988), and that the correction factor acts as a scalar for canopy closure, scaling down VI response in open canopies dominated by contributions from the understorey.

It is interesting to speculate that the same background "contamination" that some authors have attempted to eliminate with mid-infrared correction factors (e.g. Brown *et al.*, 2000; Pocewicz *et al.*, 2004) may well represent important wildlife habitat information such as seasonal food sources and ground cover in the understorey. Rather than discarding this information, it would seem desirable to investigate the feasibility of separating the understorey contribution from the overall LAI_e signal and preserving it for subsequent habitat analysis. In addition, this research also attempted to track changes in LAI across the growing season in an attempt to capture phenological changes that may represent an important facet of vegetation dynamics and a key component of the final information base.

Accupar ceptometers were used to obtain APAR measurements at 76 locations south of Hinton and Edson in the central portion of the study area (Figure 4-14). Ground stations were visited twice during the 2002 field season: once in the late spring/early summer period from June 19 to July 5, and again in the late summer period from August 14 to September, roughly matching the coincident Landsat 7 ETM+ scenes acquired on

June 13 and August 23. At each visit, measurements taken at 1.3 metres and ground level were used to characterize canopy LAI_e (LAI_{eCan}) and total LAI_e (LAI_{eTot}), respectively.

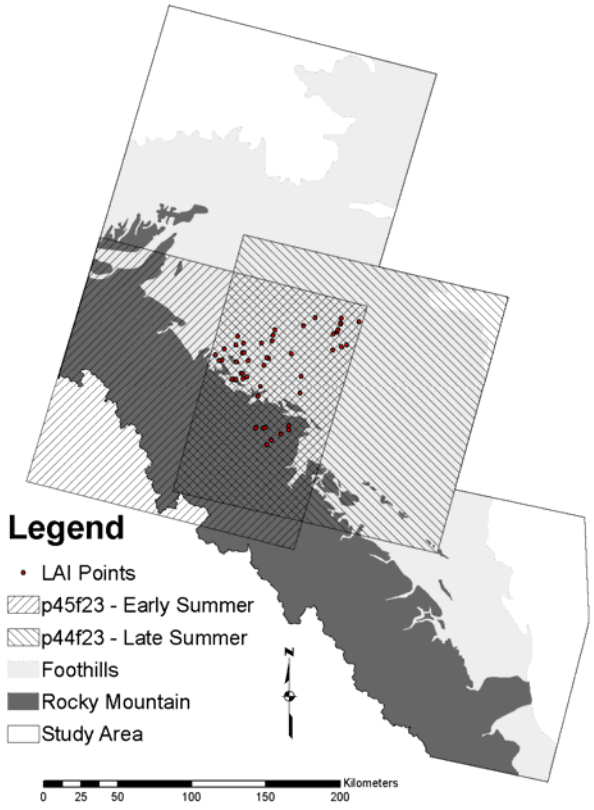

Figure 4-14: Location of field points used in early- and late-summer LAI_e modelling.

AccuPAR PAR-80 Ceptometers are composed of 80 adjacent 1 cm^2 PAR instruments distributed along a bar. A data logger within the sensor records mean PAR values measured along the bar as well as the percentage cover of sunflecks. The sunfleck data can be used to measure canopy gap fraction directly (e.g. Barradas *et al.*, 1998), but the technique is not suitable for use in coniferous forests, where the penumbral effect – partial shadows between regions of complete sunlight and complete shade cast by needles

from tall canopies – makes sunflecks difficult to distinguish (Jonckheere *et al.*, 2004). Estimating gap fraction based on transmitted PAR inversion is much more reliable under most conditions (Normal and Jarvis, 1974). Under this scenario, LAI is calculated as

$$LAI = \frac{\left[\left(1 - \frac{1}{2K}\right) f_b - 1\right] \ln \tau}{A(1 - 0.47 f_b)}$$

Equation 4-14

where f_b is the fraction of incident PAR that is beam, K is the extinction coefficient, and τ is the ratio of PAR measured below the canopy to PAR above the canopy. A is calculated as

$$A = 0.283 + 0.785a - 0.159a^2$$

Equation 4-15

where a is the leaf absorptivity in the PAR band, and is assumed to be 0.9 (Decagon Devices, Inc., 2001). The extinction coefficient, K, is calculated as

$$K = \frac{1}{2\cos\theta}$$

Equation 4-16

where θ is the zenith angle of the sun, in radians. The estimates of PAR necessary to calculate τ were acquired by ceptometer measurements collected within field sample plots and an additional reading taken in the middle of a clearing at least 1.5-times the height of the canopy – often a nearby road or well site. The fraction of the incident PAR that is beam, f_b, was estimated by taking an additional *above canopy* PAR reading with the

ceptometer wand shaded by an arm held one metre above the instrument. Under diffuse light conditions, f_b=0 and equation 4-13 simplifies to

$$LAI = \frac{-\ln \tau}{A}$$

Equation 4-17

Under these conditions, measurements of f_b and θ are unnecessary, and the procedure becomes quite simple.

Software necessary to perform the above series of calculations was written in the Cold Fusion programming language and served over the Internet in order to enable decentralized processing by multiple field personnel. The source code for the web application can be found in Appendix C. The application itself can be accessed at http://earthsystems.ucalgary.ca/Ceptometer.

Simple linear regression was used to model LAI_e as a function of spectral VIs derived from coincident Landsat imagery. The simple ratio (SR) and NDVI – both with and without the mid-infrared correction factor – made up the suite of explanatory variables used in model development. Exponential transformations were used to approximate the non-linear relationship expected between LAI_e and spectral VI (Chen and Cihlar, 1996; White *et al.*, 1995). Attempts were made to model LAI_{eCan} and LAI_{eTot} in both the early and late-summer time periods.

Although not a core component of this research, an additional set of analyses were performed to explore the ability of satellite sensors to tease apart the understorey component of LAI_e (LAI_{eUn}). The relative LAI_{eUn} – calculated as LAI_{eUn}/ LAI_{eTot} – was regressed against the mid-infrared correction factor, c. The work is the product of David

Couroux's B.Sc. Honour's thesis, and is reported more fully in Couroux (2004) and Couroux *et al.* (2005).

4.2.3.2 Model Application and Map Product Development

While the TM-derived LAI_e estimates produced interesting snapshots of vegetation phenology at two key periods of the summer, the extent was limited to the relatively small portion of the study area covered by the two specific Landsat scenes. The second phase of the process involved using MODIS data to expand the estimates over the entire study area and across additional time frames. Lacking the field measurements required to characterize LAI_e over a 250-metre pixel, the TM-based models were used to scale up estimates to the resolution of MODIS. This was accomplished by re-sampling the Landsat-derived estimates of LAI_e to a 250-metre grid using bilinear interpolation, then regressing the modelled values of LAI against the MODIS VI products. The strategy for matching *source* TM models with *destination* MODIS models was similar to that employed in model extension for crown closure and species composition: a random sample of 500 points was used to extract source LAI_e values and destination VIs in order to construct the statistical model. The resulting coefficients were then applied to the destination scene in order to estimate LAI_e across the entire study area.

Chapter 5: Remote Sensing Map Production - Results and Discussion

5.1 Digital Map Products

5.1.1 Land Cover

The contingency matrix describing the results of the level I classification is shown in Table 5-1. eCognition and the object-oriented approach to land cover classification proved very effective for performing the relatively simple task of separating vegetation and shadow from non vegetation, with an overall accuracy of 99% (Kappa=0.975). The only errors occurred in the alpine zone of the Rocky Mountain region, where two thinly vegetated alpine meadows were mis-classified as rock. Since the Vegetation class includes all terrain with greater than 6% green vegetation cover, a certain amount of confusion amongst thinly vegetated and non-vegetated sites was expected.

Table 5-1; Land cover level I contingency matrix.

		Observed			
		Vegetation & Shadow	No Vegetation	TOTAL	USER'S
Predicted	Vegetation & Shadow	184		184	100%
	No Vegetation	2	46	48	96%
	TOTAL	186	46	232	
	PRODUCER'S	99%	100%		

Overall accuracy: 99.1%; Kappa: 0.975

The level II land cover results are summarized in Table 5-2. Once again, the overall accuracy is quite high, at 94% (Kappa=0.911). Of the individual classes, only shrub generated substantial amounts of confusion, with a producer's accuracy of just 74%. Inspection of previous field records revealed common field classification errors between Shrub and Herbaceous classes – particularly in the abundant wetland zones in the northern and central portions of the study area. While most of these errors were corrected for this exercise, they illustrate the confusing array of physiographic conditions (and resulting spectral response patterns) observed in this land cover category. The Herbaceous class produced accuracies in the low 80% range. Part of this is due to the confusion with Shrub already discussed; other minor discrepancies occurred in the transition zones with Trees and Barren Land in the alpine zone. All of the non-vegetated categories were well separated, benefiting both from clear cut spectral response patterns (e.g. Snow/Ice, Barren Land) and convenient use of topographic decision rules (Water, Shadow).

Table 5-2: Land cover level II contingency matrix.

		Observed									
		Trees	Herbs	Shrubs	Shadow	Water	Barren Land	Snow/Ice	Cloud	TOTAL	USER'S
Predicted	Trees	119		5						124	96%
	Herbs	1	25	4						30	83%
	Shrubs		2	25						27	92%
	Shadow				3					3	100%
	Water					10				10	100%
	Barren Land		2				22			24	92%
	Snow/Ice							7		7	100%
	Cloud								7	7	100%
	TOTAL	120	29	34	3	10	22	7	7	232	
	PRODUCER'S	99%	82%	74%	100%	100%	100%	100%	100%		

Overall accuracy: 94.0%; Kappa: 0.911

The contingency matrix for land cover level III is shown in Table 5-3. The main objective of this level of analysis was the separation of wetland vegetation surfaces from upland – an important distinction from a habitat perspective. From a producer's standpoint, this goal was largely achieved, with class accuracies for Upland/Wetland Trees/Herbs all above 83%. However, the inclusion of the new wetland classes introduced substantial accuracies of commission, with user's accuracies of just 53% and 71% for Wetland Trees and Wetland Herbs, respectively. Wetland trees displayed confusion with upland trees and shrubs. The upland/wetland trees confusion reflects the spectral similarity of high-crown-closure treed wetlands and adjacent uplands; the shrub

issue has already been discussed. Wetland Herbs displayed confusion with Shrubs, and – somewhat surprisingly – Upland Trees. The Wetland Herb class displayed a significant amount of spectral variance across the image, reflecting the different types of fens, bogs, marshes, and peripheral shoreline areas that constitute this category. Since I had a relatively small number of test sites for the two wetland categories, these errors did not substantially impact the overall classification statistics (91.8% overall accuracy; Kappa=0.904). However, the tendency to over-classify the wetland portions of the study area is documented in the accuracy analysis and should be borne in mind.

Table 5-3: Land cover Level III contingency matrix.

		Observed											
		Upland Trees	Wetland Trees	Upland Herbs	Wetland Herbs	Shrubs	Shadow	Water	Barren Land	Snow/Ice	Cloud	TOTAL	USER'S
Predicted	Upland Trees	106	1			2						109	97%
	Wetland Trees	4	8			3						15	53%
	Upland Herbs			20		3						23	87%
	Wetland Herbs	1			5	1						7	71%
	Shrubs			2		25						27	93%
	Shadow						3					3	100%
	Water							10				10	100%
	Barren Land			2					22			24	92%
	Snow/Ice									7		7	100%
	Cloud										7	7	100%
	TOTAL	111	9	24	5	34	3	10	22	7	7	232	
	PRODUCER'S	95%	89%	83%	100%	74%	100%	100%	100%	100%	100%		

Overall accuracy: 91.8%; Kappa: 0.904

Colour map composites showing each level of the classification hierarchy are shown in Figure 5-1.

5.1.2 Crown Closure

5.1.2.1 Source Models

Candidate models of crown closure were constructed from three groups of variables: TM data alone (CCTM), DEM data alone (CCDEM), and TM plus DEM data together (CCTMDEM). Summaries of each of each of these models for the *source* areas are shown in Table 5-4. Since models dealing with spectral data were constructed on a per-scene basis, there are four *source* areas originating from the Phase 2 study area of the Grizzly Bear Project: the Rocky Mountain and Foothills regions of p44r23 and p45r23. Models based on DEM variables alone are free of WRS scene constraints, so there are only two *source* models covering the entire Foothills and Rocky Mountain portions of the study area, respectively.

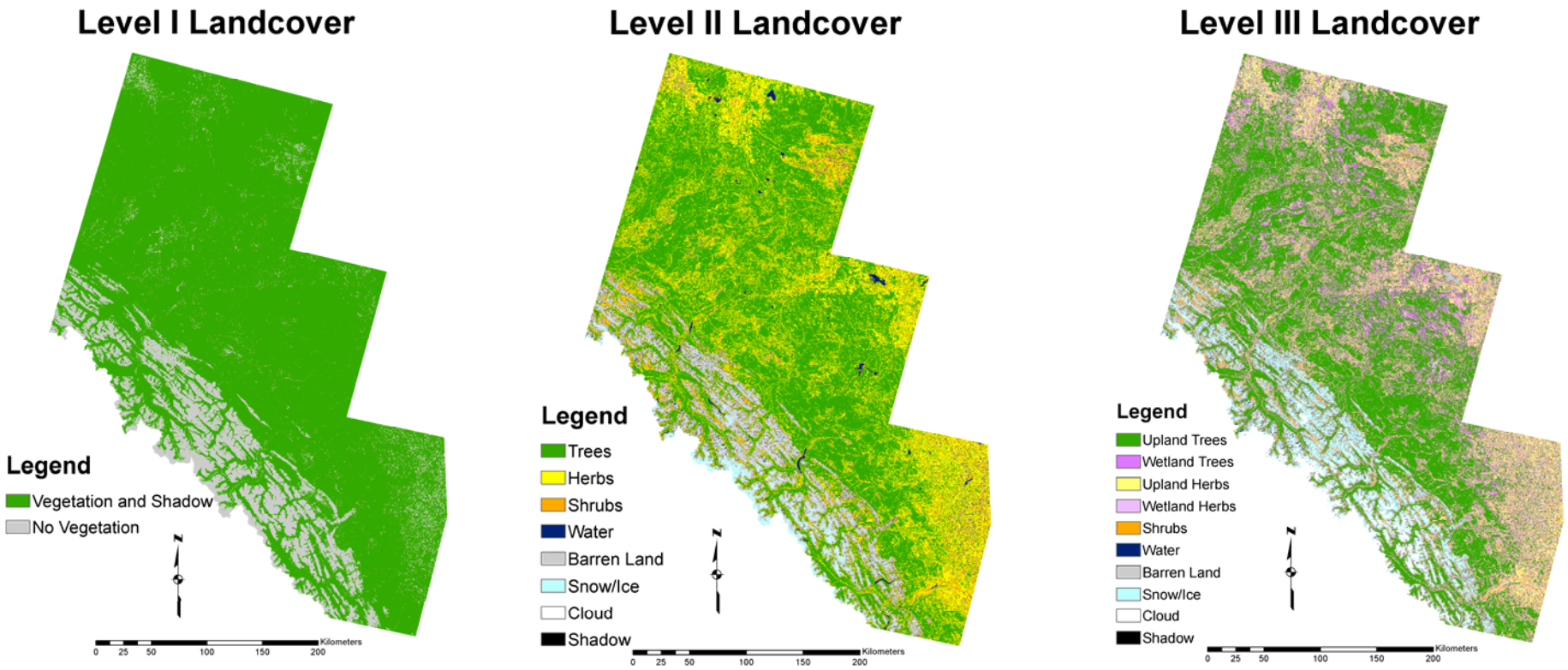

Figure 5-1: Land cover levels I, II, and III.

Table 5-4: Summaries of crown closure candidate models in the source areas.

TM			
Model	**Equation**	**r^2**	**Standard Error**
p45r23 Foothills	Y=(0.0289*Wet)-4.3681	0.49	0.1804 on 44 D.F.
p45r23 Mountains	Y=(0.0226*Wet)-3.1279	0.36	0.1954 on 82 D.F.
p44r23 Foothills	Y=(0.0378*Wet)-5.9808	0.60	0.1796 on 71 D.F.
p44r23 Mountains	Y=(0.0228*Wet)-3.2287	0.40	0.1868 on 68 D.F.
DEM			
Model	**Equation**	**r^2**	**Standard Error**
Foothills	Y=(0.004*Slp)+0.8347	0.01*	0.2733 on 99 D.F.
Mountains	Y=(0.0135*Slp)+0.7403	0.12	0.2484 on 98 D.F.
TMDEM			
Model	**Equation**	**r^2**	**Standard Error**
p45r23 Foothills	Y=(0.0326*Wet)+(0.0148*Inc)-5.6048	0.56	0.1692 on 43 D.F.
p45r23 Mountains	Y=(0.0213*Wet)+(0.0079*Inc)+(0.0088*Slp)-3.3643	0.50	0.1758 on 80 D.F.
p44r23 Foothills	Y=(0.0418*Wet)-(0.0002*Elev)+(0.0137*Inc)-6.9502	0.65	0.1685 on 69 D.F.
p44r23 Mountains	Y=(0.0191*Wet)-(0.0057*Inc)+(0.0119*Slp)-2.895	0.55	0.1638 on 66 D.F.

* Not significant at $p<0.05$

All four of the models based on TM data alone were statistically significant ($p<0.001$) in both of the source areas, with coefficients of determination ranging from 0.36 to 0.6. In each case, the minimal adequate model contained only one linear variable: wetness. While experiments were performed with quadratics and interaction terms in each of the candidate models, no consistent evidence could be discovered to suggest that these effects had a statistically significant impact on model performance. The positive relationship between wetness and crown closure is consistent with observations made in

previous studies (Hunt, 1991; Cohen and Spies, 1992; Cohen *et al.*, 1995) that suggests wetness indices and other measures that contrast middle-infrared reflectance are related to the structural complexity of the forest canopy and the optical depth of water in leaves. That relationship appears to extend to crown closure, which is an indirect measure of the amount of canopy in a pixel. Coefficients of determination and standard errors indicate that spectral models of crown closure from the Foothills region explained generally more of the observed variance than those in the Rocky Mountain region. This result is not unexpected, given the more pronounced influence of topography in high-relief terrain both on vegetation structure on the ground and spectral response in the image. The *topographic effect* – the deleterious effects of topography on image analysis – is a well-documented but incompletely understood phenomenon that image analysts find very difficult to account for (Kimes and Kirchner, 1981; Dymond, 1992; Dubayah and Rich, 1995). While strategies for ameliorating some of these effects do exist (e.g. Civco, 1989; Richter, 1997; Riano *et al.*, 2003) none of them were implemented in this project; a factor that may have limited the effectiveness of spectral models, particularly in the high-relief portions of the study area.

Of the two models based on DEM variables alone, only the Rocky Mountains one was statistically significant, with a coefficient of determination of 0.12. Slope was the only variable that qualified for this relatively weak model, indicating a generally positive relationship with crown closure possibly reflected in the occurrence of open forests and wetlands in the flat riparian zones of some alpine valleys. The CCDEM model for the Foothills region generated a statistically insignificant coefficient of determination of just

0.02, illustrating the inability of topographic variables alone to accurately account for the full range of crown closure variability across that terrain.

In all cases, the lowest standard errors and highest coefficients of determination were achieved with models constructed from the combined CCTMDEM variable set. The Foothills models both displayed positive relationships with wetness and incidence angle, with the p44r23 model also including a weak yet statistically significant negative contribution from elevation. Both Rocky Mountain models included positive contributions from wetness and slope, matching some of the trends noted previously. Incidence also qualified for both Mountain models – with a negative sign in p44r23 and a positive sign in p45r23.

While standard errors and coefficients of determination provide some information on the performance of candidate models, analyses involving independent test data are much more meaningful. The results of 2-, 3-, and 4-class crown closure classifications (Table 5-5) are summarized in Figure 5-2. The overall trends regarding model quality noted with the preliminary model statistics continue with the test data. Models constructed from DEM variables alone (CCDEM) contained almost no predictive value, with Kappa statistics <0.2, indicating results the same or just slightly better than random chance. The highest classification accuracies were generally produced by CCTMDEM models incorporating both spectral and topographic predictor variables; CCTM models tended to be slightly less accurate. As expected, crown closure in the two-class configuration (0-50%, 51-100%) produced the highest overall accuracies, generating *good* or *very good* (Table 5-6) Kappa scores of over 0.75 in all but one case. The lone exception was the CCTM model for p44r23 with a fair Kappa coefficient of 0.375 for the

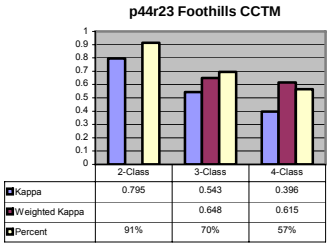

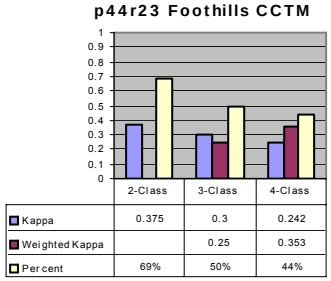

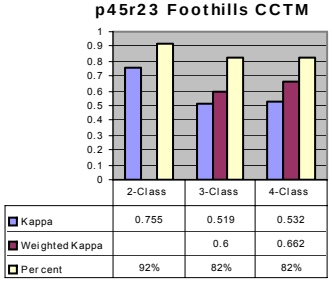

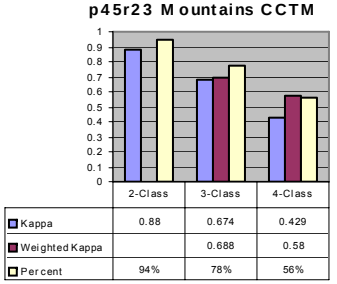

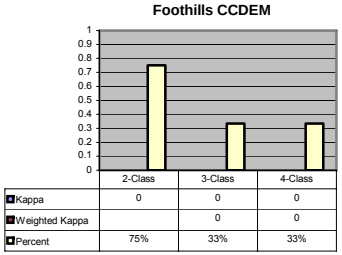

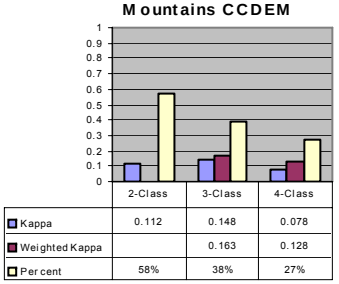

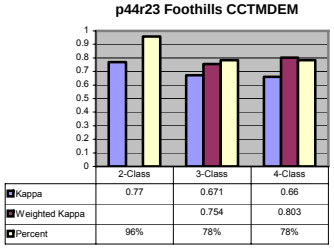

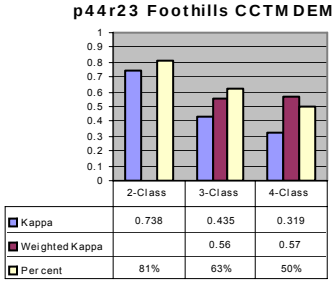

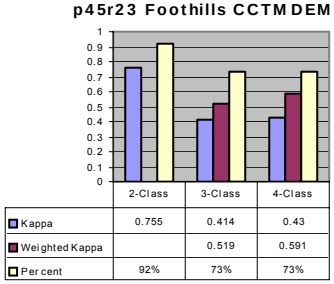

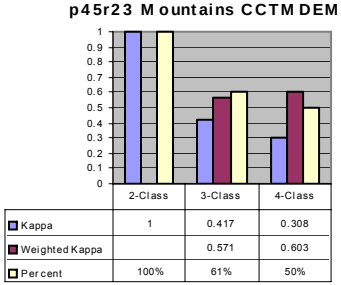

Figure 5-2: Kappa, weighted Kappa, and percent accuracies for classifications of three aggregate crown closure classes. 2-class (0-50%; 51%=100%), 3-class (0-50%, 51-70%, 71-100%), and 4-class (0-30%, 31-50%, 51-70%, 71-100%).

two-class aggregate. The TMDEM model of the same region, however, increased Kappa to a more acceptable 0.738. Increasing the class count to three (0-50%, 51-70%, 71-100%) generally dropped classification accuracies into the *moderate* 0.4-0.6 Kappa range, while a four-class configuration based on the provincial AVI standard (0-30%, 31-50%, 51-70%, 71-100%) generally produced *fair* Kappa statistics in the 0.2-0.4 range. Once again, the models from the Foothills natural region tended to perform slightly better than those from the Rocky Mountains, perhaps reflecting the greater impact of topographically induced noise in the spectral variables. The weighted Kappa statistics reported for the three- and four-class configurations are all slightly higher than the basic Kappa scores, because the standard measure does not take into account the degree of disagreement between classes. Since the classes in these cases are ordinal – i.e. class D is closer to class C than class B – not all misclassifications are of equal severity. The weighted statistic takes these factors into account, and could be argued to provide a more meaningful measure of accuracy than the un-weighted score (Cohen, 1968).

Table 5-5: Crown closure class configurations used in source model testing.

Configuration	Classes
Two-Class	0-50%; 51-100%
Three-Class	0-50%; 51-70%; 71-100%
Four-Class	0-30%; 31-50%; 51-70%; 71-100%

Table 5-6: Level of agreement guidelines based on the Kappa statistic, after Altman (1991).

Agreement Rating	Kappa Coefficient Range
Poor	<0.2
Fair	0.21-0.4
Moderate	0.41-0.6
Good	0.61-0.8
Very Good	0.81-1.0

Some interesting observations regarding error patterns can be made from scatterplots of predicted versus observed crown closure summarized in Figure 5-3. An ideal model would produce a tight grouping along a trend line passing through the origin with a slope of 1 and a Y-intercept of 0. The lack of predictive capacity for the DEM models across the full range of crown closure observations is indicated by the nearly flat (0.003 and 0.014) slopes and large (51 and 56) intercepts. The models predict consistently high values of crown closure – producing accuracies in this range similar to those that would be expected from random assignments – and gross exaggerations in stands with low values. This trend of over-predicting crown closure in the low range is observed consistently throughout most the models, though not nearly so pronounced. The error structures of the TMDEM models are generally better than those produced from TM data alone, with slightly tighter groupings and trend lines closer to the ideal.

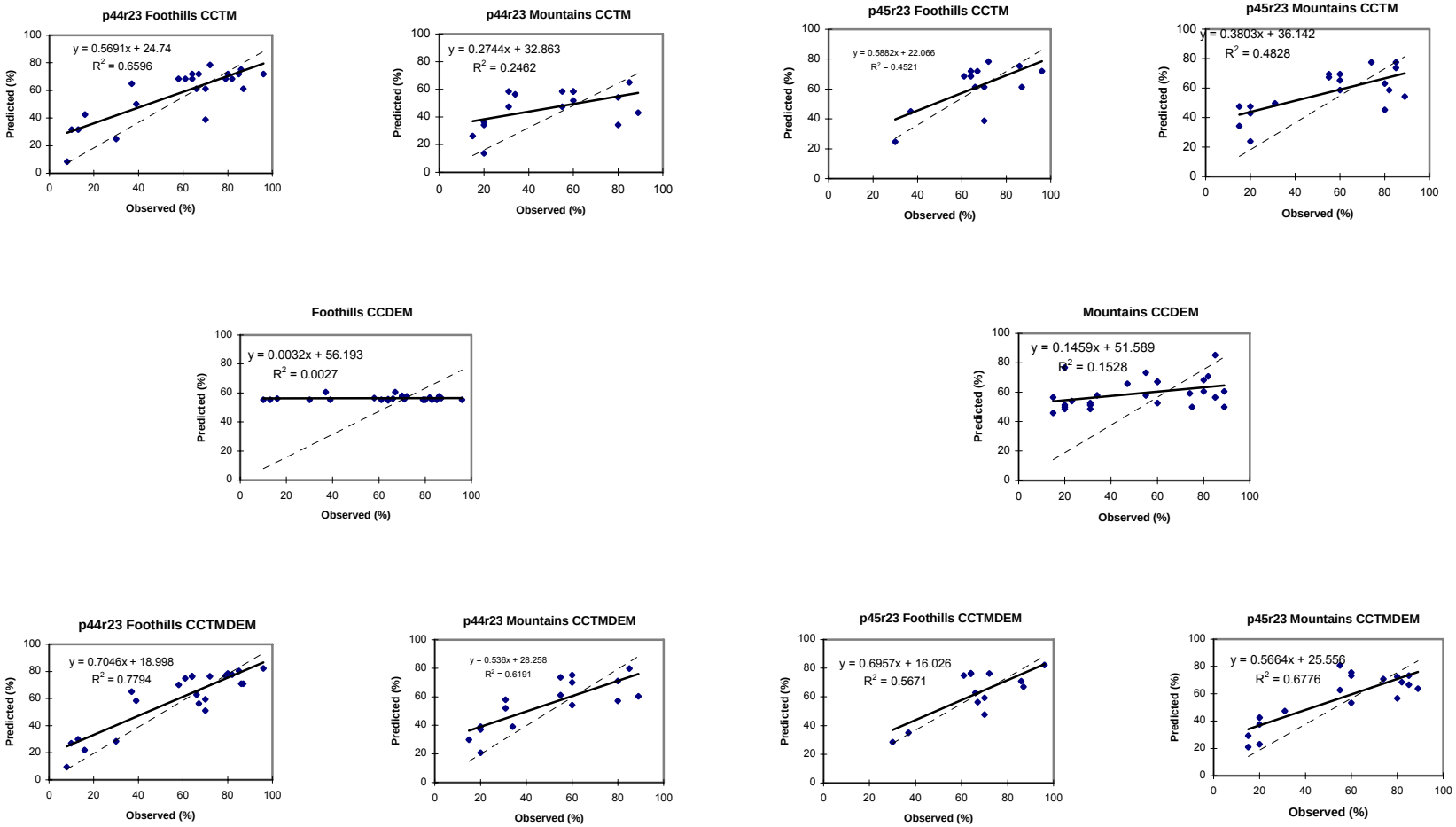

Figure 5-3: Crown closure model predictions versus field observations for independent test data in the source area

5.1.2.2 Destination Models and Model Extension

The explanatory variables in the destination scene models were identical to those qualifying for the source scenes with few exceptions (Table 5-7). The tasseled cap derivative wetness was the only explanatory variable included in the CCTM series, while CCTMDEM models in the Mountain region contained positive contributions from wetness, incidence, and slope. Wetness, and incidence angle both qualified for TMDEM variables in the Foothills region, with a small negative contribution coming from elevation in p43r24. It bears mentioning once again that both of the destination models in the Rocky Mountain natural region of p43r24 resulted from a *double extension*, since the area did not overlap either of the two Rocky Mountain source areas. In those cases, the destination model from the Mountain portion of p44r24 also served as the source model for p43r24.

The general quality of the model extension procedure is reflected in the difference statistics calculated in the overlap portions of the map. In all cases (Table 5-7 again) the mean and median difference of crown closure estimates from source and destination models was between +/– 1 %. Visual evidence of the technique's performance can be seen in the elimination of seam lines that affected draft versions of the crown closure map that attempted to apply model equations across orthomosaic scene boundaries (Figure 5-4). While the accuracy of the predictions remains a function of the quality of the source model, the integrity of the predictor variables, and the homogeneity of the ground scene, it seems clear that the stratified, per-scene approach to model building and extension has succeeded in solving the problem of creating seamless continuous-variable map products across large-area mosaics.

Table 5-7: Crown closure destination model summaries and difference statistics calculated for the overlap sections.

Crown Closure Destination Models			
TM			
Model	Equation	Mean Diff.	Median Diff.
p45r22 Foothills	Y=(0.0226*Wet)-3.6340	1	1
p44r24 Mountains	Y=(0.0154*Wet)-1.6389	1	0
p43r24 Foothills	Y=(0.0232*Wet)-2.9912	-1	0
p43r24 Mountains	Y=(0.0137*Wet)-1.1256	0	0
TMDEM			
Model	Equation	Mean Diff.	Median Diff.
p45r22 Foothills	Y=(0.0253*Wet)+(0.0130*Inc)-4.6591	0	0
p44r24 Mountains	Y=(0.0139*Wet)+(0.0045*Inc)+(0.0080*Slp)-1.6419	1	0
p43r24 Foothills	Y=(0.024*Wet)-(0.0001*Elev)+(0.0101*Inc)-3.3410	0	0
p43r24 Mountains	Y=(0.0117*Wet)+(0.0031*Inc)+(0.0073*Slp)-1.2373	-1	0

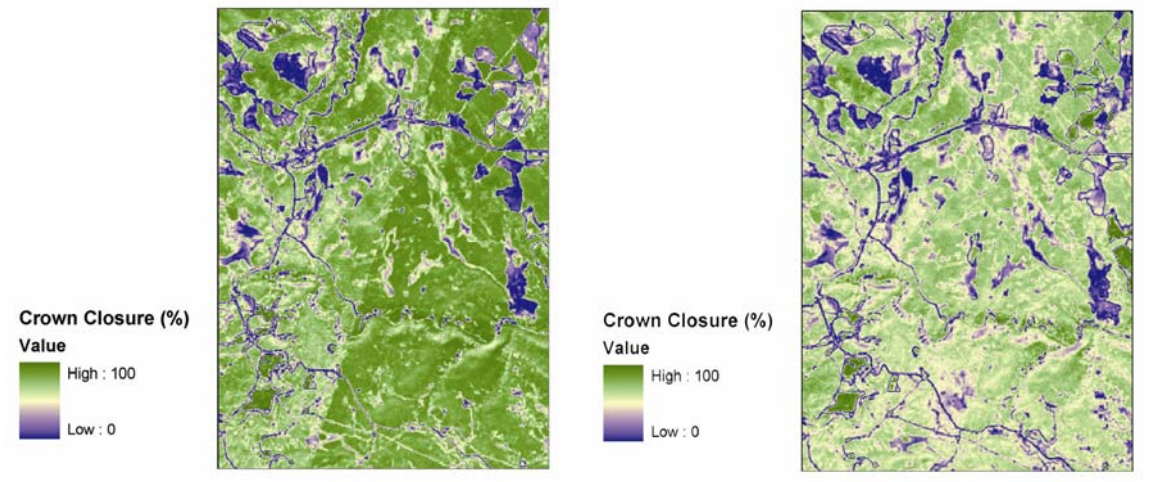

Figure 5-4: Seam line elimination from continuous-variable models. The map on the left was constructed using a single equation applied across an orthomosaic boundary. The map on the right was developed using stratified per-scene analysis and model extension.

5.1.2.3 Aggregate Map Composite

Summaries of the accuracies of 2-, 3-, and 4-class crown closure maps derived from TM, DEM, and TM-DEM variable sets are shown in Figure 5-5. The statistics were generated from independent test data not used in model construction, and include ground observations from three of the four destination scenes. No reliable field data from the Rocky Mountain portion of p43r24 was available – unfortunate, since this was the *double extension* portion of the map, and it would have been interesting to assess the accuracy of that area.

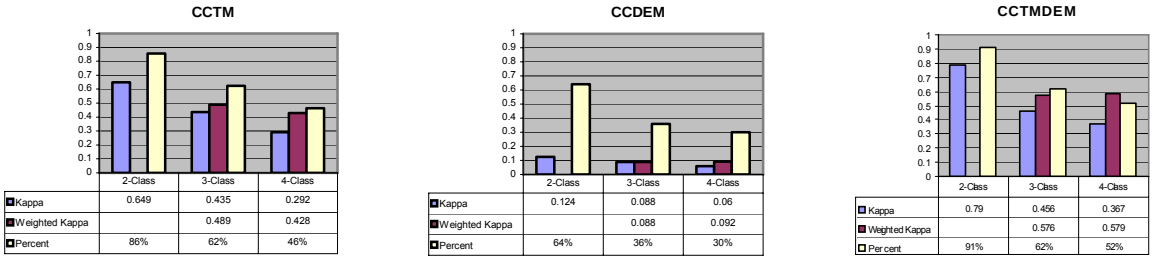

Figure 5-5: Kappa, weighted Kappa, and percent accuracy statistics of three aggregate crown closure classifications: 2-class (0-50%; 51-100%), 3-class (0-50%; 50-70%; 71-100%), and 4-class (0-30%; 31-50%; 51-70%; 71-100%).

The previous patterns noted within the source scenes continued when the model was extended over the entire map. The highest overall accuracies were produced with the combined CCTMDEM data set, with Kappa statistics ranging from 0.79 (91%) for two crown closure classes to 0.37 (52%) for the four-class set. CCTM models produced slightly lower accuracies, ranging from 0.65 (86%) to 0.29 (46%). Once again, the DEM models proved incapable of modelling crown closure beyond much more than chance

agreement, with Kappas ranging from 0.124 to 0.06. Error patterns shown in scatterplots of predicted versus observed crown closure for independent test points (Figure 5-6) once more reveal a tendency to over-predict crown closure values in the low range in both the CCTM and CCDEM models. The slightly tighter and more regular form of the CCTMDEM model's scatterplot reflects the higher accuracies observed in the Kappa statistics.

The final, continuous-variable crown closure map, based on combined spectral and topographic models developed across natural region-stratified source areas in the core of the study area and extended piece-wise across other scenes in the mosaic is shown in Figure 5-7. Statistical analyses using independent test sites suggested that this map is best used in an aggregate two-class configuration (Open: 0-50% and Closed: 51-100%), under which scenario we might expect very good accuracies in the 90% range (Kappa=0.8). A three-class configuration would be expected to yield moderately accurate results in the 65% (Kappa=0.5) range, while attempting to extract four crown closure classes would result in just fair accuracies around 50% (Kappa=0.4). Such a scenario might well be suitable if a little leeway regarding categorical precision is acceptable, since weighted Kappa statistics – those that account for ordered classes where a one-class disagreement is not penalized as severely as other more serious errors – suggest moderately accurate results in the Kappa=0.58 range with the four-class map. Regardless, the flexibility lies in the hands of the end user – to apply the product in the fashion that best suits the application.

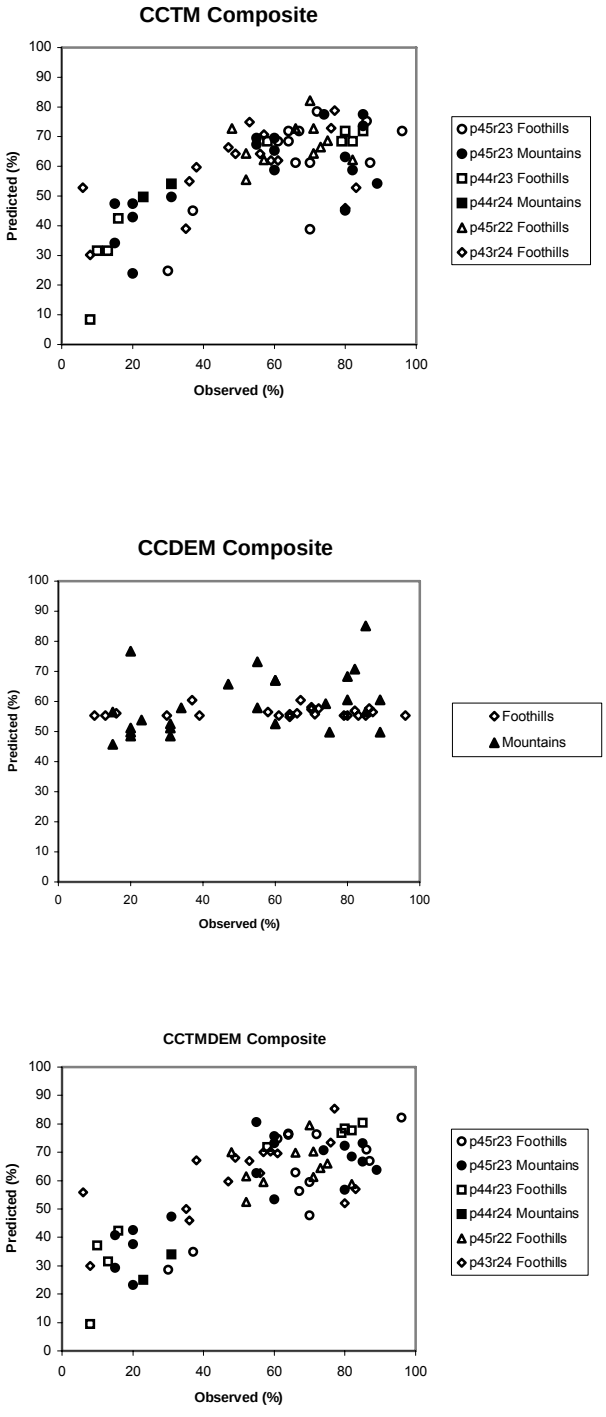

Figure 5-6: Crown closure model predictions versus field observations for independent test data.

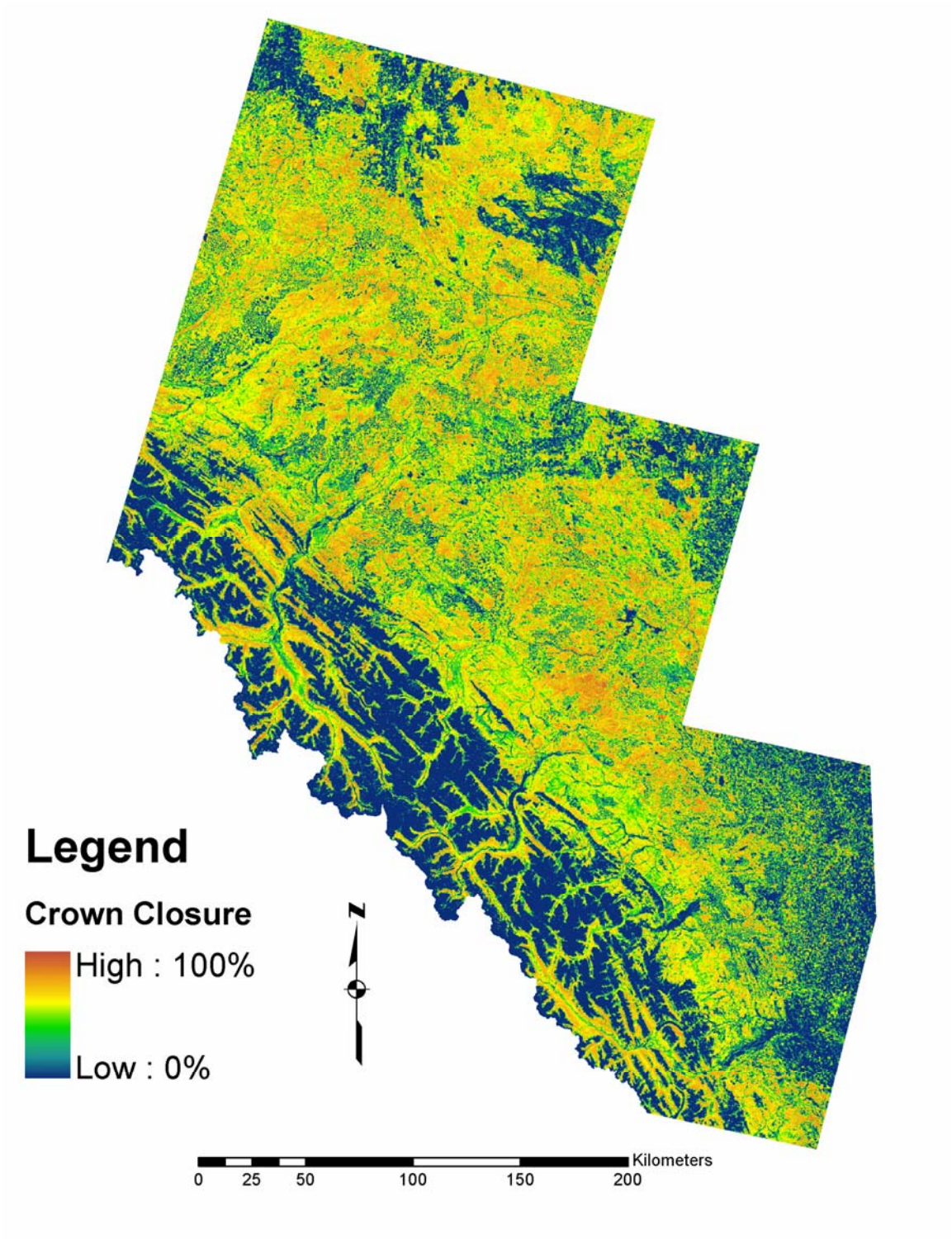

Figure 5-7: Continuous-variable map of crown closure modelled from spectral and topographic variables at 30-metre resolution. The product is a composite of CCTMDEM source models extended in a stratified piecewise fashion across the study area.

5.1.3 Species Composition

5.1.3.1 Source Models

As in the case with crown closure models in the previous sections, candidate models of species composition were constructed from three groups of variables: TM data alone (SCTM), DEM data alone (SCDEM), and TM plus DEM data together (SCTMDEM). Summaries of each of each of these models for the source areas are shown in Table 5-8. As with crown closure models, those dealing with spectral data were performed on a per-scene basis in order to avoid seam lines with the finished products. However, they were not stratified by natural region, since there were not enough points in the Rocky Mountains – particularly within broadleaf and mixed plots – to develop stable models. As a result, there are only two sources scenes for model development: p44r23 and p45r23. Models based on DEM variables alone are free of WRS scene constraints, so there is only one model, which covers the entire study area.

Of the three candidate models evaluated in this modelling exercise, the TMDEM models – those based on both spectral and topographic variables – consistently showed the greatest AIC support. All three of the topographic variables qualified for both source models, suggesting strong topographic controls on the distribution of broadleaf and coniferous and trees in the study area. The proportion of coniferous trees measured in the field displayed a direct relationship to DEM-derived measurements of elevation and incidence angle, and an inversely relationship to local slope. In western Alberta,

Table 5-8: Summaries of species composition candidate models in the source areas.

p45r23			
Model	**Equation**	**AIC**	**Residual Deviance**
SCTM	ln(p/1-p)=(0.4645376*Bright)-(0.4891548*Green)+(0.2949501+Wet)- 46.3816202	1017	920 on 189 D.F.
SCDEM	ln(p/1-p)=(0.005575367*Elev)-(0.076216613*Slp)-5.699852754	1032	1292 on 190 D.F.
SCTMDEM	ln(p/1-p)=(0.054441354*Bright)-(0.175900519*Green)+(0.003758458*Elev)-(0.045612475*Slp)+(0.120496764*Inc)-0.167521106	988	703 on 187 D.F.
Null Model			1663 on 192 D.F.
p44r23			
Model	**Equation**	**AIC**	**Residual Deviance**
SCTM	ln(p/1-p)=(-0.1213879*Green)-(0.1156707*Wet)+29.9484436	1086	800 on 203 D.F.
SCDEM	ln(p/1-p)=(0.005486834*Elev)-(0.106288433*Slp)-5.332853814	1114	1368 on 203 D.F.
SCTMDEM	ln(p/1-p)=(-0.142734694*Green)-(0.045642346*Wet)+(0.004178619*Elev)-(0.039307682*Slp)+(0.171034587*Inc)+7.178821814	1031	523 on 200 D.F.
Null Model			1688 on 205 D.F.

broadleaf trees are generally found in the lower elevations with gentle slopes and higher local incidence angles. Two spectral variables also qualified for the mixed models: brightness and greenness in p45r23 and greenness and wetness for p44r23. Both models displayed an inverse relationship between coniferous proportion and greenness, reflecting the fact that broadleaf-dominated pixels tend to be greener than their coniferous-dominated counterparts, likely due to the smaller amount of shadow in broadleaf stands. This is consistent with the findings of Cohen *et al.* (2001) in Oregon. Additional spectral patterns were less consistent, and likely reflect the variable nature of vegetation patterns observed across the very large study area.

The results of accuracy assessment involving independent test data arranged in two-, three-, and four-class species composition configurations (Table 5-9) are

summarized in Figure 5-8. Overall, the trends in these analyses reflect those noted with AIC and residual deviance in the preliminary model statistics. Models constructed from DEM data alone performed very poorly, producing Kappa and weighted Kappa statistics firmly in the *poor* range <0.2, indicating results very similar to those that could be expected from random assignment. As with the models describing crown closure, the highest classification accuracies were produced by CCTMDEM models that incorporated both spectral and topographic predictor variables. CCTM models produced from spectral variables alone tended to be slightly less accurate. As expected, the highest accuracies were achieved with the least-demanding two-class configuration (0-50%, 51-100%), with Kappa scores of 0.79 and 0.61 (i.e. *very good* and *good* according to Altman's (1991) guidelines summarized in Table 5-5) for p44r23 and p45r23, respectively. Kappa scores fell to *moderate* levels of 0.56 and 0.50 for the three-class configuration of 0-20% (pure conifer), 21-80% (mixed), and 81-100% (pure broadleaf) break points used in Phase I and II of the Grizzly Bear Research Program and published in Franklin *et al.* (2001). Similar *moderate* Kappa scores (0.55 and 0.45 for p44r23 and p45r23, respectively) were achieved in the more detailed four-class configuration. Weighted Kappa statistics that consider the non-ordinal nature of the three- and four-class crown closure configurations are all slightly higher than the basic Kappa scores, reflecting statistics that weight the severity of misclassifications (Cohen, 1968).

Table 5-9: Species composition class configurations used in source model testing.

Configuration	Classes
Two-Class	0-50%; 51-100%
Three-Class	0-20%; 21-80%; 81-100%
Four-Class	0-20%; 21-50%; 51-80%; 81-100%

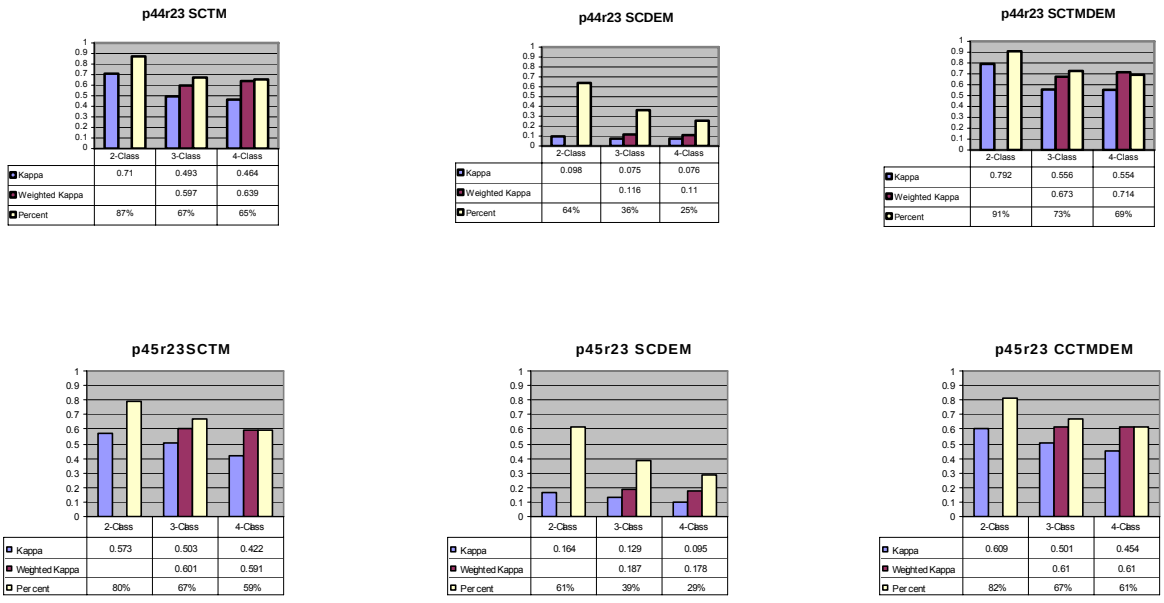

Figure 5-8: Kappa, weighted Kappa, and percent accuracies for classification of three aggregate species composition classes. Two-class (0-50%; 51-100%), three-class (0-20%; 21-80%; 81-100%), and four-class (0-20%; 21-50%; 51-80%; 81-100%).

Of some interest is the observation that models for the p44r23 source area performed somewhat better than those from p45r23. The same pattern was noted in the models for crown closure, and likely reflects the more serious influence of the topographic effect created by the rugged terrain in the western portion of the study area. Once again, these results suggest that future efforts to correct for topographic noise in the preprocessing phase would be worth investigating.

Scatterplots of predicted versus observed species composition for each variable set over the two source areas are shown in Figure 5-9. Once again, the lack of predictive capacity in DEM-based models alone for predicting species composition across large areas is graphically apparent. The error structure for SCTMDEM models are slightly better than their SCTM counterparts, but both models tend to over-predict the proportion of coniferous trees in some mixed stands. In other cases, pure coniferous stands – usually open stands with lush understories – display under-predicted coniferous proportions.

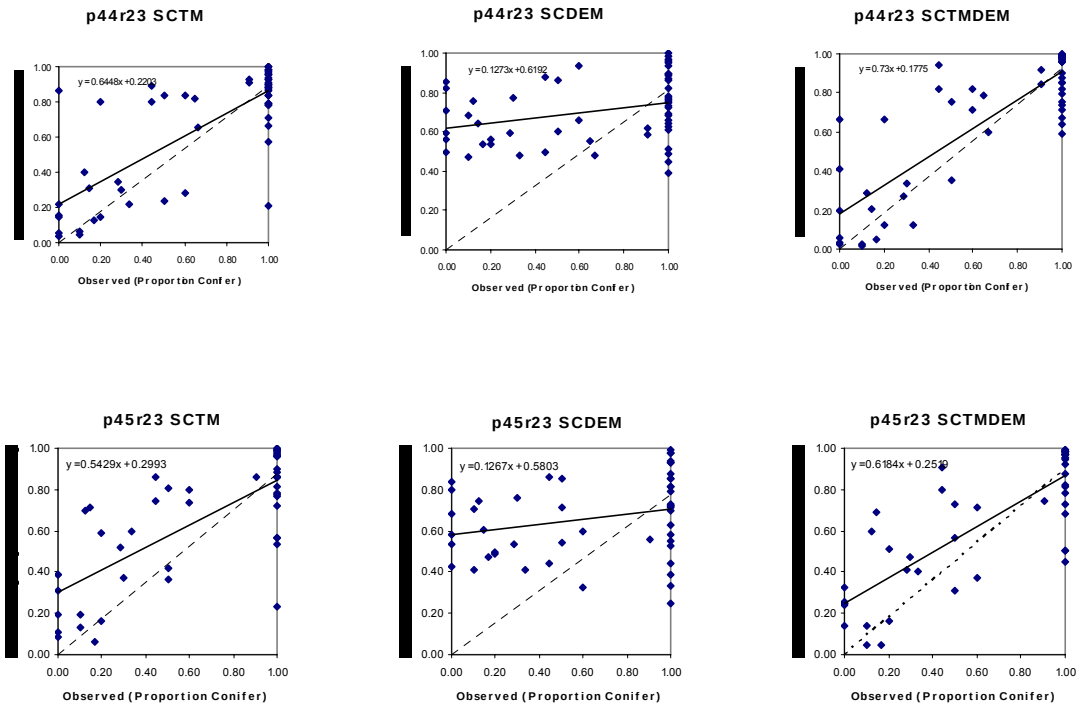

Figure 5-9: Species composition model predictions versus field observations for independent test data in the source area.

5.1.3.2 Destination Models and Model Extension

Table 5-10 summarizes the SCTM and SCTMDEM models for the destination scenes in the mosaic, as derived through model extension in the overlap portions of the study area. The pattern of explanatory variables qualifying for source and destination models for species composition were not as consistent as those observed in the crown closure case. Whether this suggests instability in the model extension or simply reflects the more complex nature of species composition patterns across the study area is unknown. Two of the tasseled cap variables qualified for each spectral model, but there are few discernible patterns. However, greenness was the only tasseled cap derivative to qualify for any of the SCTMDEM series of models, displaying once again the inverse relationship between greenness and proportion of coniferous trees noted in the two source areas. Also similar is the influence of topographic controls on species composition reflected in the consistent qualification of topographic variables in the blended TMDEM models.

Table 5-10 also provides the mean and median differences between species composition estimates from source and destination models in the overlap portions of the study area, providing a basic indicator of extension quality. In all cases, the extension revealed differences less than 4%. Once again, these results – combined with visual inspection of the finished map products – point to the success of the stratified, per-scene approach to model building and extension for producing seamless map products over large, multi-scene areas.

Table 5-10: Species composition destination model summaries and difference statistics calculated for the overlap sections.

Species Composition Destination Models			
SCTM			
Model	Equation	Mean Diff.	Median Diff.
p45r22	ln(p/1-p)=(-0.09993824*Bright)-(0.06579041*Wet)+18.11026970	0	-0.04
p44r24	ln(p/1-p)=(0.133335*Bright)-(0.1885151*Green)+7.2046243	0	-0.01
p43r24	ln(p/1-p)=(-0.12789990*Green)-(0.05711102*Wet)+19.55256868	0	-0.01
SCTMDEM			
Model	Equation	Mean Diff.	Median Diff.
p45r22	ln(p/1-p)=(-0.094818168*Green)+(0.004553026*Elev)-(0.057619126*Slp)+(0.098650115*Inc)-0.828845111	0	0
p44r24	ln(p/1-p)=(-0.07802001*Green)+(0.003938658*Elev)+(0.088267777*Inc)-1.91234777	0	0
p43r24	ln(p/1-p)=(-0.140161307*Green)+(0.003808408*Elev)+(0.121758117*Inc)+0.903450454	0	0

5.1.3.3 Aggregate Map Composite

Summaries of the accuracy assessment for two-, three-, and four-class species composition maps derived from the SCTM and SCTMDEM models derived from the source portions of the study area and extended through the destination scenes are shown in Figure 5-10. Once again, statistics were generated from independent test data that were not used in model construction. Unfortunately, test points are not evenly distributed across the full study area, and reflect a concentration of field data from the central portion. However, test points did exist for four of the five map pieces, and the statistics reflect these.

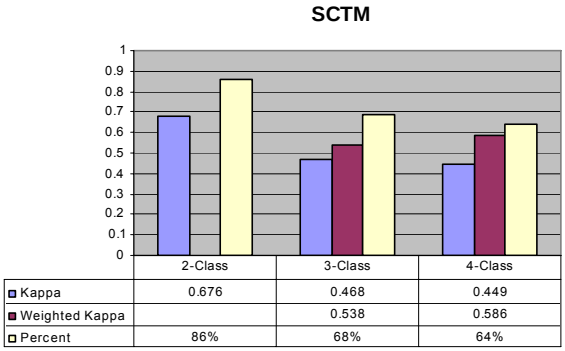

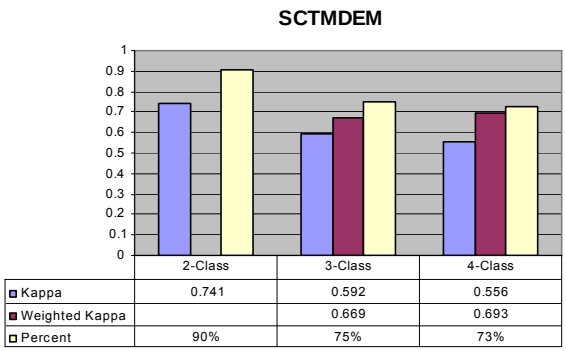

Figure 5-10: Kappa, weighted Kappa, and percent accuracy statistics of the three aggregate species composition classifications: 2-class(0-50%; 51-100%), 3-class (0-20%; 21-80%; 81-100%), and 4-class (0-20%; 21-50%; 51-80%; 81-100%).

In general, the accuracy patterns across the aggregated map composite reflect those noted for the source areas. The highest overall accuracies were produced by the combined SCTMDEM data set, with Kappa statistics ranging from 0.74 (90%) for the two-class configuration to 0.56 (73%) for the more detailed four-class arrangement. Composite maps based on spectral variables alone (SCTM) produced somewhat lower accuracies ranging from 0.68 (86%) for two classes to 0.45 (64%) for four. Error patterns shown in scatterplots of predicted versus observed species composition for the independent test points (Figure 5-11) once again reveal the slightly better overall performance of the combined SCTMDEM data set, as well as the tendency to over-estimate the coniferous portion of some mixed stands.

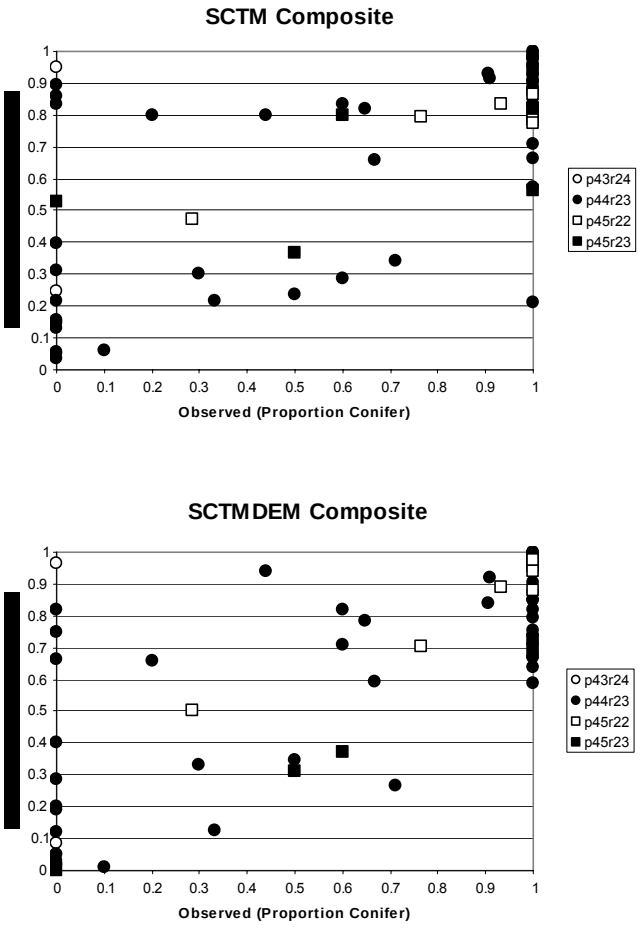

Figure 5-11: Species composition model predictions versus field observations for independent test data.

The final, continuous-variable map of species composition – as measured by the proportion of coniferous trees – is shown in Figure 5-12. The map is based on combined spectral and topographic models developed in the field data-rich central portions of the study area and extended in a piece-wise fashion to adjacent Landsat scenes. Statistical analysis of independent test sites suggests the map would be most accurate in a two-class (0-50%; 51-100%) configuration, in which it could be expected to yield good results in the 90% range (Kappa=0.74). Maps organized into more detailed three (0-20%; 21-80%;

81-100%) and four (0-20%; 21-50%; 51-80%; 81-100%) class configurations would be expected to produce moderately accurate results in the 75% (Kappa=0.59) to 73% (Kappa=0.56) range.

5.1.4 Leaf Area Index

Observed values of LAI_e measured in the field ranged from 0.62 to 6.71 for LAI_{eTot} and 0 to 6.16 for LAI_{eCan}; very similar to the range of values noted in LAI studies conducted in similar landscapes, including Hall *et al.* (2003) in northern Alberta, Wulder *et al.* (1996) in the Kananaskis Country, and White *et al.* (1997) in Glacier National Park. Table 5-11 summarizes the measured values by cover type and season, and while the small sample size makes it difficult to make definitive statements, some interesting trends can be observed. For example, while dense conifer stands produced the highest canopy and total LAI_e values overall, broadleaf stands produced slightly higher mean values. Predictably, treed sites of all types produced higher mean LAI_e values than those without trees, with the lowest values observed on herbaceous lands. As expected, LAI_{eTot} was higher than LAI_{eCan} in all cases, suggesting that understorey growth contributes measurably to the LAI_e values measured in this study area. The greatest contrasts were observed in regenerating forests, where generally open canopies permit the development of lush understories that contribute significantly to the total. The contrast is generally not as great among treed targets, but can vary widely depending on the complexity of the stand and amount of undergrowth. Dense canopies with thin understories produce very similar canopy and total LAI_e measurements, while complex stands or stands with dense

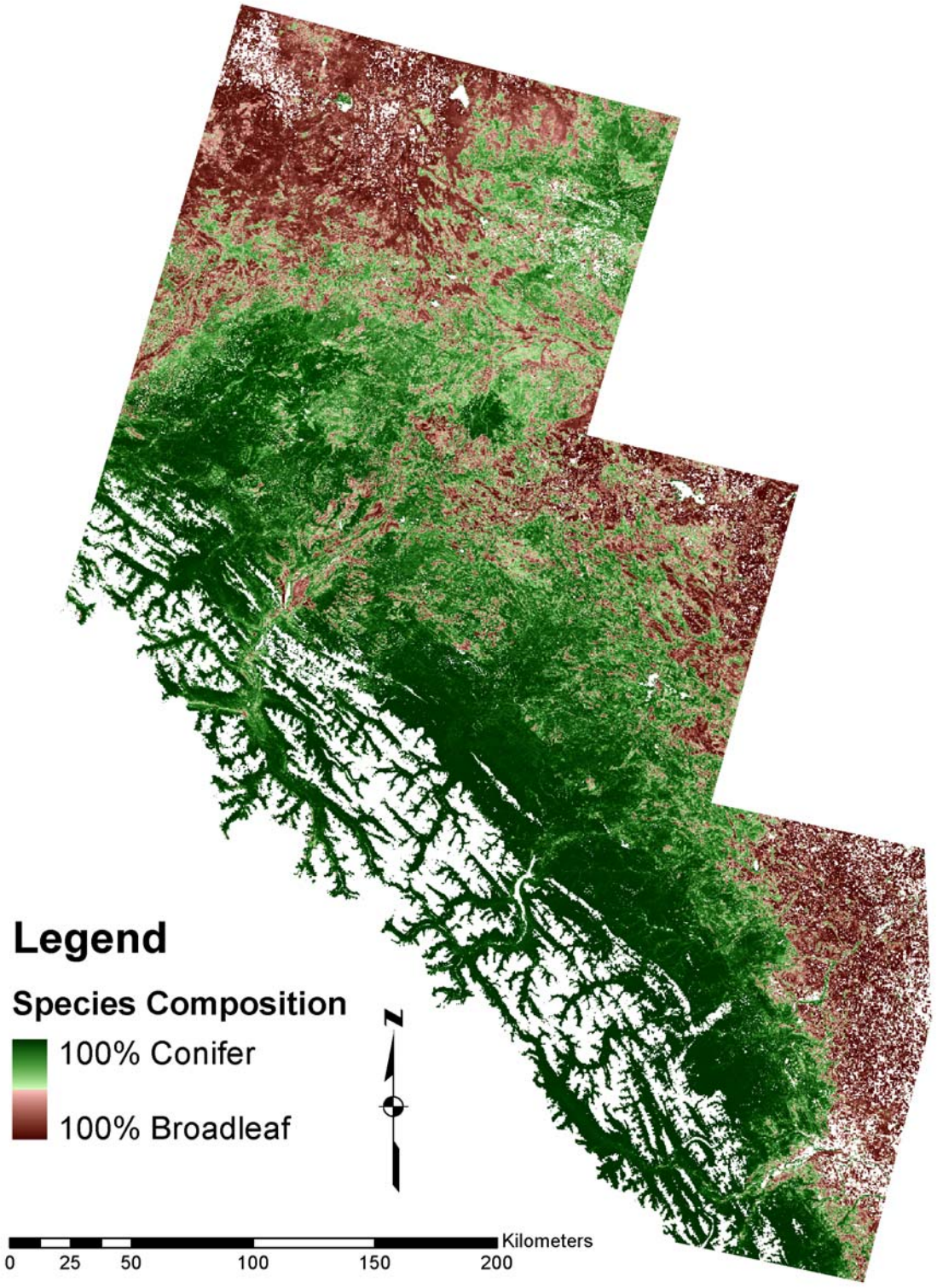

Figure 5-12: Continuous-variable map of species composition (% conifer) modelled from spectral and topographic variables at 30-metre resolution. The product is a composite of SCTMDEM source models extended in a piecewise fashion across the study area.

undergrowth can produce substantial differences between LAI_{eCan} and LAI_{eTot} (Figure 5-13). All cover types showed measurable mean LAI_e growth over the summer growing season with the exception of herbaceous sites, which experienced senescence. Even LAI_{eCan} in coniferous stands showed a modest increase from a mean of 3.32 to 4.05. Whether this is due to a measurable increase in leaf area or some other external factor is difficult to say. Much larger and more noticeable seasonable differences could be detected in total LAI_e; particularly in mixed or broadleaf stands, which tended to have denser growth in the understorey. The broadleaf stand shown in the left side of Figure 5-13 had a canopy LAI_e of 2.1 on June 22 and 2.5 on August 21, while LAI_{eTot} over the same time frame changed from 3.4 to 4.9. Clearly, the largest change occurred in the understorey, which increased its contribution from 38% of LAI_{eTot} in the early summer to 51% at the end of summer. This pattern stands in sharp contrast to the conifer stand on the right side of Figure 5-13, with almost no understorey and little LAI_e variability from June to September.

5.1.4.1 Landsat Source Models

Summaries of the Landsat candidate models from early hyperphagia are shown in Table 5-12. Coefficients of determination for LAI_{eCan} ranged from 0.29 to 0.52. VIs using the mid-infrared correction factor – $NDVI_c$ and SR_c – were significantly higher than their uncorrected counterparts, with $NDVI_c$ producing the best result (r^2=0.52). This observation confirms the findings of Nemani *et al.* (1993) and White *et al.* (1997). Interestingly, early summer estimates of LAI_{eTot} were also best predicted with *c*-corrected VIs. In this case $NDVI_c$ and SR_c both produced r2 values of 0.46; significantly better

than the 0.39 and 0.37 produced by their non-corrected NDVI and SR counterparts. This observation appears suggests that the value of the mid-infrared correction factor may go beyond that of a simple background scalar. In this study, the correction factor improves estimates of LAI_{eTot} as well.

Table 5-11: Summary statistics for LAI_e values measured in the early and late hyperphagia periods of 2002.

		Early Hyperphagia (n=32)				Late Hyperphagia (n=43)			
		Mean	**S.D.**	**Min.**	**Max.**	**Mean**	**S.D.**	**Min.**	**Max.**
Coniferous	Canopy LAI	3.32	0.87	1.91	5.29	4.05	1.07	2.23	6.16
	Total LAI	4.03	0.90	2.77	5.48	4.62	1.15	2.26	6.39
Broadleaf	Canopy LAI	3.46	1.15	2.37	5.06	-	-	-	-
	Total LAI	4.28	1.67	2.99	6.71	-	-	-	-
Mixed	Canopy LAI	2.69	1.53	1.61	3.77	5.43	-	5.43	5.43
	Total LAI	3.55	1.22	2.69	4.41	5.49	-	5.49	5.49
Forest Regeneration	Canopy LAI	1.58	1.30	0	3.47	1.97	1.56	0	4.09
	Total LAI	2.79	1.64	0.81	4.77	3.01	1.86	0.91	5.57
Shrub	Canopy LAI	1.61	-	1.61	1.61	1.38	0.44	0.96	1.84
	Total LAI	2.69	-	2.69	2.69	2.94	1.20	1.97	4.28
Herbaceous	Canopy LAI	0	0	0	0	0	0	0	0
	Total LAI	1.71	1.53	0.74	3.47	0.62	0.62	0.62	0.62
Treed Wetland	Canopy LAI	1.4	-	1.4	1.4	1.86	0.54	1.24	2.78
	Total LAI	2.34	-	2.34	2.34	2.95	0.82	1.91	4.03
Herbaceous Wetland	Canopy LAI	0	-	0	0	0.75	1.70	0.63	0.87
	Total LAI	0.74	-	0.74	0.74	1.56	0.07	1.51	1.61

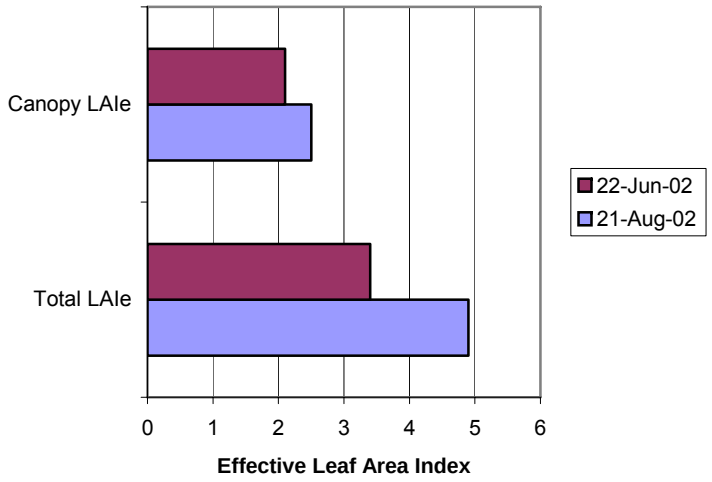

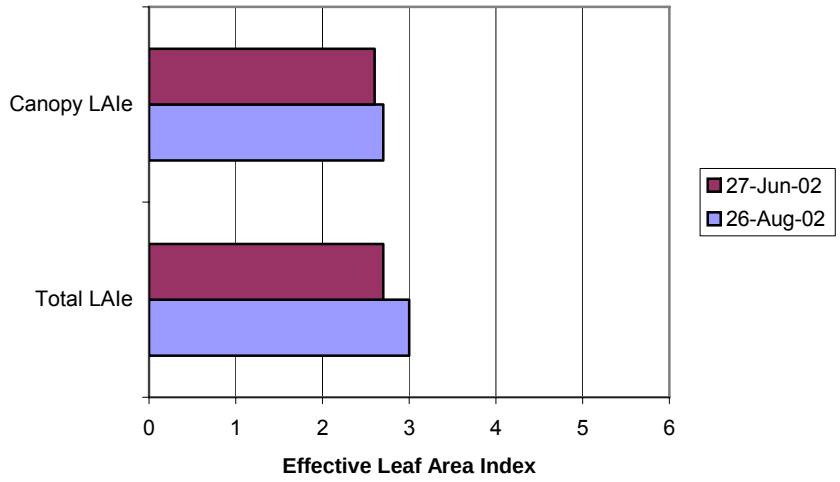

Figure 5-13: Structural and seasonal variability of LAI_e in broadleaf stand with dense understorey (left) and conifer stand with sparse understorey (right).

The coefficients of determination for all the early summer models of were in the *moderate* range, varying from 0.29 to 0.52. The image upon which these models were based suffered from patchy atmospheric contamination that could not be corrected – a common issue with June imagery in the study area. The quality of the remote sensing scene clearly had an impact on the ability to accurately model LAI during the early hyperphagia time period.

Table 5-12: Summaries of early hyperphagia LAI_e candidate models from TM data.

	Canopy LAI_e		Total LAI_e	
	r^2	Equation	r^2	Equation
NDVI	0.34	$y=0.29e^{3.92NDVI}$	0.39	$y=0.65^{e3.18NDVI}$
NDVIc	0.52	$y=0.61e^{3.51NDVIc}$	0.46	$y=1.33^{e2.41NDVI}$
SR	0.29	$y=0.43^{e0.50SR}$	0.37	$y=0.84^{e0.41SR}$
SRc	0.49	$y=0.67^{e0.51SRc}$	0.46	$y=1.38^{e0.36SRc}$

Summaries of candidate models for the late hyperphagia time frame are shown in Table 5-13. The patterns observed in these results mirror those from the early summer, but with significantly stronger results; due no doubt to the superior quality of the late-summer imagery. Canopy LAI_e models had r^2 values ranging from 0.32 to 0.82. Once again, VIs with the mid-infrared correction factor performed significantly better than those without the correction factor, with $NDVI_c$ (r^2= 0.82) performing the best. The correction factor had a less pronounced impact on the models of LAI_{eTot}, but again the best results were produced by $NDVI_c$ (r^2=0.76) and SR_c (r^2=0.75).

Table 5-13: Summaries of late summer LAI_e candidate models from TM data.

	Canopy LAI_e		Total LAI_e	
	r^2	Equation	r^2	Equation
NDVI	0.55	$LAI_e=0.08e^{4.98NDVI}$	0.63	$LAI_e=0.18e^{4.40NDVI}$
NDVIc	0.82	$LAI_e=0.46e^{3.35NDVIc}$	0.76	$LAI_e=0.94e^{2.61NDVIc}$
SR	0.36	$LAI_e=0.62e^{0.24SR}$	0.41	$LAI_e=1.03e^{0.21SR}$
SRc	0.76	$LAI_e=0.56e^{0.31SRc}$	0.75	$LAI_e=1.03e^{0.25SRc}$

An interesting pattern noted in both the early and late-hyperphagia time frames is that the NDVI-based VIs were significantly better than SR in predicting LAI_{eCan}, but there was very little difference in their ability to predict LAI_{eTot}. The physical reason behind this observation is unknown, but may be due to the differences in VI response to increasing LAI values. A key feature of the NDVI lies in the ratioing concept, which is widely cited as a strength of the index as a factor for reducing certain types of multiplicative noise: illumination differences, cloud shadows, atmospheric attenuation, and certain topographic effects (Lillesand and Kieffer, 2000). While NDVI is functionally equivalent to the simple ratio in that NDVI=SR-1/SR+1, the NDVI approximates a logarithmic stretch of the simple ratio such that low LAI vegetation values span a greater range of values (Myneni *et al.*, 1995). Figure 5-14 shows the relationship between NDVI and SR over the plots used in this analysis. While all VIs begin to display saturation at LAI values greater than about 2 (Huete et al., 1999), the NDVI's tendency to asymptote more quickly than the simple ratio is such that its advantages begin to level off as LAI increases. Since values of LAI_{eTot} tend to be higher

than LAI_{eCan}, the relative advantages and disadvantages of the NDVI and SR may even out, such that there is no appreciable difference in their respective performances.

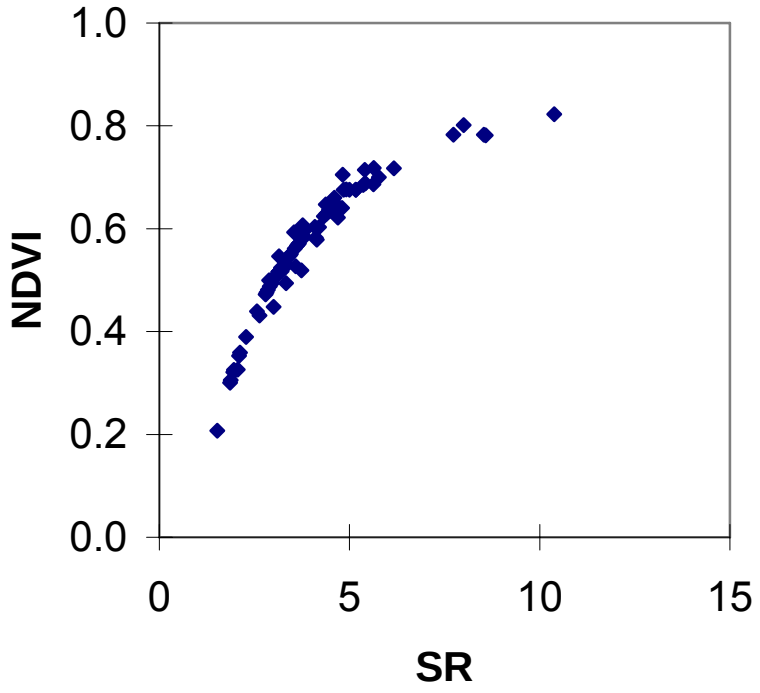

Figure 5-14: Relationship between NDVI and SR in the sites used to model LAI_e in this study.

The relationship between LAI_{eUs} and the mid-infrared correction factor, c, are summarized in Table 5-14. Early hyperphagia and late hyperphagia observations produced r^2 values of 0.37 and 0.57, respectively. Once again, the weaker early hyperphagia model is likely due to the relatively poor quality of the June, 2002 imagery. The moderate positive relationship observed between LAI_{eUs} and c is similar to White *et al.*'s (1997) findings in Montana, and seem to confirm a causal relationship between understorey LAI and the mid-infrared correction factor. Additional work surrounding

this issue – including a more thorough analysis of LAI_{eUs} and an attempt to map LAI_{eUs} spatially across the landscape with ETM+ imagery can be found in Couroux (2004).

Table 5-14: Summary of relative LAI_{eUS} vs. MIR correction factor models.

	Early Hyperphagia Relative LAI_{eUs}		Late Hyperphagia Relative LAI_{eUs}	
	r^2	Equation	r^2	Equation
MIR Correction Factor	0.37	Rel. LAI_{eUs}=0.52c+0.14	0.57	Rel. LAI_{eUs}=0.52c+0.18

5.1.4.2 MODIS Destination Models

The source models with the highest explanatory abilities were used to generate spatial estimates of LAI_e across the respective source imagery: p45f23 for the early hyperphagia period and p44f23 for the late hyperphagia. These in turn were scaled to 250-metre spatial resolution to match the corresponding MODIS 14-day composite VIs. Summaries of simple linear regression models linking scaled estimates of LAI_e from Landsat to explanatory variables from MODIS are shown in Table 5-15. Of the two MODIS-based models generated for each time period, only the ones using NDVI were statistically significant, achieving r^2 values of 0.51 and 0.51 for the early and late-hyperphagia stage, respectively. The model based on EVI data had coefficients of determination less than 0.05 for each time period. This result was surprising, given the supposedly more sophisticated nature of the EVI, and its enhanced ability to account for canopy background and atmospheric effects (Huete et al., 1999). The complete failure of this index to model Landsat-scaled estimates of LAI_e over two separate time periods, combined with the acceptable performance of corresponding NDVI measures from the same dataset, suggests some sort of data issue with the EVI. Since the index relies on

specific correction factors for background and atmospheric resistance, it is possible that its poor performance may be the result of processing errors in the MOD13 product development cycle. A definitive answer to this puzzling result would require further investigation. Fortunately, the presence of the legacy NDVI in the MOD13 data set allowed the mapping of LAI_e over the entire study area to continue.

Table 5-15: Summary of models linking scaled LAI_e (Landsat) to MODIS VIs.

	Early Hyperphagia		Late Hyperphagia	
	r^2	Equation	r^2	Equation
NDVI	0.51	$LAI_e=0.4332e^{0.0003NDVI}$	0.58	$LAI_e=0.1e^{0.0005NDVI}$
EVI	0.01*	$LAI_e=2.1804e^{0.0001EVI}$	0.05*	$LAI_e=2.2771e^{0.0002EVI}$

* Not significant at $p<0.05$

The final maps of LAI_e for the early and late-hyperphagia phases of 2003 are shown in Figure 5-15. Generated through a two-step process involving empirical modelling of ground-measured LAI to 30-metre NDVIc data from Landsat, followed by a resampling to 250-metres and subsequent extension over the entire study area via MODIS NDVI, the maps reflect moderate-resolution estimates of vegetation amount at two key time periods, and a basic foundation for characterizing phenological changes across the summer growing season.

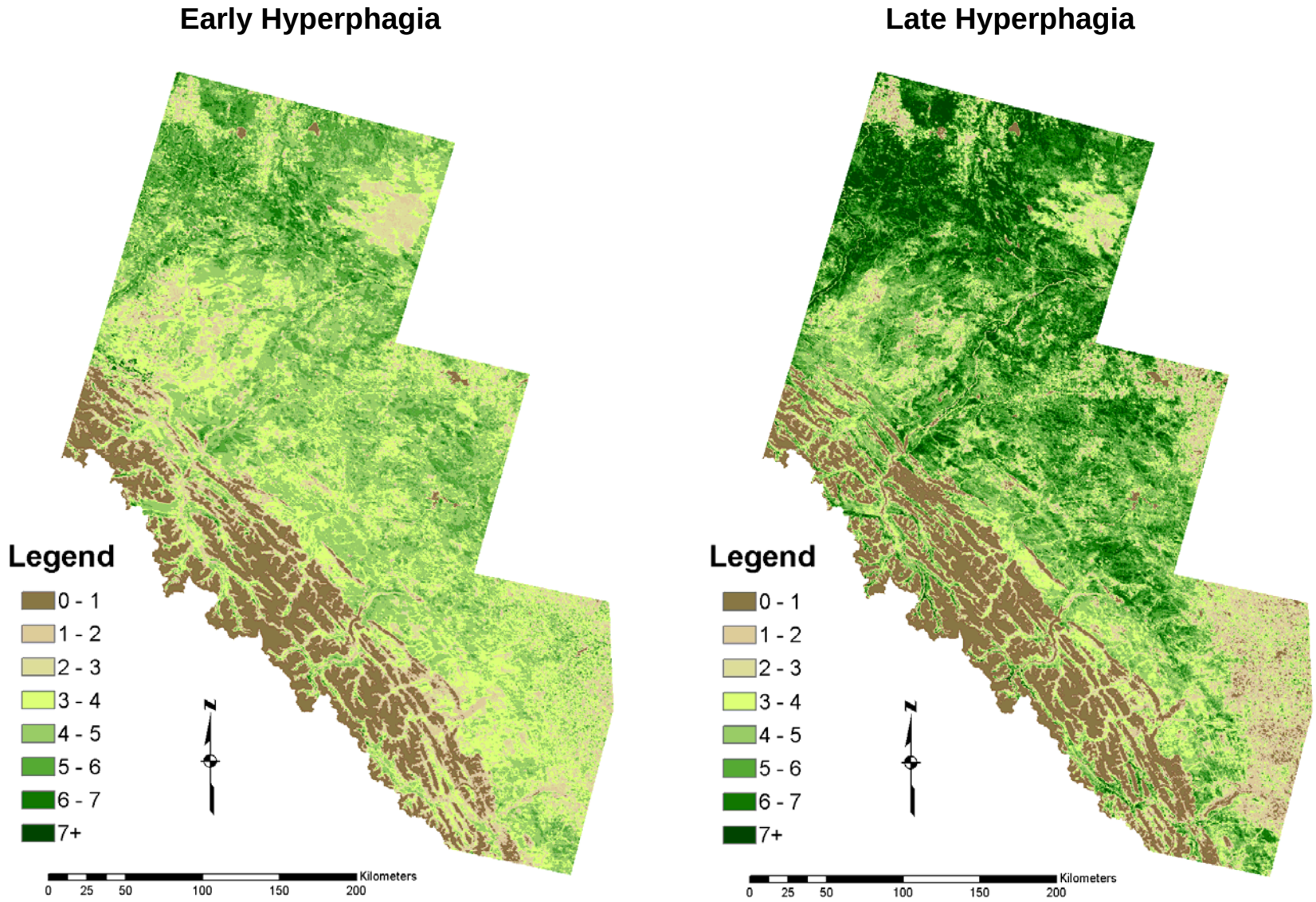

Figure 5-15: Total LAI maps of the study area for early hyperphagia and late hyperphagia, 2003.

5.2 Re-Coding, Re-Classing, and Composite Map Production

The end result of the multi-scale, attribute-based approach to vegetation and land cover information extraction developed in this research is a multi-layer composite of the land and vegetation information products, including layers for land cover, crown closure, species composition, and LAI (Figure 5-16). This stands in sharp contrast to the single-layer classification map generated by most large-area remote sensing projects, and adds significant new dimensions of quality and flexibility to the final product. By separating categorical information products that vary at the stand level – land cover – from attributes like LAI and crown closure that operate at the tree/gap level and vary continuously across the landscape, two key objectives have been realized. First, a framework has been created that matches diverse information needs with appropriate and effective image processing techniques. Based on hierarchy theory and the remote sensing scene model, this framework provides a foundation for complex information extraction that is more effective than the indiscriminate application of classification techniques. Second, the generation of multiple – and, where appropriate, continuous – estimates of individual attributes across the study area resulted in a land cover/vegetation information database with exceptional flexibility. By maintaining high-order information, the system provides managers with divergent needs the opportunity to define categories that suit their individual application. By re-coding, re-classing, and combining information from the vegetation/land cover information base with geospatial layers from other GIS sources, the potential exists to produce a large number of information products potentially suitable for a broad range of habitat mapping/environmental management objectives. For example,

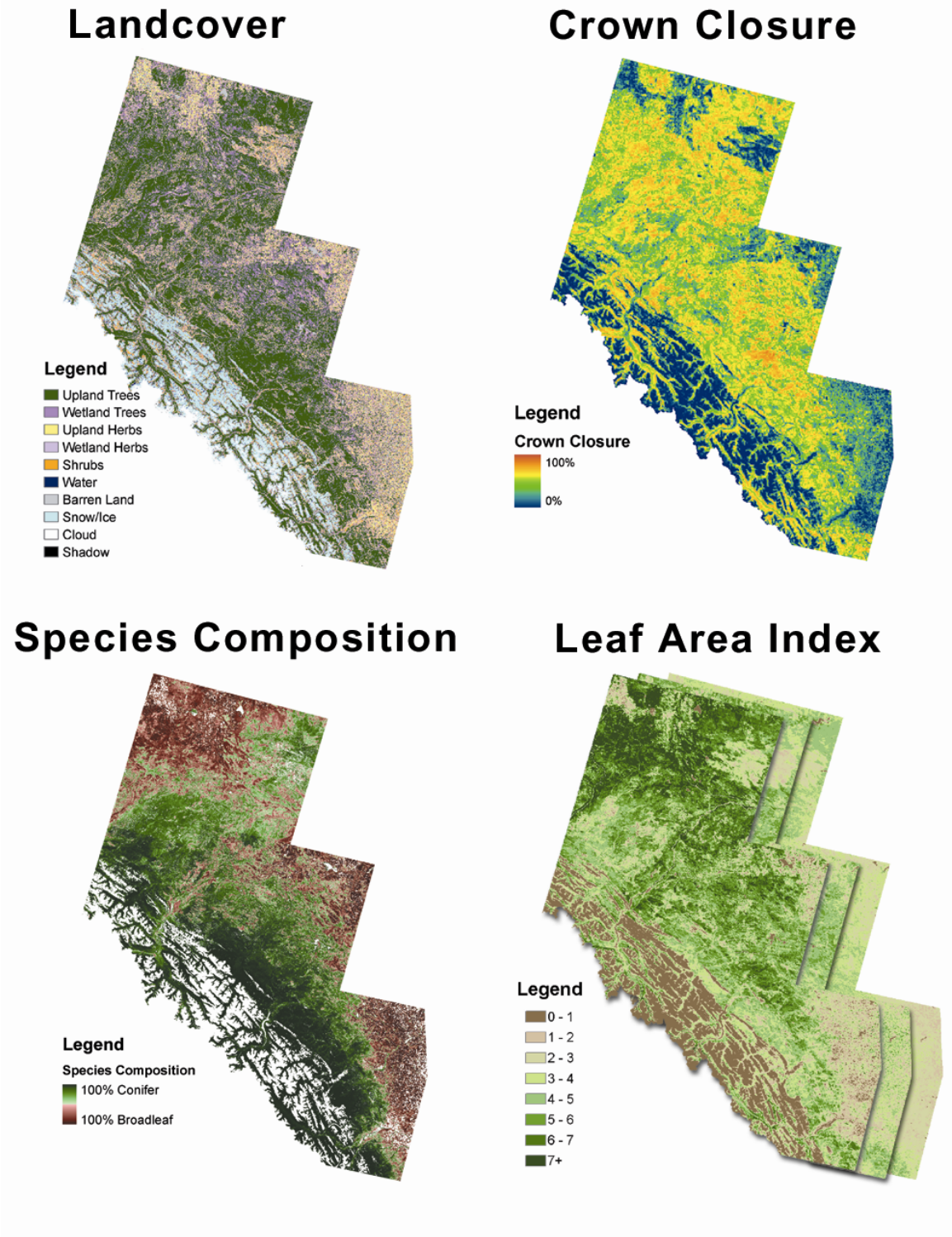

Figure 5-16: Major geospatial products used in the characterization of land cover and vegetation in the study area.

Figure 5-17 shows examples of three different map products generated over a small portion of the study area using simple procedures in a GIS environment. Figure 5-17A depicts vegetation structure with three classes of forest species composition: pure conifer (>70% coniferous), pure broadleaf (<30% broadleaf), and mixed forest (30-70% coniferous), but only two crown closure classes: open (<50% crown closure) and closed (>50% crown closure). The prevalence of old-growth conifer forests in this portion of the study area – the Athabasca valley in Jasper National Park – creates a map dominated by the *closed coniferous forest* class. However, the simple process of re-generating the map with a three-class configuration of crown closure: open (<30% crown closure), medium (30-70% crown closure), and dense (>70% crown closure) produces a product – Figure 5-17B with much more structural detail in the forests common to in this part of the study area. Contrasting these two *structural* vegetation maps is the *phenological* view of vegetation shown in Figure 5-17C. In this case, the map was generated to highlight three categories of LAI change across the summer growing season: LAI senescence (LAI decreasing between June and August), LAI no change (LAI remaining the same between June and August), and LAI growth (LAI increasing between June and August). Configured in this way, the information base presents a markedly different view of the study area, highlighting the substantial increase of foliage observed in the upper valley slopes.

This exceptional adaptibility is a key advantage that reduces the need for constant re-investment (or the pain of chronic dissatisfaction) that is often experienced with inflexible classification-based products. For example, Figure 5-18 shows a simplified flow chart for generating a land cover/vegetation map roughly analogous to Franklin *et*

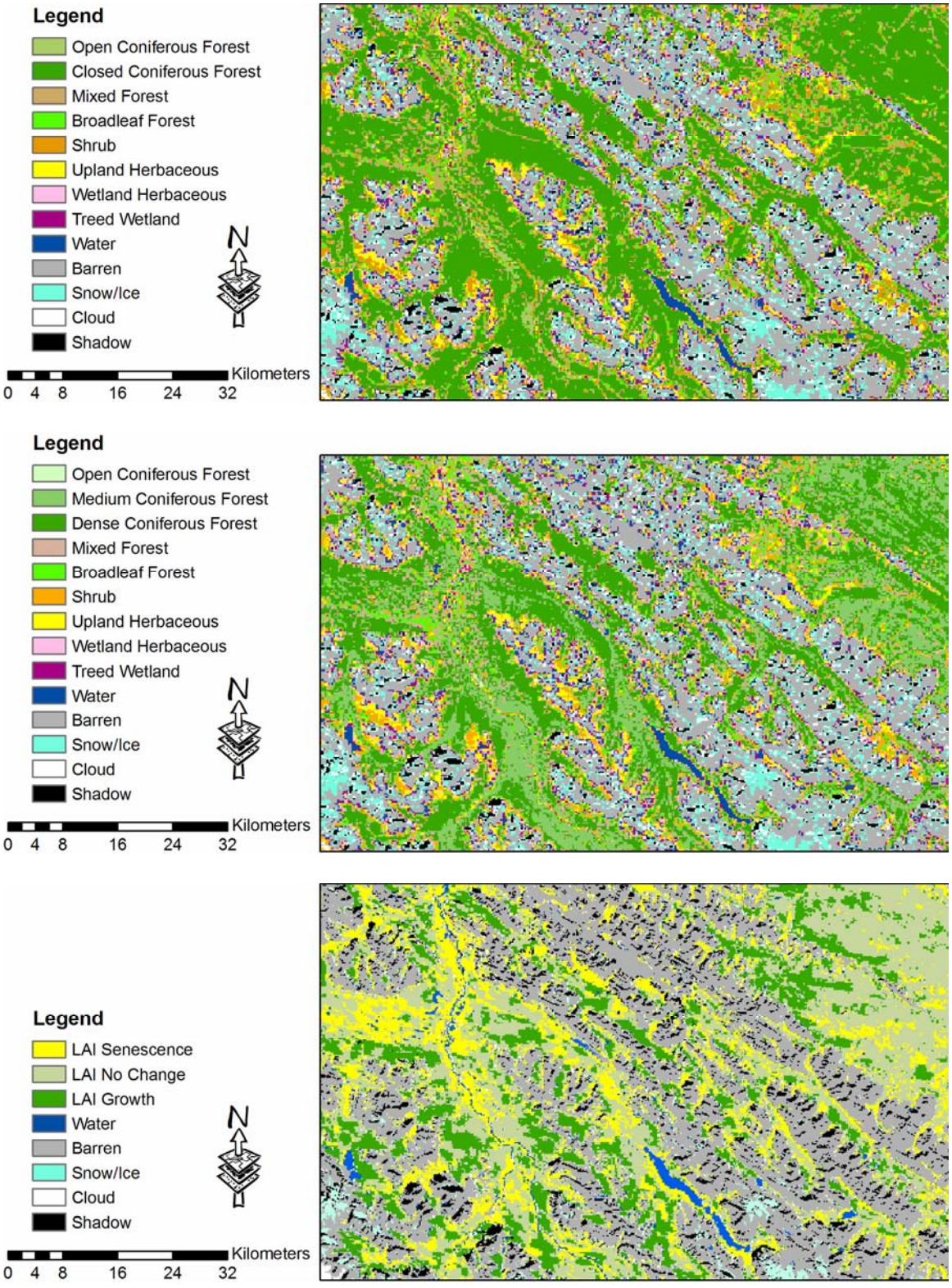

Figure 5-17: Examples of the flexible composite map capability of the current land/vegetation information base. Maps shown here cover a small portion of the study area and were generated through simple re-classing and merging procedures in a GIS environment.

al.'s (2001) legacy "Integrated Decision Tree" map that formed the foundation for much of the early work in the Foothills Model Forest Grizzly Bear Research Program. The resulting map product is shown in Figure 5-19.

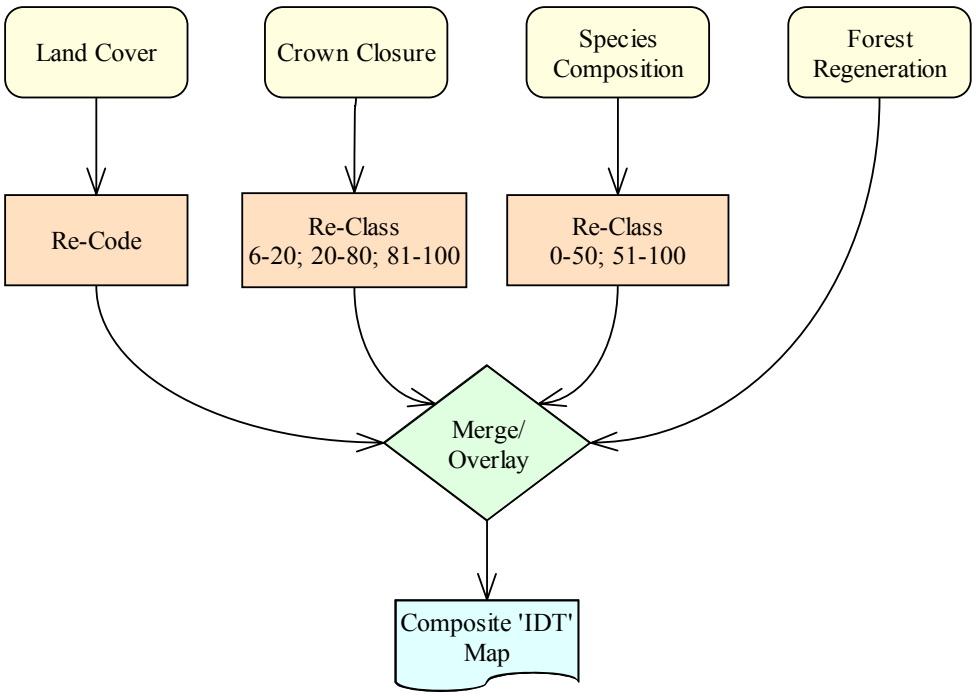

Figure 5-18: Simplified flow chart illustrating the production of sample composite map from land cover/vegetation information base generated in this research.

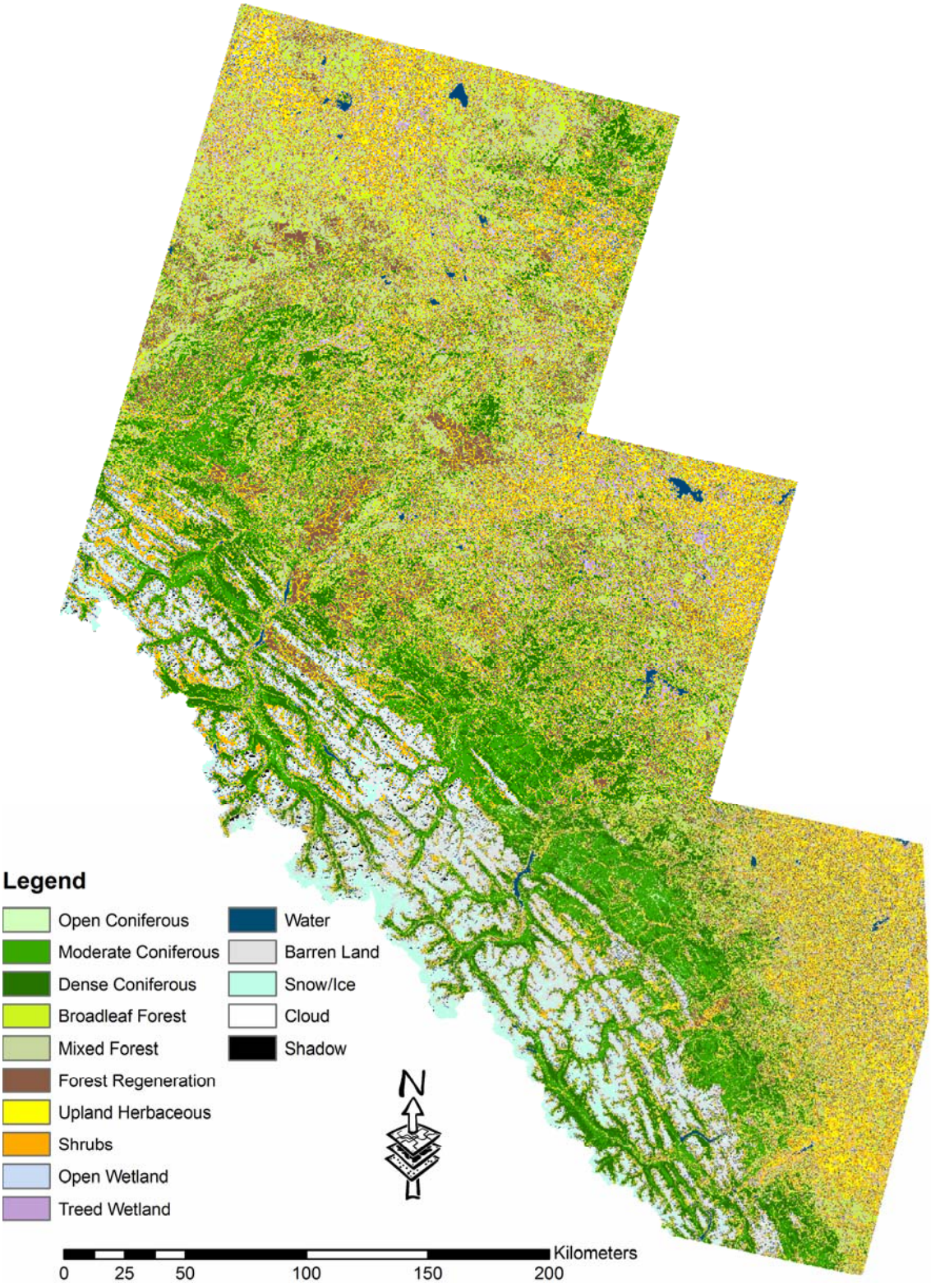

Figure 5-19: Sample composite map of land cover and vegetation generated from research information layers in a GIS environment.

5.3 Chapter Summary

A sophisticated, satellite-based database of land cover and vegetation has been developed for a 100,000 km^2 study area in west-central Alberta, creating an effective case study of the multi-scale, attribute-based framework developed in this thesis to support the development of wildlife habitat maps across large, multi-jurisdictional areas. The information base consists of multiple layers designed to characterize four separate attributes: land cover, crown closure, species composition, and LAI phenology. Generated through a combination of object-oriented classification, conventional regression, and generalized linear models, the products represent a high-quality, flexible information base constructed over a challenging multi-jurisdictional environment.

Chapter 6: Remote Sensing and Forest Inventory for Grizzly Bear Habitat Mapping and Resource Selection Analysis

Contemporary strategies for wildlife habitat mapping (Manly *et al.*, 2002), biodiversity analysis (Scott *et al.*, 1993), and animal movement modeling (Bian, 2001; Musiega and Kazadi, 2004) require the use of spatially explicit environmental map layers, such as those derived from air photos and satellite imagery. These data are commonly processed for a variety of environmental attributes, including vegetation cover (Hines and Franklin, 1997; Carroll *et al.*, 1998; McClain and Porter, 2000; Lauver *et al.*, 2002), land use (Osborne *et al.*, 2001; Dash Sharma *et al.*, 2004; Witztum and Stow, 2005), landscape structure (Ripple *et al.*, 1997; Peery *et al.*, 1999; Hargis *et al.*, 1999; Hansen *et al.*, 2001), and phenology (Verlinden and Masogo, 1997; Leimgruber *et al.*, 2001; Serneels and Lambin, 2001; Ciarniello et al., 2002). The extent to which wildlife studies and management activities have come to rely on these remote sensing-derived products is illustrated by Glenn and Ripple's (2004) survey of 44 such works published in *The Journal of Wildlife Management* between 2000 and 2002. The assumption underlying each of these efforts is that the chosen environmental map products are an effective representation of the natural landscape, and an appropriate source of information for the given application. The validity of these assumptions is an active research issue, and the topic of on-going concern within the scientific and resource management communities.

Researchers and managers selecting the land cover/vegetation information layers upon which to base their projects must choose between adapting an existing information source and creating custom products of their own. Many jurisdictions maintain detailed

land inventory databases designed to aid in the management and conservation of public lands. The Alberta Vegetation Inventory (AVI) of Alberta, Vegetation Resource Inventory of British Columbia, and Forest Resource Inventory of Ontario are examples of Canadian inventories retained in public jurisdictions managed for timber harvest. Public lands in the U.S. under the stewardship of the National Forest Service are covered by the Forest Inventory Analysis, while the Bureau of Land Management maintains a variety of inventories, including those acquired under the National Environmental Policy Act, the Abandoned Land Mines program, and various species-directed initiatives.

Inventory databases offer an attractive alternative for many wildlife studies because they reduce or eliminate the cost and burden of production. In addition, existing inventory database systems often contain highly detailed information, and are usually distributed in convenient GIS formats. However, the utility of these data sets may be limited by issues of consistency, accuracy, and availability, depending on the scope and needs of the project (e.g. Throgmartin *et al.*, 2004).

Concerns about the suitability of existing datasets have prompted many wildlife studies to produce their own environmental information from satellite or airborne remote sensing products, particularly for projects involving large areas (e.g. Scott *et al.*, 1993) that stretch beyond a single jurisdiction. The strategy is tempting, given the allure of high-quality information perfectly suited to the needs of the study. However, the challenges associated with effectively integrating remote sensing into multidisciplinary projects are daunting (McDermid *et al.*, 2005), and the potential for mistakes is high. Glenn and Ripple (2004) pointed out the lack of widely accepted standards surrounding the use of digital maps in wildlife habitat mapping studies, and the differences resulting

from the use of data from different sources. A wide variety of remote sensing-based mapping strategies are available, ranging from relatively inexpensive maps generated with well-known unsupervised classification techniques (e.g. Townshend, and Justice, 1980) to complex and expensive environmental databases produced through sophisticated mapping and modeling procedures (e.g. J. Franklin *et al.*, 2000). Depending on the approach and strategy adopted, the remote sensing portion of the program can range from a relatively minor component to a major consumer of project resources.

Even with the necessary resources in place, the question remains: Which mapping strategy is most effective? Are pre-existing inventory databases up to the task? If new information from remote sensing is necessary, must a sophisticated environmental dataset be developed, or would a less complicated land-cover map provide a suitable (and less costly) alternative? To help address these questions, three sources of environmental information were examined: (i) a pre-existing forest inventory, (ii) the high-cost remote sensing product developed in this research, and (iii) a lower-cost remote sensing alternative produced by another environmental mapping initiative operating within the study area. The goal was to evaluate the utility of three environmental data sources that represent options commonly available to modern wildlife management projects. The evaluation was accomplished by first appraising the quality of the three data sets and, second, by investigating their capacity to explain patterns of grizzly bear (*Ursus arctos*) telemetry locations across the study area. In a previous publication, Franklin *et al.* (2002) highlighted the marked difference observed between maps generated from satellite image classification versus those produced from a land inventory database. This study builds upon the theme of that work, and extends it to its logical conclusion.

6.1 Data Sets

6.1.1 Environmental Data Source #1: The Alberta Vegetation Inventory (Pre-existing Inventory Data)

The Alberta Vegetation Inventory (AVI) is the provincial standard for forest inventory on Alberta's public lands, and embodies the familiar GIS-based inventory products that serve forest resource managers in many jurisdictions (Leckie and Gillis, 1995). Generated through manual interpretation of aerial photographs, the AVI is produced by provincial and private photo-interpretation experts who map "homogeneous" polygons on the basis of tone, texture, pattern, size, shape, shadow, and association. Once delineated, these polygons are assigned attributes associated with timber productivity, moisture regime, crown closure, height, tree species composition, and age (Alberta Sustainable Resource Development, 1991). Attributes are generated through a blend of ground reference information and the subjective experience of professional interpreters. The quality and consistency of the AVI is maintained through field checks and provincial certification, but the information's accuracy is not quantitatively assessed. Overall, the polygonal format of the data is designed primarily to suit forest harvest management needs at the stand level, and the two-hectare minimum mapping unit means that many of the smaller ecological details on the landscape are missed. However, the level of forest structural information is unsurpassed by any other large-area information source in the region, and the AVI forms the basis of virtually all forest management decisions on Alberta's public lands.

The AVI has one major drawback for large-area wildlife studies such as the Foothills Model Forest Grizzly Bear Research Program, in that it is a jurisdictional

database and therefore not available across the entire study area. As with most such provincial forest inventories, it is only maintained on lands managed for timber harvest. Parks, private lands, protected areas, First Nations reserves, and other *white zone* regions of the study area are not covered by the AVI (Figure 6-1). As such, our analysis in this data source is limited only to regions in which AVI data was available.

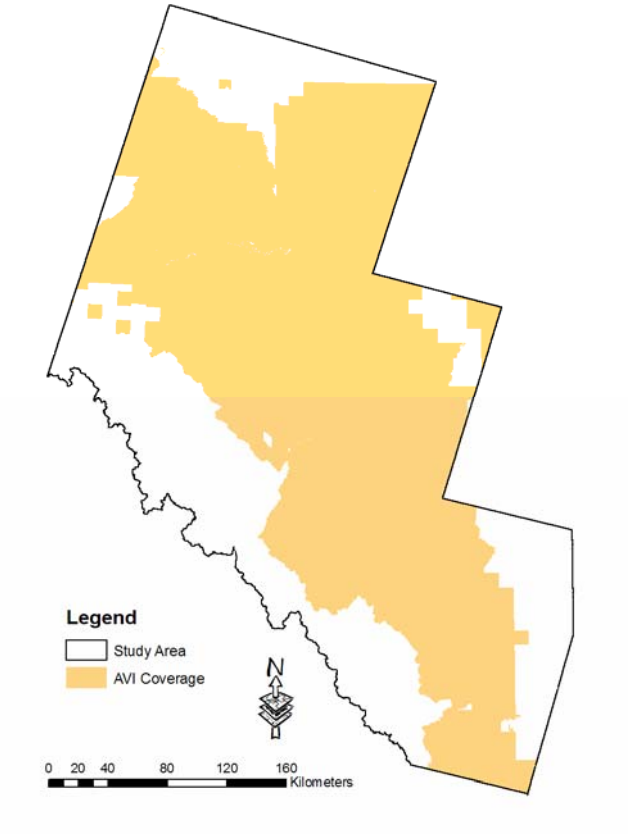

Figure 6-1: AVI coverage in the study area.

6.1.2 Environmental Data Source #2: The Alberta Ground Cover Characterization (Low-cost Remote Sensing Alternative)

The Alberta Ground Cover Characterization (AGCC) is an on-going initiative between the University of Alberta and its partners in the provincial and federal government to map the land cover across the forested portions of Alberta using Landsat data. The AGCC mapping protocol employs a "hierarchical classification" strategy in which unsupervised classification/hyperclustering techniques are used to derive land cover information from amongst 45 spectral classes. The approach proceeds iteratively, beginning with known features such as roads, water bodies, clear cuts, and burns, and moves systematically through increasing levels of detail. While the AGCC legend has a total of 73 potential classes (Table 6-1), the typical number encountered in any given region is considerably less. Imagery used in production of AGCC maps come from the Landsat Thematic Mapper (TM) and Enhanced Thematic Mapper Plus (ETM+) instruments, and are drawn primarily from public domain archives such as Geogratis (www.geogratis.ca) and Global Land Cover Facility at the University of Maryland (glcf.umiacs.umd.edu). The AGCC maps of the current study area are derived from five ETM+ scenes acquired from 1999 to 2002 (Table 6-2).

The unsupervised classification procedures used by the AGCC require a substantial amount of manual interpretation in order to label the raw spectral classes that are the product of spectral clustering. Technicians are trained to view a variety of colour composites of the imagery in order to separate subtle variations in land cover. The field work component of the procedure is designed primarily to provide technical personnel with an overview of the major vegetation types encountered in a region, and is quite

Table 6-1: AGCC classification legend.

Anthropomorphic	Urban and Industrial			Undifferentiated Urban and Industrial Features
				Urban
				Commercial and industrial
				Major roads, highway and railways
				Cutlines and Trails
				Surface mines (coal) gravel pits, spoil piles
				Farmstead and/or ranch (including shelter belts)
	Agricultural			Undifferentiated Agriculture
				Cropland
				Irrigated Land
				Agricultural Clearing
	Clearcuts			Undifferentiated clear-cut
				Graminoid (grasses/sedges) dominated clear-cut
				Tree/shrub dominated clear-cut
				Tree (replanted - immature trees, <20 years old) dominated clearcut
	Burns			Undifferentiated burn
				Graminoid (grasses/sedges) dominated burn
				Tree/shrub dominated burn
				Tree dominated burn
				New Burn
				Herbaceous Burn
Uplands	Forested Land	Coniferous Dominated Forest	Closed	Closed Fir
				Closed Black Spruce
				Closed Pine
				Closed White Spruce
				Closed Undifferentiated Conifer
			Open	Open Fir
				Open Black Spruce
				Open Pine
				Open White Spruce
				Open Undifferentiated Conifer
		Deciduous Dominated Forest	Closed	Closed Aspen, Balsam Poplar and/or Birch and/or Birch
				Riparian Poplar
			Open	Open Aspen, Balsam Poplar and/or Birch and/or Birch
		Mixed Wood Dominated Forest	Closed	Closed Coniferous Dominated Mixedwood
				Closed Deciduous Dominated Mixedwood
				Closed Coniferous and Deciduous Mixedwood
			Open	Open Coniferous Dominated Mixedwood
				Open Deciduous Dominated Mixedwood
				Open Coniferous and Deciduous Mixedwood
	Shrub Land	Closed Shrub Land (streams and coulees)		Closed Riparian Shrub
				Closed Coulee Shrub Thicket
				Closed Upland Shrub
		Open Shrub Land		Open Riparian Shrub
				Open Coulee Shrub Thicket
				Open Upland Shrub
				Open Sagebrush Flat
	Grassland	Graminoids (grasses and sedges)		Fescue Grassland
				Mixed Grassland
				Sandhill Grassland
				Coulee Grassland
		Upland Fords		Upland Ford Meadow
Wetlands and Water	Wetlands			Emergent Wetlands (cattails)
				Graminoid Wetlands (sedges/grasses/forbs)
				Shrubby Wetlands (willow and birch)
				Sphagnum Bog
				Lichen Bog
				Black Spruce Bog (sphagnum understory)
				Black Spruce Bog (lichen understory)
				Undifferentiated Wetlands
				Woodland Fen (Larch Drainage Flow Patterns)
	Water			Lake, pond, reservoir, river and stream
Barren Lands				Permanent Ice and Snow
				Rock, Talus, and/or Avalanche Chute
				Exposed Soil
				Alkali Flat and/or Mud Flat
				Upland Dune Field
				Alluvial Deposit
				Beach
				Badland
				Blowout Zone
Unclassified				Cloud / Haze
				Shadow

Table 6-2: Satellite imagery used in production of the AGCC map of the study area.

Sensor	WRS Scene	Acquisition Date(s)
ETM+	Path 43 Row 24	September 23, 2001
ETM+	Path 44 Row 23	September 14, 2001
ETM+	Path 44 Row 24	September 14, 2001
ETM+	Path 45 Row 22	September 16, 1999
ETM+	Path 45 Row 23	August 23, 2002

limited compared to remote sensing projects that incorporate data-hungry supervised classification or empirical modeling procedures. As such, the AGCC products are relatively cost-effective, and represent the *low cost* end of the remote sensing spectrum evaluated in this study.

6.1.3 Environmental Data Source #3: The Foothills Model Forest Grizzly Bear Research Program (High-cost Remote Sensing Alternative)

The Foothills Model Forest Grizzly Bear Research Program (FMFGPRP) has been conducting field work in the study area since 1999, resulting in the production of a large – and expensive – collection of ground plots that have enabled the generation of the sophisticated series of remote sensing-based map products reported in this thesis. The database was generated from a multi-source digital dataset using a variety of supervised mapping and modelling techniques (Table 6-3). While produced separately, the four layers are designed to work in concert in order to provide a flexible information source capable of supporting a broad range of resource management objectives, including grizzly bear habitat mapping within the FMFGBRP project (Nielsen *et al.*, 2003; Nielsen,

2004). The FMFGPRP map layers are generated from Landsat TM and MODIS 250-meter vegetation index (Huete *et al*., 1999) data (Table 6-4), and topographic derivatives from a digital elevation model.

Table 6-3: Summary of environmental information products generated by the Foothills Model Forest Grizzly Bear Research Program.

Map Layer	Data Sources	Mapping Technique	Product
Land Cover	Landsat TM, DEM	Supervised, object-oriented classification	Ten-class classification of land cover/physiognomy
Crown Closure	Landsat TM, DEM	Multiple regression with arcsine transformation	Continuous-variable (0-100%) crown closure of 30m pixels
Species Composition	Landsat TM, DEM	Binomial-family generalized linear model with logit link	Continuous-variable (0-100%) proportion of coniferous cover in 30m pixels
LAI_e Phenology	Landsat TM, MODIS	Simple regression	Continuous-variable (0-x) estimates of effective LAI for early and late-summer time periods

Table 6-4: Satellite imagery used in the Foothills Model Forest Grizzly Bear Research Program maps of the study area.

Sensor	Scene	Acquisition Date(s)
TM	WRS Path 43 Row 24	June 17, 2003*
TM	WRS Path 44 Row 23	June 13, 2002†; July 10, 2003*
TM	WRS Path 44 Row 24	July 10, 2003*
TM	WRS Path 45 Row 22	September 3, 2003*
TM	WRS Path 45 Row 23	August 23, 2002†; September 3, 2003*
MODIS	H10v03	June 25 – July 10, 2003†, Aug 28 – September 13, 2003†, October 15 – October 31, 2003†
MODIS	H11v03	June 25 – July 10, 2003†, Aug 28 – September 13, 2003†, October 15 – October 31, 2003†

* Used for land cover, crown closure, species composition
† Used for LAI

The supervised classification and empirical modeling procedures used in the production of the FMFGPRP database required a large number of detailed ground measurements. As

such, the investment needed to create the 1125 field samples used in the creation of the current data layers is substantially greater than the limited ground checks required for the unsupervised procedures adopted by the AGCC. As such, the FMFGPRP represents the *high cost* remote sensing alternative evaluated in this study.

6.1.4 Grizzly Bear Use/Availability Data

The FMFGBRP has assembled an extensive database of telemetry locations designed to help characterize the selection of resources by grizzly bears in western Alberta. Between 1999 and 2004, 78 individual bears were captured using aerial darting and snaring techniques (Hobson, 2005). Of these, 64 animals were fitted with Televilt or Advanced Telemetry Systems global positioning system (GPS) radio collars programmed to acquire positional fixes at intervals ranging from one to four hours. For the purposes of this study, the raw data were restricted to include only individuals that generated a minimum of 50 telemetry positions (Leban *et al.* 2001) and remained within the boundaries of the study area. The resulting dataset consists of 35,572 point locations (Figure 6-2) from 34 female and 19 male bears (Table 6-5).

In order to account for seasonal variations in habitat use, the telemetry data were stratified into three time periods defined on the basis of previously observed food habits and selection patterns (Pearson and Nolan, 1976; Hamer and Herrero, 1987; Hamer *et al.*, 1991; Nielsen *et al*, 2003). The first season, occurring from May 1 to June 15, is termed

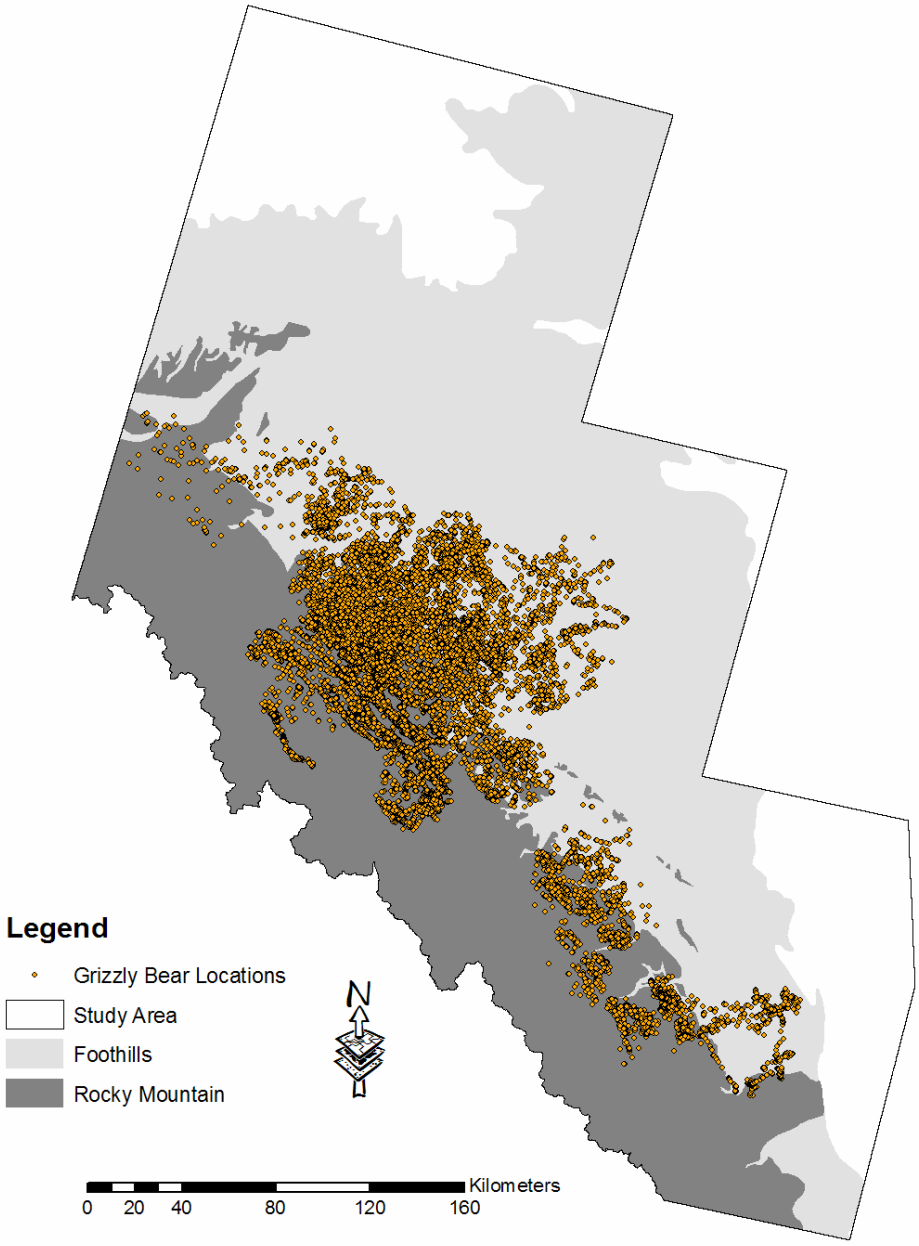

Figure 6-2: Grizzly bear telemetry locations in the study area.

Table 6-5: Summary of grizzly bears contributing to the telemetry location dataset.

Bear ID	Sex/Age class	Age†	MCP (km²)	Telemetry Locations			
				S-1*	S-2**	S-3***	Total
G001	M-adult	8.5	1629	0	68	6	74
G002	F-adult	6.5	694	150	95	48	193
G003	F-adult	6.7	849	255	349	102	706
G004	F-adult	6	474	319	1507	943	2769
G006	M-adult	16.5	1491	142	9	0	151
G007	F-adult	5	529	96	87	0	183
G008	M-adult	15.5	1827	304	490	108	902
G011	F-adult	8	484	171	151	0	322
G012	F-adult	6.5	1941	757	766	169	1692
G013	F-subadult	4	2045	0	144	0	144
G014	M-adult	10.5	2638	139	192	2	333
G016	F-adult	6	591	121	729	388	1238
G017	M-adult	8.5	1694	661	347	0	1008
G020	F-adult	5.5	987	601	850	173	1624
G023	F-adult	12	798	360	1311	289	1960
G024	M-adult	6.5	4314	372	780	289	1441
G026	F-subadult	3	1447	53	134	59	246
G027	F-adult	12	2928	222	502	231	955
G028	F-adult	7	1314	88	315	109	512
G029	M		3745	585	769	110	1464
G033	M-subadult	4	5044	555	1266	567	2388
G035	F-subadult	4	294	122	298	68	488
G036	F-subadult	3.5	1064	213	270	36	519
G037	F-subadult	4	742	61	209	99	369
G038	F-adult	15	311	79	107	31	217
G040	F-subadult	3.5	1000	430	605	278	1313
G043	M-subadult	3	1833	153	335	164	652
G044	M-subadult	3	509	78	220	131	429
G045	M-adult	6	3154	57	0	0	57
G050	M-subadult	4	903	95	89	0	184
G054	M-subadult	4	1357	0	54	0	54
G055	M-subadult	4	879	101	293	49	443
G057	F		1381	119	113	0	232
G058	M-subadult		1696	0	257	116	373
G060	F-adult		325	103	0	0	103
G061	F-subadult		593	124	363	187	674
G062	M-adult		4828	0	132	33	165
G065	F		1278	91	293	164	548
G066	M		1610	0	60	0	60
G067	F		1174	166	256	94	516
G068	M		3795	33	81	0	114
G070	F		520	0	262	158	420
G072	M		1819	267	932	358	1557
G073	F		535	56	339	19	414
G074	F		419	0	117	26	143
G075F	F		129	0	362	209	571
G092	F		299	58	120	13	191
G095	F		176	0	99	25	124
G096	F		674	0	174	58	232
G098	F		1184	0	1182	0	1182
G099	F		327	0	696	500	1196
G100	F-subadult	3.5	879	304	574	279	1157
G106	F-subadult		1692	157	269	144	570

†Age calculated as mean age during telemetry period
*Hypophagia: May 1 – June 15
**Early hyperphagia: Jun 16 – August 15
***Late hyperphagia: August 16 – October 15

hypophagia. During this time period, grizzly bear food resources are relatively limited across the landscape, and include vetches (*Hedysarum* spp.), carrion and ungulate calves, and early green herbaceous materials such horsetail (*Equisetum arvense*) and clover (*Trifolium* spp.). The second season – early hyperphagia – runs from June 16 to August 15. Early hyperphagia is characterized by increasing herbaceous forage, including cow parsnip (*Heracleum lanatum*), graminoids, sedges, and horsetails. The final season, termed late hyperphagia, runs from August 16 to October 15. During this time period, grizzly bears in the region normally seek out the fruit from buffaloberry (*Sheperdia canadensis*), blueberries, and huckleberries (*Vaccinium* spp.). It is important to note that the seasonal stratification described here represents an average of pooled multi-year observations across a very large study area. No consideration was given to inter-annual variability of habitat selection or differences within the study area caused by latitude or elevation.

While telemetry points provide information on bear *presence*, they do not contribute meaningfully to the definition of *absence*: locations on the landscape that are not used by grizzly bears. GPS collars only provide a limited sample of points on the landscape used by the individual being tracked. Locations visited by the bear between telemetry fixes, in addition to the location of uncollared grizzlies living in the study area, are completely unaccounted for. In these situations, it is appropriate to characterize *availability* rather than absence – i.e., points on the landscape that are available for use by the animal within its home range (Boyce *et al.*, 2002). In order to characterize the resources available to the GPS-collared grizzly bears used in this study, multi-annual 100% minimum convex polygon (MCP) home ranges (Figure 6-3) were defined using the

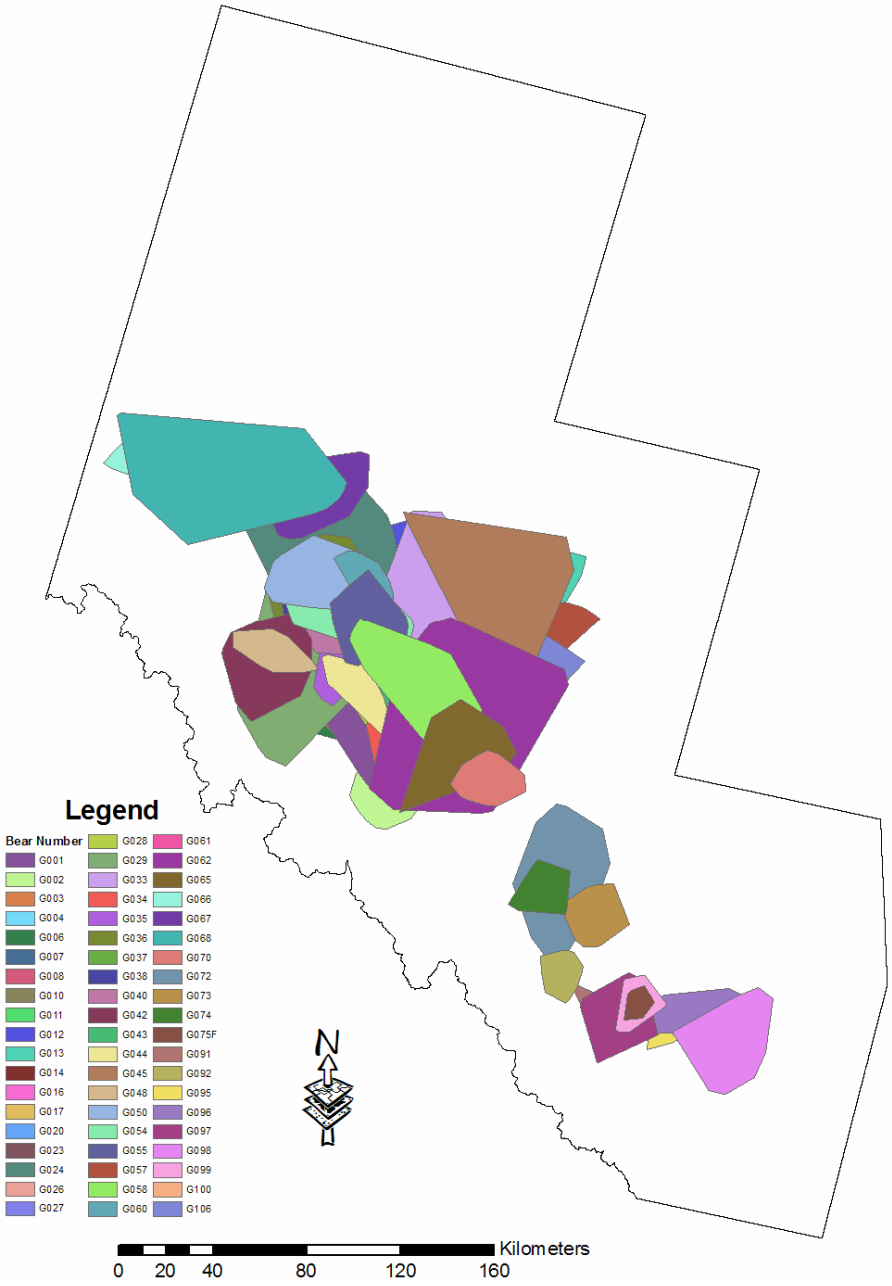

Figure 6-3: MCP home ranges for grizzly bears in the study area.

Hawth's Tools extension in ArcGIS (Beyer, 2004). A random point generator was used to select random samples within MCP home ranges at a density of roughly five points per square kilometre. Together with the grizzly bear telemetry locations, these data comprise the *presence* and *available* information suitable for both individual- and population-level resource selection analyses (Manly *et al.*, 2002).

6.2 Methods

6.2.1 Map Quality Assessment

The quality of a spatial data set is a broad issue that can relate to a variety of properties, including vagueness, precision, consistency, and completeness, among others (Worboys, 1998). In this case, the issue is further complicated by the presence of multiple data layers with widely varying characteristics. While a thorough investigation of the quality of each data source is beyond the scope of this study, several components of spatial data quality that affect each dataset's utility as a foundation for large-area wildlife work were addressed.

Map accuracy – or deviation of recorded values from true values – was evaluated using 245 independent, randomly selected test sites surveyed in the field by trained personnel. In order to establish a consistent baseline for comparing the three candidate information sources, a series of *derived* map products was produced based on land cover and structural vegetation attributes common to all three data sources (Table 6-6). While the derived maps represent a simplification of the original products and do not include some attributes that are unique to individual sources (for example, the *height* and *age* information contained in the AVI, or the LAI attributes of the FMFGBRP information

base), it does provide a framework for performing a baseline evaluation. Since the AVI does not cover the entire study area, its accuracy was assessed with a reduced set of 175 sample points. Observations were made on the basis of contingency tables and basic summary statistics such as % accuracy (user's, producer's, overall) and the kappa statistic (Cohen, 1960). Other map quality attributes – vagueness, consistency, completeness, precision, and depth – that are not as amenable to detailed statistical analyses were summarized either qualitatively or with simple summary statistics.

Table 6-6: Structural vegetation classes used to provide baseline accuracy data.

Class Label	AVI	AGCC	FMFGBRP
1. Closed Coniferous Forest	>60% Crown closure; >75% Conifer, based on basal area	>50% Crown closure; >80% Conifer, based on stem count	>50% Crown closure; >80% Conifer, based on stem count
2. Open Coniferous Forest	6-59% Crown closure; >75% Conifer, based on basal area	6-49% Crown closure; >80% Conifer, based on stem count	6-49% Crown closure; >80% Conifer, based on stem count
3. Closed Broadleaf Forest	>60% Crown closure; >75% Broadleaf, based on basal area	>50% Crown closure; >80% Broadleaf, based on stem count	>50% Crown closure; >80% Broadleaf, based on stem count
4. Open Broadleaf Forest	6-59% Crown closure; >75% Broadleaf, based on basal area	6-49% Crown closure; >80% Broadleaf, based on stem count	6-49% Crown closure; >80% Broadleaf, based on stem count
5. Closed Mixedwood Forest	>60% Crown closure; 26-74% Broadleaf, based on basal area	>50% Crown closure; 26-79% Broadleaf, based on stem count	>50% Crown closure; 26-79% Broadleaf, based on stem count
6. Open Mixedwood Forest	6-59% Crown closure; 26-74% Broadleaf, based on basal area	6-49% Crown closure; 26-79% Broadleaf, based on stem count	6-49% Crown closure; 26-79% Broadleaf, based on stem count
7. Upland Shrubs	>25% shrub cover; <6% tree cover	>25% shrub cover; <6% tree cover	>25% shrub cover; <6% tree cover
8. Upland Herbaceous	<25% shrub cover; <6% tree cover	<25% shrub cover; <6% tree cover	<25% shrub cover; <6% tree cover
9. Treed Wetland	>6% Crown closure; *wet* or *aquatic* moisture regime	>6% Crown closure; *wet* or *aquatic* moisture regime	>6% Crown closure; *wet* or *aquatic* moisture regime
10. Open Wetland	<6% Crown closure; *wet* or *aquatic* moisture regime	<6% Crown closure; *wet* or *aquatic* moisture regime	<6% Crown closure; *wet* or *aquatic* moisture regime
11. Water	>6% Standing or flowing Water	>6% Standing or flowing Water	>6% Standing or flowing Water
12. Barren Land	<6% vegetation cover	<6% vegetation cover	<6% vegetation cover

6.2.2 Resource Selection Analysis

Resource selection functions (RSFs) are any function that is proportional to the probability of use by an organism (Manly *et al.*, 2002). They have been widely employed

as tools for resource management planning, habitat mapping, cumulative effects assessment, and population viability analysis (e.g. Boyce *et al.*, 1994, Boyce and McDonald, 1999; Boyce and Waller, 2000). RSFs take the general form

$$w(x) = \exp(\beta x)$$

Equation 6-1

where $w(x)$ is the resource selection function and β is the selection coefficient of the predictor variable x. Predictor variables are normally derived from environmental datasets such as those under investigation in this study, and may be composed of land cover, vegetation, structure, disturbance, and topographic measures judged *a priori* to be related to resource selection of the organism under investigation (Burnham and Anderson, 2001). In this study, RSFs were employed not for their ecological insight, but rather as a quantifiable means of judging the relative utility of the three candidate information sources as foundations for supporting grizzly bear habitat research and operational management objectives.

While the term *RSF* can apply to a number of statistically rigorous procedures designed to predict animal occurrence (Manly *et al.*, 2002), the prevailing methods employ binomial generalized linear models (GLM) – usually logistic regression – based on presence/absence or presence/available data such as those assembled here for grizzly bears (Boyce *et al.*, 2002). With data such as these, conventional linear regression strategies are not appropriate, because the dependent variable is binary (present/available – 1/0) instead of unbounded. In addition, linear regression fitted by least squares assumes that errors are normally distributed with a constant variance and mean of zero; conditions

that are clearly not met by binary animal location data. GLMs relax the assumption of unbounded dependent variables through link functions, and employ error structures that account for non-normal residual errors (Crawley, 2002).

To evaluate the AVI, AGCC, and FMFGBRP datasets being examined in this study, a series of candidate RSF models was constructed in the statistical package S-Plus using binomial-family GLMs with log links. Separate models were developed for male and female bears during each of the three observed time frames: hypophagia, early hyperphagia, and late hyperphagia. A stepwise procedure based on Akaike's Information Criterion (AIC) (Burnham and Anderson, 1998) was used in the development of minimum adequate models, with decisions confirmed through chi-square tests and analyses of variance. Candidate models were constructed using variables from each of the three data sets separately, and evaluated against each other using the AIC statistic and null/residual deviance.

Analyses were performed at both the population and individual levels – the "Design I" and "Design III" approaches of Manly *et al.* (2002), respectively – in order to illuminate potential differences with respect to scale. At the population level, *presence* and *available* data were sampled across the entire portion of the study area occupied by grizzly bears, with individual animals not identified (Figure 6-4A). Analyses at the individual level, by contrast, worked with data drawn from a single animal's home range (Figure 6-4B).

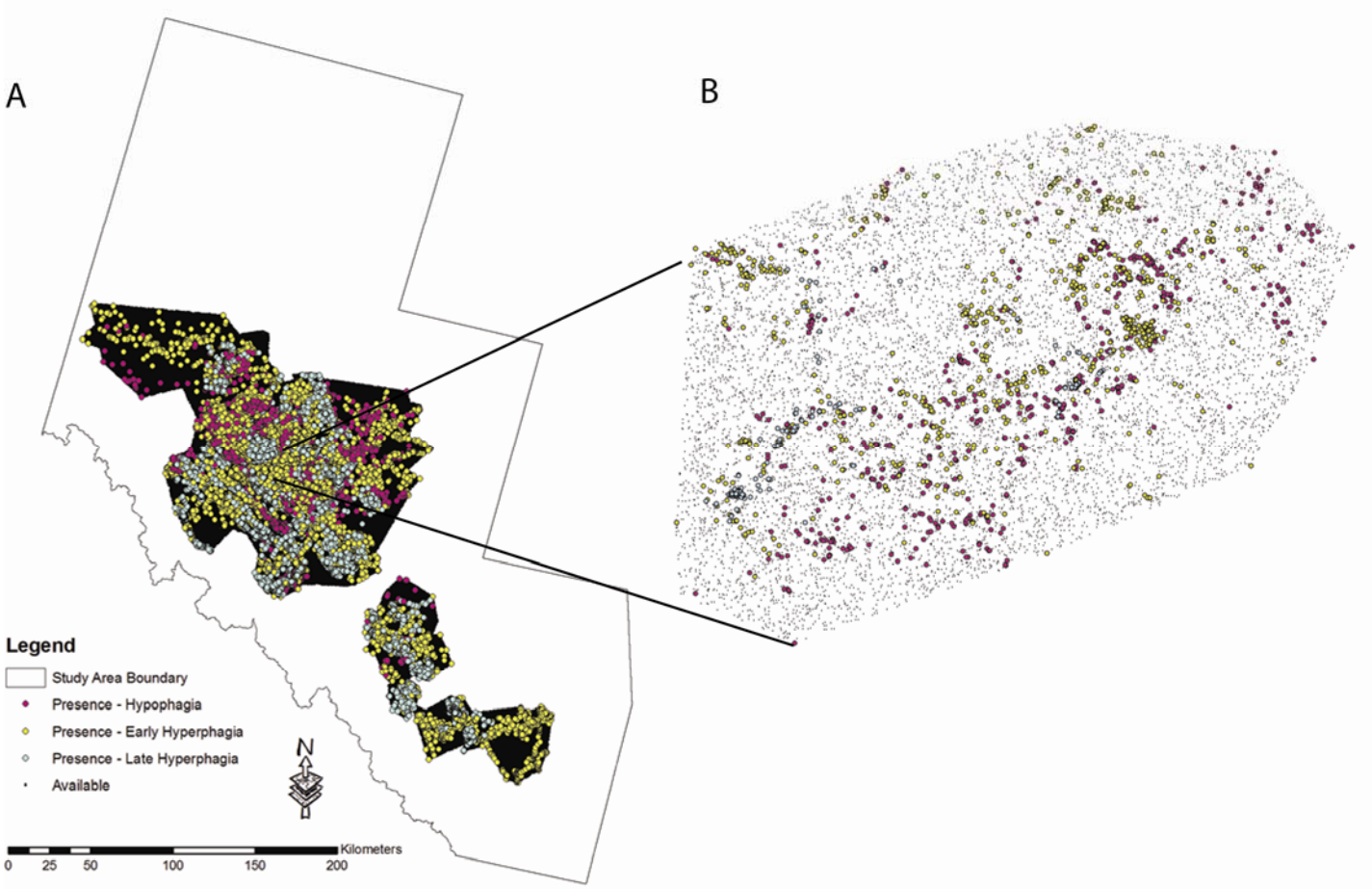

Figure 6-4: Presence-available data for population- (A) and individual- (B) level analyses. Individual shown here is G011.

A complicating factor effective at both levels of analysis revolved around the incomplete availability of the AVI within the study area. Since resource selection cannot be properly analyzed using incomplete environmental data, it was necessary to create two separate presence/absence subsets: one composed of data from all the bears, for which only remote sensing information from AGCC and FMFGBRP was available, and the second composed of data from bears whose home ranges included complete AVI coverage, for which information from all three environmental data sources was available. Since grizzly bears – particularly males – occupy such large home ranges, the *AVI-available* subset was substantially reduced from the original, containing just 14 of 34

females and one of 19 males, constrained almost exclusively to the central foothills portion of the study area (Figure 6-5). Since the AVI-based data reduction was so substantial, the population-level analyses were carried out twice: once on the reduced dataset, for which all three candidate information sources were evaluated, and once on the complete dataset, for which only the AGCC and FMFGBRP sources were evaluated. At the individual level, five bears (G070, G073, G074, G012, and G011) were selected from the reduced dataset, and formed the basis for evaluation on all three candidate information sources.

Two potential criticisms of the relatively basic modelling techniques employed here involve (i) the potential influence of autocorrelation amongst telemetry points on model parameters, and (ii) the failure to employ independent test data and other more robust statistical techniques in the assessment of model accuracy. The acknowledged presence of autocorrelation in GPS location data means an increased chance of Type I errors due to underestimated variances associated with model coefficients. A number of approaches, including data rarification (e.g. Swihart and Slade, 1985) and variance inflators (e.g. Nielsen *et al.*, 2002) are available to help account for these factors. However, the purpose of this exercise was limited to the relative evaluation of individual variables and datasets, not the pronouncement statistical inferences based on absolute model coefficients. Rigorous evaluation of error patterns – critical if the purpose of the models included the production of grizzly bear habitat maps or other secondary applications – was judged to be similarly unnecessary, given the present needs and the lack of effort spent on producing *best possible* models. A more complete series of

analyses performed in the context of broader information objectives can be found in Nielsen (2004).

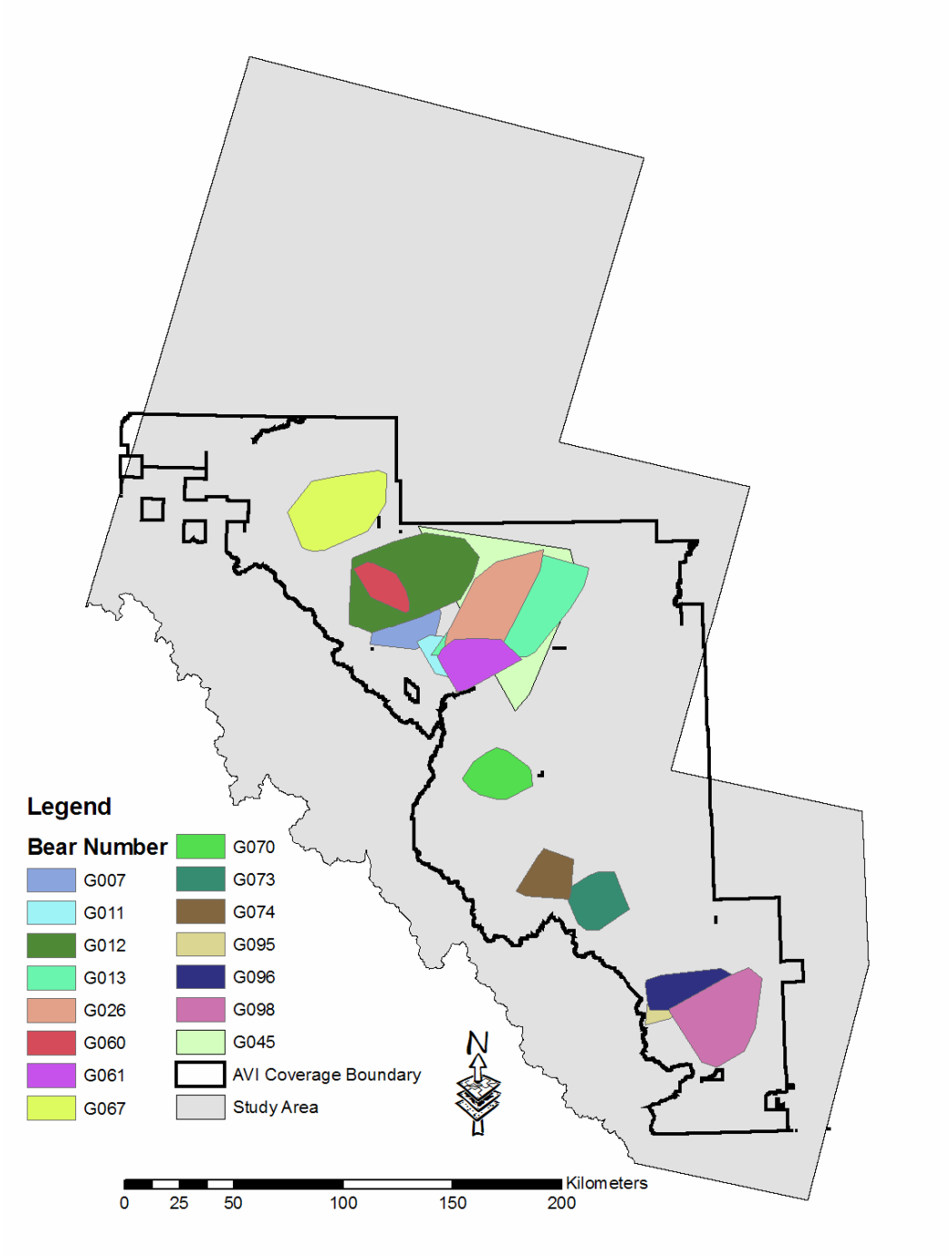

Figure 6-5: MCP home ranges for grizzly bears in portions of the study area with AVI coverage.

6.3 Results and Discussion

6.3.1 Map Accuracy

Results of the accuracy assessments on the derived map products based on each of the three candidate data sources are summarized in Table 6-7. The map derived from the FMFGBRP – the *high cost* remote sensing products – performed the best overall, with a map accuracy of approximately 78% (Kappa=0.75). The ACGG map achieved a 55% overall accuracy (Kappa=0.48), while the AVI-based product – evaluated using the reduced dataset of 175 test points – had an overall accuracy of about 45% (Kappa=0.40). Individual (Producer's) class accuracies varied widely for each data source: 50-100% for the FMFGBRP, 0-76% for the AGCC, and 14-100% for the AVI. None of the three information sources mapped the observed wetland classes with better than 53% accuracy, reflecting the complexity of wetlands in the study area, the difficulty in achieving appropriate ground data for producing high-quality maps of these features, and the generally higher emphasis placed on upland classes.

Complete confusion matrices for the FMFGBRP-, AGCC-, and AVI-based derived products are shown in Tables 6-8, 6-9, and 6-10, respectively. While generally producing the best overall results, the FMFGBRP map tended to over-estimate crown closure, resulting in confusion between open and closed treed classes. Pure conifer and broadleaf classes were mapped well, but some of the mixedwood sites were mislabelled as pure. Shrub and upland herbaceous lands were predictably confused, while spectrally and topographically distinct classes such as water and unvegetated were consistently well separated.

Table 6-7: Summary of class accuracies (Producer's), overall accuracy, and Kappa statistic for derived maps based on three candidate data sources.

Class Label	AVI		AGCC		FMFGBRP	
	N	Accuracy (%)	N	Accuracy (%)	N	Accuracy (%)
1. Closed Coniferous Forest	38	60.5	57	61.4	57	89.5
2. Open Coniferous Forest	7	71.4	8	50.0	8	62.5
3. Closed Broadleaf Forest	17	41.2	17	35.3	17	76.5
4. Open Broadleaf Forest	1	100	1	0	1	100
5. Closed Mixedwood Forest	29	13.8	33	42.4	33	69.7
6. Open Mixedwood Forest	0	-	0	-	0	-
7. Upland Shrubs	17	29.4	26	53.8	26	73.1
8. Upland Herbaceous	23	39.1	28	64.3	28	75.0
9. Treed Wetland	15	53.3	15	20.0	15	53.3
10. Open Wetland	8	25.0	8	12.5	8	50.0
11. Water	4	100	11	72.3	11	100
12. Barren Land	16	68.8	41	75.6	41	85.4
OVERALL (%)		45.1		54.7		78.0
KAPPA		0.40 (fair)		0.48 (moderate)		0.75 (good)

The AGCC product did a good job with spectrally unique classes such as water and unvegetated areas, but performed only moderately well with the more difficult designation of tree species composition and crown closure. Open coniferous forests were significantly over-estimated, and the map was unable to consistently separate pure broadleaf classes from spectrally similar mixedwood and dense shrubs. While none of the map sources performed well with the wetland classes, the poor performance of the AGCC product in these areas may have been exacerbated by the lack of topographic information from a digital elevation model.

The AVI map performed reasonably well in the closed, homogeneous tree stands, but displayed low class accuracies with other non-treed vegetation. Above all, this likely reflects the primary purpose of the AVI as a timber management tool, and the large mismatch in scale between this particular map product and ground plots used to assess it. The two-hectare minimum mapping unit used in the production of the AVI combined with a focus on operational timber management likely leads human interpreters to emphasize large, commercially viable forest stands while simplifying natural variability at smaller scales. If nothing else, these observations illustrate the issues associated with using pre-existing data sources for purposes outside of their original intent.

Table 6-8: Contingency matrix for structural vegetation map derived from FMFGBRP data products.

		Observed													
		Closed Conifer	Open Conifer	Closed Broadleaf	Open Broadleaf	Closed Mixedwood	Open Mixedwood	Upland Shrub	Upland Herbaceous	Treed Wetland	Open Wetland	Water	Unvegetated	TOTAL	USER'S (%)
Predicted (FMFGBP)	Closed Conifer	51	1			3		1		1				57	89.5
	Open Conifer	1	5					1		2			1	10	50.0
	Closed Broadleaf	1		13		4			1					19	68.4
	Open Broadleaf			2	1				1					4	25.0
	Closed Mixedwood	3	1	2		23								29	79.3
	Open Mixedwood	1				1				3				5	0
	Upland Shrub		1			1		19	3	1				25	76.0
	Upland Herbaceous							4	21				5	30	70.0
	Treed Wetland					1				8	2			11	72.3
	Open Wetland							1			4			5	80.0
	Water										1	11		12	91.7
	Unvegetated								2		1		35	38	92.1
	No Data														
	TOTAL	57	8	17	1	33	0	26	28	15	8	11	41	245	
	PRODUCER'S (%)	89.5	62.5	76.5	100	69.7	-	73.1	75.0	53.3	50.0	100	85.4		

Overall accuracy: 78.0% Kappa: 0.75 (good)

Table 6-9: Contingency matrix for structural vegetation map derived from AGCC.

		Observed													
		Closed Conifer	Open Conifer	Closed Broadleaf	Open Broadleaf	Closed Mixedwood	Open Mixedwood	Upland Shrub	Upland Herbaceous	Treed Wetland	Open Wetland	Water	Unvegetated	TOTAL	USER'S (%)
Predicted (AGCC)	Closed Conifer	35	2			6		1	2	1		2	2	51	68.6
	Open Conifer	9	4		1					1				15	26.7
	Closed Broadleaf	1	1	6		4				2			1	15	40.0
	Open Broadleaf													0	-
	Closed Mixedwood	4	1	4		14				2				25	56.0
	Open Mixedwood													0	-
	Upland Shrub	1		5		3		14	4	1	2			30	46.7
	Upland Herbaceous			1		1		7	18	1	3		5	36	50.0
	Treed Wetland			1		3		1		3	1			9	33.3
	Open Wetland					1		2	1	3	1			8	12.5
	Water	2				1		1		1	1	8	1	15	53.3
	Unvegetated	1							3			1	31	36	86.1
	No Data	4											1	5	
	TOTAL	57	8	17	1	33	0	26	28	15	8	11	41	245	
	PRODUCER'S (%)	61.4	50.0	35.3	0	42.4	-	53.8	64.3	20.0	12.5	72.3	75.6		

Overall accuracy: 54.7% Kappa: 0.48 (moderate)

Table 6-10: Contingency matrix for structural vegetation map derived from the AVI.

		Observed												
		Closed Conifer	Open Conifer	Closed Broadleaf	Open Broadleaf	Closed Mixedwood	Open Mixedwood	Upland Shrub	Upland Herbaceous	Treed Wetland	Open Wetland	Water	Unvegetated	TOTAL	USER'S (%)
Predicted (AVI)	Closed Conifer	23	1			3			2		1		1	31	74.2
	Open Conifer	9	5	1		3		2		4			1	25	20.0
	Closed Broadleaf			7		2							1	10	70.0
	Open Broadleaf			4	1									5	20.0
	Closed Mixedwood	2				4								6	66.7
	Open Mixedwood	4		3		14			1	1				23	0
	Upland Shrub		1	1				5	5	1			1	14	35.7
	Upland Herbaceous							2	9		3		1	15	60.0
	Treed Wetland					2		1		8	2			13	61.5
	Open Wetland							6	1	1	2			10	20.0
	Water											4		4	100
	Unvegetated							1	5				11	17	64.7
	No Data			1		1								2	
	TOTAL	38	7	17	1	29	0	17	23	15	8	4	16	175	
	PRODUCER'S (%)	60.5	71.4	41.2	100	13.8	-	29.4	39.1	53.3	25.0	100	68.8		

Overall accuracy: 45.1% Kappa: 0.40 (fair)

6.3.2 Map Quality Assessment

As stated previously, overall map quality is a function of a number of attributes, and a complete analysis requires consideration of more than just accuracy. Table 6-11 summarizes the relative rank of the candidate data sources among each of five map quality attributes: accuracy, vagueness, completion, consistency, precision, and depth. Ranking was assigned on the basis of quantifiable scalars where possible, but also includes qualitative assessments where necessary.

Table 6-11: Relative quality scores assigned to each environmental information source on the basis of accuracy, vagueness, completion, consistency, precision, and depth.

	Accuracy	Vagueness	Completion	Consistency	Precision	Depth	Total Score (Rank)
FMFGBRP	1	1	1	1	1	2	7 (1)
AGCC	2	1	1	1	3	3	11 (2)
AVI	3	1	3	3	2	1	13 (3)

None of the three information sources examined in this study suffered from problems related to vagueness. Metadata from each source outlined explicit class definitions, and information in all cases were related directly to physical ground phenomenon.

The AVI suffered substantially on the basis of map completion, since it was only available for about 65% of the study area. While the remote sensing datasets – which obviously do not conform to jurisdictional boundaries – are far more complete, they still contain *no data* values in areas of shadow, clouds, and other obstructions that can affect

the overall quality of the product. A quick analysis revealed these issues to be more prevalent in the AGCC dataset than the FMFGBRP products, particularly in the mountain and upper foothills portions of the study area, where *no data* values caused by shadows consume more than 13% of the total land area (Figure 6-4). By comparison, the *no data* component of the FMFGBRP data set in the same mountain and upper foothills zone occupies less than 3% of the total area. The difference is likely a function of increased shadows in the original AGCC source imagery combined with excess caution on the part of the human interpreter.

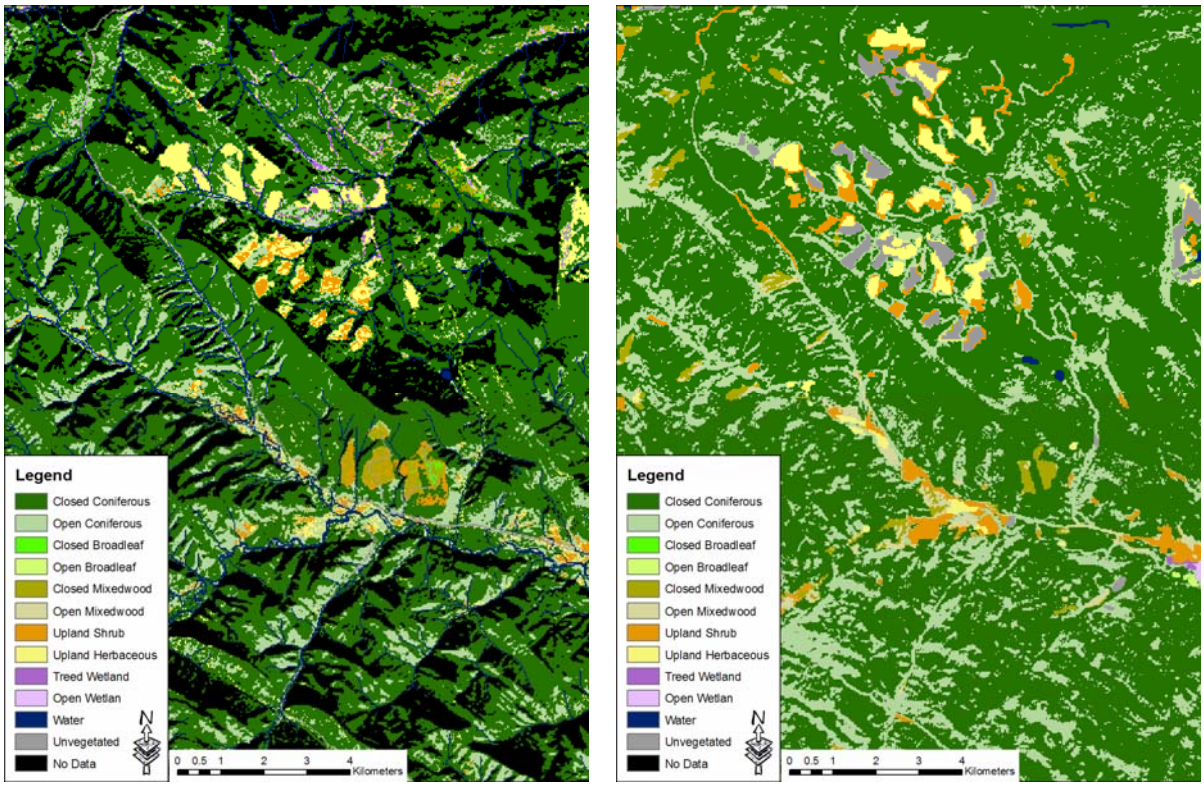

Figure 6-6: Issues related to map completion caused by shadows ('No Data') in the AGCC (left) and FMFGBRP (right) map products.

Creation and maintenance of the AVI within the study area is the responsibility of several different organizations. In the northern and central portion of the study area, individual Forest Management Agreement holders – the logging companies holding leases to operate in a given area – are responsible for producing the inventory. In the south, the responsibility lies primarily with the provincial government. Given that each of these agencies operates on a different schedule and updates may occur only once per decade or more, consistency within the AVI is an on-going concern. Even within the same organization, individual interpreters make decisions that may impact the overall consistency of the data set. Within the stratification process, a *lumper* may choose consistently larger polygons than a *splitter*, resulting in noticeable differences within the finished product (Figure 6-5). While maps derived from remote sensing – particularly large-area data sets that combine multiple image scenes across time or sensors – also have the potential for significant inconsistencies, visual inspections of the AGCC and FMFGBRP databases revealed few such issues. Careful standards relating to image preprocessing (McDermid, 2005) and production (Sanchez-Azofeifa *et al.*, 2005) have apparently eliminated most of these problems.

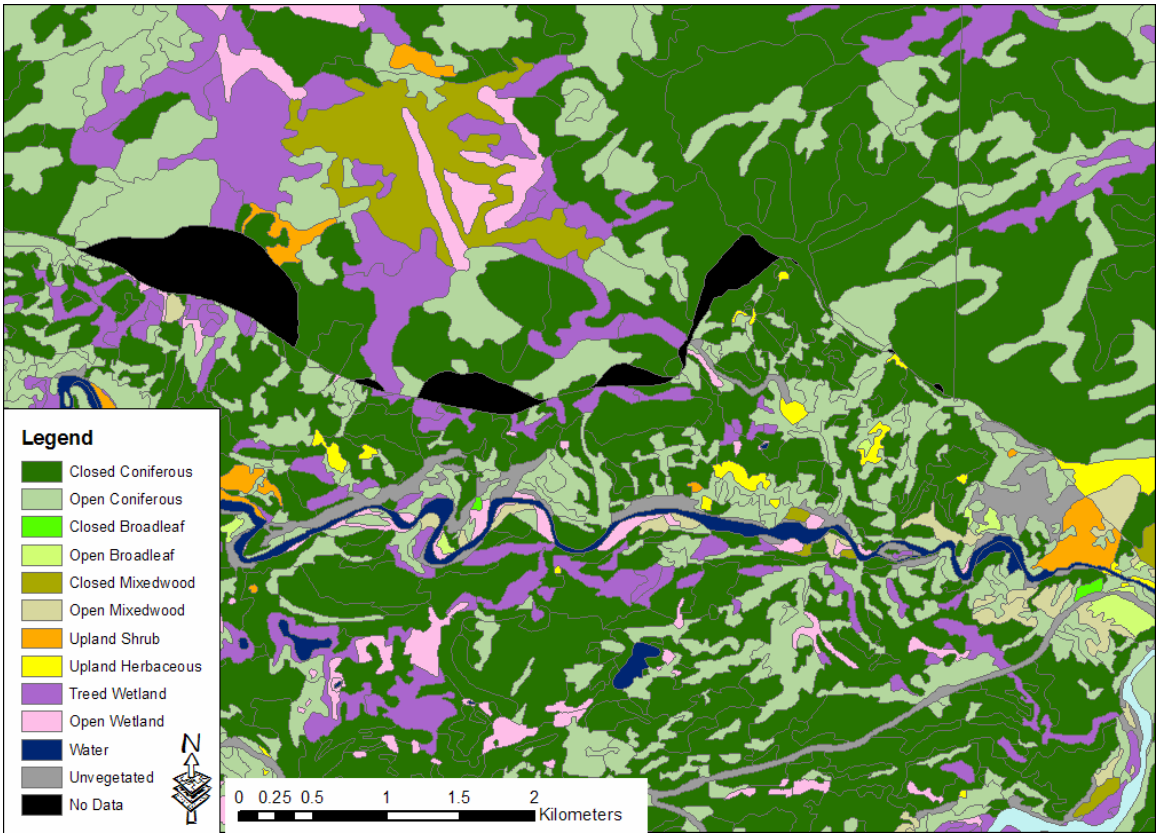

Figure 6-7: Gaps and inconsistencies in the AVI.

The level of precision afforded to a completed map product is largely a function of the procedures that went into its creation. For example, classification – the systematic arrangement of information into categories or groups – produces nominal- or ordinal-level data levels that are less precise than the interval- or ratio-level measurements upon which they are normally based. While each information source examined in this study relies on classification to some extent, the AGCC product – composed entirely of nominal- and ordinal-level classes from unsupervised cluster labelling – is the least precise. The FMFGBRP database includes continuous ratio-level estimates of crown closure, species composition, and leaf area index. While not necessarily more accurate than corresponding categorical measures, these continuous variables provide end users

with divergent needs the opportunity to define categories that suit their individual application (Cohen *et al.*, 1995). The AVI occupies the intermediate position, recording ordinal-level estimates for crown closure, interval-level measurements of species composition and age (rounded to the nearest 10), and ratio-level estimates of height.

The AGCC information source received the lowest rank with respect to information depth, since it contains just a single variable – land cover. The FMFGBRP dataset, with five separate variables, received the second position, but ranked behind the AVI with respect to depth. The AVI is widely regarded as the richest large-area information source in the province, and the only one of the three under investigation here to include three-dimensional vegetation information – height – as well as estimates of stand age, moisture regime, and productivity.

To summarize, the FMFGBRP products received the best overall rank, with a total score of 7. The AGCC map was second with a total score of 11, and the AVI was third with a total score of 13. Predictably, the results reflect the relative levels of investment tied up in the generation of each map product. High-end remote sensing databases based on large amounts of ground data, using sophisticated multi-source mapping and modeling techniques for the express purpose of the host project produced the best overall results. However, the cost of these information sources is high. Franklin *et al.* (2002) reported a cost-to-project estimate of $2.50/km for a similar high-end map from an earlier stage of the FMFGBRP. The expense is derived by extensive field programs, specialized software, and labour costs from highly trained image processing technicians. Maps based on pre-existing forest inventory data such as the AVI, on the other hand, cost the project significantly less, requiring only mid-level technical

assistance for GIS data handling. However, the overall map quality is likely to suffer from incomplete, inconsistent layers that may not match well with the goals of the study. Mid-level map remote sensing solutions with intermediate expense can be achieved through unsupervised classification techniques exemplified by the AGCC. High-quality technical expertise and sophisticated software are still required, but the need for expensive field data is significantly reduced.

6.3.3 Resource Selection Analysis

Summaries of the RSF analyses results at the population level can be found in Tables 6-12 and 6-13. Table 6-12 shows the results from the reduced data set, containing only those bears whose home ranges were covered by the AVI. Table 6-13 contains the results from the complete grizzly bear database, but is limited to candidate models derived from the two remote sensing information sources: AVI and FMFGBRP. In both cases, results are stratified by sex and time period. For female bears in the reduced dataset, FMFGBRP models received the best AIC support for all three time periods, followed by AVI and AGCC. The results suggest that *deeper* environmental databases containing information beyond categorical land cover variables are better suited to explaining female resource selection at the population level. While specific analysis of the univariate contributions of individual variables were not performed, AVI and FMFGBRP models consistently qualified non-land cover variables such as age and LAI – information that was not contained in the AGCC database. The frequent appearance of LAI and LAI change (the difference between LAI in the early and late-hyperphagia periods) in the FMFGBRP models suggests that these may be the key variables responsible for the better overall performance of the FMFGBRP information base.

There are no results for male bears at the population level, since only one male qualified for the reduced dataset – not enough to define a population. However, results from both male and female grizzly bears at the population level were available from the complete dataset outside the AVI region (Table 6-13). The patterns here were the same as those noted above, with models from the deeper FMFGBRP being ranked consistently higher than those derived using the nominal-level land cover information from the AGCC. Male bears and broader populations from both the mountain and foothills regions did not seem to affect the overall pattern of results.

Table 6-12: AIC statistics, ranks, and qualifying variables of minimum adequate models for female grizzly bears at the population level. Models derived from the reduced dataset with full AVI coverage.

Female									
	S-1			S-2			S-3		
	AIC	Rank	Variables	AIC	Rank	Variables	AIC	Rank	Variables
AGCC	85874	3	Land cover	118355	3	Land cover	63006	3	Land cover
FMFBGRP	75302	1	Land cover, LAI Change	113799	1	Early LAI, CC Land cover	58143	1	Land cover, LAI Change
AVI	75441	2	Land cover, Age	114202	2	Density, Height, Age	61127	2	Age, Density

Table 6-13: AIC statistics, ranks, and qualifying variables of minimum adequate models for male and female grizzly bears at the population level. Models derived from the full dataset with no AVI coverage.

Female									
	S-1			S-2			S-3		
	AIC	Rank	Variables	AIC	Rank	Variables	AIC	Rank	Variables
AGCC	215624	2	Land cover	278894	2	Land cover	224690	2	Land cover
FMFBGRP	199117	1	Land cover, LAI Change	277614	1	Early LAI, Land cover	200251	1	Land cover, CC, LAI Change
Male									
	S-1			S-2			S-3		
	AIC	Rank	Variables	AIC	Rank	Variables	AIC	Rank	Variables
AGCC	204397	2	Land cover	241102	2	Land cover	146949	2	Land cover
FMFBGRP	175556	1	Land cover, CC, Early LAI	218565	1	Land cover, Early LAI	111093	1	Land cover, LAI Change

Summaries of the RSF analyses results for the five selected bears at the individual level can be found in Table 6-14. Once again, it seems clear that environmental data sets containing depth beyond land cover are superior for explaining resource selection at the individual level. Models derived from the AGCC database were consistently ranked lower than those from the deeper AVI and AGCC information sources. Age, density, LAI, and crown closure were frequently selected in the final minimum adequate models, and received better AIC support than models constructed from AGCC-derived land cover alone. However, there seems very little to choose between AVI- and FMFGBRP-based models at the individual level, with both sources contributing top-ranked models: seven out of ten cases for FMFGBRP and three out of ten for AVI. There seemed to be no discernable patterns regarding time period related to these observations; concrete conclusions – if they exist – would require a more detailed analysis.

A summary of the mean rankings observed for models at the individual and population levels, as well as an overall ranking of all trials is shown in Table 6-15. Models from the FMFGBRP dataset were ranked number one overall, followed by the AVI and AGCC. The firm advantage of the AVI and FMFGBRP data sets over the land cover-only AGCC offering illustrate the additional explanatory power contained in datasets with additional variables such as age, height, LAI, and crown closure. The closeness of the overall ranking of the AVI and FMFGBRP models – particularly at the individual level – suggests that one source has no clear-cut advantage over the other, and that either might serve effectively as foundations for grizzly bear research and operational management activities, depending on the scope and needs of the individual project. The major limitation of the AVI information base is its incomplete coverage, particularly in the mountain regions and with respect to male grizzly bears with extensive home ranges.

Table 6-14: AIC statistics, ranks, and qualifying variables of minimum adequate models for selected male and female grizzly bears at the individual level.

G070									
	S-1			S-2			S-3		
	AIC	Rank	Variables	AIC	Rank	Variables	AIC	Rank	Variables
AGCC				7179	3	Land cover			
FMFBGRP				6803	2	Land cover, Late LAI, CC			
AVI				6700	1	Land cover, Density, Height			
G073									
	S-1			S-2			S-3		
	AIC	Rank	Variables	AIC	Rank	Variables	AIC	Rank	Variables
AGCC	4424	3	Land cover	7934	3	Land cover	5989	3	Land cover
FMFBGRP	3933	1	Land cover, LAI Change, CC	7484	2	Land cover, LAI Change, CC	5347	1	Land cover, LAI Change
AVI	4136	2	Land cover, Age, Density	7481	1	Density, Age, Total Conifer	5429	2	Density, Age, Total Conifer
G074									
	S-1			S-2			S-3		
	AIC	Rank	Variables	AIC	Rank	Variables	AIC	Rank	Variables
AGCC				6072	3	Land cover			
FMFBGRP				4309	1	Early LAI, CC			
AVI				4827	2	Density, Age, Total Conifer			
G012									
	S-1			S-2			S-3		
	AIC	Rank	Variables	AIC	Rank	Variables	AIC	Rank	Variables
AGCC	23392	3	Land cover	24708	3	Land cover	14509	3	Land cover
FMFBGRP	23020	1	Early LAI, CC	23250	1	LAI Change, CC	11304	1	LAI Change, SC
AVI	23813	2	Density, Height, Age	23937	2	Land cover, Age	12461	2	Density
G011									
	S-1			S-2			S-3		
	AIC	Rank	Variables	AIC	Rank	Variables	AIC	Rank	Variables
AGCC	6281	3	Land cover	6099	3	Land cover			
FMFBGRP	5484	1	Early LAI, CC	6009	2	Land cover, LAI Change			
AVI	5737	2	Density, Height, Age	5729	1	Density, Height, Age			

Table 6-15: Mean rank summary of minimum adequate models for at the individual, population, and combined (both individual and population) levels.

	Individual	Population	Overall
AGCC	3	3	3
FMFBGRP	1.3 (1)	1	1.2 (1)
AVI	1.7 (2)	2	1.8 (2)

6.4 Conclusions

Three sources of environmental information that are commonly employed in support of modern wildlife research and management projects were evaluated on the basis of two factors: overall map quality, and the ability to explain grizzly bear habitat use, as observed through RSF models of telemetry presence/availability data. The three candidate information sources examined were (i) the Alberta Vegetation Inventory, typifying the pre-existing forest inventory databases that are common across productive forested lands throughout North America; (ii) the Alberta Ground Cover Characterization land-cover map, representing a relatively low-cost remote sensing information product derived through unsupervised classification and limited field data; and (iii) the Foothills Model Forest Grizzly Bear Research Program information base generated in this dissertation, representing a relatively high-cost remote sensing information source comprised of land cover, crown closure, species composition, and LAI phenology, derived through supervised classification and empirical modelling techniques using large amounts of field data. Map quality – judged here as a function of accuracy, vagueness, consistency, completeness, precision, and depth – ranked the high-cost FMFGBRP information source the highest. The AVI – the deepest information source of the three – suffered from incomplete coverage across the study area, spatial inconsistencies, and low

accuracy at the point scale used in this study. The AGCC map occupied the middle quality position, with good consistency, but lower accuracy and issues related to map completeness caused by excessive shadows in the mountain and upper foothills regions. In terms of their ability to explain observed patterns of grizzly bear telemetry locations across the study area, a series of resource selection function models displayed the importance of information depth beyond the basic land cover information contained in the low-cost AGCC information set. AVI- and FMFGBRP-based models both ranked consistently higher in terms of AIC support at both the individual and population levels, but the AVI was limited by incomplete coverage, particularly with the exceptionally large home ranges occupied by male bears, as well as individuals occupying multi-jurisdictional lands in the upper foothills and mountain regions.

To summarize, existing inventory data sources such as the AVI seem capable of supporting grizzly bear research and management objectives in regions where coverage is complete, but must be judged ineffective across the entire study area. Issues related to map quality – particularly coverage, consistency, and accuracy at the sub-stand level – are of particular concern. Low-cost remote sensing alternatives, while certainly capable of producing higher-quality map products over large, multi-jurisdictional areas, display consistently lower capacities for explaining observed patterns of grizzly bear habitat use. High-cost remote sensing products – such as those developed in this research for the Foothills Model Forest Grizzly Bear Research Program – appear to have the depth necessary to explain occurrence patterns at levels as good as or better than those observed for the AVI, and can still be produced consistently and effectively across large areas. As

such, they are the recommended strategy for wildlife studies conducted across large, multi-jurisdictional study areas.

Chapter 7: Summary and Conclusions

A strong alliance is forming between remote sensing and ecology in order to address the challenges of habitat mapping and other aspects of contemporary wildlife management. Unfortunately, the effectiveness of this partnership has so far been hindered by miscommunication and a lack of common understanding between the *tools* experts – practitioners of remote sensing, GIS, and other spatial techniques – and *applications* personnel with expertise in wildlife management and biology. Pioneering work has demonstrated the promise of geospatial tools in cross-disciplinary ecology, but an effective application strategy has yet to be formalized. Classification, per-pixel modelling, and spatio-temporal pattern analysis techniques provide useful tools in the wildlife management arena, but scientists and resource managers require guidance for their practical application.

At the outset of this endeavour, three major research goals were established:

1. A methodological approach for creating high-quality, spatially explicit environmental information over large areas must be articulated,
2. Robust strategies for creating attribute-based maps of land cover, crown closure, species composition, and LAI phenology must be established, and
3. The effectiveness of these new products for supporting operational management objectives over large, multi-jurisdictional areas must be determined.

The following paragraphs briefly summarize the successful achievement of these goals.

1. During the course of this research, a methodological framework has been developed to enable the competent application of remote sensing for large-area, multi-jurisdictional habitat mapping. Grounded in hierarchy theory and the

remote sensing scene model, the approach advocates the identification of key physical processes operating on the landscape, followed by the selective application of multiple techniques matched to data sources specifically designed to extract H- and L-resolution information, as appropriate. This is fundamentally different than the single-map, classification-based strategies typical of most remote sensing/wildlife studies, in its recognition that land and vegetation information exists at a variety of spatial and temporal scales, and that no single map is capable of capturing the full range of variability observed in reality. Also, by focussing on multiple attributes and the production of continuous, high-order variables wherever possible, the approach results in the generation of a multi-source information base flexible enough to support multiple management objectives – a desirable attribute that should reduce the need for frequent re-investment commonly experienced with inflexible, nominal-level classification products.

2. Robust strategies were developed for the creation of a four-attribute database of land cover, crown closure, species composition, and LAI phenology over a study area covering more than 100,000 km^2 of rugged, multi-jurisdictional terrain in west-central Alberta. Generated through a blend of object-oriented classification, conventional regression, and generalized linear modelling of Landsat, MODIS, and topographic data, the exercise represents a successful case study carried out under exceptionally challenging conditions. Accuracy assessment of individual model components revealed generally good results. The land-cover map, produced through object-oriented classification of spectral and topographic

variables using the software package eCognition, had an overall accuracy of 91.8% (Kappa=0.904). The continuous-variable crown closure map, based on combined spectral and topographic models developed across natural region-stratified source areas in the core of the study area and extended piece-wise across the remainder of the study area, displayed accuracies in the 90% range (Kappa=0.8) for map aggregates based on a two-class configuration, 65% (Kappa=0.5) for a three-class configuration, and 50% (Kappa=0.4) for a four-class configuration. The continuous-variable species composition map – again based on combined spectral and topographic models – displayed accuracies in the 90% range (Kappa=0.7) for map aggregates based on a two-class configuration, 73% (Kappa=0.6) for a three-class configuration, and 73% (Kappa=0.6) for a four-class configuration. Empirical models of effective LAI developed during the key early and late-hyperphagia time periods achieved r^2 values of 0.52 and 0.82, respectively, using the mid infrared-corrected versions of the Normalized Difference Vegetation Index (NDVIc).

3. In order to assess the effectiveness of these new products for supporting operational management objectives over large, multi-jurisdictional areas, a series of experiments were designed to measure the thesis database against two alternative sources of environmental information: (i) the Alberta Vegetation Inventory – the provincial forest inventory database – and (ii) the Alberta Ground Cover Characterization – a remote sensing land cover product produced through traditional unsupervised classification techniques by technicians at the University of Alberta's Earth Observation Systems Laboratory. The three candidate

information bases were assessed in terms of both map quality and their ability to explain patterns of grizzly bear telemetry locations. In both cases, the thesis database produced the best overall results.

To conclude, the multi-scale, attribute-based framework for environmental information extraction developed in this thesis provides an effective strategy for generating consistent, high-quality land and vegetation information over large, multi-jurisdictional areas. The Landsat- and MODIS-based products generated over the challenging, 100,000-km^2 study area serve as an effective case study, demonstrating the superior quality of the information base as both a source of map products and a foundation for operational grizzly bear research and wildlife habitat mapping.

7.1 Research Contributions

With a study area roughly half the size of the United Kingdom, this project ranks among the largest and most ambitious satellite mapping exercises ever conducted in Alberta. In achieving this milestone, a number of research contributions have been secured. First, an extensive review regarding the role of remote sensing in large-area habitat mapping and other ecological applications was compiled. Published as McDermid *et al.* (2005), the work articulated the philosophical foundation that would go on to guide all subsequent mapping activities. In addition to this theoretical work, a number of methodological contributions have also been made. Most obvious is the development of the multi-scale, attribute-based information-extraction strategy that forms the core of this project, and its subsequent application across a large, challenging study area. Methodological contributions were also made concerning operational strategies for radiometric

processing and model extension for the elimination of seam lines in multi-scene remote sensing products. Perhaps most significant, however, are the application-based contributions of this work. The map comparison material presented in Chapter 6 represents the first known evaluation of traditional inventory and remote sensing-based alternatives for grizzly bear habitat mapping, and forms a significant contribution to the wildlife literature. Looking forward, the demonstrated utility of the remote sensing-based information products for these and other applications, including forthcoming work in the study area with mountain caribou and elk forage biomass, reveals the flexibility of the approach developed here, and sets the stage for articulating a broader geospatial approach for large-area, multi-jurisdiction resource management.

The Foothills Model Forest Grizzly Bear Research Program (FMFGBRP), the project within which the bulk of this research was conducted, was honoured by the Alberta provincial government in 2004 with an Emerald Award for Environmental Excellence in the *Research and Innovation* category. The tools, procedures, and products developed in the context of that project have been adopted as a core part of the long-term conservation strategy for grizzly bear in Alberta. In the early part of 2005, the Foothills Model Forest held a series of industry workshops designed to introduce the new planning tools developed through research in the FMFGBRP – including the remote sensing-based products presented in this thesis – to managers and executives in the forestry and oil/gas industries. In opening these workshops, Doug Sklar, the Executive Director of Sustainable Resource Development in the province stated that "the next series of forest management plans will be expected to use these tools". The remote sensing-based mapping strategies developed in this research continue to form the foundation for

spatially explicit land cover and vegetation information in the FMFGBRP as it expands both north and south as part of its stated goal to map all the known grizzly bear habitat in the province.

7.2 Suggestions for Future Research

While the current work contains a number of substantial research contributions, the multi-disciplinary realm of remote sensing in wildlife and resource management is still relatively undeveloped, and a large number of research issues yet remain. The following suggestions are among the most relevant topics arising from the work reported in this thesis.

Several issues arose during the administration of this project, but were deemed to be outside the scope of the current investigation. For example, the land cover/vegetation mapping and modelling work conducted within this research was designed primarily around natural vegetation communities occurring outside of regenerating areas formed by cut blocks, burns, and other disturbance features. While the products certainly cover these areas, observations made in the preliminary stages of this project suggested that the patterns and processes operating in cut blocks and other regenerating surfaces are fundamentally different than those in surrounding undisturbed lands. Future research should attempt to identify the key attributes occurring within these regions, and develop maps and models specifically tuned to these important environments.

A second issue arising out of this research involves the issue of topographic correction. The *topographic effect* – the deleterious effects of topography on image analysis – is a well-documented but incompletely understood phenomenon that image analysts find very difficult to account for (Kimes and Kirchner, 1981; Dymond, 1992;

Dubayah and Rich, 1995). While strategies for ameliorating some of these effects do exist (e.g. Civco, 1989; Richter, 1997; Riano *et al.*, 2003) none of them were implemented in this project; a factor that may have limited the effectiveness of spectral models and classification results, particularly in the high-relief portions of the study area. Future research efforts should employ an approach similar to the one adopted for atmospheric correction to evaluate and identify the most effective strategy for operational topographic correction, and document the impacts of topographic correction on the resulting products. One potentially serious limitation in this work revolves around the lack of a high-quality DEM over the full study area. Both major topographic data sources – the Alberta provincial DEM as well as the DMTI model used in this project – are relatively low-quality models generated through the interpolation of contour lines. The lack of a quality DEM not only limits the ability to perform effective topographic correction, but seriously hinders the potential role of geomorphometric derivatives in general mapping and modelling activities. In general, the lack of high-quality topographic information stands out as among the most serious limitations of this work. Future efforts to engage higher-quality DEMs, such as the recently acquired interferometric RADAR product covering Banff National Park, would be productive.

While the core strategy of the framework developed in this research – the identification of key physical attributes of the landscape, followed by the selection of intelligent, scale-sensitive strategies for mapping them – has already been established, a large amount of work remains regarding the application of this strategy. In particular, two key areas require attention: (i) the evaluation of new data, and (ii) the development of new products. For many years, the number of reliable options for obtaining satellite

imagery was quite limited. However, the large number of recent launches has lead to the emergence of a new era with an unprecedented number of choices regarding spectral, spatial, and temporal resolution. The utility of these new data sources for characterizing key land cover/vegetation attributes needs to be evaluated. In particular, data fusion techniques involving LiDAR (e.g. Miller, 2003; Asner, *et al.*, 2002) and interferometric RADAR (e.g. Treuhaft, *et al.*, 2004; Asner *et al.*, 2000) hold the potential to expand the information potential of satellite imagery over vegetated surfaces beyond the two-dimensional limitations of optical data towards a much more meaningful characterization of three-dimensional structure. In regards to new products, future efforts should work towards a much more meaningful multi-scale characterization of natural vegetated landscapes. Priorities include better spatial characterizations of broad-scale entities, such as the natural region- and subregion-based classes of Achuff (1992), as well as other more detailed vegetation attributes including age, height, density, and forest composition at the species level. The potential also exists to characterize vegetation phenology much more thoroughly than the rough preliminary attempts contained in this work by exploiting the full potential of high-temporal-resolution sensor systems such as MODIS. Future research should also build on the work of Couroux *et al*. (2005) in the attempt to tease apart the ecologically significant contributions of the understorey from the complete phenology measurements recorded by the sensor.

One of the initial objectives stated in this research involved creating a methodological framework that would generate an information base flexible enough to support multiple resource management objectives. With the current set of products now in place over a substantial portion of Alberta, the exciting opportunity exists to apply

these data to projects outside of the original FMFGBRP. With this in mind, a number of new research initiatives are already under way. For example, a collaboration with researchers in the Ya Ha Tinda Elk and Wolf Project will attempt to use the environmental database developed in this thesis to explain elk movement and habitat selection patterns. Of particular interest is the application of MODIS phenology curves to map changes in herbaceous forage biomass: a key component of elk habitat. In another initiative, Parks Canada has provided support the complete mapping of the five Rocky Mountain parks: Banff, Jasper, Yoho, Kootenay, and Waterton Lakes using the approach developed in this thesis. The first field season was completed in the summer of 2005, and a second is scheduled for 2006. The resulting database is slated to replace the outdated Ecological Land Classification, and will contribute immediately towards such pressing management issues as Mountain Pine Beetle mapping and monitoring, Mountain Caribou habitat assessment, Whitebark Pine mapping and monitoring, and avalanche hazard assessment. The challenges posed by these and other management issues on the multi-use, multi-jurisdictional lands of western Canada will fuel future research activities for years to come.

References

Achuff, P. L., 1992: *Natural Regions, Subregions, and Natural History Themes of Alberta: A Classification for Protected Areas* Management. Alberta Environmental Protection, Edmonton, Alberta.

Allen, T. R., 2000: Topographic normalization of Landsat Thematic Mapper data in three mountain environments. *Geocarto International*, Vol. 15, pp. 13-19.

Anderson, J. R., E. E. Hardy, J. T. Roach, and R. E. Witmer, 1976: *A Land Use and Land Cover Classification System for Use with Remote Sensor Data*. U.S. Geological Survey Professional Paper 964, Washington, DC.

Apps, M. J., W. A. Kurz, S. J. Bukema, and J. S. Bhatti, 1999: Carbon budget of the Canadian forest products sector. *Environmental Science and Policy*, Vol. 2, No. 1, pp. 25-41.

Asner, G. P., R. N. Treuharft, and B. E. Law, 2000: Vegetation structure from quantitative fusion of hyperspectral optical and radar interferometric remote sensing. *AVIRIS Proceedings: 2000*. http://popo.jpl.nasa.gov/docs/workshops/00_docs/Asner_2_web.pdf accessed 09/01/05.

Asner, G. P., M. Palace, M. Keller, and R. Pireira, Jr., 2002: Estimating canopy structure in an Amazon forest from laser range finder and Ikonos satellite imagery. *Biotropica*, Vol. 34, No. 4, pp. 483-492. http://www.google.com/url?sa=t&ct=res&cd=1&url=http%3A//asnerlab.stanford.edu/publications/peerpublications/asner_etal_Biotropica_2002.pdf&ei=5pgbQ6mAM7-aYMqB3YML accessed 09/01/05.

Asrar, G., R. B. Myneni, and B. J. Choudhury, 1992: Spatial heterogeneity in vegetation canopies and remote sensing of absorbed photosynthetically active radiation: a modelling study. *Remote Sensing of Environment*, Vol. 41, pp. 85-101.

Atkinson, P. M. and A. R. L. Tatnall, 1997: Neural networks in remote sensing. *International Journal of Remote Sensing*, Vol. 18, No. 4, pp. 699-709.

Austen, M. J. W., C. M. Francis, D. M. Burke, and M. S. W. Bradstreet, 2001: Landscape context and fragmentation effects on forest birds in southern Ontario. *Condor*, Vol. 103, pp. 701-714.

Baatz, M. and A. Schape, 1999: Object-oriented and multi-scale image analysis in semantic networks. In *Proceedings of the 2nd International Symposium on Optimization of Remote Sensing,* Enschede, Netherlands.

Barandela, R. and M. Juarez, 2002: Supervised classification of remotely sensed data with ongoing learning capability. *International Journal of Remote Sensing*, Vol. 23, No. 22, pp. 4965 – 4970.

Baret, F., G. Guyot, A. Begue, P. Maurel, and A. Podaire, 1988: Complementarity of middle infrared with visible and near-infrared reflectance for monitoring wheat canopies. *Remote Sensing of Environment*, Vol. 26, pp. 213-225.

Barradas, V. L., H. G. Jones, and J. A. Clark, 1998: Sunfleck dynamics and canopy structure in a *Phaseolus vulgaris* canopy. *International Journal of Biometeorology*, Vol. 42, No. 1, pp. 34-43.

Bauer, M. E., T. E. Burk, A. R. Ek, P. R. Coppin, S. D. Lime, T. A. Walsh, D. K. Walters, W. Befort, and D. F. Heinzen, 1994: Satellite inventory of Minnesota forest resources. *Photogrammetric Engineering and Remote Sensing*, Vol. 63, pp. 59-67.

Begon, M., Harper, J.L. and Townsend, C.R., 1990. Ecology: Individuals, Populations and Communities, 2nd edition. Blackwell, Boston.

Beyer, H., 2004: *Hawth's Tools: An Extension for ArcGIS*. http://www.spatialecology.com accessed 08/04/05.

Binaghi, E. P. Madella, M. Grazia Montesano, and A. Rampini, 1997: Fuzzy contextual classification of multisource remote sensing images. *IEEE Transactions on Geoscience and Remote Sensing*, Vol. 28, pp. 540-551.

Bolstad, P. V. and S. T. Gower, 1990: Estimation of leaf area index in fourteen southern Wisconsin forest satnds using a portable radiometer. *Tree Physiology*, Vol. 7, pp. 115-124.

Bolstad, P. V. and T. M. Lillesand, 1992: Flexible integration of satellite imagery and thematic spatial data. *Photogrammetric Engineering and Remote Sensing*, Vol. 58, No. 7, pp. 965-971.

Bolstad, P. V. and S. T. Gower, 1992: Improved classification of forest vegetation in northern Wisconsin through a rule-based combination of soils, terrain, and Landsat Thematic Mapper data. *Forest Science,* Vol. 38, No. 1, pp. 5–20.

Borak, J. S. and A. H. Strahler, 1999: Feature selection and land cover classification of a MODIS-like data set for a semiarid environment. *International Journal of Remote Sensing*, Vol. 20, pp. 919-938.

Borboroglu, G. P., P. Yorio, P. D. Boersma, H. Del Valle, and M. Bertellotti, 2002: Habitat use and breeding distribution of Magellanic Penguins in northern San Jorge Gulf, Patagonia, Argentina. *Auk*, Vol. 119, pp. 233–239.

Boyce, M. S., and L. L. McDonald, 1999: Relating populations to habitats using resource selection functions. Trends in Ecology and Evolution, Vol. 14, pp. 268-272.

Boyce, M. S., J. S. Meyer, and L. L. Irwin, 1994: Habitat-based PVA for the northern spotted owl. In: Fletcher, D.J., Manly, B.F.J. (Eds.), *Statistics in Ecology and Environmental Monitoring, Otago Conference Series No. 2*. University Otago Press, Dunedin, New Zealand, pp. 63-85.

Boyce, M. S., P. R. Vernier, S. E. Nielsen, and F. K. A. Schiemgelow, 2002: Evaluating resource selection functions. *Ecological Modelling*, Vol. 157, pp. 281-300.

Boyce, M. S., J. Waller, 2000: The application of resource selection functions analysis to estimate the number of grizzly bears that could be supported by habitats in the Bitterroot ecosystem. In: C. Servheen (Ed.), *Grizzly Bear Recovery in the Bitterroot Ecosystem. Final Environmental Impact Statement*. Appendix 21B. US. Fish & Wildlife Service, Missoula, Montana, USA, pp. 6-231-6-241.

Brodley, C. and M. Friedl, 1999: Identifying mislabeled training data. Journal of *Artificial Intelligence Research*, Vol. 11, pp. 131-167.

Brown de Colstoun, E. C., M. H. Story, C. Thompson, K. Commisso, T. G. Smith, and J. R. Irons, 2003: National park vegetation mapping using multitemporal Landsat 7 data and a decision tree classifier. Remote Sensing of Environment, Vol. 85, pp. 316-327.

Burnham, K.P. and D. R. Anderson, 1998: *Model Selection and Inference: A Practical Information-Theoretic Approach*. Springer-Verlag, New York, New York, USA.

Burnham, K. P. and D. R. Anderson, 2001: Kullback-Leibler information as a basis for strong inference in ecological studies. *Wildlife Biology*, Vol. 28, pp. 111-119.

Butera, C., 1986: A correlation and regression analysis of prevent canopy closure and TM spectral response for selected forested sites in the San Juan National Forest, Colorado. *I.E.E.E. Transactions on Geoscience and Remote Sensing*, Vol. GE-24, pp. 122-129.

Carroll, C., W. J. Zielinski, and R. F. Noss, 1999: Using presence-absence data to build and test spatial habitat models for the fisher in the Klamath region, USA. *Conservation Biology*, Vol. 13, No. 6, pp. 1344-1359.

Chander, G. and B. Makham, 2003: *Revised Landsat TM Radiometric Calibration Procedures and Post-Calibration Dynamic Ranges.* United States Geological Survey publication. http://landsat7.usgs.gov/documents/L5TMCal2003.pdf accessed 09/01/05.

Chason, J. W., D. D. Baldocchi, and M. A. Huston, 1991: Comparison of direct and indirect methods for estimating forest canopy leaf area. *Agriculture and Forest Meteorology*, Vol. 57, pp. 107-128.

Chavez Jr., P. S., 1988: An improved dark-object subtraction technique for atmospheric scattering correction of multispectral data. *Remote Sensing of Environment*, Vol. 24, pp. 459-479.

Chen, J. M. and T. A. Black, 1992: Defining leaf area index for non-flat leaves. *Plant Cell and Environment*, Vol. 15, pp. 421-429.

Chen, J. M. and J. Cihlar, 1996: Retrieving leaf area index of boreal conifers using Landsat TM images. *Remote Sensing of Environment*, Vol. 55, pp. 153-162.

Chrisman, N. R., 1989: Modelling error in overlaid categorical maps. In M. Goodchild and S. Gopal (Eds.) *Accuracy of Spatial Databases*. Taylor and Francis, Philidelphia, PA, pp. 21-34.

Ciarniello, L. M., M. S. Boyce, and H. Beyer, 2002: *Grizzly Bear Habitat Selection Along the Parsnip River, British Columbia*. A report prepared for the British Columbia Ministry of Forests, Prince George Forest Region, 24 p. http://web.unbc.ca/parsnip-grizzly/progress/RSF_Grizzly.pdf accessed 09/01/05.

Cihlar, J., 2000: Land cover mapping of large areas from satellites: status and research priorities. *International Journal of Remote* Sensing, Vol. 2, No. 6 /7, pp. 1093-1114.

Cihlar, J., J. Chen, Z. Li, G. Fedosejevs, M. Adair, W. Park, R. Fraser, A. Trishchenko, B. Guindon, and D. Stanley, 2002: GeoComp-n, an advanced system for the processing of coarse and medium resolution satellite data. Part 2: biophysical products for the northern ecosystem. *Canadian Journal of Remote Sensing*, Vol. 28, No. 1, pp. 21-44.

Cihlar, J., D. Manak, and N. Voisen, 1994: AVHRR bidirection reflectance effects and compositing. *Remote Sensing of Environment*, Vol. 60, pp. 35-57.

Civco, D. L., 1989: Topographic normalization of Landsat Thematic Mapper digital imagery. Photogrammetric Engineering and Remote Sensing, Vol. 55, No. 9, pp. 1303-1309.

Clausi, D.A., 2002: An analysis of co-occurrence texture statistics as a function of grey level quantization. *Canadian Journal of Remote Sensing*, Vol. 28, No. 1, pp. 45-62.

Cohen J., 1960: A coefficient of agreement for nominal scales. *Educational and Psychological Measurement*, pp. 37-46.

Cohen J., 1968: Weighted kappa: Nominal scale agreement with provision for scaled disagreement or partial credit. *Psychological Bulletin*, Vol. 70, pp. 213-220.

Cohen, W.B., 1991: Response of vegetation indices to changes in three measures of leaf water stress. *Photogrammetric Engineering and Remote Sensing*, Vol. 57, pp. 195–202.

Cohen WB, Spies TA, Alig RJ, Oetter DR, Maiersperger TK, Fiorella M., 2002: Characterizing 23 years (1972–1995) of stand replacement disturbance in western Oregon forests with Landsat imagery. *Ecosystems* Vol. 5, pp. 122–137.

Cohen, W. B., T. K. Maiersperger, S. T. Gower, and D. P. Turner, 2003: An improved strategy for regression of biophysical variables and Landsat ETM+ data. *Remote Sensing of Environment*, Vol. 84, pp. 561-571.

Cohen, W. B., T. K. Maiersperger, T. A. Spies, and D. R. Otter, 2001: Modelling forest cover attributes as continuous variables in a regional context with Thematic Mapper data. International Journal of Remote Sensing, Vol. 22, No. 12, pp. 2279-2310.

Cohen, W. B. and T. A. Spies, 1992: Estimating structural attributes of douglas-fir/western hemlock forest stands from Landsat and SPOT imagery. *Remote Sensing of Environment,* Vol. 41, pp. 1-17.

Cohen, W. B., T. A. Spies, and M. Fiorella, 1995: Estimating the age and structure of forests in a multi-ownership landscape of western Oregon, U.S.A. *International Journal of Remote Sensing*, Vol. 16, No. 721-746.

Colinvaux, P. A., 1986: *Ecology*. Wiley, New York.

Collin, P. H. 1988: *Dictionary of Ecology and the Environment*. Peter Collin Publishing, London.

Colwell, J. E. 1974: Vegetation canopy reflectance. *Remote Sensing of Environment*, Vol. 3, pp. 175-183.

Conese, C., M. A. Gilabert, F. Maselli, and L. Bottai, 1993: Topographic normalization of TM scenes through the use of an atmospheric correction method and digital terrain models. *Photogrammetric Engineering and Remote Sensing*, Vol. 59, No. 12, pp. 1745-1753.

Corsi, F., E. Dupre, and J. Boitani, 1998: Large-scale model of wolf distribution in Italy for conservation planning. *Conservation Biology*, Vol. 13, No. 1, pp. 150-159.

Corsi, F., J. De Leeuw, and A. Skidmore, 2000: Modeling species distribution with GIS. In L. Boitani and T. K. Fuller (Eds.), *Research Techniques in Animal Ecology:* Controversies and Consequences. Columbia University Press, New York.

Couroux, D. A., 2004: wef. Unpublished B.Sc. Honours Thesis, Department of Geography, University of Calgary.

Couroux, D. A., S. E. Franklin, and G. J. McDermid, 2005: Estimating canopy and understorey LAI with Landsat ETM+ imagery in the Foothills Model Forest. *Canadian Journal of Remote Sensing*, in review.

Cousins, S. H., 1993: Hierarchy in ecology: its relevance to landscape ecology and geographic information systems. In R. Haines-Young, D. R. Green, and S. Cousins (Eds.), *Landscape Ecology and Geographic Information Systems*. Taylor & Francis, New York, pp. 75-86.

Crawley, M. J., 2002: *Statistical Computing, an Introduction to Data Analysis Using S-Plus*. Wiley, West Sussex, England.

Crist, E. P. and R. C. Cicone, 1984: A physically based transformation of Thematic Mapper data - The TM Tasseled Cap. *IEEE Transactions on Geoscience and Remote Sensing*, Vol. GE-22, pp. 256 - 263.

Curran, P. J., J. Dungan and H. L. Gholz, 1992: Seasonal LAI measurements in slash pine using Landsat TM. *Remote Sensing of Environment*, Vol. 39, pp. 3-13.

Culvenor, D. S., 2003: Extracting individual tree information: A survey of techniques for high spatial resolution imagery. In M. A. Wulder and S. E. Franklin (Eds.), *Remote Sensing of Forest Environments: Concepts and Case Studies*. Kluwer Academic Publishers, Boston, pp. 255-278.

Curran, P. J., J. L. Dungan, and H. L. Gholz, 1992: Seasonal LAI in slash pine estimated with Landsat TM. *Remote Sensing of Environment*, Vol. 1992, pp. 3-13.

Danks, F. S. and D. R. Klein, 2002: Using GIS to predict potential wildlife habitat: a case study of muxoxen in northern Alaska. *International Journal of Remote Sensing*, Vol. 23, No. 21, pp. 4611-4632.

Davis, F. W. and S. Goetz, 1990: Modelling vegetation pattern using digital terrain data. *Landscape Ecology*, Vol. 4, No. 1, pp. 69-80.

Deering, D. W., 1978: *Rangeland reflectance characteristics measured by aircraft and spacecraft sensors*. Unpublished Ph.D. dissertation, Texas A&M University, College Station, TX.

De Leeuw, J., W. K. Otticilo, A. G. Toxopeus, and H. H. T. Prins, 2002: Applications of remote sensing and geographic information systems in wildlife mapping and modelling. In: A. Skidmore and H. Prins (Eds.) *Environmental Modelling With GIS and Remote Sensing*, Taylor and Francis, London.

Decagon Devices, Inc., 2001: *AccuPAR Linear PAR/LAI Ceptometer Model PAR-80 Operator's Manual*. Decagon Devices, Inc., Pullman, WA.

Dechka, J. A., D. R. Peddle, S. E. Franklin, and G. B. Stenhouse, 2000: Grizzly bear habitat mapping using evidential reasoning and maximum likelihood classifiers: a comparison. *Proceedings, 22nd Canadian Symposium on Remote Sensing*, Victoria, BC, pp. 393-402.

DeFries, R. S. and A. S. Belward, 2000: Global and regional land cover characterization from satellite data: and introduction to the special issue. *International Journal of Remote Sensing*, Vol. 21, No. 6-7, pp. 1083-1092.

DiGregio, A. and L. J. M Jansen, 2000: *Land Cover Classification System (LCCS): Classification Concepts and User Manual*. Food and Agriculture Organization of the United Nations, Rome. http://www.africover.org/download/manuals/LCCSMS20.pdf accessed 09/01/05.

Dubayah, R. O. and P. M. Rich, 1995: Topographic collar radiation models for GIS. *International Journal of Geographic Information Systems*, Vol. 9, pp. 405-419.

Dymond, J. R., 1992: Nonparametric modelling of radiance in hill country for digital classification of aerial photographs. *Remote Sensing of Environment*, Vol. 39, pp. 95-102.

Edwards, T. C., G. G. Moisen, and D. R. Cutler, 1998: Asssessing map accuracy in a remotely sensed, ecoregion-scale cover map. *Remote Sensing of Environment*, Vol. 63, pp. 73-83.

Edwards, T. C., G. G. Moisen, T. S. Frescino, and J. J. Lawler, 2002: Use of forest inventory analysis information in wildlife habitat modelling: a process for linking multiple scales. *Proceedings of the FIA Science Symposium*, Traverse City, MI.

Elvidge, C.D. and Z. Chen, 1995: Comparison of broad-band and narrow-band red and near-infrared vegetation indicies. Remote Sensing of Environment, Vol. 54, pp. 38-48.

Elvidge, C. D., D. Yuan, R. D. Weerackoon, and R. S. Lunetta, 1995: Relative radiometric normalization of Landsat Multispectral Scanner (MSS) data using an automatic scattergram-controlled regression. *Photogrammetric Engineering and Remote Sensing*, Vol. 61, pp. 1255-1260.

Eve, M.D., and J.W. Merchant, 1998: *A National Survey of Land Cover Mapping Protocols Used in the Gap Analysis Program*. http://www.calmit.unl.edu/gapmap accessed 09/01/05.

Fahsi, A., Tsegaye, T., W. Tadesse, and T. Coleman, 2000: Incorporation of digital elevation models with Landsat-TM data to improve land cover classification. *Forest Ecology and Management*, Vol. 128, No. 1, pp. 57-64.

Fassnacht, K. S., S. T. Gower, J. M. Norman, and R. E. McMutrie, 1994: A comparison of optical and direct methods for estimating foliage surface area in forests. *Agriculture and Forest Meteorology*, Vol. 71, pp. 183-207.

Fayyad, U. M., and K. B. Irani, 1992: On the handling of continuous-valued attributes in decision tree generation. *Machine Learning*, Vol. 8, pp. 87-102.

Fazakas, Z. and M. Nilsson, 1996: Volume and forest cover over southern Sweden using AVHRR data calibrated with TM data. *International Journal of Remote Sensing*, Vol. 17, No. 9, pp. 1701-1709.

Fleming, M. D. and R. M. Hoffer, 1975: *Computer-Aided Analysis of Landsat-1 MSS Data: A Comparison of Three Approaches, Including a 'Modified Clustering' Approach*. Laboratory for Application of Remote Sensing Informations Note 072475. Purdue University, West Lafayette, Indiana.

Foody, G. M., 1996a: Approaches for the production and evaluation of fuzzy land cover classifications from remotely sensed data. *International Journal of Remote Sensing*, Vol. 17, pp. 1317-1340.

Foody, G. M., 1996b: Fuzzy modelling of vegetation from remotely sensed imagery, *Ecological Modelling*, Vol. 85, No. 1, Pages 3-12.

Foody, G. M., 1999: The continuum of classification fuzziness in thematic mapping. *Photogrammetric Engineering and Remote Sensing,* Vol. 65, pp. 443-451.

Foody, G. M., 2002: State of land cover classification accuracy assessment. *Remote Sensing of Environment*, Vol. 80, pp. 185-201.

Forman, R. T. T. and M. Godron, 1986: *Landscape Ecology*. Wiley, New York.

Franklin, J., 1995: Predictive vegetation mapping: geographic modeling of biospatial patterns in relation to environmental gradients. *Progress in Physical Geography*, Vol. 19, pp. 474-499.

Franklin, J. and J. Stephenson, 1996: *Integrating GIS and Remote Sensing to Produce Regional Vegetation Databases: Attributes Related to Environmental Modeling*. http://www.sbg.ac.at/geo/idrisi/gis_environmental_modeling/sf_papers/franklin_janet/my_paper.html accessed 09/01/05.

Franklin, J., S. R. Phinn, C. E. Woodcock, and J. Rogan, 2003: Rationale and conceptual framework for classification approaches to assess forest resources and properties.

In M. A. Wulder and S. E. Franklin (Eds.), *Remote Sensing of Forest Environments: Concepts and Case Studies*. Kluwer Academic Publishers, Boston, pp. 279-300.

Franklin, J. and C. E. Woodcock, 1997: Multiscale vegetation data for the mountains of southern California. In D. A. Quattrochi and M. F. Goodchild (Eds), *Scale in Remote Sensing and GIS*. Lewis Publishers, New York, pp. 141-168.

Franklin, S. E., 1991: Image transformations in mountainous terrain and the relationship to surface patterns. *Computers and Geoscience*, Vol. 17, pp. 1137-1149.

Franklin, S. E., 2001: *Remote Sensing for Sustainable Forest Management*. Lewis Publishers, New York.

Franklin, S. E., D. R. Connery, and J. E. Williams, 1994: Classification of alpine vegetation using Landsat Thematic Mapper, SPOT HRV, and digital elevation data. *Canadian Journal of Remote Sensing*, Vol. 20, No. 1, pp. 49-58.

Franklin, S. E., R. J. Hall, L. Smith, and G. R. Gerylo, 2003: Discrimination of conifer height, age, and crown closure classes using Landsat-5 TM imagery in the Canadian Northwest Territories. *International Journal of Remote Sensing*, Vol. 24, No. 9, pp. 1823-1834.

Franklin, S. E. and G. J. McDermid, 1993: Empirical relations between digital SPOT HRV and CASI imagery and lodgepole pine (*Pinus contorta*) forest stand parameters. *International Journal of Remote Sensing*, Vol. 14, pp. 2331-2348.

Franklin, S. E. and J. E. Moulton, 1990: Variability and classification of Landsat Thematic Mapper spectral response in southwest Yukon. *Canadian Journal of* Remote Sensing, Vol. 16, pp. 2-13.

Franklin, S. E., G. B. Stenhouse, M. J. Hansen, C. C. Popplewell, J. A. Dechka, and D. R. Peddle, 2001: An integrated decision tree approach (IDTA) to mapping land cover using satellite remote sensing in support of grizzly bear habitat analysis in the Alberta yellowhead ecosystem. *Canadian Journal of Remote Sensing*, Vol. 27, No. 6, pp. 579-592.

Franklin, S. E. and M. A. Wulder, 2003: Remote sensing methods in high spatial resolution satellite data land cover classification of large area. *Progress in Physical Geography*, Vol. 26, No. 2, pp. 173-205.

Frescino, T. S., T. C. Edwards, and G. G. Moisen, 2001: Modeling spatially explicit forest structural attributes using generalized additive models. *Journal of Vegetation Science*, Vol. 12, pp. 15-26.

Friedl, M. A. and C. E. Brodley, 1996: Decision tree classification of land cover from remotely sensed data. *Remote Sensing of Environment*, Vol. 61, pp. 399-409.

Fung, T. and E. F. LeDrew, 1987: Application of principal components analysis to change detection. *Photogrammetric Engineering and Remote Sensing*, Vol. 53, No. 12, pp. 1649-1658.

Gadd, B., 1986: *Handbook of the Canadian Rockies.* Corax Press, Jasper, Alberta.

Gardner, R. H., Kemp, W. M., Kennedy, V. S. and Petersen, J. E. (eds), 2001: *Scaling Relations in Experimental Ecology*. Columbia University Press.

GeoAnalytic, 1999: *Application of Evidential Reasoning to the classification of Grizzly bear habitat using Landsat TM and Ancillary Data*. Milestone Report 1. Canada Centre for Remote Sensing.

Gillis, M. D., 2001: Canada's national forest inventory (responding to current information needs). *Environmental Monitoring and Assessment*, Vol. 67, Nos. 1&2, pp. 121-129.

Goel, 1988: Models of Vegetation Canopy Reflectance & Their Use in Estimation of Biophysical Parameters from Reflectance Data. Gordon and Breach Publishing Group (Now Taylor and Francis), New York, 222 p.

Goodchild, M. F., 1989: Modelling error in objects and fields. In M. Goodchild and S. Gopal (Eds.) *Accuracy of Spatial Databases*. Taylor and Francis, Philidelphia, PA, pp. 107-113.

Gould, W. A., S. Edlund, S. Zoltai , M. Raynolds, D. A. Walker and H. Maier, 2002: Canadian arctic vegetation mapping. *International Journal of Remote Sensing*, Vol. 23, No. 21, pp. 4597-4609.

Goward, S. N., B. L. Markham, D. G. Dye, W. Dulaney, and J. Yang, 1991: Normalized difference vegetation index measurements from the Advanced Very High Resolution Radiometer. *Remote Sensing of Environment*, Vol. 35, pp. 257-277.

Graetz, R. D., 1990: Remote sensing of terrestrial ecosystem structure: an ecologist's pragmatic view. In: Hobbs, R. J. and H. A. Mooney (Eds.), *Remote Sensing of Biosphere Functioning*, Springer, New York, pp. 5-30.

Gu, D. and A. Gillespie, 1998: Topographic normalization of Landsat TM images of forest based on subpixel sun-canopy-sensor geometry. *Remote Sensing of Environment*, Vol. 64, pp. 166-175.

Gustafson, E. J., 1998: Quantifying landscape spatial pattern: What is the state of the art? *Ecosystems*, Vol. 1, No. 1, pp. 143-156.

Hall, F. G., D. E. Strebel, J. E. Nickeson, and S. J. Goetz, 1991: Radiometric rectification: Toward a common radiometric response among multidate, multisensor images. *Remote Sensing of Environment*, Vol. 35, pp. 11-27.

Hall, L. S., P. R. Krausman, and M. L. Morrison, 1997: The habitat concept and a plea for standard terminology. *Wildlife Society Bulletin*, Vol. 25, No. 1, pp. 173-182.

Hall, R. J., D. P. Davidson, and D. R. Peddle, 2003: Ground and remote estimation of leaf area index in Rocky Mountain forest stands, Kananaskis, Alberta. *Canadian Journal of Remote Sensing*, Vol. 29, No. 3, pp. 411-427.

Hamer, D. and S. Herrero, 1987: Grizzly bear food and habitat in the front ranges of Banff National Park, Alberta. *Proceedings, Seventh International Conference on Bear Research and Management*, pp. 199-213.

Hamer, D., S. Herrero, and K. Brady, 1991: Food and habitat use by grizzly bears, *Ursus arctos*, along the continental divide in Waterton Lakes National Park, Alberta. *Canadian Field Naturalist*, Vol. 105, pp. 325-329.

Hansen, M., DeFries, R., Townshend, J. R. G. and Sohlberg, R., 2000, Global land cover classification at 1km resolution using a decision tree classifier, International Journal of Remote Sensing. 21: 1331-1365.

Hansen, M., R. Dubayah, and R. DeFries, 1996: Classification trees: an alternative to traditional land cover classifiers. *International Journal of Remote Sensing*, Vol. 17, No. 5, pp. 1057-1081.

Hay, G. J., P. Dube, A. Bouchard, and D. J. Marceau, 2002: A scale-space primer for exploring and quantifying complex landscapes. *Ecological Modelling*, Vol. 153, pp. 27-49.

Haralick, R. M., K. Shanmugan, and I. Dinstien, 1973: Textural features for image classification. *IEEE Transactions on Systems, Man and Cybernetics*, Vol. 3, pp. 610-621.

Hargis, C. D., J. A. Bissonette, and D. L. Turner, 1999: The influence of forest fragmentation and landscape pattern on American martens. Journal of Applied Ecology, Vol. 36, pp. 157-172.

Harris, P. and S. Ventura, 1995: The integration of geographic data with remotely sensed imagery to improve classification in an urban area. *Photogrammetric Engineering and Remote Sensing*, Vol. 61, No. 8, pp. 993-998.

Herr, Andrea M., and Lloyd P. Queen, 1993: Crane habitat evaluation using GIS and remote sensing. *Photogrammetric Engineering and Remote Sensing,* Vol. 59, pp. 1531-1538.

Hines, E. M. and J. Franklin, A sensitivity analysis of a map of habitat quality for the California Spotted Owl (*Strix occidentalis occidentalis*) in southern California. *Proceedings, Second International Symposium on Biology and Conservation of Owls of the Northern Hemisphere*. http://www.ncrs.fs.fed.us/epubs/owl/HINES.PDF accessed 09/01/05.

Hobson, D., 2005: Bear capturing and handling. *Foothills Model Forest Grizzly Bear Research Program 1999-2003 Final Report*. Foothills Model Forest, Hinton, Alberta. http://www.fmf.ca/GB/GB_report7.pdf accessed 08/06/05.

Hoffer, R. M., 1994: Challenges in developing and applying remote sensing to ecosystem management. In V. A. Sample (Ed.) *Remote Sensing and GIS in Ecosystem Management*. Island Press, Washington, pp. 25-40.

Homer, C, C. Huang, L. Yang, and B. Wylie, 2002: *Development of a Circa 2000 Land cover Database for the United States*. U. S. Geological Survey, U. S. Department of the Interior. http://land cover.usgs.gov/pdf/asprs_final.pdf accessed 09/01/05.

Homer, C., R. Ramsey, T. C. Edwards, Jr., and A. Falconer, 1997: Landscape cover-type modelling using a multi-scene Thematic Mapper mosaic. *Photogrammetric Engineering and Remote Sensing*, Vol. 63, pp. 59-67.

Hoving, C. L., Harrison, D. J., Krohn, W. B., Joseph, R. A., O'Brien, M., 2005: Broad-scale predictors of Canada Lynx occurrence in eastern North America. *Journal of Wildlife Management*: Vol. 69, No. 2, pp. 739–751.

Huang, C., C. Comer, and L. Yang, 2003: Regional forest land cover characterization using medium spatial resolution satellite data. In M. A. Wulder and S. E. Franklin (Eds.) *Remote Sensing of Forest Environments: Concepts and Case Studies*. Kluwer Academic Publishers, Boston, pp. 389-410.

Huete, A., C. Justice, and W. van Leeuwen, 1999: *MODIS Vegetation Index (MOD 13) Algorithm Theoretical Basis Document*. Version 3. http://modis.gsfc.nasa.gov/data/atbd/atbd_mod13.pdf accessed 09/01/05.

Huete, A. R. and A. W. Warrick, 1990: Assessment of vegetation and soil water regimes in partial canopies with optical remotely sensed data. *Remote Sensing of Environment*, Vol. 32, pp. 155-167.

Huguenin, R. L., M. A. Karaska, D. Van Blaricom, and J. R. Jensen, 1997: Subpixel classification of bald d cypress and tupelo gum trees in Thematic Mapper imagery. *Photogrammetric Engineering and Remote Sensing*, Vol. 63, pp. 717-725.

Hunt, E. R., Jr., 1991: Airborne remote sensing of canopy water thickness from leaf spectrometer data. *International Journal of Remote Sensing*, Vol. 12, pp. 643-649.

Hutchinson, C. F., 1982: Techniques for combining Landsat and ancillary data for digital classifcation improvement. *Photogrammetric Engineering and Remote Sensing*, Vol. 48, pp. 123-130.

Hutchinson, M. F., 1989: A new method for gridding elevation and stream line data with automatic removal of pits. *Journal of Hydrology*, Vol. 106, pp. 211-232.

Irons, J. R. and G. W. Peterson, 1981: Texture transforms of remote sensing data. *Remote Sensing of Environment*, Vol. 11, pp. 359-370.

Jackson, V. L., Laack, L. L., Zimmerman, E. G. 2005: Landscape metrics associated with habitat use by ocelots in south Texas. *Journal of Wildlife Management*, Vol. 69, No. 2, pp. 733–738.

James, M. E. and S. N. V. Kalluri, 1994: The Pathfinder AVHRR land data set: An improved coarse resolution data set for terrestrial monitoring. *International Journal of Remote Sensing*, Vol. 15, No. 17, pp. 3347-3363.

Jarvis, P. G. and J. W. Leverenz, 1983: Productivity of temperate, deciduous, and evergreen forests. In: O. L. Lange, P. S. Nobel, C. B. Osmond, and H. Ziegler (Eds.) *Encyclopedia of Plant Physiology*, Vol. 12D, Physiological Plant Ecology, IV. Springer-Verlag, Berlin.

Jensen, J. R., 1996: *Introductory Digital Image Processing, a Remote Sensing Perspective*. Prentice-Hall, Upper Saddle River, NJ.

Jensen, J. R. and D. C. Cowen, 1999: Remote sensing of urban/suburban infrastructure and socio-economic attributes. *Photogrammetric Engineering and Remote Sensing*, Vol. 65, pp. 611-622.

Jones, K. B., 1986: Amphibians and reptiles. In A. Y. Cooperider, R. J. Boyd, and H. R. Stuart (eds), *Inventory and Monitoring of Wildlife Habitat*, U.S. Bureau of Land Management, Denver, CO, pp. 267-290.

Jupp, D. L. B., A. H. Strahler, and C. E. Woodcock, 1988: Autocorrelation and regularization in digital images: I. Basic theory. *IEEE Transactions on Geoscience and Remote Sensing*, Vol. 26, No. 4, pp. 463-473.

Jupp, D. L. B., A. H. Strahler, and C. E. Woodcock, 1989: Autocorrelation and regularization in digital images: II. Simple image models. *IEEE Transactions on Geoscience and Remote Sensing*, Vol. 27, No. 3, pp. 247-258.

Justice, C. O., A. Belward, J. Morisette, P. Lewis, J. Privette, and F. Baret, 2000: Developments in the 'validation' of satellite sensor products for the study of the

land surface. *International Journal of Remote Sensing*, Vol. 21, No. 17, pp. 3383-3390.

Kauth, R. J. and G. S. Thomas, 1976: The Tasseled Cap – a graphical description of the spectral-temporal development of agricultural crops as seen by Landsat. *Proceedings of the Symposium on Machine Processing of Remotely Sensed Data*, Purdue University, West Lafayette, Indiana, pp. 4B41-4B51.

Kay, J., 1991: A non-equilibrium thermodynamic framework for discussing ecosystem integrity. *Environmental Management*, Vol. 15, No. 4, pp. 483-495.

Kerr, R. M., 1986: Habitat mapping. In A. Y. Cooperrider, J. B. Raymond, and H. R. Stuart (Eds.), *Inventory and Monitoring of Wildlife Habitat*. U. S. Department of the Interior, Bureau of Lands, Denver, Co, pp. 49-72.

Kimes, D. S. and J. A. Kirchner, 1981: Modeling the effects of various radiant transfers in mountainous terrain on sensor response. *IEEE Transactions on Geoscience and Remote Sensing*, Vol. 19, pp. 100-108.

Kimes, D. S., R. F. Nelson, W. A. Salas, and D. L. Skole, 1999: Mapping and secondary tropical forest and forest age from SPOT HRV data. *International Journal of Remote Sensing*, Vol. 20, pp. 3625-3640.

Kobler, A. and Adamic, M., 1999: Brown bears in Slovenia: identifying locations for construction of wildlife bridges across highways. *ICOWET III Proceedings*, Missoula, Montana. http://www11.myflorida.com/emo/sched/kobler_p.pdf accessed 09/01/05.

Krausman, P. R. 1999: Some basic principles of habitat use. In: K. L. Launchbaugh, K. D. Sander, J. C. Mosley (eds.), *Grazing Behavior of Livestock and Wildlife*. University of Idaho Forest, Wildlife, & Range Experimental Station Bulletin No. 70, p. 85-90.

Krebs, C.J., 1985. *Ecology: The Experimental Analysis of Distribution and Abundance, Third Edition*, Harper and Row, New York, 800 p.

Kuncheva, L. I. and L. C. Jain, 1999: Nearest neighbor classifier: simultaneous editing and feature selection. *Pattern Recognition Letters*, Vol. 20, pp 1149-1156.

Kurki, S., A. Nikula, P. Helle, and H. Linden, 1998: Abundance of red fox and pine marten in relation to the composition of boreal forest landscapes. *Journal of Animal Ecology*, Vol. 67, pp. 874-886.

Lambin, E. F., 1996: Change detection at multiple temporal scales: seasonal and annual variations in landscape variables. *Photogrammetric Engineering and Remote Sensing*, Vol. 62, pp. 931-938.

Landsat Project Science Office, 1998: *Landsat 7 Science Data Users Handbook*. NASA Goddard Space Flight Centre, Green Belt, Maryland. http://ltpwww.gsfc.nasa.gov/IAS/handbook/handbook_toc.html accessed 09/01/05.

Lauver, C. L., W. H. Busby, and J. L. Whistler, 2002: Testing a GIS model of habitat suitability for a declining grassland bird. *Environmental Management*, Vol. 30, No. 1, pp. 88-97.

Law, B. E., A. Cesatti, D. D. Baldocchi, 2001: Leaf area distribution and radiative transfer in open-canopy forest; implications for mass and energy exchange. *Tree Physiology*, Vol. 21, pp. 777-787.

Law, B. E. and R. H. Waring, 1994: Remote sensing of leaf area index and radiation intercepted by understory vegetation. *Ecological Applications*, Vol. 4, No. 2, pp. 272-279.

Le Dantec, V., E. Dufrene, and B. Saugier, 2000: Interannual and spatial variation in maximum leaf area index of temperate deciduous stands. *Forest Ecology and Management*, Vol. 134, pp. 71-81.

Leban, F. A., M. J. Wisdom, E. O. Garton, B. K. Johnson, and J. G. Kie, 2001: Effects of sample size on the performance of resource selection analyses. In: J. J. Millspaugh and J. M. Marzluff (Eds.), *Radio-Tracking and Animal Populations*. Academic Press, New York, USA, pp. 291-307.

Lehmkuhl, J. F., and M. G. Raphael, 1993: Habitat pattern around spotted owl locations on the Olympic Peninsula, Washington. *Journal of Wildlife Management,* Vol. 57, pp. 302-315.

Lillesand, T. M., 1994: Strategies for improving the accuracy and specifity of large-area, satellite-cased land cover inventories. *Proceedings of the Symposium, Mapping and GIS,* Athens, GA, Vol. 30, pp. 23-30.

Lillesand, T. M., 1996: A protocol for satellite-based land cover classification in the upper Midwest. In J. M. Scott, T. H. Tear, and F. W. Davis (Eds.), *Gap Analysis: A Landscape Approach to Biodiversity Planning*. American Society for Photogrammetry and Remote Sensing, Bethesda, Maryland, pp. 103-118.

Lim K, Treitz P, Wulder M, St-Onge B, and Flood M., 2003: Lidar remote sensing of forest structure. *Progress in Physical Geography*, Vol. 27, No. 1, pp. 88-106.

Lindeman, R. L., 1942: The trophic-dynamic aspect of ecology. *Ecology*, Vol. 23, pp. 399-418.

Loveland, T., J. Merchant, D. Ohlen, and J. Brown, 1991: Development of a land-cover characteristics database for the contimerous United States. *Photogrammetric Engineering and Remote Sensing*, Vol., 57, 1453-1463.

Lunetta, R. S., R. Alvarez, C. M. Edmonds, J. G. Lyon, C. D. Elvidge, R. Bonifaz, and C. Garcia, 2002: NALC/Mexico land-cover mapping results: implications for assessing landscape condition. *International Journal of Remote Sensing*, Vol. 23, No. 16, pp. 3129-3148.

MacMillan, R. A., T. C. Martin, T. J. Earle, and D. H. McNabb, 2003: Automated analysis and classification using high-resolution digital elevation data: applications and issues. *Canadian Journal of Remote Sensing*, Vol. 29, No. 5, pp. 592-602.

Maiden, M., 1994: The Pathfinder project. *International Journal of Remote Sensing,* Vol. 15, pp. 3333-3345.

Manis, G., J. Lowry and R. D. Ramsey, 2001: Preclassification: An ecologically predictive landform model. *GAP Analysis Bulletin No. 10,* United States Geological Survey.

Manly, B.F., L. McDonald, D.L. Thomas, Trent L. McDonald, and Wallace P. Erickson, 2002: *Resource Selection by Animals: Statistical Design and Analysis for Field Studies*. Kluwer Academic Publishers, Boston.

Mather, P., 1999: *Computer Processing of Remotely Sensed Images: An Introduction.* Wiley, New York.

Marceau, D. J. and G. J. Hay, 1999: Remote sensing contributions to the scale issue. *Canadian Journal of Remote Sensing*, Vol. 25, No. 4, pp. 357-366.

May, C. A., Petersburg, M. L., Gutierrez, R. J.. 2004: Mexican Spotted Owl nest- and roost-site habitat in northern Arizona. *Journal of Wildlife Management*, Vol. 68, No. 4, pp. 1054–1064.

Mayhew, S. and A. Penny, 1992: *The Concise Oxford Dictionary of Geography*. Oxford University Press, Oxford, U.K.

Mazerolle, D. F. and K. A. Hobson, 2002: Consequences of forest fragmentation on territory quality of male Ovenbirds breeding in western boreal forests. *Canadian Journal of Zoology*, Vol. 80, pp. 1841-1848.

McClain, B. J. and W. F. Porter, 2000: Using satellite imagery to assess large-scale habitat characteristics of the Adirondack Park. *Environmental Management* Vol. 26, pp. 553-561.

McDermid, G. J. and S. E. Franklin, 1995: Remote sensing and geomorphometric discrimination of slope processes. *Zeitschrift fur Geomorphologie N. F.,* Supplement Band 101, pp. 165-185.

McDermid, G. J., A. Pape, M. S. Chubey, and S. E. Franklin, 2003: Object-oriented analysis for change detection. *Proceedings, 25th Canadian Symposium on Remote Sensing*.

McDermid, G. J., S. E. Franklin, and E. F. LeDrew, 2005: Remote sensing for large-area habitat mapping. *Progress in Physical Geography,* Vol. 29, No. 4.

McGarigal, K., and B. J. Marks: 1995: *FRAGSTATS: spatial pattern analysis program for quantifying landscape structure*. USDA Forest Service General. Tech. Rep. PNW-351.

McGovern, E. A., N. M. Holden, S. M. Ward, and J. F. Collins, 2002: The radiometric normalization of multitemporal Thematic Mapper imagery of the midlands of Ireland – a case study. *International Journal of Remote Sensing*, Vol. 23, No. 4, pp. 751-766.

McLaren, B. E., and S. P. Mahoney, 2001: Comparison of forestry-based remote sensing methodologies to evaluate woodland caribou habitat in non-forested areas of Newfoundland. *Forestry Chronicle*, Vol. 77, No. 5, pp. 866-873.

Meadows J. S., and J. D. Hodges, 2002: Sapwood area as an estimator of leaf area and foliar weight in cherrybark oak and green ash. *Forest Science*, Vol. 48, No. 1, pp. 69-76.

Mencuccini. M., and J. Grace, 1995: Climatic influences on the leaf area sapwood area ratio in Scots pines. *Tree Physiology*, Vol. 15, pp. 1-10.

Merriam-Webster, 1998: *Webster's Revised Unabridged Dictionary*. C. & G. Merriam Company, Springfield, Massachusetts. http://www.dictionary.com accessed 09/01/05.

Meyer, P., K. I. Itten, T. Kellenberger, S. Sandmeier, and R. Sandmeier, 1993: Radiometric corrections of topographically induced effects on Landsat TM data in an alpine environment. *ISPRS Journal of Photogrammetry and Remote Sensing*, Vol. 48, No. 4, pp. 17-28.

Meyer, M. and L. Werth, 1990: Sateliite data: management panacea or potential problem? *Journal of Forestry*, Vol. 88, No. 9, pp. 10-13.

Miller, C. J., 2003: Fusion of high-resolution lidar elevation data with hyperspectral data to characterize tree canopies. *Proceedings, SPIE The International Society for Optical Engineering* Vol. 4381, pp. 246-252.

Mladenoff, D. J. and G. E. Host, 1994: Ecological perspective: Current and potential applications of remote sensing and GIS to ecosystem analysis. In V. A. Sample (Ed.), *Remote Sensing and GIS in Ecosystem Management*. Island Press, Washington, pp.218-242.

Moisen, G. G. and T. C. Edwards, Jr., 1999: Use of generalized linear models and digital data in a forest inventory of northern Utah. *Journal of Agricultural, Biological, and Environmental Statistics*, Vol. 4, pp. 372-390.

Moore, W. G., 1967: *A dictionary of geography*. London: A. & C. Black.

Moore, I. D., R. B. Grayson, and A. R. Ladson, 1991: Digital terrain modelling: a review of hydrological, geomorphological, and biological applications. *Hydrological Processes*, Vol. 5, No. 1, pp. 3-30

Morrison, M. L., B. G. Marcot, and R. W. Mannan, 1992: *Wildlife-Habitat Relationships: Concepts and Applications*. University of Wisconsin Press, Madison.

Murai, H. and S. Omatu, 1997: Remote sensing image analysis using a neural network and knowledge-based processing. *International Journal of Remote Sensing*, Vol. 18, No. 4, pp. 811-828.

Mustard, J. F., 1993: Relationships of soil, grass, and bedrock over the Kaweah Serpentine Melange through mixture analysis of AVIRIS data. *Remote Sensing of Environment*, Vol. 44, pp. 293-308.

Myneni, R.B., Hall, F.G., Sellers, P.J., and Marshack, A.L., 1995, The interpretation of spectral vegetation indices, *IEEE Transactions on Geoscience and Remote Sensing*, Vol. 33, pp. 481-486.

Narayana, A., H. U. Solanki, B. G. Krishna, and A. Narain, 1995: Geometric correction and radiometric normalization of NOAA AVHRR data for fisheries applications; International Journal of Remote Sensing, Vol. 16, pp. 765-771.

Natural Resources Canada, 1995: *Land Cover Map of Canada*. Natural Resources Canada, Ottawa. http://www.ccrs.nrcan.gc.ca/ccrs/rd/apps/landcov/map_e.html accessed 09/01/05.

Nemani, R., L. Pierce, S. W. Running, and L. Band, 1993: Forest ecosystem processes at the watershed scale: sensitivity to remotely sensed leaf area index estimates. *International Journal of Remote Sensing*, Vol. 14, pp. 2519-2534.

Nielsen, S.E., Boyce, M.S., Stenhouse, G.B., Munro, R.H.M., 2003: Development and testing of phonologically driven grizzly bear habitat models. *Ecoscience,* Vol. 10, pp. 1−10.

Norman, J. M. and P. G. Jarvis, 1974: Photosynthesis in sitka spruce (*Picea sitchensis* (Bong.) C*arr*.) III. Measurements of canopy structure and interception of Radiation. *Journal of Applied Ecology*, Vol. 12, pp. 839-878.

Norris D. R., M. T. Theberge, and J. B. Theberge, 2002: Forest composition around wolf dens in eastern Algonquin Provincial Park, Ontario. *Canadian Journal of Zoology* Vol. 80, pp. 866-872.

Nuemann, H. H., G. D. Den Hartog, and R. H. Shaw, 1989: Leaf area measurements based on hemispheric photographs and leaf litter collection in a deciduous forest during autumn leaf fall. *Agriculture and Forest Meteorology*, Vol. 45, pp. 325-345.

Odum, E. P., 1971: *Fundamentals of Ecology*. W. B. Sanders Co., Philadelphia, PA, 574 p.

Ohmann, J. L. and M. J. Gregory, 2002: Predictive mapping of forest composition and structure with direct gradient analysis and nearest neighbor imputation in coastal Oregon, U.S.A.. *Canadian Journal of Forest Research,* Vol. 32, pp. 725-741.

Osborne, P. E., J. C. Alonso, and R. G. Bryant, 2001: Modelling landscape-scale habitat using GIS and remote sensing: a case study with great bustards. *Journal of Applied Ecology*, Vol. 38, pp. 458-471.

Osko, T. J., Hiltz, M. N., Hudson, R. J., Wasel, S. M. 2004: Moose habitat preferences in response to changing availability. *Journal of Wildlife Management*, Vol. 68, No. 3, pp. 576–584.

Palma, L. P. Beja, and M. Rodrigues, 1999: The use of sighting data to analyze Iberian lynx habitat and distribution. *Journal of Applied Ecology*, Vol. 36, pp. 812-824.

Pax-Lenney, M., C. E. Woodcock, S. A. Macomber, S. Gopal, and C. Song, 2001: Forest mapping with a generalized classifier and Landsat TM data. *Remote Sensing of Environment*, Vol. 77, pp. 241-250.

Pearson, A. M. and J. Nolan, 1976: *The Ecology of the Grizzly Bear (Ursus arctos L.) in Jasper National Park – Report for 1975*. Canadian Wildlife Service, Edmonton, Alberta, Canada.

Peddle, D. R., 1995: Knowledge formulation for supervised evidential classification. *Photogrammetric Engineering and Remote Sensing*, Vol. 61, pp. 409-417.

Peddle, D. R., F. G. Hall, and E. F. LeDrew, 1999: Spectral mixture analysis and geometric-optical reflectance modeling of boreal forest biophysical structure. *Remote Sensing of Environment*, Vol. 67, pp. 288-297.

Peterson, D. L., M. A. Spanner, S. W. Running, and K. B. Teuber, 1987: Relationship of Thematic Mapper simulator data to leaf area index of temperate coniferous forests. *Remote Sensing of Environment*, Vol. 22, pp. 323-341.

Piwowar, J. M. and E. F. LeDrew, 1996: Principal components analysis of arctic ice conditions between 1978 and 1987 as observed from the SSMR data record. *Canadian Journal of Remote Sensing*, Vol. 22, No. 4, pp. 390-403.

Phinn, S. R., 1998: A framework for selecting appropriate remotely sensed data dimensions for environmental monitoring and management. *International Journal of Remote Sensing*, Vol. 19, No. 17, pp. 3457-3463.

Plummer, S. E., 2000: Perspectives on combining ecological process models and remotely sensed data. *Ecological Modelling*, Vol. 129, pp. 169-186.

Pocewicz, A. L., P. Gessler, and A. P. Robinson, 2004: The relationship between effective plant area index and Landsat spectral response across elevation, solar insolation, and spatial scales in a northern Idaho forest. *Canadian Journal of Forest Research*, 34, 465-480.

Pu, R. and P. Gong, 2004: Wavelet transform applied to EO-1 hyperspectral data for forest LAI and crown closure mapping. *Remote Sensing of Environment*, Vol. 91, pp. 212-224.

Qi, J., A. R. Huete, M. S. Moran, A. Chehbouni, and R. D. Jackson, 1993: Interpretation of vegetation indices from multi-temporal SPOT images. *Remote Sensing of Environment*, Vol. 44, pp. 89-101.

Radeloff, V. C., A. M. Pidgeon, and P. Hostert, 1999: Habitat and population modelling of roe deer using an interactive geographic information system. *Ecological Modelling*, Vol. 114, pp. 287-304.

Read, J. M. and N. S. N. Lam, 2002: Spatial methods for characterizing land cover and detecting land-cover changes for the tropics. *International Journal of Remote Sensing*, Vol. 23, No. 12, pp. 2457-2474.

Reese, H. M., T. M. Lillesand, D. E. Nagel, J. N. Stewart, R. A. Goldmann, T. E. Simmons, J. W. Chipman, and P. A. Tessar, 2002: Statewide land cover derived from multiseasonal Landsat TM data: a retrospective of the WISCLAND project. *Remote Sensing of Environment*, Vol. 82, pp. 224-237.

Reeves, M. C., J. C. Winslow, and S. W. Running, 2001: Mapping weekly rangeland vegetation productivity using MODIS algorithms. *Journal of Rangeland Management*, Vol. 54, pp. A90-A105.

Rhoads A.G., S. P. Hamburg, T. J. Fahey, T. G. Siccama, and R. Kobe, 2004: Comparing direct and indirect methods of assessing canopy structure in a northern hardwood forest. *Canadian Journal of Forest Research*, Vol. 34, No. 3, pp. 584-591.

Riano, D., E. Chuvieco, J. Salas, and I Aguado, 2003: Assessment of different topographic corrections in Landsat-TM data for mapping vegetation types. *IEEE Transactions on Geoscience and Remote Sensing*, Vol. 41, No. 5, pp. 1056-1061.

Richter, R., 1997: Correction of atmospheric and topographic effects for high spatial resolution satellite imagery. *International Journal of Remote Sensing*, Vol. 18, pp. 1099-1111.

Ripley, B. D., 1996: *Pattern Recognition and Neural Networks*. Cambridge University Press, Cambridge.

Rogan, J., J. Franklin, and D. Roberts, 2002: A comparison of methods for monitoring multitemporal vegetation using Thematic Mapper imagery. *Remote Sensing of Environment*, Vol. 80, pp. 143-156.

Roseberry, J. L., 1998: Landscape characteristics and spatial patterns of eastern cottontail abundance in Illinois. *Transactions of the Illinois State Academy of Science*, Vol. 91, No. 3-4, pp. 167-178.

Roughgarden, J., S. W. Running, and P. A. Matson, 1991: What does remote sensing do for ecology? *Ecology*, Vol. 72, No. 6, pp. 1918-1922.

Rushton, S. P., P. W. W. Lurz, R. Fuller, and P. J. Garson, 1997: Modelling the distribution of the red and grey squirrel at the landscape scale: a combined GIS and population dynamics approach. *Journal of Applied Ecology*, Vol. 34, No. 5, pp. 1137-1154.

Satterwhite, M. B., 1984: Discriminating vegetation and soils using Landsat MSS and Thematic Mappber bands and band ratios. *Proceedings, American Society of Photogrammetry*, Vol. 2, pp. 479-485.

Scarth, P. and S. Phinn, 2000: Determining forest structural attributes using an inverted geometric-optical model in the mixed eucalypt forests, south-east Queensland, Australia. *Remote Sensing of Environment*, Vol. 71, pp. 141-157.

Scepan, J., 1999: Thematic validation of high-resolution global land-cover data sets. *Photogrammetric Engineering and Remote Sensing*, Vol. 65, pp. 1051-1060.

Schriever, J. R. and R. G. Congalton, 1995: Evaluating seasonal variability as an aid to cover type mapping from Landsat Thematic Mapper data in the northeast. *Photogrammetric Engineering and Remote Sensing*, Vol. 61, pp. 321-327.

Shinozaki, K., K. Yoda, K. Hozumi, and T. Kira, 1964a: A quantitative analysis of plant form – the pipe model theory. I. Basic analyses. *Japanese Journal of Ecology*, Vol. 14, pp. 97-105.

Shinozaki, K., K. Yoda, K. Hozumi, and T. Kira, 1964b: A quantitative analysis of plant form – the pipe model theory. II. Further evidence of the theory and its application in forest ecology. *Japanese Journal of Ecology*, Vol. 14, pp. 133-139.

Skidmore, A. (Ed.), 2002: Environmental Modelling with GIS and Remote Sensing. Taylor and Francis, New York.

Skidmore, A. K., and A. Gauld, 1996: Classification of kangaroo habitat distribution using three GIS models. *International Journal of Geographical Information Systems*, Vol. 10, No. 4, pp. 441-454.

Smith, N. J., 1991: Predicting radiation attenuation in stands of Douglas fir. *Forest Science*, Vol. 37, pp. 1213-1223.

Smith, J. L. D., S. C. Ahern, and C. McDougal, 1998: Landscape analysis of tiger distribution and habitat quality in Nepal. *Conservation Biology*, Vol. 12, pp. 1338–1346.

Song, C., C. E. Woodcock, K. C. Seto, M. P. Lenney, and S. A. Macomber, 1999: Classification and change detection using Landsat TM data: When and how to correct atmospheric effects? *Remote Sensing of Environment*, Vol. 75, pp. 230-244.

Spanner, M. A., L. L. Pierce, D. L. Peterson, and S. W. Running, 1990: Remote sensing of temperate coniferous forest leaf area index. The influence of canopy closure, understorey vegetation, and background reflectance. *International Journal of Remote Sensing*, Vol. 11, pp. 95-111.

Stehman, S. V. and R. L. Czaplewski, 1998: Design and analysis for thematic map accuracy assessment: fundamental principles. *Remote Sensing of Environment*, Vol. 64, pp. 331-344.

Stelfox, H. A. and G. R. Ironside. 1982: Land/wildlife integration no. 2. Proceedings of a technical workshop to discuss the incorporation of wildlife information into ecological land surveys. *Ecological Land Classification Series*, No. 17, Lands Directorate, Environment Canada.

Stenberg, P., S. Linder, H. Smolander, and J. Flowerellis, 1994: Performance of the LAI-2000 Plant Canopy Analyzer in estimating leaf area index of some scots pine stands. *Tree Physiology*, Vol. 14, pp. 981-995.

Strahler, A. H., C. E. Woodcock, and J. A. Smith, 1986: On the nature of models in remote sensing. *Remote Sensing of Environment*, Vol. 20, pp. 121-139.

Strong, W. L., 1992: *Ecoregions and Ecodistricts of Alberta*. Alberta Forestry, Lands, and Wildlife Publication, Edmonton, Alberta.

Tarboton, D. G., 1997: A new method for the determination of flow directions and upslope areas in grid digital elevation models. *Water Resources Research*, Vol. 33, No. 2, pp. 309-319.

Swihart, R. K. and N. A. Slade, 1985: Testing for independence of observations in animal movement. *Ecology*, Vol. 66, pp. 1176-1184.

Thomas, D. L. and E. J. Taylor, 1990: Study designs and tests for comparing resource use and availability. *Journal of Wildlife Management*, Vol. 54, pp. 322-330.

Throgmartin, W. E., A. L. Gallant, M. G. Knutson, T. J. Fox, and M. J. Suarez, 2004: Commentary: A cautionary tale regarding use of the National Land Cover Dataset 1992. *Wildlife Society Bulletin*, Vol. 32, No 3, pp. 970-978.

Tokola, T., J. Sarkeala, and M. Van der Linden, 2001: Use of topographic correction in Landsat TM-based forest interpretation in Nepal. *International Journal of Remote Sensing*, Col. 22, No. 4, pp. 551-563.

Toutin, T., 1995: Multisource data integration: comparison of geometric and radiometric methods. *International Journal of Remote Sensing*, Vol. 16, No. 15, pp. 2795-2811.

Townshend, J. R. G. and Justice, C. 1980: Unsupervised classification of MSS Landsat data for mapping spatially complex vegetation. *International Journal of Remote Sensing*, Vol. 1, No. 2, pp. 105-120.

Townsend, P. A. and J. R. Foster, 2002: Terrain normalization of AVIRIS and Hyperion imagery in forested landscapes. In R. O. Green (Ed.), *Proceedings of the Eighth JPL Airborne Earth Science Workshop*, Pasedena, CA.

Treitz, P.M. and P.J. Howarth, 2000: Integrating spectral, spatial and terrain variables for forest ecosystem classification. *Photogrammetric Engineering and Remote Sensing*, Vol. 66, No. 3, pp. 305-317.

Trotter, C., 1991: Remotely sensed data as an information source for geographical information systems in natural resource management: A review. *International Journal of Remote Sensing,* Vol. 5, No. 2, pp. 225-239.

Treuhaft, R. N. B. E. Law, and G. P. Asner, 2005: Forest attributes from radar interferometric structure and its fusion with optical remote sensing. *Bioscience*, Vol. 54, No. 6, pp. 561-571.

Turner, D., W. Cohen, R. Kennedy, K. Fassnacht, and J. Briggs, 1999; Relationships between leaf area index and Landsat TM spectral vegetation indices across three temperate zone sites. *Remote Sensing of Environment*, Vol. 70, pp. 52-68.

Turner, M. G., R. H. Gardner, and R. V. O'Neill, 2001: *Landscape Ecology in Theory and Practice Pattern and Process*. Springer-Verlag, New York.

United States Fish and Wildlife Service, 1980a: Habitats as a basis for environmental assessment. *Ecological Service Manual 101*, U. S. Department of Interior, Fish and Wildlife Service, Division of Ecological Services, Government Printing Office, Washington, D. C., 26 p.

United States Fish and Wildlife Service, 1980b: Habitat Evaluation Procedures (HEP). *Ecological Service Manual 102*, U. S. Department of Interior, Fish and Wildlife Service, Division of Ecological Services, Government Printing Office, Washington, D. C., 84 p.

Urban, D. L., R. V. O'Neill, and H. H. Shugart, Jr., 1987: Landscape ecology. *Bioscience*, Vol. 37, 119-127.

Van Tighem, K. J. and G. L. Holroyd, 1983: *Ecological (Biophysical) Land Classification of Banff and Jasper National Parks*, *Vol. 2: Soil and Vegetation Resources.*. Parks Canada.

Veregin, H., 1989: *Accuracy of Spatial Databases: Annotated Bibliography*. Technical Paper No. 89, National Center for Geographic Information Analysis, University of California, Santa Barbara, CA.

Verlinden, A. and R. Masogo, 1997: Satellite remote sensing of habitat suitability for ungulates and ostrich in the Kalahari of Botswanna. *Journal of Arid Environments*, Vol. 35, pp. 563-574.

Vermonte, E. and Y. J. Kaufman, 1995: Absolute calibration of AVHRR visible and near-infrared channels using ocean and cloud views. *International Journal of Remote Sensing*, Vol. 16, pp. 2317-2340.

Vinluan, J. N. and J. D. De Alban, 2001: Evaluation of Landsat ETM+ data for coastal habitat assessment in support of fisheries management. *Proceedings, 22nd Asian Conference on Remote Sensing*, Singapore. http://www.crisp.nus.edu.sg/~acrs2001/pdf/289vinlu.pdf accessed 09/01/05.

Wagner, W., A. Luckman, J. Vietmeier, K. Tansey, H. Balzter, C. Schmullius, M. Davidson, G. Gaveau, M. Gluck, T. Le Toan, S. Quegan, A. Shvidenko, A. Weismann, and J. J. Yu, 2003: Large-scale mapping of boreal forest in Siberia using ERS tandem coherence and JERS backscatter data. *Remote Sensing of Environment*, Vol. 85, pp. 125-144.

Walker, D. A., W. A. Gould, H. A. Maier, and M. K. Raynolds, 2002: The circumpolar arctic vegetation map: AVHRR-derived base maps, environmental controls, and integrated mapping procedures. *International Journal of Remote Sensing*, Vol. 23, No. 1, pp. 4551-4570.

Wallin, D. O., C. C. H. Elliot, H. H. Shugart, C. J. Tucker, and F. Wilhelmi, 1992: Satellite remote sensing of breeding habitat for an African weaver-bird. *Landscape Ecology*, Vol. 7, No. 2, pp. 87-99.

Waring, R. H., P. E. Schroeder, and R. Oren, 1982: Application of the pipe model theory to predict canopy leaf area. *Canadian Journal of Forest Research*, Vol. 12, No. 3, pp. 556-560

Watson, D. J., 1947: Comparative physiological studies in the growth of field crops. I. Variation in net assimilation rate and leaf area between species and varieties, and within and between years. *Annals of Botany*, Vol. 11, pp. 41-76.

Welles, J. M., 1990: Some indirect methods of measuring canopy structure. *Remote Sensing Reviews*, Vol. 5. pp. 31-43.

Welles, J. M. and J. M. Norman, 1991: Istrument for indirect measurement of canopy architecture. *Agriculture Journal*, Vol. 83, Vol. 818-825.

White, J. D., S. W. Running, R. Nemani, R. E. Keane, and K. C. Ryan, 1997: Measurement and remote sensing of LAI in Rocky Mountain montane ecosystems. *Canadian Journal of Forest Resources*, Vol. 27, pp. 1714-1727.

Whittaker R. H., S. A. Levin, and R. B. Root, 1973: Niche, habitat, and ecotope. *American Naturalist,* Vol. 107, pp. 321–338.

Wolter, P. T., D. J Mladenoff., G. E. Host, and T. R. Crow, 1995: Improved forest classification in the northern lakes states using multi-temporal Landsat imagery. *Photogrammetric Engineering and Remote Sensing*, Vol. 61, pp. 1129-1143.

Wood, J. E., M. D. Gillis, D. G. Goodenough, R. J. Hall, D. G. Lecki, J. L. Luther, and M. Wulder, 2002: Earth Observation for Sustainable Development of Forests (EOSD): Project Overview. *Proceedings of the 2002 IEEE International Geoscience and Remote Sensing Symposium (IGARSS 2002) and the 24th Canadian Symposium on Remote Sensing*, Toronto, Ontario.

Woodcock, C. E. and V. J. Harward, 1992: Nested-hierarchical scene models and image segmentation. *International Journal of Remote Sensing*. Vol. 13, pp. 3167-3187.

Woodcock, C. E., S. A. Macomber, M. Pax-Lenney, and W. B. Cohen, 2001: Monitoring large areas for forest change using Landsat: generalization across space, time and Landsat sensors. *Remote Sensing of Environment*, Vol. 78, pp. 194-203.

Woolf, A., C. K. Nielsen, T. Weber, and T. J. Gibbs-Kieninger, 2002: Statewide modelling of bobcat, *Lynx rufus*, habitat in Illinois, USA. *Biological Conservation*, Vol. 104, pp. 191-198.

Worboys, M., 1998: Imprecision in finite resolution spatial data. *GeoInformatica*, Vol. 2, pp. 257-279. http://www.spatial.maine.edu/~worboys/mywebpapers/geoinformatica1998.pdf accessed 09/01/05.

Wulder, M. A., 2002: Mapping the land cover of the forested area of Canada with Landsat data. *Proceedings of the 2002 IEEE International Geoscience and Remote Sensing Symposium (IGARSS 2002) and the 24th Canadian Symposium on Remote Sensing*, Toronto, Ontario.

Wulder, M. A., J. A. Dechka, M. A. Gillis, J. E. Luther, R. J. Hall, A. Beaudoin, and S. E. Franklin, 2003: Operational mapping of the land cover of the forested area of Canada with Landsat data: EOSD land cover program. *The Forestry Chronicle*, Vol. 79, No. 6, pp. 1075-1083.

Wulder, M., A. LeDrew, S. Franklin, and M. Lavigne, 1998: Aerial image texture information in the estimation of northern deciduous and mixed wood forest leaf area index (LAI). Remote Sensing of Environment, Vol. 64, pp. 64-76.

Wyatt, B., Billington, C., De Bie, K., De Leeuw, J., Greatorex-Davies, N., Luxmoore, R., 1994: *Guidelines for land cover and land use description and classification*. Final Report to UNEP/FAO/ITC/ITE/WCMC, Huntingdon.

Yapp, R. H., 1922: The concept of habitat. *Journal of Ecology*, Vol. 10: pp. 1-17.

Zhu, Z. and Waller, E., 2003: Global forest cover mapping for the United Nations Food and Agriculture Organization Forest Resources Assessment. *Forest Science*, Vol. 49, pp. 369-380.

Zonneveld I. S., 1995: *Land Ecology. An Introduction to Landscape Ecology as a Base for Land Evaluation, Land Management and Conservation*. SPB Academic Publishing, Amsterdam.

Appendix A: Field Sheet

University of Calgary 2003 Field Sheet							Entered ☐
Plot # E: N:	Date/Time:				Ground	Chopper	
	Crew:						
	Weather:			Cloud/Light:			
Field E:		GPS Error:			Photos:		
Field N:		GPS Elev:					
Dry	Mesic	Wet	Aquatic	Slope:		Aspect:	
Disturbance:							

Field Calls	
Grizzly Bear:	AGCC:
AVI Level 1:	AVI Level 2:

Plot Description/Comments

	Species	Height	DBH	HLC	Sap	Age	Comments
1							
2							
3							
4							
5							
6							
7							
8							
9							
10							
11							
12							
13							
14							
15							
16							
17							
18							
19							
20							
21							
22							
23							
24							

Densiometer					Hemispherical Photography
	N	E	S	W	
C					
NE					
NW					
SE					
SW					

Ceptometer							
		C	NE	NW	SE	SW	Notes and Comments
1.3 m	1:						
	2:						
	3:						
	4:						
0.3 m	1:						
	2:						
	3:						
	4:						
Ground	1:						
	2:						
	3:						
	4:						

Clearsky Before Direct Beam:	Diffuse Beam:
Clearsky After Direct Beam:	Diffuse Beam:

Cover Composition				
Strata	Species	Cover % (per strata)	Cover % (all strata)	Comments
	Litter/Deadfall			
	Soil			
	Rock			
	Water			

Appendix B: Cold Fusion Code for Ceptometer Web Application

```
<!--- act_globals.cfm --->

<cfparam name="url.fuseaction" default="">

<style type="text/css">
<!--
.btn {cursor:hand;font-family:Verdana,"MS Sans Serif",Charcoal,Chicago,Arial;font-weight:normal;font-
size:smaller;background-color:#efefef;}
body,table,tr,td,th,tt {}
-->
</style>
```

```
<!--- index.cfm --->

<!DOCTYPE HTML PUBLIC "-//W3C//DTD HTML 4.0 Transitional//EN">

<html>
<cfinclude template="act_globals.cfm">

<head>
	<title>Ceptometer Processing Form</title>
</head>

<body bgcolor="#FFFFFF" marginheight="0" marginwidth="0" leftmargin="10" topmargin="10">

<table border="0" cellpadding="5" cellspacing="0" width="550" align="center">
	<tr>
		<td bgcolor="#cccc99" align="center" valign="middle" width="100%">
			<cfswitch expression=#url.fuseaction#>
				<cfcase value="process">
					<font face="Arial" > <b>Calculation
Results</b></font>
				</cfcase>
				<cfcase value="getform">
					<font face="Arial" > <b>Ceptometer Entry
Form</b></font>
				</cfcase>
				<cfdefaultcase>
					<font face="Arial" > <b>LAI From Ceptometer
Processing</b></font>
				</cfdefaultcase>
			</cfswitch>
		</td>
	</tr>

	<cfswitch expression=#url.fuseaction#>
		<cfcase value="getform">
			<cfif form.lightconditions IS "diffuse">
				<cfinclude template="dsp_diffuseinstructions.cfm">
```

```
                        <cfinclude template="frm_diffuseform.cfm">
                    <cfelse>
                        <cfinclude template="dsp_directinstructions.cfm">
                        <cfinclude template="frm_directform.cfm">
                    </cfif>
                </cfcase>
                <cfcase value="process">
                    <cfif form.lightconditions IS "diffuse">
                        <cfinclude template="act_diffuseprocess.cfm">
                    <cfelse>
                        <cfinclude template="act_directprocess.cfm">
                    </cfif>

                </cfcase>
                <cfdefaultcase>
                        <cfinclude template="dsp_lightinstructions.cfm">
                        <cfform action="index.cfm?fuseaction=getform" method="POST"
enablecab="Yes">
                                <tr>
                                        <td bgcolor="#ffffff" align="center" valign="middle"
width="100%">
                                                <font face="arial">
                                                        <cfinput type="Radio"
name="lightconditions" value="diffuse" required="Yes" message="You must select the light conditions
under which the measurements were taken."> Diffuse
                                                <cfinput type="Radio"
name="lightconditions" value="direct"> Direct
                                                </font>
                                        </td>
                                </tr>
                                <tr>
                                        <td bgcolor="#cecece" align="center"
valign="middle" width="100%">
                                                <input type="submit" value="Submit">
<input type="reset" value="Reset">
                                        </td>
                                </tr>
                        </cfform>
                </cfdefaultcase>
        </cfswitch>
</table>

</body>
</html>
```

```
<!--- dsp_lightinstructions.cfm --->

<tr>
        <td bgcolor="#efefef" align="left" valign="middle" width="100%">
                Please specify the light conditions under which your ceptometer readings were acquired:
        </td>
</tr>
```

```
<!--- dsp_diffuseinstructions.cfm --->
```

```
<tr>
	<td bgcolor="#efefef" align="left" valign="middle" width="100%">
		Measurements acquired under diffuse light conditions are the simplest for LAI
determination, since they do not require direct beam calculations or assumptions regarding canopy
structure. All that is required are above- and below-canopy PAR measurements.<br><br>
		Use the form below to enter the ceptometer measurements acquired in the field:
	</td>
</tr>
```

```
<!--- frm_diffureform.cfm --->

<cfform action="index.cfm?fuseaction=process" method="POST" enablecab="Yes">
	<input type="hidden" name="lightconditions" value="diffuse">
	<tr>
		<td bgcolor="#ffffff" align="center" valign="middle" width="100%">
			<font face="arial">
				<cfinput type="Text" name="abovecanopy" message="You must enter
an integer value for above canopy PAR" validate="integer" required="Yes" size="15"> Above canopy
PAR<br>
				<cfinput type="Text" name="belowcanopy" message="You must enter
an integer value for below canopy PAR" validate="integer" required="Yes" size="15"> Below canopy
PAR<br>
			</font>
		</td>
	</tr>
	<tr>
		<td bgcolor="#cecece" align="center" valign="middle" width="100%">
			<input type="submit" value="Submit"> <input type="reset" value="Reset">
		</td>
	</tr>
</cfform>
```

```
<!--- dsp_directinstructions.cfm --->

<tr>
	<td bgcolor="#efefef" align="left" valign="middle" width="100%">
		In addition to above- and below-canopy PAR measurements, readings acquired under
direct light conditions require estimates of beam fraction and solar zenith angle to calculate the extinction
coefficient for the canopy. Further assumptions must also be made concerning the distribution of leaves in
the canopy. The calculations made in this application assume a spherical distribution, which is accurate for
most canopies.<br><br>
		Use the form below to enter the condition and light measurements acquired in the field:
	</td>
</tr>
```

```
<!--- frm_directform.cfm --->

<cfform action="index.cfm?fuseaction=process" method="POST" enablecab="Yes">
	<input type="hidden" name="lightconditions" value="direct">
	<tr>
		<td bgcolor="#ffffff" align="center" valign="middle" width="100%">
```

```
<table border=0 cellpadding="1"  width="100%">
	<tr>
		<td width="100%" colspan="2" align="center">
			<font face="arial">
				Date:
				<cfselect name="Month" message="Please
specify the complete date/time of measurement" required="Yes">
					<option value="1"> January
					<option value="2"> February
					<option value="3"> March
					<option value="4"> April
					<option value="5"> May
					<option value="6"> June
					<option value="7" selected> July
					<option value="8"> August
					<option value="9"> September
					<option value="10"> October
					<option value="11"> November
					<option value="12"> December
				</cfselect>
				<cfselect name="Day" message="Please
specify the complete date/time of measurement" required="Yes">
					<option value="1"> 1
					<option value="2"> 2
					<option value="3"> 3
					<option value="4"> 4
					<option value="5"> 5
					<option value="6"> 6
					<option value="7" selected> 7
					<option value="8"> 8
					<option value="9"> 9
					<option value="10"> 10
					<option value="11"> 11
					<option value="12"> 12
					<option value="13"> 13
					<option value="14"> 14
					<option value="15"> 15
					<option value="16"> 16
					<option value="17"> 17
					<option value="18"> 18
					<option value="19"> 19
					<option value="20"> 20
					<option value="21"> 21
					<option value="22"> 22
					<option value="23"> 23
					<option value="24"> 24
					<option value="25"> 25
					<option value="26"> 26
					<option value="27"> 27
					<option value="28"> 28
					<option value="29"> 29
					<option value="30"> 30
					<option value="31"> 31
				</cfselect>
				<cfselect name="Year" message="Please
specify the complete date/time of measurement" required="Yes">
```

```
                                                <option value="2002"> 2002
                                                <option value="2003" selected>
2003
                                                <option value="2004"> 2004
                                                <option value="2005"> 2005
                                        </cfselect>
                                        Time:
                                        <cfselect name="Hour" message="Please
specify the complete date/time of measurement" required="Yes">
                                                <option value="1"> 1
                                                <option value="2"> 2
                                                <option value="3"> 3
                                                <option value="4"> 4
                                                <option value="5"> 5
                                                <option value="6"> 6
                                                <option value="7"> 7
                                                <option value="8"> 8
                                                <option value="9"> 9
                                                <option value="10"> 10
                                                <option value="11"> 11
                                                <option value="12" selected> 12
                                        </cfselect> :
                                        <cfselect name="Minute" message="Please
specify the complete date/time of measurement" required="Yes">
                                                <option value="00" selected> 00
                                                <option value="05"> 05
                                                <option value="10"> 10
                                                <option value="15"> 15
                                                <option value="20"> 20
                                                <option value="25"> 25
                                                <option value="30"> 30
                                                <option value="35"> 35
                                                <option value="40"> 40
                                                <option value="45"> 45
                                                <option value="50"> 50
                                                <option value="55"> 55
                                        </cfselect>
                                        <cfselect name="ampm" message="Please
specify the complete date/time of measurement" required="Yes">
                                                <option value="AM"> AM
                                                <option value="PM" selected> PM
                                        </cfselect>
                                </font>
                        </td>
                </tr>
                <tr>
                        <td width="50%">
                                <font face="arial">
                                        <cfinput type="Text" name="latitude"
message="You must enter an integer value for latitude" validate="float" required="Yes" size="15"
value="51.03"> Latitude*
                                </font>
                        </td>
                        <td width="50%">
                                <font face="arial">
```

```
                                                <cfinput type="Text" name="longitude"
message="You must enter an integer value for longitude" validate="float" required="Yes" size="15"
value="115.05"> Longitude*
                                                </font>
                                        </td>
                                </tr>
                                <tr>
                                        <td width="100%" colspan="2">
                                                <font face="arial">
                                                        <cfinput type="Text"
name="standardmeridian" message="You must enter an integer value for standard meridian"
validate="integer" required="Yes" size="15" value="105"> Standard Meridian*
                                                </font>
                                        </td>
                                </tr>
                                <tr>
                                        <td width="100%" colspan="2">
                                                <font face="arial">
                                                        <cfinput type="Text"
name="abovecanopydirect" message="You must enter an integer value for above canopy direct PAR"
validate="integer" required="Yes" size="15"> Above canopy direct PAR
                                                </font>
                                        </td>
                                </tr>
                                <tr>
                                        <td width="100%" colspan="2">
                                                <font face="arial">
                                                        <cfinput type="Text"
name="abovecanopydiffuse" validate="integer" required="No" size="15"> Above canopy diffuse PAR**
                                                </font>
                                        </td>
                                </tr>
                                <tr>
                                        <td width="100%" colspan="2">
                                                <font face="arial">
                                                        <cfinput type="Text" name="belowcanopy"
message="You must enter an integer value for below canopy PAR" validate="integer" required="Yes"
size="15"> Below canopy PAR
                                                </font>
                                        </td>
                                </tr>
                        </table>
                </td>
        </tr>
        <tr>
                <td bgcolor="#cecece" align="left" valign="middle" width="100%">
                        *The default Lat/Long values given are for the Kananaskis Field Station.<br>
                        **Leave blank if unavailable. A standard beam fraction value of 0.881 will be
used<br><br>
                        <div align="center"><input type="submit" value="Submit"> <input
type="reset" value="Reset"></div>
                </td>
        </tr>
</cfform>
```

```
<!--- act_diffuseprocess.cfm --->

<cfset tau=form.belowcanopy/form.abovecanopy>
<cfset LAI=(log(tau)/0.86)*-1>

	<tr>
		<td bgcolor="#ffffff" align="left" valign="middle" width="100%">
			<font face="arial"><strong>LAI:
<cfoutput>#decimalformat(LAI)#</strong></cfoutput>
		</td>
	</tr>
	<form action="index.cfm" method=POST>
		<tr>
			<td align="center">
				<font  face="Arial"><input type=submit class=btn value='Calculate
Another One'></font>
			</td>
		</tr>
	</form>
```

```
<!--- act_directprocess.cfm --->

<!--- Set the date/time based on input form --->
<cfif (form.ampm IS "PM") and (form.hour LT 12)>
	<CFSET theDate = CreateDateTime(form.year, form.month, form.day, (form.hour+12),
form.minute, "00")>
<cfelseif (form.ampm IS "AM") and (form.hour IS 12)>
	<CFSET theDate = CreateDateTime(form.year, form.month, form.day, "00", form.minute, "00")>
<cfelse>
	<CFSET theDate = CreateDateTime(form.year, form.month, form.day, form.hour, form.minute,
"00")>
</cfif>

<!--- Calculate Julian day --->
<cfif ((form.Month IS "1") OR (form.Month IS "2"))>
	<cfset form.Month=form.Month+12>
	<cfset form.Year=form.Year-1>
</cfif>
<cfset A=form.Year/100>
<cfset B=A/4>
<cfset C=2-A+B>
<cfset E=365.25*(form.Year+4716)>
<cfset F=30.6001*(form.Month+1)>
<cfset JD=C+form.Day+E+F-1524.5>

<!--- Calculate day of the year --->
<cfset J=dayofyear(thedate)>

<!--- Calculate solar declination --->
<cfset AA=0.6224+(0.0172*J)>
<cfset BB=0.03345*Sin(AA)>
<cfset CC=4.869+(0.0172*J)+BB>
<cfset DD=0.39785*sin(CC)>
<cfset Declination=ASIN(DD)>
```

```
<!--- Convert degrees latitude to radians --->
<cfset radian_latitude=form.latitude*0.01745329252>

<!--- Convert clock time to decimal time --->
<cfset time=hour(theDate)+(minute(theDate)/60)>

<!--- Correct time for daylight savings --->
<cfset time=time-1>

<!--- Calculate the time of solar noon --->
<cfset LC=(form.standardmeridian-longitude)/15>
<cfset theta=(279.575 + 0.986*JD)*pi()/180>
<cfset ET=(-104.7*sin(theta)+596.2*sin(2*theta)+4.3*sin(3*theta)-12.7*sin(4*theta)-429.3*cos(theta)-
2.0*cos(2*theta)+19.3*cos(3*theta))/3600>
<cfset timesolarnoon=(12-LC-ET)>

<!--- Calculate solar zenith angle --->
<cfset W=0.2618*(time-timesolarnoon)>
<cfset X=cos(radian_latitude)*cos(Declination)*cos(W)>
<cfset Y=sin(radian_latitude)*sin(Declination)+(X)>
<cfset szenith=acos(Y)>

<!--- Calculate beam fraction --->
<cfif form.abovecanopydiffuse IS NOT "">
        <cfset beam_fraction=1-(abovecanopydiffuse/abovecanopydirect)>
<cfelse>
        <cfset beam_fraction=0.881>
</cfif>

<!--- Leaf absorptivity estimate --->
<cfparam name="leaf_absorptivity" default="0.9">

<!--- Calculate extinction coefficient --->
<cfset A=0.283+0.785*leaf_absorptivity-0.159*leaf_absorptivity>
<cfparam name="leaf_angle_distribution" default="1"> <!--- Assumes spherical distribution --->
<cfset K=(1/(2*cos(szenith)))>

<!--- Calculate fPAR --->
<cfset this_fPAR=belowcanopy/abovecanopydirect>

<!--- Calculate primitives for LAI=((1-1/2*K)*beam_fraction-1)*Log(this_fPAR)/A*(1-
0.47*beam_fraction)--->
<cfset AAA=(1/(2*K))>
<cfset BBB=(1-AAA)>
<cfset CCC=((BBB*beam_fraction)-1)>
<cfset DDD=(log(this_fPAR))>
<cfset numerator=(DDD*CCC)>
<cfset denominator=(A*(1-(0.47*beam_fraction)))>
<cfset this_LAI=numerator/denominator>

<tr>
        <td bgcolor="#ffffff" align="left" valign="middle" width="100%">
                <font face="arial">Day of the Year: <cfoutput>#round(J)#</cfoutput><br>
                <font face="arial">Julian Day: <cfoutput>#round(JD)#</cfoutput><br>
                <font face="arial">Decimal Time: <cfoutput>#decimalformat(time)#</cfoutput><br>
```

```
                    <font face="arial">Time of Solar Noon (decimal time):
<cfoutput>#decimalformat(timesolarnoon)#</cfoutput><br>
                    <font face="arial">Declination (radians):
<cfoutput>#decimalformat(Declination)#</cfoutput><br>
                    <font face="arial">Sloar Zenith Angle (radians):
<cfoutput>#decimalformat(szenith)#</cfoutput><br>
                    <font face="arial">Beam Fraction:
<cfoutput>#decimalformat(beam_fraction)#</cfoutput><br>
                    <font face="arial">Extinction Coefficient:
<cfoutput>#decimalformat(K)#</cfoutput><br>
                    <font face="arial">fPAR: <cfoutput>#decimalformat(this_fPAR)#</cfoutput><br>
                    <font face="arial"><strong>LAI:
<cfoutput>#decimalformat(this_LAI)#</cfoutput></strong><br>
          </td>
</tr>
<form action="index.cfm" method=POST>
          <tr>
                    <td align="center">
                              <font  face="Arial"><input type=submit class=btn value='Calculate Another
One'></font>
                    </td>
          </tr>
</form>
```

Appendix C: List of Acronymns

AGCC	Alberta Ground Cover Characterization
AIC	Akaike's Information Criterion
ANN	Artificial Neural Network
APAR	Absorbed Photosynthetically Active Radiation
AVHRR	Advanced Very High Resolution Radiometer
AVI	Alberta Vegetation Inventory
CCDEM	Crown Closure Model From DEM Variables
CCTM	Crown Closure Model From TM Variables
CCTMDEM	Crown Closure Model From TM and DEM Variables
DBH	Diameter at Breast Height
DEM	Digital Elevation Model
DN	Digital Number
EOS	Earth Observing System
EOSD	Earth Observation for the Sustainable Development of Forests
ETM+	Enhanced Thematic Mapper Plus
FMFGBRP	Foothills Model Forest Grizzly Bear Research Program
FPAR	Fraction of Absorbed Photosynthetically Active Radiation
GAP	Gap Analysis Program
GIS	Geographic Information System
GLM	Generalized Linear Model
GPS	Global Positioning System
IDT	Integrated Decision Tree
IDTA	Integrated Decision Tree Approach
kNN	Mean Nearest Neighbour
LAI	Leaf Area Index
LAI_e	Effective Leaf Area Index
LAI_{eCan}	Canopy Effective Leaf Area Index
LAI_{eTot}	Total Effective Leaf Area Index
LAI_{eUs}	Understorey Effective Leaf Area Index
LiDAR	Light Detection and Ranging
MCP	Minimum Convex Polygon
MLC	Maximum Likelihood Classifier
MODIS	Moderate Resolution Imaging Spectroradiometer
MSS	Multispectral Scanner
NDVI	Normalized Difference Vegetation Index
$NDVI_c$	Mid Infrared-Corrected Normalized Difference Vegetation Index
NN	Nearest Neighbour
PAR	Photosynthetically Active Radiation
PIF	Pseudo-Invariant Feature
RMSE	Root Mean Square Error
RADAR	Radio Detection and Ranging
RSF	Resource Selection Function
SCDEM	Species Composition Model From DEM Variables

SCTM	Species Composition Model From TM Variables
SCTMDEM	Species Composition Model From TM and DEM Variables
SR	Simple Ratio
SR_c	Mid Infrared-Corrected Simple Ratio
SJWCP	South Jasper Woodland Caribou Project
TM	Thematic Mapper
TOA	Top of Atmosphere
VI	Vegetation Index
WRS	Worldwide Reference System